

8. SITE 652: LOWER SARDINIAN MARGIN¹

Shipboard Scientific Party²

HOLE 652A

Date occupied: 18 January 1986

Date departed: 28 January 1986

Time on hole: 10 days, 13 hr

Position: 40°21.30'N 12°08.59'E

Water depth (sea level, corrected m, echo-sounding): 3446.0

Water depth (rig floor, corrected m, echo-sounding): 3457.0

Bottom felt (m, drill pipe length from rig floor): 3470.5

Total depth (m): 4191.6

Penetration (m): 721.1

Number of cores: 75

Total length of cored section (m): 721.1

Total core recovered (m): 445.7

Core recovery (%): 61.2

Deepest sedimentary unit cored:

Depth sub-bottom (m): 683.5

Nature: calcareous sandstones and siltstones.

Age: unknown, possibly Messinian.

Measured vertical sound velocity (km/s): 3.3 km/s

Igneous or metamorphic basement: None

Principal Results: The sediments recovered are divided into two major divisions: Pliocene/Pleistocene hemipelagic marine sediments from 0 to 188 mbsf, underlain by barren, gypsiferous, calcareous sandy mud and mudstone interbedded with minor chemical sediments from 188 to 721 mbsf. The Pliocene/Pleistocene sediments can be further divided into two units (Units I and II) primarily based on their calcium carbonate content; the pre-Pliocene sediments can be divided in two units (Units IV and V) based on sedimentary structures and the abundance of chemical sediments. A 40-cm-thick transition zone (Unit III) divides the Pliocene/Pleistocene hemipelagic sediments from the barren pre-Pliocene sediments.

Coring Results

In more detail, the recovered lithologies were (Fig. 1):

Sedimentary Unit I: Cores 107-652A-1R to -6R; depth: 0-55.4 mbsf; age: Pleistocene. This unit consists mainly of gray calcareous muds and gray muds, with volcanic glass as a common minor constituent. Carbonate content averages 22%. The succession includes four distinct sapropel layers; preliminary geochemical data suggest that these sapropels contain a mixture of marine and continental organic lipids.

Sedimentary Unit II: Cores 107-652A-7R to -20R; depth: 55.4-188.2 mbsf; age: early Pleistocene-Pliocene. Sedimentary unit II consists of marly nannofossil oozes with higher carbonate content (average 48%) than in Unit I. Four more sapropel layers were found in the upper 22 m of the unit. The interval between 65 and 113 mbsf contains abundant volcanic glass. From 176 to 180 mbsf, the dominant olive gray color grades downsection into yellowish-red and brownish yellow tones, followed by intense reds and browns directly above the Miocene/Pliocene boundary. The boundary was determined by the last appearance of *in-situ* planktonic foraminifera at 188.2 mbsf.

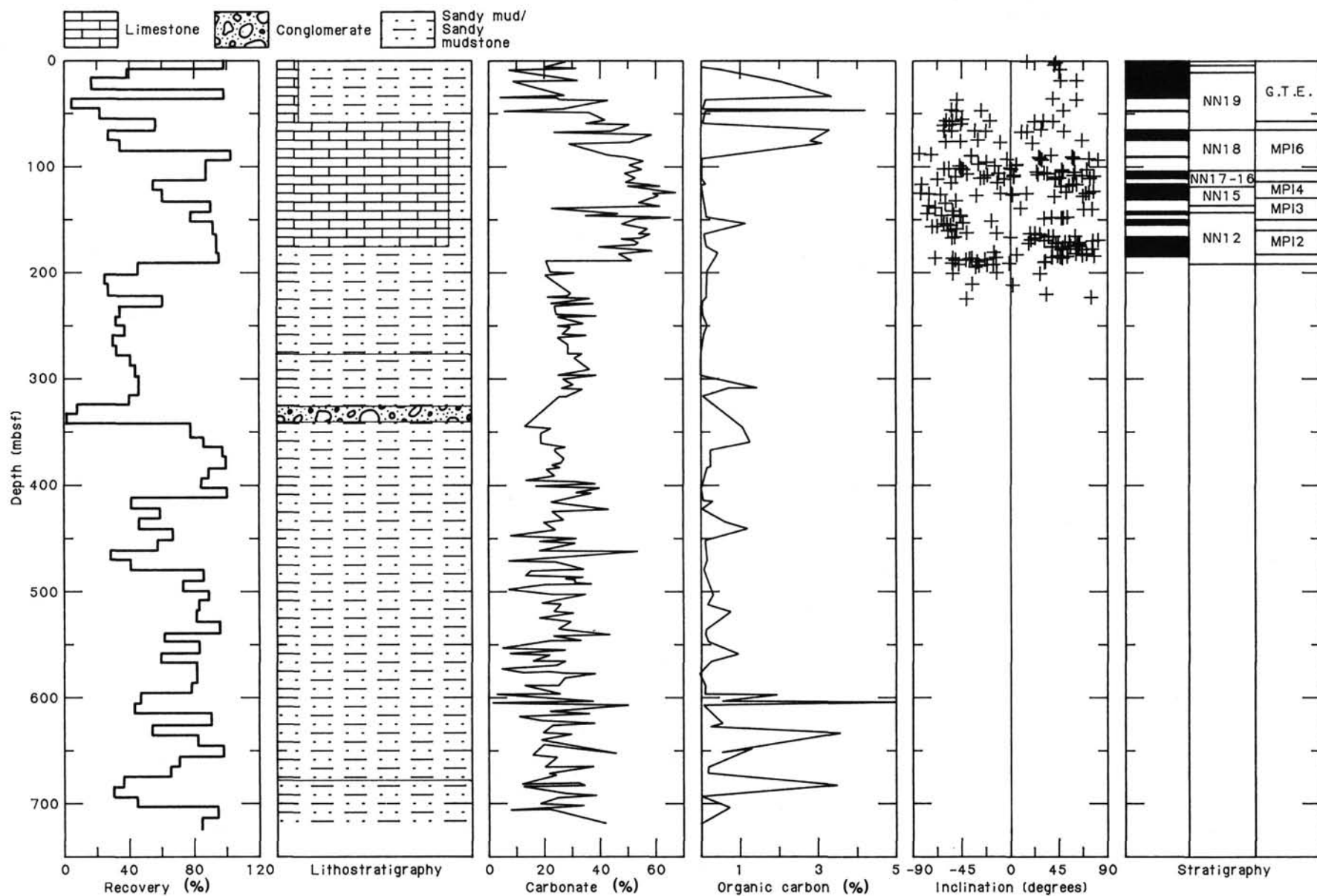
Sedimentary Unit III: Interval 107-652A-20R-6, 52-92 cm depth: 188.2-188.6 mbsf; age: latest Messinian. This unit is a transitional interval between the normal marine Pliocene and the barren Messinian sediments. The unit is composed of a succession of centimeter-thick layers of strongly colored (red, strong brown, reddish gray, light gray, greenish gray, and gray) clays and muds. The deepest occurrence of rare *in-situ* nannofossils was at 188.4 mbsf.

Sedimentary Unit IV: Interval 107-652-20R-6, 92 cm to -36R-CC; depth: 188.6-344.3 mbsf; age: probable late Messinian. The interval from 189 to 286 mbsf is dominated by gray, thinly-bedded, normally-graded, gypsum- and carbonate-bearing, sandy mud, interpreted as turbidites. From 286 to 335 mbsf the lithological components are the same but the sedimentary structures differ in that there are reversely-graded sequences, frequent water escape structures, syn-sedimentary microfaults, and microbreccias; the shallowest occurrence of authigenic calcium sulfate and halite-dissolution molds occurs here. The unit was barren except for three specimens of *Ammonia beccarii tepida* and two fragments which may be from the brackish water ostracod *Cyprideis*, all found at 277 mbsf. The lowest core of the unit (335-345 mbsf) recovered only 14 smooth, rounded pebbles of sedimentary and low-grade metamorphic origin. The collection of varied lithologies represented by the pebbles occurs on land in the southern Apennine and the Sicilian Maghrebide mountain chains; this suite of rocks is unknown in Sardinia, Calabria, or on the Marchi Seamount.

Sedimentary Unit V: Core 107-652A-37R to -75R; depth: 344.8-721.1 mbsf; age: undetermined (probable Messinian). The interval from 345 to 684 mbsf is characterized by a succession of dark gray, graded and cross-bedded, gypsum- and carbonate-bearing sandy muds,

¹ Kastens, K. A., Mascle, J., Auroux, C., et al., 1987. *Proc., Init. Repts. (Pt. A), ODP*, 107.

² Kim A. Kastens (Co-Chief Scientist), Lamont-Doherty Geological Observatory, Palisades, NY 10964; Jean Mascle (Co-Chief Scientist), Laboratoire de Géodynamique Sous-Marine, Université Pierre et Marie Curie, BP 48, 06230 Villefranche-sur-Mer, France; Christian Auroux, Staff Scientist, Ocean Drilling Program, Texas A&M University, College Station, TX 77843; Enrico Bonatti, Lamont-Doherty Geological Observatory, Palisades, NY 10964; Cristina Broglia, Lamont-Doherty Geological Observatory, Palisades, NY 10964; James Channell, Department of Geology, 1112 Turlington Hall, University of Florida, Gainesville, FL 32611; Pietro Curzi, Istituto di Geologia Marina, Via Zamboni, 65, 40127 Bologna, Italy; Kay-Christian Emeis, Ocean Drilling Program, Texas A&M University, College Station, TX 77843; Georgette Glaçon, Laboratoire de Stratigraphie et de Paléogéologie, Centre Saint-Charles, Université de Provence, 3, Place Victor Hugo, 13331 Marseille Cedex, France; Shiro Hasegawa, Institute of Geology, Faculty of Science, Tohoku University, Aobayama, Sendai, 980, Japan; Werner Hieke, Lehrstuhl für Allgemeine, Angewandte und Ingenieur-Geologie, Abt. Sedimentforschung und Meeresgeologie, Technische Universität München, Lichtenbergstrasse 4, D-8046 Garching, Federal Republic of Germany; Floyd McCoy, Lamont-Doherty Geological Observatory, Palisades, NY 10964; Judith McKenzie, Department of Geology, University of Florida, 1112 Turlington Hall, Gainesville, FL 32611; Georges Mascle, Institut Dolomieu, Université Scientifique et Médicale de Grenoble, 15 Rue Maurice Gignoux, 38031 Grenoble Cedex, France; James Mendelson, Earth Resources Laboratory E34-366, Department of Earth, Atmospheric and Planetary Sciences, Massachusetts Institute of Technology, 42 Carleton Street, Cambridge, MA 02142; Carla Müller, Geol.-Paläont. Institut, Universität Frankfurt/Main, 32-34 Senckenberg-Anlage, D-6000 Frankfurt/Main 1, Federal Republic of Germany (current address: 1 Rue Martignon, 92500 Rueil-Malmaison, France); Jean-Pierre Réhault, Laboratoire de Géodynamique Sous-Marine, Université Pierre et Marie Curie, BP 48, 06230 Villefranche-sur-Mer, France; Alastair Robertson, U.S. Geological Survey, 345 Middlefield Road, Menlo Park, CA 94025 (current address: Department of Geology, Grant Institute, University of Edinburgh, Edinburgh, EH9 3JW, United Kingdom); Renzo Sartori, Istituto di Geologia Marina, Via Zamboni, 65, 40127 Bologna, Italy; Rodolfo Sprovieri, Istituto di Geologia, Corso Tukory, 131, Palermo, Italy; Masayuki Torii, Department of Geology and Mineralogy, Faculty of Science, Kyoto University, Kyoto, 606, Japan.



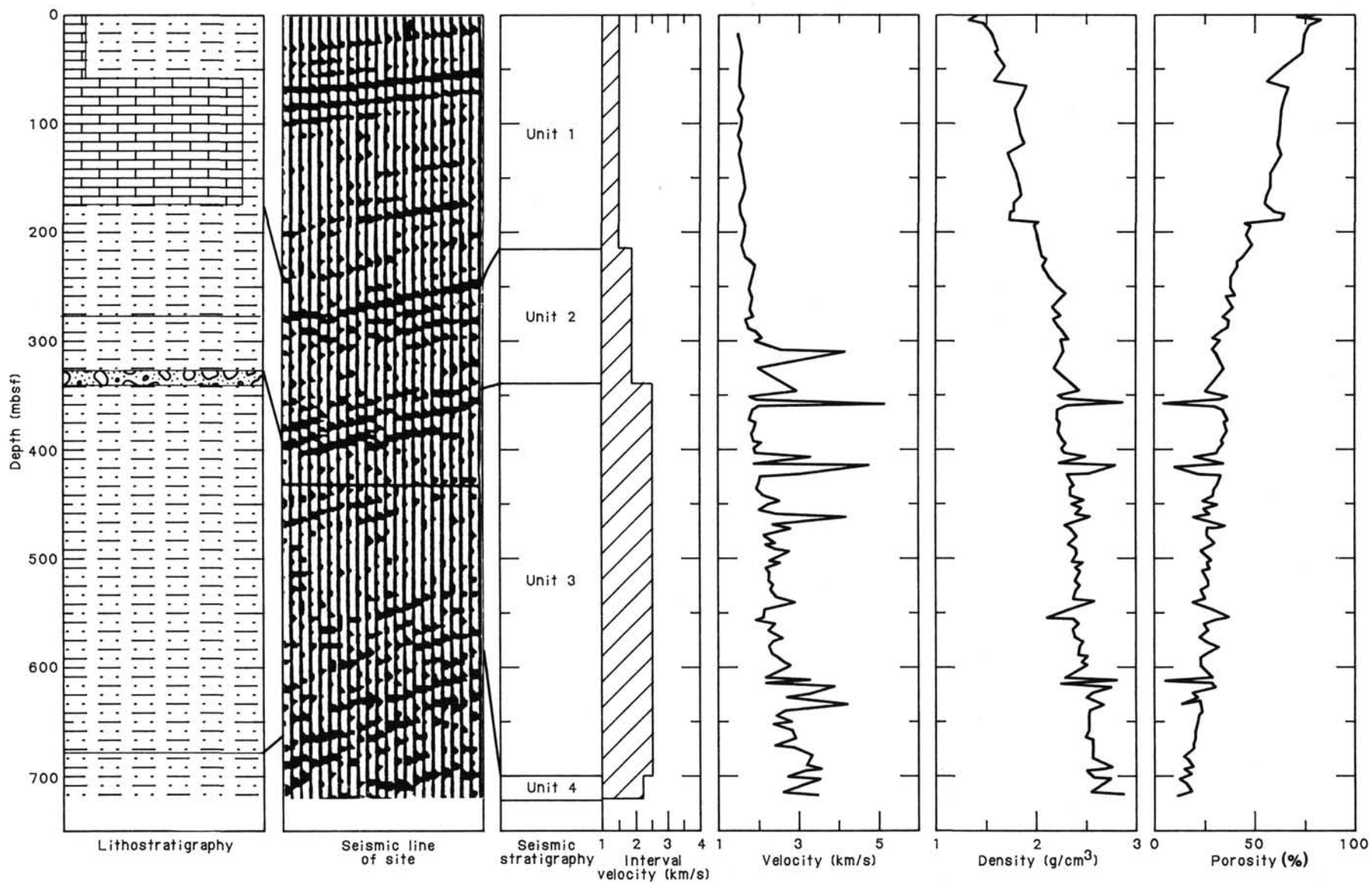


Figure 1. Summary of measurements made at Site 652.

with several cyclic zones containing crystalline anhydrite as thick as 5 cm showing "chicken-wire" texture. Rare scattered plant debris, one algae-rich layer, thin finely-laminated organic carbon-rich layers, and numerous bright red (hematite?) and yellow (limonite?) millimetric horizons of inferred continental derivation are locally present. Within the interstitial waters, Ca^{2+} , Mg^{2+} , sulfate, and chlorinity reach maximum concentrations at about 500 mbsf; this suggests that the pore water chemistry of the entire sediment column is dominated by dissolution of evaporites in sedimentary Unit V. From 684 to 721 mbsf, sedimentary Unit V is well-indurated and consists mainly of dark gray calcareous siltstones, sandstones and claystones, containing highly-variable detrital elements, including pelagic micrite, platform carbonate debris, metamorphic lithic fragments, and detrital dolomite, calcite, and gypsum.

Downhole Measurements

Five successful heat flow measurements gave a thermal gradient of $14^\circ\text{C}/100\text{ m}$, for an average heat flow of about 4 HFU. The hole

was logged between 78 mbsf and approximately 375 mbsf with a DIL/LSS/GR/CALI combination and a GST/NGT/CNT combination. The GST data proved valuable for identifying clay-rich/clay-poor cycles in sedimentary Units IV and V (the inferred Messinian sequence).

BACKGROUND AND OBJECTIVES

Regional Setting and Previous Work

Site 652 lies on the lowermost eastern Sardinian continental margin in the central Tyrrhenian Sea (Figs. 2 and 3). The eastern Sardinian margin is an example of the class of "passive" or "Atlantic-type" margins in which continental crust has been stretched and thinned by listric normal faulting (Malinverno et al., 1981; Fabbri et al., 1981; Moussat, 1983; Rehault et al., 1986). Seismic refraction experiments reveal an eastward-thinning conti-

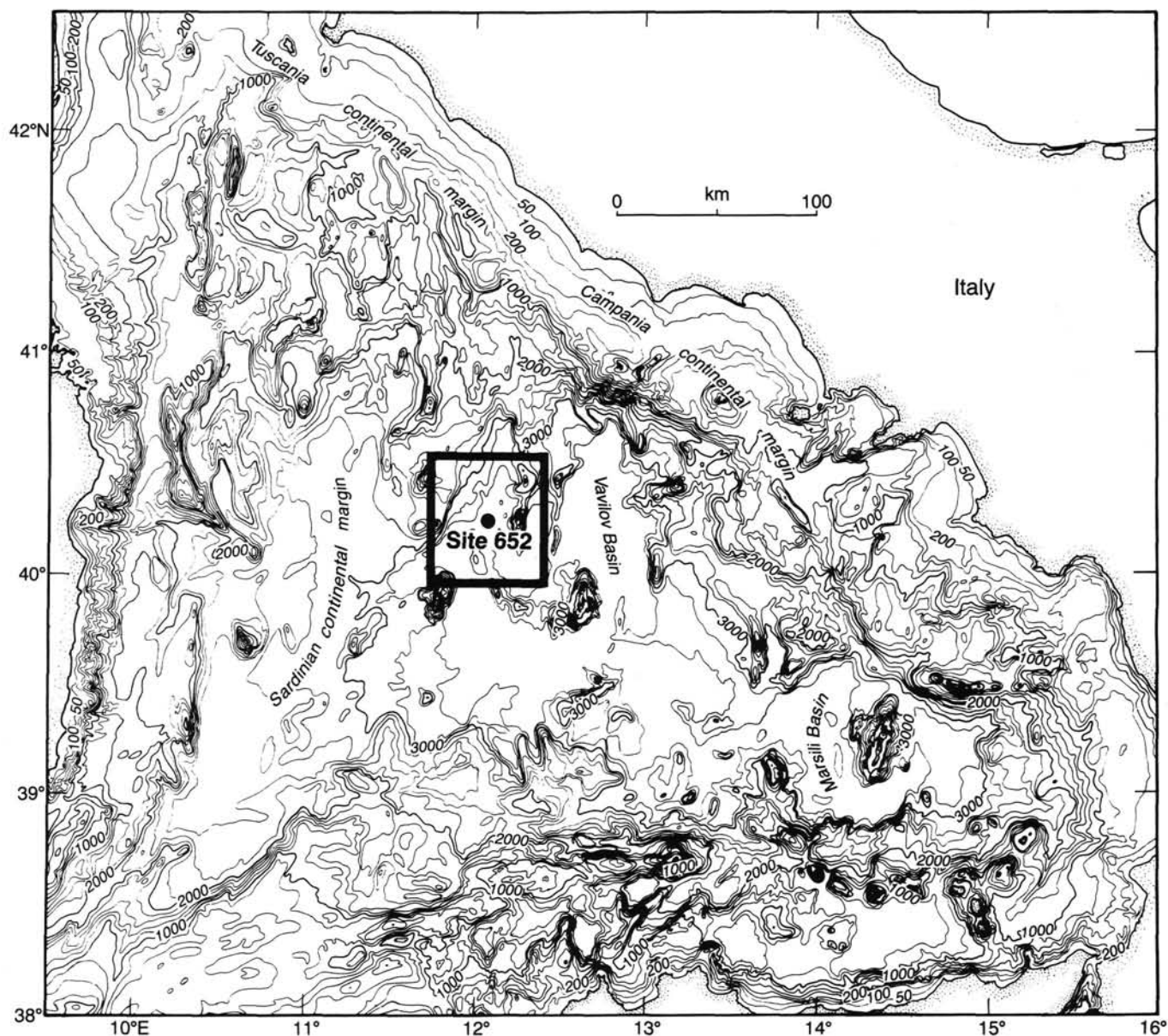


Figure 2. Site 652 is located on a small tilted block on the lowermost Sardinian continental margin, west of the Vavilov Basin. Contours in meters from International Bathymetric Chart of the Mediterranean.

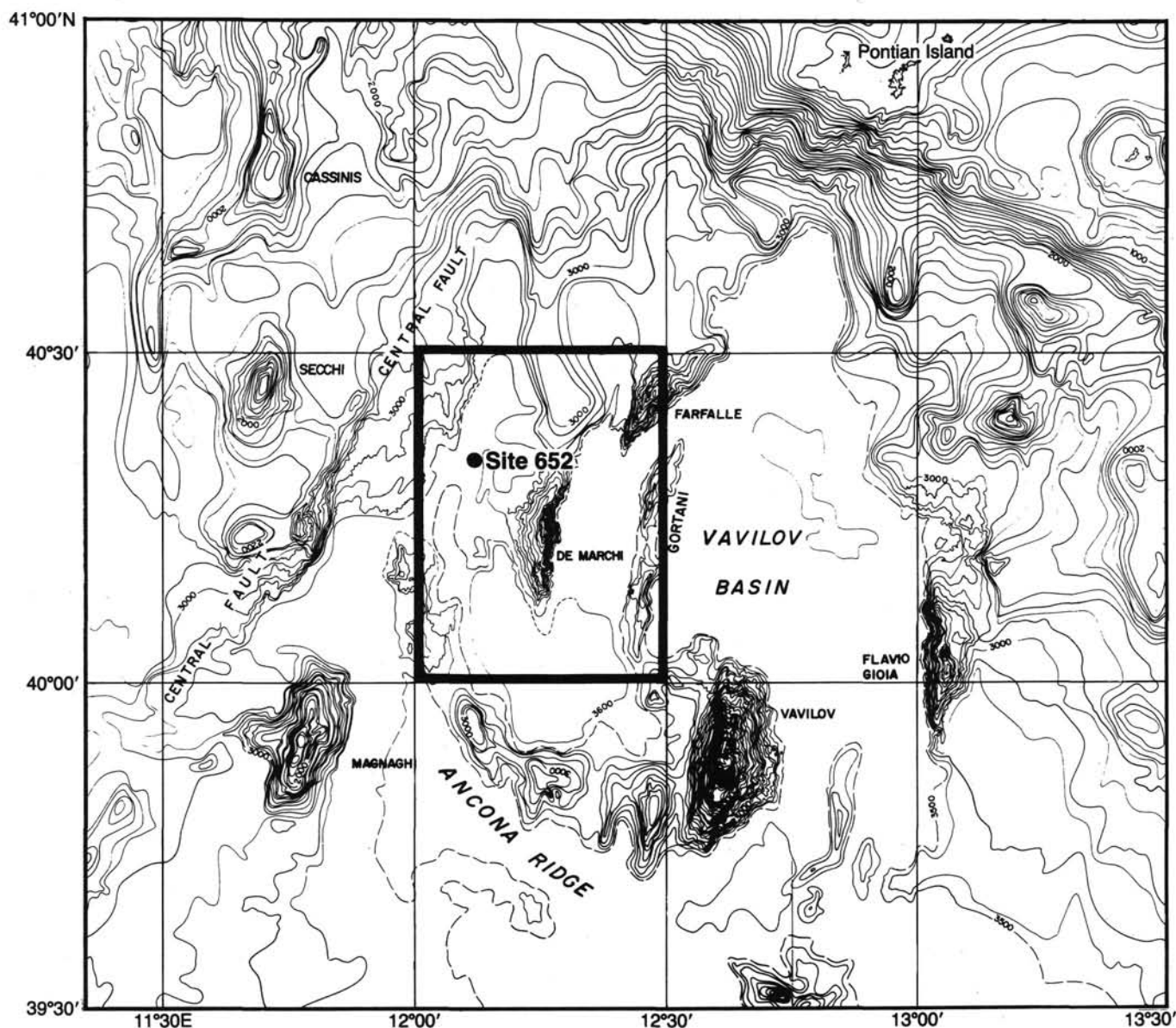


Figure 3. A northeast-trending bathymetric scarp, the so-called Central Fault, lies west of the site. Prominent asymmetric seamounts, the de Marchi and Farfalle Seamounts, lie east of the site.

mental crust (Fig. 4; Recq et al., 1984; Steinmetz et al., 1983), and seismic reflection profiles illustrate fracturing of the lower margin into a series of small, fault-bounded, tilted blocks (Figs. 4 and 5; Morelli, 1970; Finetti et al., 1970; Finetti and Morelli, 1973; Fabbri and Curzi, 1979; Moussat, 1983; Rehault et al., 1984a).

Relative to most other passive continental margins, the Sardinian margin offers to researchers the advantage of adjoining a basin which is relatively young, and a land area which sheds a relatively sparse sediment supply. Thus the early rifting history is not deeply buried and is unusually accessible to drilling. In contrast to most well-studied passive margins, this study area bounds a marginal basin or back-arc basin. Young seafloor in back-arc basins is typically deeper than seafloor of the same age in mature oceans; this implies that back-arc basin seafloor follows a different subsidence curve.

As at other passive continental margins, seismic reflection lines across the Sardinian margin reveal the existence of three distinct sedimentary sequences which are inferred to have been

deposited prior to, during, and after stretching of the continental crust (Figs. 6 and 7). The lowermost unit, the pre-rift sequence, comprises subparallel seismic reflectors with a uniform dip. Typically the dip is landward (westward) although eastward dipping pre-rift sediments are seen on some fault-bounded blocks. This lowermost unit is interpreted as strata that were flat-lying when deposited, and then subsequently tilted en masse when the fault-bounded block rotated. The middle unit, the syn-rift sequence, comprises dipping reflectors with the same sense of dip as the pre-rift sequence; however the magnitude of the dip increases downsection within the syn-rift sequence, such that individual layers within the sequence, and the syn-rift sequence as a whole, thicken downdip. The middle unit is interpreted as strata that maintained a horizontal depositional surface while the fault-bounded block gradually tilted under them. The uppermost unit, the post-rift sequence, comprises subparallel, subhorizontal reflectors. This uppermost unit is interpreted as strata that were deposited after motion ceased on the faults bounding the block. The cessation of tilting is inferred to coincide with the end of

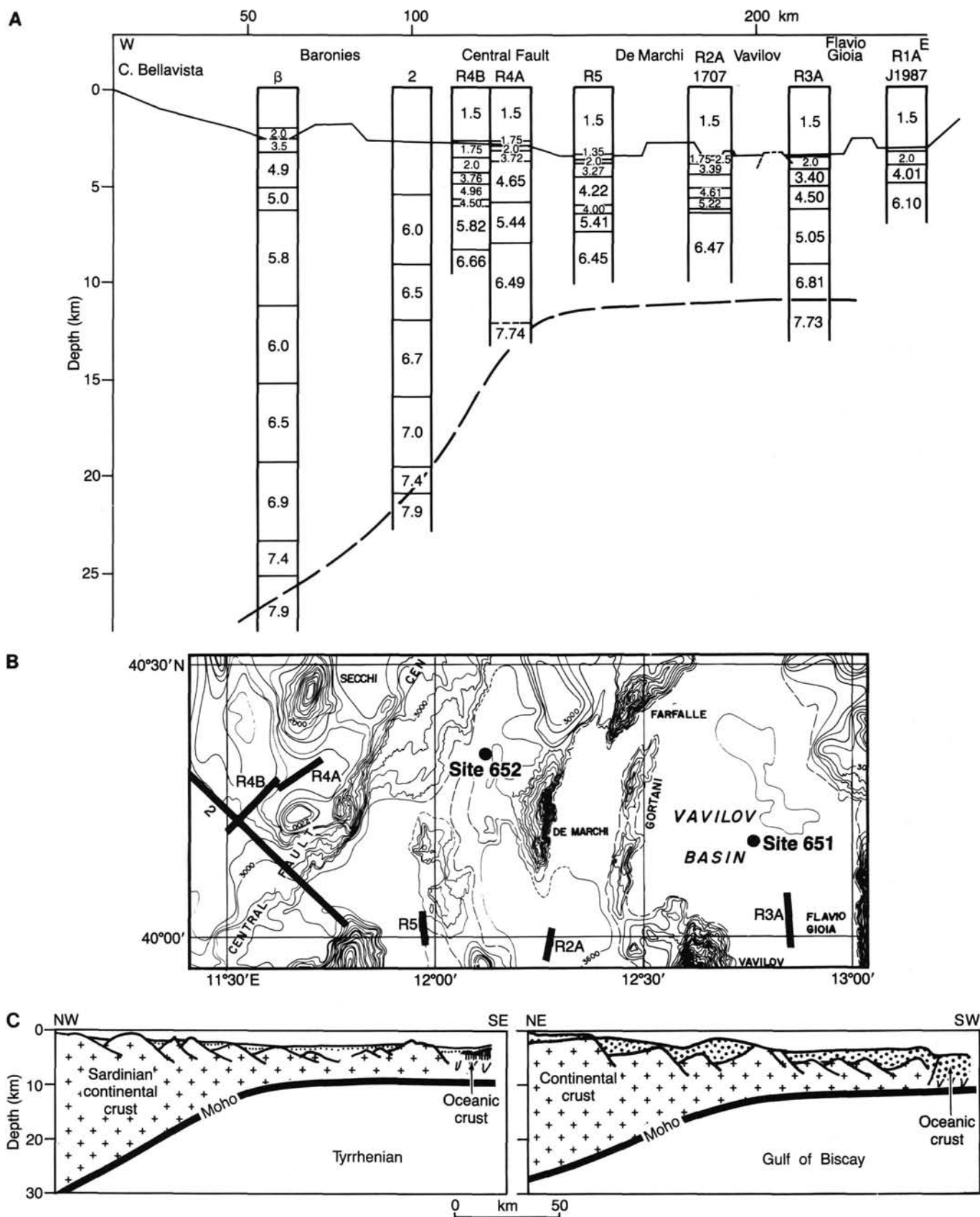


Figure 4. A. Crustal section of the Sardinian margin and Vavilov Basin deduced from refraction data (after Recq et al., 1984). B. Location of refraction experiments in the vicinity of Sites 651–652. C. Comparison between the general cross section of the Sardinian continental margin and the Gulf of Biscaye northern margin (after Malinverno et al., 1981).

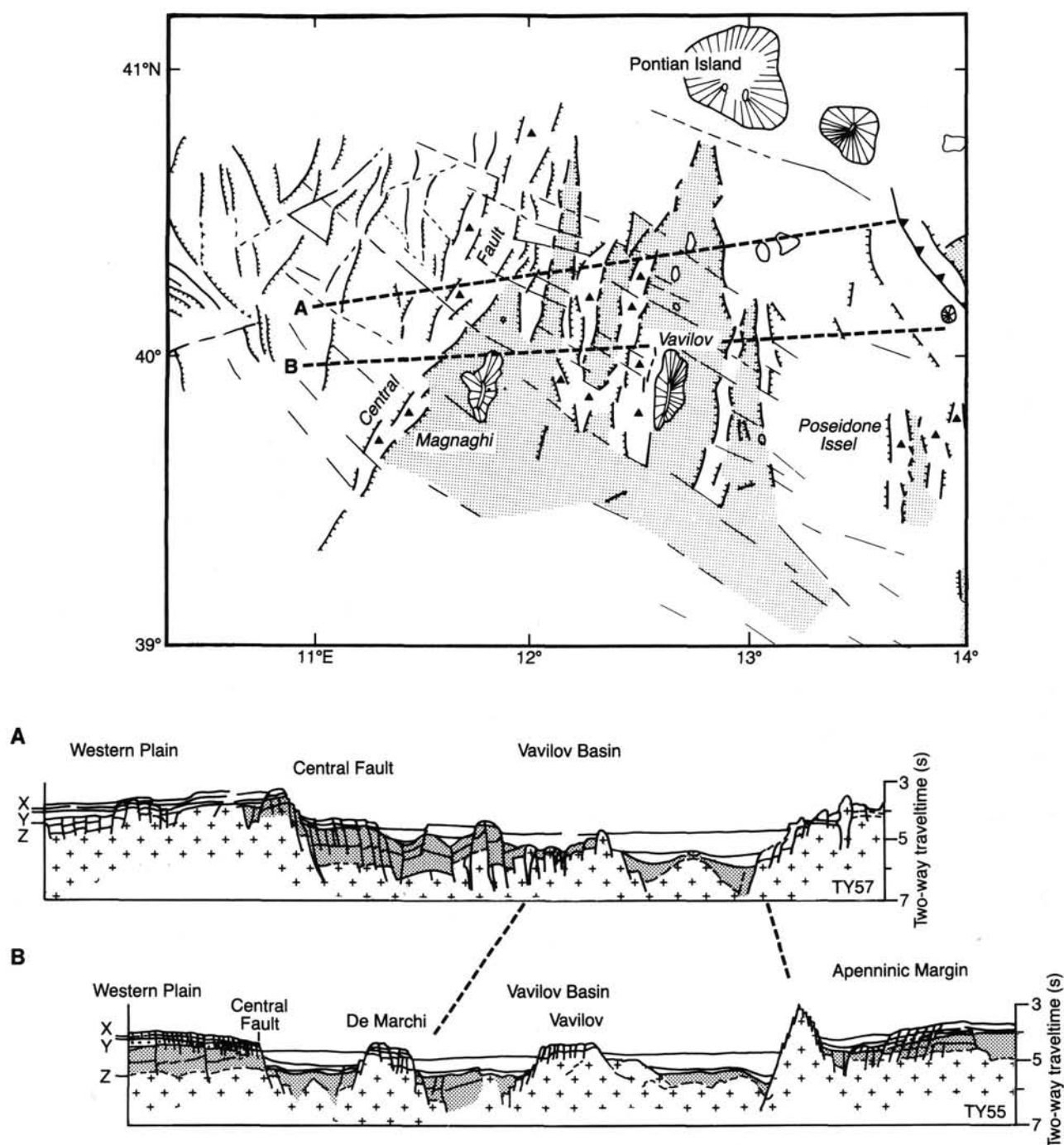


Figure 5. Upper. Schematic structural diagram of the lowermost Sardinian margin and adjacent Vavilov Basin (after Rehault et al., 1987). Shaded area: extension of the main bathymetric plain. The general structural trend of the margin is northeast (Central Fault), but subtle N 110°–N 120° lineaments, possibly transfer faults, are detected in the bathymetry. Lower. Two east-west cross sections from the Sardinian margin to the Tuscanian (Apenninic) margin. + + +: acoustic basement; shaded area: inferred pre-Pliocene sediments; dots: evaporitic facies (Messinian) (After Rehault et al., 1987).

the continental stretching stage and the beginning of formation of oceanic-type crust along the axis of the basin.

The timing of pre-, syn-, and post-rift phases in the Tyrrhenian Sea is poorly constrained; elucidating this was the major objective of Sites 652 and 654. There was widespread agreement that the post-rift sequence is Pliocene to Pleistocene (Fabbri and Curzi, 1979; Malinverno et al., 1981; Moussat, 1983; Rehault et

al., 1984b). According to the pioneering hypothesis of Selli and Fabbri (1971), who proposed a Pliocene age for the central Tyrrhenian Sea, one may expect the syn-rift sequence to be late-pre-Pliocene.

Site 652 is located (Figs. 7 and 8) in an elongate, north-trending slope basin, on the landward (western) side of a small tilted block, near the inferred transition between thinned continental

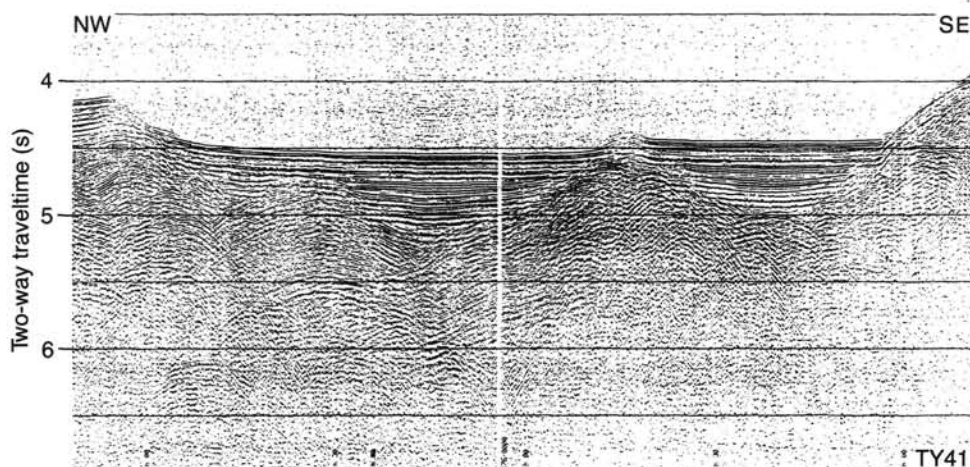


Figure 6. Single channel seismic line collected in the vicinity of Site 652 (see location on Fig. 8). Air-gun line TY41 (LGSM *Villefranche*), parallel to site survey line ST01, showing the tilted block on which the site was chosen.

and oceanic crust. The sediments on this particular tilted block are landward (westward) dipping, implying this block is bounded by seaward-dipping listric normal faults.

Immediately to the west of the site lies a north-northeast-trending, east-facing system of scarps known as the *Faïlle Centrale* or Central Fault (Fabbri et al., 1981; Fig. 3). The Central Fault appears to be a fundamental structural lineament of the Tyrrhenian Sea. Physiographically, the Central Fault separates the lower Sardinian slope, with water depths averaging greater than 3000 m, from the middle slope, where water depths are generally shallower than 3000 m.

Immediately to the east of the site lies a north-northeast-trending, asymmetric ridge known as Monte de Marchi or de Marchi Seamount (Fig. 3). de Marchi Seamount borders the Vavilov Basin and is interpreted as the easternmost tilted block of the continental margin (Figs. 3 and 5) (Moussat, 1983; Rehault et al., 1986). Dredge hauls on de Marchi Seamount have clearly demonstrated its continental nature, yielding phyllites, limestones, and granites of Carboniferous to Neogene age (Colantoni et al., 1981). Dives by submersibles made recently along the steep slopes of de Marchi Seamount have shown many outcrops of deformed phyllites and massive limestones cut by north-northeast- and northwest-trending faults (Gennesseaux et al., 1986).

Objectives

Passive Continental Margin Evolution

The primary objective at Site 652 was to document the timing of extension and subsidence of a young passive continental margin, by dating the contact between pre- and syn-rift sediments and between syn- and post-rift sediments. The timing and rate of extension and subsidence were to be compared to those at other passive margins, with the expectation that the subsidence history of this very small basin, bounded on two sides by collisional interactions, might differ significantly from passive margins fronting open oceans.

In addition to deciphering the subsidence history of the single block on which Site 652 is situated, the results from this site should permit extrapolation to adjacent blocks. Prominent reflectors present in the half-graben fill at Site 652 have been mapped throughout the Sardinian margin (Moussat, 1983); using ages for these reflectors determined at Site 652, it should be possible

to approximate the timing of tilting of other blocks on which the same reflectors are detected.

Messinian Paleoenvironment

A secondary objective at Site 652 was to recover Messinian facies in an area where the existence and/or nature of Messinian deposits appeared uncertain on seismic grounds (Fabbri and Curzi, 1979). MCS line ST01 (Fig. 7) shows a strong reflector (slightly faulted, at about 220 ms), dipping toward the west, which has been tentatively interpreted as of Messinian age but of unknown nature (Rehault et al., 1986). Malinverno et al. (1981) mapped this area as a subaerial Messinian facies, possibly alluvial. Moussat (1983) stressed the apparent absence of the B₂ sequence (evaporitic sequence) in an area near Site 652.

Pre-Messinian Paleoenvironment

According to the seismic stratigraphic interpretation of Moussat (1983), the uppermost part of the inferred pre-Messinian seismic sequence is involved in the syn-rift filling of half-grabens, whereas deeper parts of the sequence are presumably pre-rift. Thus the potential recovery of Tortonian and possibly older sediments during drilling at Site 652 would increase our understanding of the evolution of the Tyrrhenian area prior to rifting. Of particular interest was the determination of whether marine conditions existed prior to the most recent phase of extension and tilting; such an observation would support the suggestion that the Tyrrhenian has experienced multiple phases of extension (Moussat, 1983; Rehault et al., 1984a).

Site Selection

Site 652 was intended to decipher the extensional and subsidence history of the lower margin, as close as possible to the ocean/continent transition. The site was therefore positioned on the easternmost tilted, fault-bounded block whose seismic reflection profiles exhibit an unambiguous geometry of apparent pre-, syn-, and post-rift sediments. The precise position of the site, at shotpoint 4250 on seismic line ST01 (Fig. 7), is constrained in the downdip direction (west) by the increasing thickness of the syn-sedimentary unit; the inferred pre-rift sediments would be too deep to reach in a single-bit hole farther west. In the updip direction (east), the location is constrained for safety considerations to avoid a recently active fault.

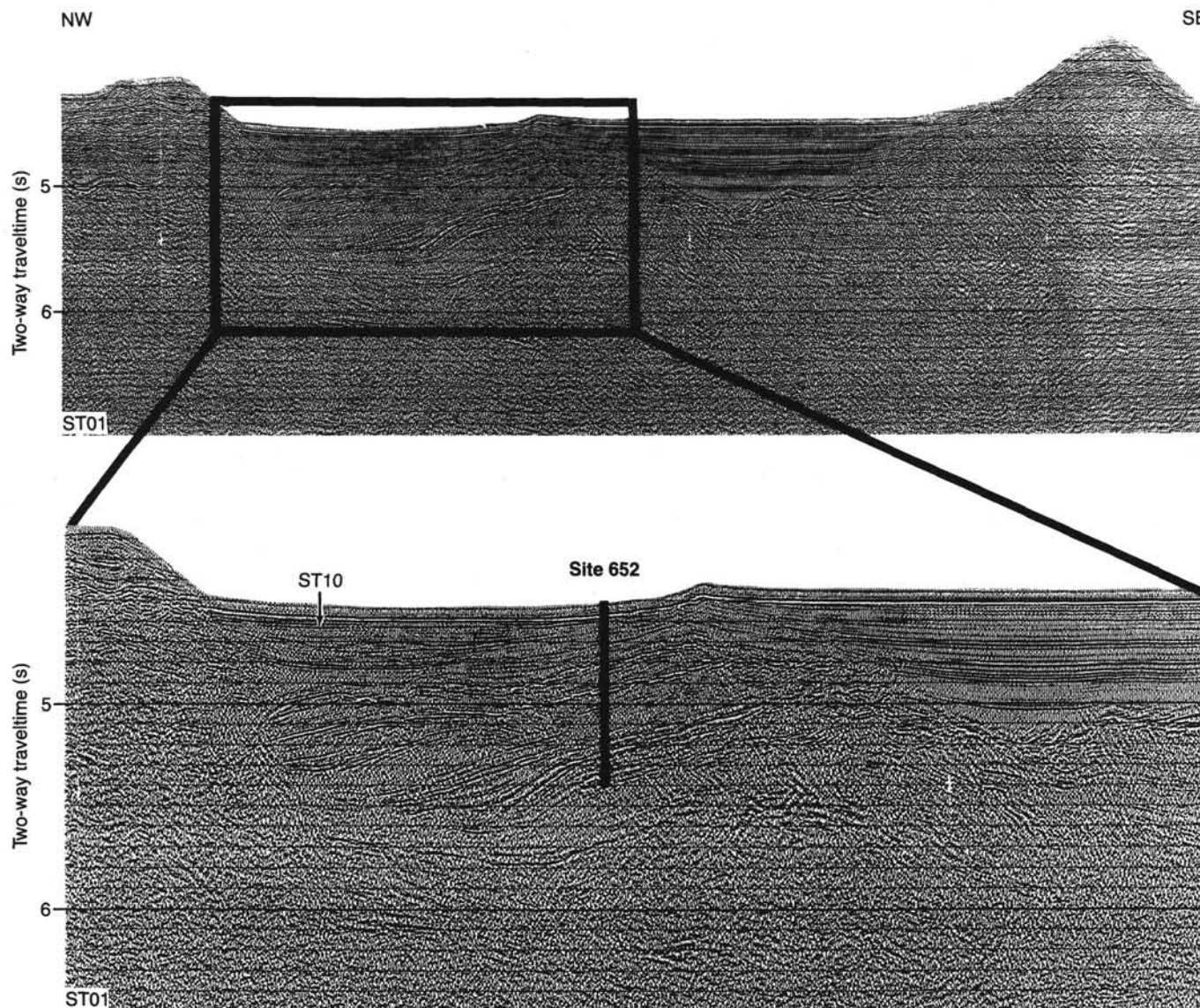


Figure 7. Section of multichannel seismic line ST01 across the lowermost Sardinian margin. Site 652 is located on a small tilted block wedged between the Central Fault and de Marchi Seamount (to the east). Note the geometric arrangement of the different reflectors, suggesting pre-rift, syn-rift, and post-rift sedimentary sequences.

OPERATIONS

Strategy

A major objective of Site 652 was to reach the contact between inferred pre-rift and syn-rift sediment on a fault-bounded tilted block. Since this contact lay at approximately 700 mbsf, rotary coring was the technique chosen. Heat flow measurements were planned at 40-m-intervals. The proposed logging program consisted of standard Schlumberger logs plus GST and/or borehole televiwer, depending on time available and geology encountered.

There was no contingency plan for an offset second hole because the location of the site was tightly constrained by geological and safety considerations.

The approach to the site was planned to duplicate site survey line ST01 from east-southeast to west-northwest. The tilted block trends slightly east of north; thus an approach along course 300° ensured that small across-track deviations from plan would be relatively harmless, although along-track positioning would be

critical. Because the acceptable drilling location was so tightly constrained, a first pass was planned to calibrate the site survey multichannel profile with the *Resolution's* single channel seismic profile, to be followed by the beacon drop on a second east-southeast pass. The time of the beacon drop was to be determined from the single channel seismic profile. Since the site lay on a westward-sloping seafloor, final position of the ship relative to the beacon could be adjusted with respect to water depth, with the constraint that the proposed site had a water depth 72 m deeper than the crest of a small knoll 1.1 km east-southeast of the site.

Approach to Site

On the transit from Site 651 to the turning point for the Site 652 approach, the ship was navigated using the global positioning system (GPS). As the turning point was approached, Loran C was giving positions approximately 1 1/2 mi southwest of the GPS positions (as had been the case for the approach to Site 651). However the transit satellite fix at 2347 on 17 January

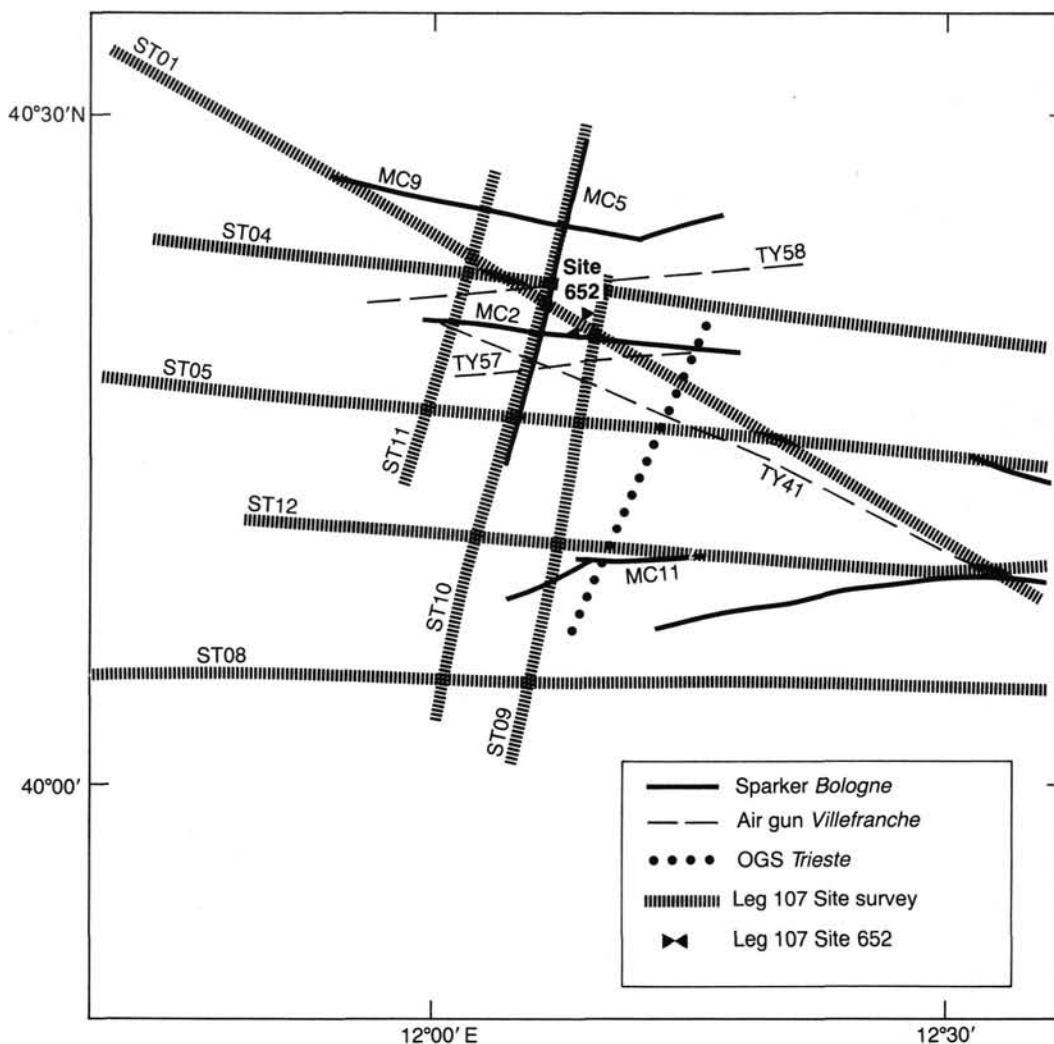


Figure 8. Site 652 location and seismic lines in the vicinity of the site. Most of the seismic data are single channel lines, with the exception of the Leg 107 site survey data collected in 1985.

agreed with the GPS rather than the Loran positions, so the turn to begin the survey was made on the GPS position.

At 0021 on 18 January the ship slowed to 6 kt and changed course to 303°. Two Bolt 80 in.³ water guns and a 500-m Tele-dyne streamer were deployed beginning at 0028. Processing, filtering, and recording techniques for seismic data are described in the "Underway Geophysics" section, this chapter. Bathymetric data were also collected at 12 and 3.5 kHz during the approach.

Soon after the turn the discrepancy between the Loran and GPS fixes increased to up to 5 nmi and it was noted that the Loran C warning lights for cycle skip were lit for both master/slave pairs. There were no more usable Loran data from that time until approximately an hour after the beacon drop. Until the end of the night GPS window (at 0140), the ship was navigated using GPS; transit satellites at 0122 and 0132 plus the crossing of de Marchi Seamount at the appropriate time confirmed the GPS position. The ship then continued on the same heading at the same speed, navigating by dead reckoning. At 0240 the ship crossed the target site. Agreement between the site survey and *Resolution* data was excellent on both seismic and 3.5 kHz profiles. The dead-reckoned *Resolution* position agreed well with the site survey position.

The ship continued west-northwest for 4 more miles to verify the agreement between site survey and *Resolution* data. At 0317 a Williamson turn to heading 116° was initiated. As the turn was completed an unpredicted transit satellite fix arrived (time 0318, elevation 66°) which showed the ship to be north of the desired track. As the ship ran east-southeast, it quickly became obvious that both the bathymetry and the sub-bottom geology differed drastically from those on either the site survey profile or the *Resolution* west-northwest-bound track. The beacon drop was therefore deferred to a third pass over the site. This decision was confirmed by transit satellite fixes at 0420 and 0506 which both showed the ship even farther north than the dead-reckoned position. Motivated by the 0507 satellite fix, the ship changed course to 130° at 0439 to steer back down to the desired track. The east-southeast pass was prolonged until 12°20'E because the satellite alerts predicted that this strategy would give us two satellites with good elevations on the west-northwest beacon-dropping pass.

A Williamson turn back to course 300° was initiated at 0621. A transit satellite fix at 0657 confirmed our position on the desired line. However, when we crossed the northern edge of de Marchi seamount at 0707, the water depth was 50 m deeper than on our first pass, suggesting we were 0.5 mi north of our

first track. Consequently, the ship altered course to 298° at 0710. As the target site was approached, both the bathymetry and the seismic data agreed with the site survey data, and the decision to drop on this pass was reconfirmed. The beacon was dropped at 0820 on 18 January at a dead-reckoned position of 40°21.01'N, 12°08.86'E.

The ship continued with the same heading and speed while waiting for a satellite fix scheduled for 0837 to tie the end of the dead reckoned track. This fix did not come in, so the seismic gear was pulled and the ship reversed course to return to the beacon. With the ship in dynamic positioning mode over the beacon, the water depth was found to be 70 m deeper than at the crest of the small knoll east of the site (as opposed to 72 m on the site survey profile). This difference was judged to be less than the measurement error, and the decision was made to drill at the beacon.

The average position of GPS and transit satellite fixes received while on station gave a final position of 40°21.30'N, 12°08.59'E. The Loran position determined from the X and Z slaves was 40°21.19'N, 12°08.40'E. Loran time delays were as follows: X, 13127; Z, 13127. The Loran signal from the Y slave was unusable.

Coring

A conventional rotary (RCB) coring system bottom hole assembly was run with a long tooth core bit. The precision depth recorder (PDR) depth at the site was 3457 m (corrected) but side echoes suggested that spud depth might be deeper. This proved to be the case when a water core was taken at a depth close to 3457 m. Actual bottom was located at 3470.5 m with a mud-line punch core.

Routine RCB cores in muds and oozes continued from the mud line down to core 24R at 228 mbsf (Table 1). At the Miocene/Pliocene boundary, recovery dropped markedly, from 64% in the calcareous muds and marly nannofossil oozes of lithostratigraphic Units I and II, to 38% in the gypsiferous sandy silts and calcareous clays and muds of lithostratigraphic Unit IV. The change in recovery corresponds to an abrupt downsection decrease in carbonate content from greater than 50% to less than 30%; perhaps the higher carbonate content makes the core sticky enough to avoid falling out of the liner.

Successful heat flow runs were made at 36, 75, 113, 151, and 190 mbsf. While recovering the heat flow probe following Core 107-652A-24R, the sand line parted at the crown sheave. Fortunately, the lower portion of the line tangled itself into a knot faster than the weight could pull it downhole and the heat flow tool was left suspended about 1000 m off bottom. The line and heat flow tool were painstakingly recovered. Approximately 7 hr were lost in this maneuver, but the potentially much more devastating loss of the hole was avoided. The batteries in the heat flow probe were dead on arrival; since the Uyeda probe holds data in volatile memory, thermistor data from this lowering were lost.

Routine RCB coring continued in stiff mud and mudstone. While drilling Core 107-652A-35R, four distinct changes of formation were noted: the first 3 m drilled similarly to the previous several cores; the next 3 m dropped down almost instantly; the next meter was hard and slow to drill and caused considerable torquing of the drill string; and the final 2 m were hard but did not cause torquing. Recovery in this core was only 0.8 m; the material resembled the overlying cores and probably came from the upper 3 m of the cored interval. Core 107-652A-36R was hard and slow to drill (64 min) but did not cause torquing. Recovery in Core 107-652A-36R consisted of 14 rounded pebbles in the core catcher. Considerable geological significance has been read into these 14 pebbles (see "Lithostratigraphy" and "Discussion and Conclusions" sections, this chapter), so it is inter-

Table 1. Coring summary for Site 652.

Core no.	Date (Jan. 1986)	Time	Sub-bottom depths (m)	Length cored (m)	Length recovered (m)	Recovery (%)
1R	18	1930	0.0-3.6	3.6	3.6	99.4
2R	18	2100	3.6-17.0	13.4	5.2	38.6
3R	18	2230	17.0-26.7	9.7	1.8	18.5
4R	19	0015	26.7-36.4	9.7	9.6	98.9
5R	19	0345	36.4-45.8	9.4	0.4	4.6
6R	19	0515	45.8-55.4	9.6	2.0	20.9
7R	19	0700	55.4-64.9	9.5	5.3	55.4
8R	19	0830	64.9-74.5	9.6	2.6	27.1
9R	19	1130	74.5-84.2	9.7	3.3	34.2
10R	19	1315	84.2-93.8	9.6	9.7	101.5
11R	19	1500	93.8-103.0	9.2	8.1	88.0
12R	19	1630	103.0-112.7	9.7	8.4	86.8
13R	19	2015	112.7-122.3	9.6	5.3	54.7
14R	19	2200	122.3-131.9	9.6	5.8	60.6
15R	19	2315	131.9-141.5	9.6	8.7	90.3
16R	20	0130	141.5-151.2	9.7	7.6	78.4
17R	20	0500	151.2-160.8	9.6	8.9	92.3
18R	20	0630	160.8-170.5	9.7	9.1	93.5
19R	20	0815	170.5-180.2	9.7	9.0	92.6
20R	20	0945	180.2-189.8	9.6	9.1	94.7
21R	20	1315	189.8-199.7	9.9	4.5	45.1
22R	20	1445	199.7-209.1	9.4	2.4	25.4
23R	20	1630	209.1-218.7	9.6	2.6	26.6
24R	20	1815	218.7-228.4	9.7	6.0	62.0
25R	21	0515	228.4-238.1	9.7	3.4	34.5
26R	21	0715	238.1-247.7	9.6	3.1	32.3
27R	21	0900	247.7-257.4	9.7	3.6	37.4
28R	21	1045	257.4-267.1	9.7	3.0	30.4
29R	21	1245	267.1-276.7	9.6	3.0	31.4
30R	21	1500	276.7-286.3	9.6	4.0	41.3
31R	21	1715	286.3-295.9	9.6	4.3	44.6
32R	21	1930	295.9-305.6	9.7	4.6	47.0
33R	21	2130	305.6-315.3	9.7	4.6	47.4
34R	21	2330	315.3-325.0	9.7	4.0	40.9
35R	22	0130	325.0-334.7	9.7	0.8	8.3
36R	22	0400	334.7-344.3	9.6	0.1	1.0
37R	22	0600	344.3-354.0	9.7	7.7	79.3
38R	22	0815	354.0-363.7	9.7	8.3	85.6
39R	22	1030	363.7-373.4	9.7	9.4	96.9
40R	22	1245	373.4-383.0	9.6	9.5	99.1
41R	22	1515	383.0-392.7	9.7	8.7	89.8
42R	22	1730	392.7-402.4	9.7	8.3	85.4
43R	22	2000	402.4-412.1	9.7	9.7	100.4
44R	22	2200	412.1-421.8	9.7	4.0	41.4
45R	23	0000	421.8-431.5	9.7	5.7	59.0
46R	23	0230	431.5-441.1	9.6	4.4	45.8
47R	23	0430	441.1-450.7	9.6	6.5	67.7
48R	23	0630	450.7-460.3	9.6	5.6	58.3
49R	23	0830	460.3-470.0	9.7	2.7	27.6
50R	23	1045	470.0-479.6	9.6	3.9	41.0
51R	23	1330	479.6-489.2	9.6	8.3	86.0
52R	23	1600	489.2-498.8	9.6	7.1	73.8
53R	23	1915	498.8-508.5	9.7	8.6	89.1
54R	23	2300	508.5-518.1	9.6	7.9	82.5
55R	24	0300	518.1-527.8	9.7	8.0	82.1
56R	24	0700	527.8-537.4	9.6	9.2	95.8
57R	24	1030	537.4-546.6	9.2	5.7	61.7
58R	24	1330	546.6-556.3	9.7	8.1	83.9
59R	24	1715	556.3-566.0	9.7	5.7	58.8
60R	24	2115	566.0-575.6	9.6	7.9	81.9
61R	25	0000	575.6-585.2	9.6	7.9	82.6
62R	25	0315	585.2-594.9	9.7	7.7	79.0
63R	25	0645	594.9-604.5	9.6	4.5	46.6
64R	25	1000	604.5-614.2	9.7	4.2	43.6
65R	25	1245	614.2-624.5	10.3	9.3	89.8
66R	25	1530	624.5-634.2	9.7	5.2	54.0
67R	25	1900	634.2-643.8	9.6	8.0	83.1
68R	25	2245	643.8-653.4	9.6	9.4	97.7
69R	26	0200	653.4-663.1	9.7	6.9	71.0
70R	26	0500	663.1-672.8	9.7	6.4	66.2
71R	26	0830	672.8-682.5	9.7	3.5	35.7
72R	26	1115	682.5-692.2	9.7	2.9	30.3
73R	26	1430	692.2-701.9	9.7	4.3	44.5
74R	26	2000	701.9-710.5	8.6	8.1	94.5
75R	27	0130	710.5-721.1	10.6	9.0	84.9

esting to note that drilling characteristics of Cores 107-652A-35R and -36R suggest that the pebble horizon and associated unusual lithologies may be as thick as 15 m.

Below the pebble horizon, in the gypsum-bearing clay and silt sequence of lithostratigraphic Unit Va, recovery improved to 71%. Core disturbance was minimal, especially for rotary coring, with fine laminae, microfaults, and slump structures beautifully preserved. As Core 107-652A-37R came on deck, the sea-going tug *Jumbo Primo* arrived from Naples with mail and a variety of other supplies and materials which had not reached the vessel in Malaga. Later that same day, a film crew from Dutch National Television arrived by helicopter; they stayed aboard the vessel for 3 days filming routine shipboard activities.

Starting with Core 107-652A-52R at 500 mbsf, the rate of penetration dropped from 16 m/hr to 9 m/hr to less than 5 m/hr in the space of four cores. The cores themselves did not give evidence of a change in lithology to account for this apparent resistance to penetration; bit problems were suspected although no abnormal signs of torque, cone wobble, or other normal signs of bit wear were detected. The rate of penetration slowed still further at the contact between the siltstones and mudstones of lithostratigraphic Unit Va and the indurated siltstones and sandstones of Unit Vb (683 mbsf). Cores 107-652A-74R and -75R required more than 3 hr apiece to cut. The core diameter during the previous 24 hr of coring had decreased from 2-3/8" to 2-1/8" suggesting that the bit cones were beginning their terminal wobble. According to any reasonable interpretation of the seismic stratigraphy, the pre-rift/syn-rift contact at 730 ms sub-bottom had been penetrated by this time. Although deeper penetration would have been laboriously achievable, the next anticipated lithologic change (an internal reflector within the pre-rift sequence) would have been days away at the rate of penetration experienced on the previous two cores. This goal was not considered worth the time, and the hole was terminated at 721 mbsf. Despite the poor rate of penetration, the overall recovery for the hole was very impressive for RCB coring.

Logging

The hole was cleaned with a 20 bbl high viscosity mud sweep and left full of sea water. The bit was released successfully, and the pipe was pulled to the logging depth of 100 mbsf (with pipe down). The first suite of logs comprised the dual induction log (DIL), long spacing sonic (LSS), gamma ray (GR), and caliper (CALI). This string passed easily through the Pliocene-Pleistocene section, but the pre-Pliocene section of the hole was very irregular, with diameter variations from less than 5 to greater than 13 in. over a few meters. The tools stopped completely at a bridge at 367 mbsf, and the hole was logged up from there.

A second suite of logging tools (gamma spectroscopy tool, compensated neutron tool, and natural gamma tool: GST-CNT-NGT) was made up and run in the hole. This suite was all 3-5/8-in. diameter tools with no caliper or centralizer springs. In spite of this, the second run was stopped at an impassable bridge at 268 mbsf and was forced to log up from there.

The pipe was then run to bottom without rotation or circulation. A weak bridge was knocked out at 365 mbsf, and the remainder of the hole was found to be open. Seawater was circulated for 30 min, and the pipe was pulled to 259 mbsf for a third logging run to try to gain access to the lower portion of the hole. The third logging run again consisted of the GST-CNT-NGT combination and again stopped at a bridge, this time at 369 mbsf. The interval from there to the bottom of the pipe was logged and the tool was retrieved, ending the logging exercises for the site.

Although it was frustrating not to be able to log the bottom of the hole, the logged interval did include both the Miocene/Pliocene boundary and the intra-Messinian pebble horizon. The

impenetrable bridge encountered at about 370 mbsf on logging runs 1 and 3 as well as on the wiper trip is near the top of lithostratigraphic Unit V, in which calcium sulfate in discrete layers was first encountered. This correlation suggests that the narrowing of the hole may be associated with the volume increase associated with the transformation of anhydrite to gypsum in the presence of water.

The hole was filled with weighted mud and abandoned. The pipe end arrived on deck at 2120 on January 28 as the ship got underway for Site 653 (TYR 2).

LITHOSTRATIGRAPHY

Lithologic Description

Introduction

Sediments recovered at Site 652 are divided into two major categories (Fig. 9): Pliocene/Pleistocene hemipelagic biogenic marine sediments from 0 to 188.2 mbsf (Cores 107-652A-1R to 107-652A-20R-6, 97 cm) and pre-Pliocene terrigenous and chemical sediments from 188.6 to 721.1 mbsf (Cores 107-652A-20R-6, 97 cm, to 107-652A-75R); a 40-cm transition zone lies between the two. The Pliocene/Pleistocene sediments are further divided into two units based on their calcium carbonate content, and the pre-Pliocene sediments are also divided into two units based on other lithologic and sedimentologic criteria. Together with the transitional unit, five lithostratigraphic units are described.

Pliocene/Pleistocene

Unit I: 0-55.4 mbsf (Cores 107-652A-1R through 107-652A-6R). This unit comprises gray calcareous muds and muds. Average carbonate concentration is 22% (27 samples). Volcanic glass is commonly mixed within the sediment as well as pumice. Tephra layers do not occur. Thin sandy levels mainly comprised of foraminifers are frequent. This unit is entirely Pleistocene.

Four distinct sapropel layers were identified: (1) 18.41-18.54 mbsf (Core 107-652A-3R-1, 141-150 cm to 107-652A-3R-2, 0-4 cm); (2) 24.14-24.30 mbsf (Core 107-652A-4R-5, 114-130 cm), (3) 24.48-24.83 mbsf (Core 107-652A-4R-5, 148-150 to 107-652A-4R-6, 0-33 cm), (4) 46.17-46.32 mbsf (Core 107-652A-6R-1, 37-52 cm). See discussion on sapropels below.

Unit II: 55.4-188.2 mbsf (Cores 107-652A-7R to 107-652A-20R-6, 50 cm). Marly nannofossil oozes, with an average carbonate content of 48% (54 samples), dominate in Unit II. The age is early Pleistocene-Pliocene. Between 64.9 and 112.7 mbsf (Cores 107-652A-8R to -12R) the sediments are foraminiferal, marly nannofossil oozes; they contain abundant volcanic glass (10%-35%) as minor lithologies. Between 55.4 and 176.5 mbsf (Cores 107-652A-7R to 107-652A-19R-4) the color of the sediment is more or less an olive gray to gray with frequent overprinting by yellowish brown tones. Dark gray layers throughout this interval are graded volcanic ashes, now highly altered. From 176.5 to 180.2 mbsf (Cores 107-652A-19R-5 and -6R), the marly nannofossil oozes are yellowish red and brownish yellow progressing downsection to more intense reds and strong browns directly above the Miocene/Pliocene boundary at 188.2 mbsf (Core 107-652A-20R-6, 50-51 cm). The boundary was determined by the last appearance of *in-situ* planktonic foraminifers.

Four sandy mudstone intervals, the thicknesses of which cannot be measured because of fracturing during drilling, occur between 103.0 and 112.7 mbsf (Core 107-652A-12R-1, 38-50 cm, 107-652A-12R-3, 125-128 cm, -12R-4, 90-102 cm and -12R-4, 111-119 cm), which corresponds to an interval with a decreased sedimentation rate. Between 116 and 147 mbsf, the carbonate content is generally very high, sometimes reaching 60%. The boundary between lower and upper Pliocene is located within this interval at 131.9 mbsf, corresponding to the maximum per-

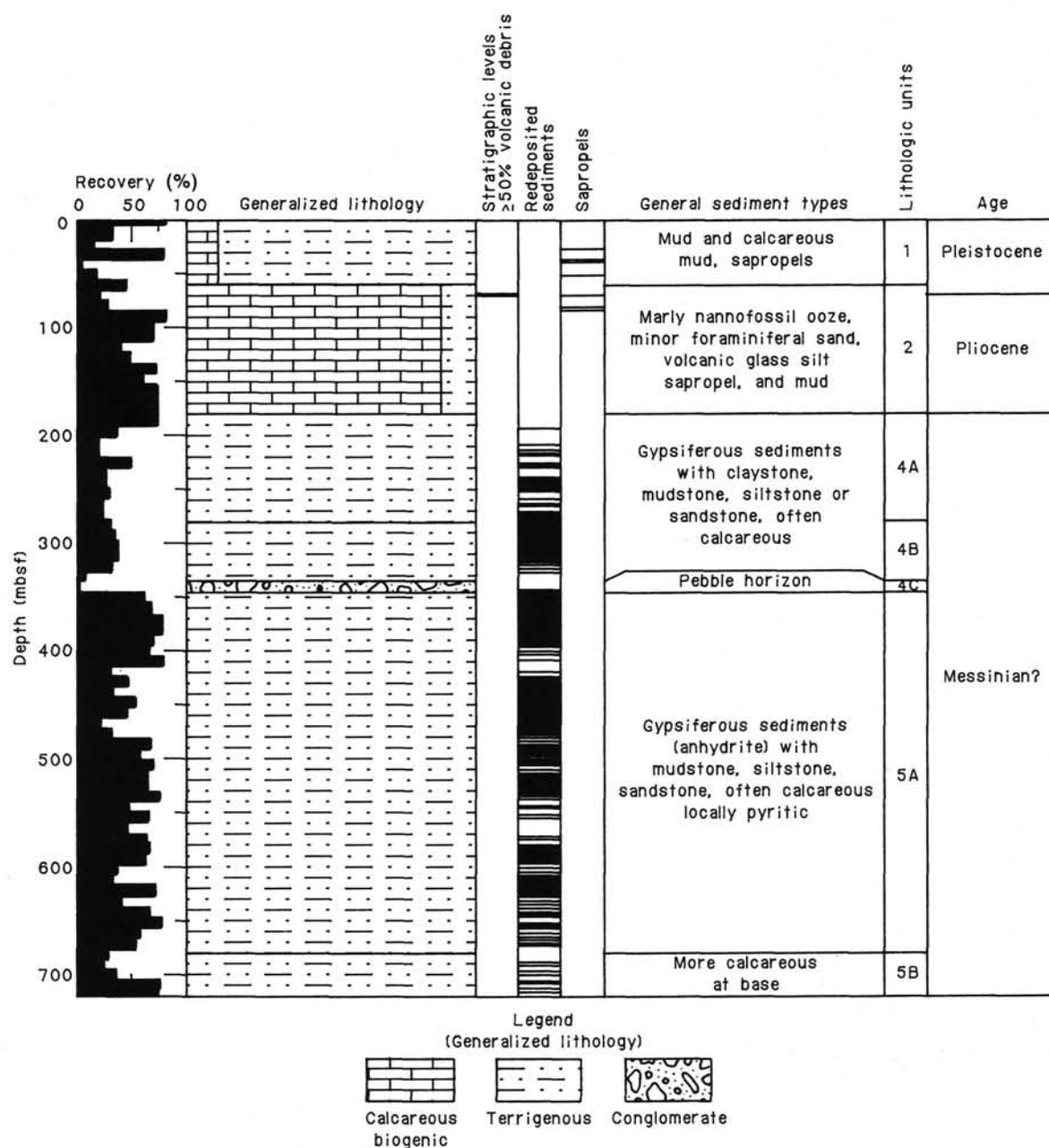


Figure 9. Synthetic lithologic column and drilling recovery at Site 652.

centage of carbonate. However, between 136.8 and 144.6 mbsf (Core 107-652A-15R-4 to 16R-3) there is a brief significant decrease in carbonate content, which is reflected by a decrease in sedimentation rate (see "Biostratigraphy" section, this chapter) but has no visual lithologic expression. Between 141.5 and 151.2 mbsf (Core 107-652A-16R), a temporary downhole lithologic change to nannofossil ooze occurs as well documented by an increased carbonate content within this interval.

Sapropels occur at: (1) 60.10–60.25 mbsf (Core 107-652A-7R-4, 20–35 cm), (2) 66.04–66.06 mbsf (Core 107-652A-8R-1, 114–116 cm), (3) 76.36–76.41 mbsf (Core 107-652A-9R-2, 36–41 cm) and (4) 76.93–76.99 mbsf (Core 107-652A-9R-2, 93–99 cm). See discussion on sapropels below.

Only the uppermost part of this unit is Pleistocene, the boundary between Pleistocene and Pliocene being situated at about 85

mbsf. There is no obvious lithologic expression of this boundary.

Two occurrences of the characteristic gray clay of the underlying sediments of the uppermost part of Unit IV appear sandwiched between the distinctly colored marly nannofossil oozes of the lowermost part of Unit II at 187.8 mbsf (Core 107-652A-20R-6, 0–4 cm) and 187.1 mbsf (Core 107-652A-20R-5, 83–88 cm).

Transitional Zone

Unit III: 188.2–188.6 mbsf (Core 107-652A-20R-6, 52–92 cm). This 40-cm transitional interval ranges between the occurrence of marine planktonic foraminifers at the top and the Messinian sediments at the base. It is characterized by a succession of from 0.5- to 4.0-cm-thick layers of strongly colored clays and muds (Fig. 10). The basal contact is marked by a distinct color

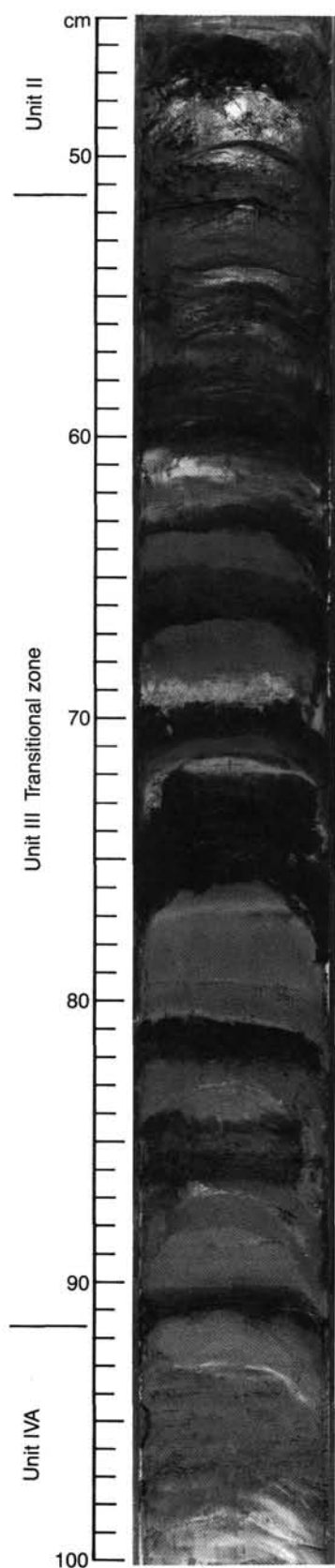


Figure 10. The alternation of distinctly colored layers within the 40-cm-thick transitional zone (Unit III) and the contacts with the overlying Pliocene (Unit II) and underlying Messinian (Unit IV) sediments (Core 107-652A-20R-6, 45–100 cm).

change with the underlying homogeneous, gray, gypsiferous dolomitic clays, the latter with a carbonate content of 20.1%. Moving down through the transitional interval the dominant colors of the alternating layers change from red and strong brown at the top of the unit to reddish gray becoming light gray and grayish green to gray at the base of the unit. This dramatic color change represents a transition from marine Pliocene to a pre-Pliocene sedimentation environment. The deepest occurrence of rare *in-situ* nannofossils was observed within the transitional zone at 188.4 mbsf (Core 107-652A-20R-6, 70 cm). The calcareous component of the sediments decreases rapidly from about 50% just above the top of Unit III (e.g. 51.4% at 187.6 mbsf, Core 107-625A-20R-5, 135–138 cm), to the lower values of Unit IV. The red color of the upper part of the transitional interval and the earliest Pliocene sediments is probably produced by the presence of iron oxides. The red color becomes progressively less intense upward, disappearing at 176.5 mbsf (Core 107-652A-19R-5) near the top of the MP11 foraminiferal zone, which was recognized at 180.2 mbsf (Core 107-652A-19R, CC).

Pre-Pliocene

The pre-Pliocene is represented by a thick nonfossiliferous series. Pre-Pliocene sediments have been subdivided into two units to take into consideration the presence of an important conglomeratic horizon recovered between 334.70 and 344.80 mbsf.

Unit IV: 188.6–344.3 mbsf (Cores 107-652A-20R-6, 92 cm to 107-652A-36R, CC). Unit IV is divided into three subunits as follows:

Subunit IVa: 188.6–286.3 mbsf (Cores 107-652A-20R-6, 92 cm to 107-652A-30R, CC).

This subunit is characterized by a succession of thinly bedded (often < 25 cm), normally graded alternations of gypsum and carbonate-bearing sandy silts or sands and calcareous clays or muds (Fig. 11), which are interpreted as turbidites. All are gray colored. Reworked nannofossils are abundant; gypsum and carbonates are detrital. Zeolites are frequent. Micrometeorites occur in Core 107-652A-28R, CC (see “Biostratigraphy” section, this chapter, and Fig. 22).

Subunit IVb: 286.30–334.70 mbsf (Cores 107-652A-31R to -35R). The lithologic components are the same as in the preceding Subunit IVa, but the sedimentary structures differ in that there are reversely graded sequences, frequent water-escape structures, syndimentary microfaults, and microbreccias. Also, the first occurrence of crystals of authigenic calcium sulfates and the existence of cubic dissolution molds (former halite?) in the coarser intervals were noted in Cores 107-652A-33R to -35R. Examples of these chemical phenomena are illustrated in Fig. 12 (Core 107-652A-35R, 36–50 cm); mudstones with displace lenticular gypsum crystals directly overlie a sandier interval containing tiny cubic molds. Some sandstone layers are well indurated (Core 107-652A-34R-1).

Subunit IVc: 334.70–344.80 mbsf (Core 107-652A-36R). The recovery was very poor, consisting of only 14 pebbles in the core catcher. However, downhole logging data suggest that this conglomeratic horizon could be as thick as 14 m (interval 324–338 mbsf) (see “Downhole Measurements” section, this chapter), and the drilling characteristics for Cores 107-652A-35R and -36 suggest a zone of unusual lithology as thick as 15 m (see “Operations” section, this chapter). The pebbles are rounded and smooth, and some appear flattened and elongated. Maximum dimensions are 8 cm, minimum slightly more than 1 cm. Thin-section examination revealed the following lithotypes.

1. *Packstone* (Pebble no. 5). Rudistidae, green algae, benthic foraminifers (e.g., arenaceous and Miliolidae), bioclasts and biosomata of mollusks in a minor matrix con-

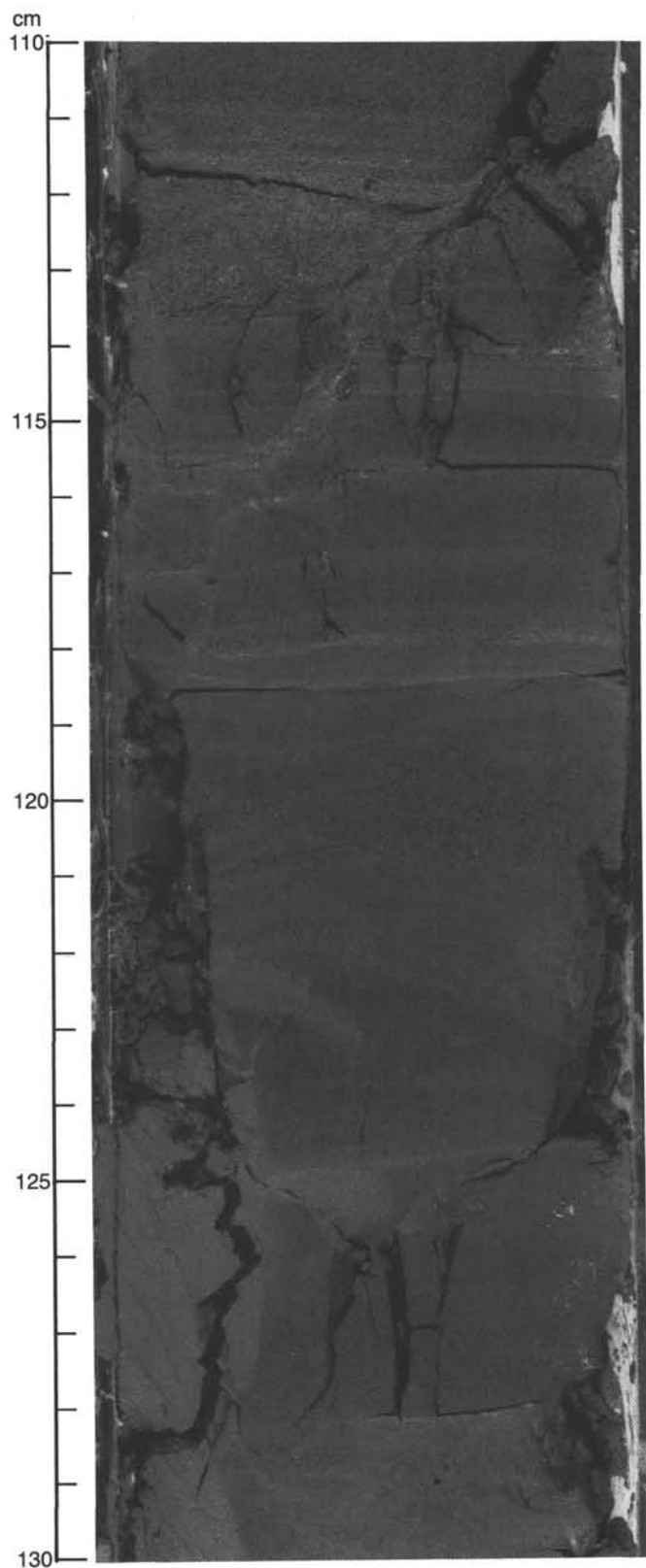


Figure 11. Several intervals of normally graded alternations of gypsum- and carbonate-bearing sandy silts and muds are shown. Notable sedimentary features in the core photograph are the sharp basal contacts between the units, the fining upward of grain size within the units, parallel laminations, and a slump structure between 121 and 123 cm. These sediments are interpreted as a turbidite sequence.

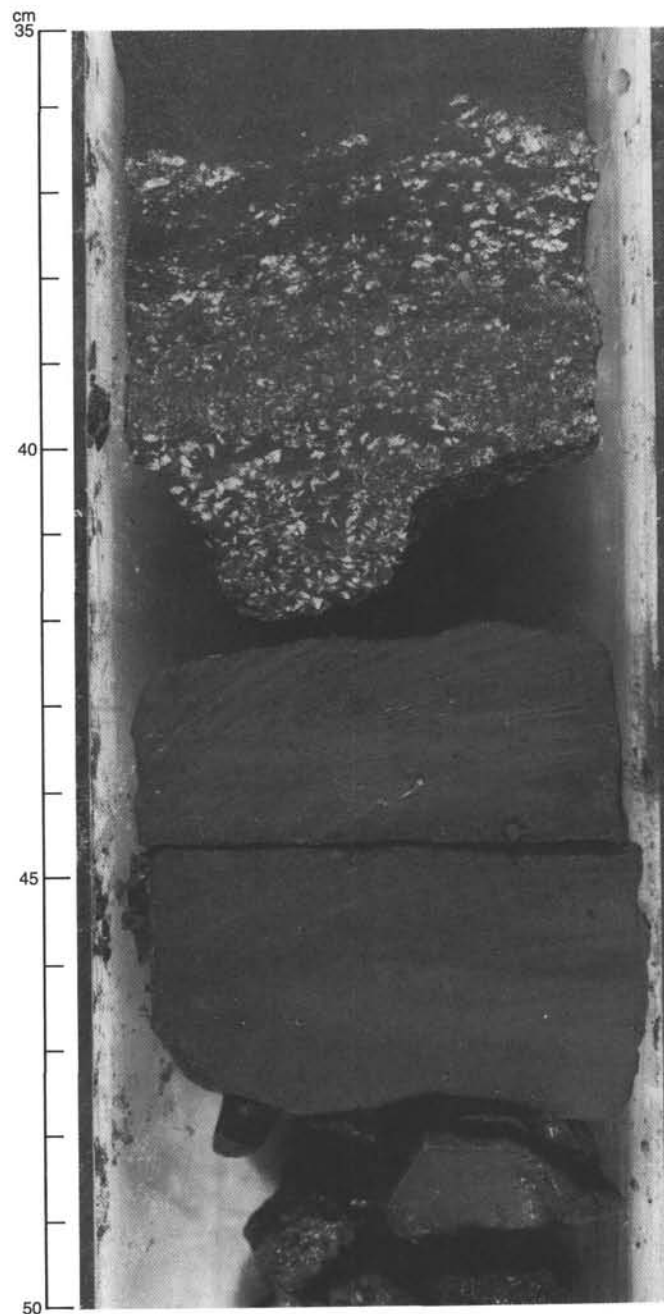


Figure 12. Displacive lenticular crystals of gypsum in a gray mudstone (Core 107-652A-35R-1, 36-42 cm) overlies a sandier mudstone containing numerous tiny cubic molds (formerly halite?) (Core 107-652A-35R-1, 42-47 cm).

taining angular quartz grains, rare ostracodes, and planktonic foraminifers. Environment: penocontemporaneous debris of rudistid carbonate platform reworked into deeper water facies. Age: Late Cretaceous.

2. *Mudstone* (Pebble nos. 3,4,6,9,12,14). Biomicrites containing abundant calcitized radiolarians. Some pebbles also contain planktonic foraminifers, including *Hedbergellae*, while one contains *Saccocoma*-like remains. Environment: open marine, pelagic. Age: spanning possibly Late Jurassic? to middle Cretaceous.

3. *Grainstone* (Pebble no. 1). Large benthic foraminifers (*Miogyopsinids*?, *Amphisteginidae*), bryozoa, red al-

gae, echinid plates, mollusk fragments, micrite fragments, rare planktonic foraminifers in scarce spar cement. Environment: high-energy, shallow (less than 100–150 m) marine bank. Age: possibly Oligocene-early Miocene.

4. *Quartzarenite* (Pebble nos. 2, 13). Quartz, often well rounded, dominant, with very rare feldspar and opaque rhombohedral grains in a spar cement.

5. *Polymictic sandstone* (Pebble nos. 7, 10). The grains, mostly angular, include: metamorphic and igneous quartz, calcite, dolomite, low-grade metamorphic lithic fragments (including carbonaceous phyllites), mafic crystals, feldspar-bearing lithic fragments (igneous?), glauconite, very rare bryozoa, mollusk fragments, and benthic foraminifers. Environment: post-orogenic nonmature deposits on continental slope or shelf. Age: a very tentative early-middle Miocene age may be assigned by comparison with surrounding regions (Amodio-Morelli et al., 1976; Grandjacquet and Mascle, 1978).

6. *Calcareous phyllites* (Pebble no. 11). Very low-grade calcareous metapelites including some ghosts and remains of biogenic origin (one benthic foraminifer and some unidentifiable grains).

Interpretation: Pebble sizes, structures, and textures suggest a nearby source which underwent subaerial erosion during the Messinian. The petrographic nature of the clasts, however, excludes the nearest structural high, de Marchi Seamount, as the only possible source, because different lithotypes crop out there (Colantoni et al., 1981; Gennesseaux et al., 1986). Other Messinian structural highs, presently covered by Pliocene-Pleistocene sediments, might represent the appropriate source area. The suite of rocks indicate a sedimentary cover related to a continental basement which is referable either to the southern Apenninic chain and/or to the Sicily Maghreb chain. Sardinian, and possibly also Calabrian-Kabilian type basements, can be ruled out as the source area since high-grade metamorphic rocks and true geologic basement were not sampled in the conglomeratic horizon, and the lithologies of the pebbles do not match the sedimentary cover cropping out in these domains.

Unit V: 344.8–721.1 mbsf (Cores 37R to 75R). Unit V is divided into two subunits as follows:

Subunit Va: 344.80–683.5 mbsf (Cores 37R to 72R-2). This unit is characterized by a monotonous succession of numerous centimeter-thick olive gray to dark gray sequences of well-graded and cross-bedded gypsum- and carbonate-bearing sand or sandy silt and well-layered clays or muds. In some intervals crystalline anhydrite as thick as 5 cm has a classic “chicken wire” texture (Fig. 13) between the sequences. Although the anhydrite intervals may represent the deposition of a chemical precipitate in a subaqueous environment, later stage displacive growth of anhydrite nodules in the sediment is documented by the disrupted laminae overlying the nodules (Fig. 13). The frequent coalescing of smaller discrete nodules into continuous layers was noted. Also noted were apparent gypsum layers with a satin-spar texture which have been overgrown by secondary anhydrite nodules. The temperature estimated from the geothermal gradient for the depth (~400 mbsf) where the anhydrite occurs is approximately 70°C (see “Downhole Measurements” section, this chapter) and the interstitial waters at these depths have salinities more than double that of seawater (see “Geochemistry” section, this chapter). Under these temperature and salinity conditions anhydrite, not gypsum, would be the stable phase of calcium sulfate (Hardie, 1967), which is in agreement with the above observations.

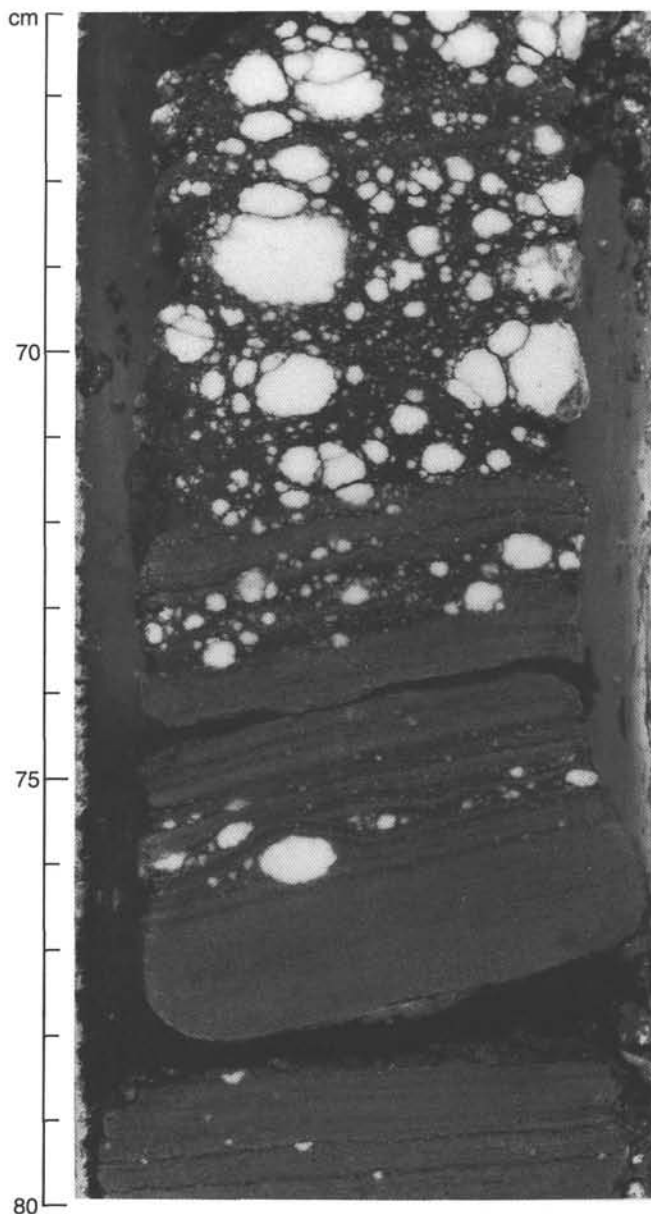


Figure 13. Discrete nodules of white anhydrite have grown displacively in a gray sandy mudstone, in places disrupting the fine laminations of the host sediment (Core 107-652A-44R-3, 66–80 cm).

From the frequency and thickness of the sulfate layers, it is possible to distinguish seven second-order cycles with increasing amount of sulfates toward the top of each cycle. These are in Core 107-652A-37R (344.30–354.0 mbsf), Cores 107-652A-38R to -43R (354.0–412.10 mbsf), Core 107-652A-44R (412.10–421.80 mbsf), Core 107-652A-47R (441.10–450.70 mbsf), Core 107-652A-54R (508.50–518.10 mbsf), Core 107-652A-60R to -62R (566.0–594.9 mbsf) and Core 107-652A-70R (663.10–672.80 mbsf).

Very thin, millimetric, red and yellow horizons appear in Cores 107-652A-50R to -53R (470.0–497.60 mbsf), -56R (527.80–537.40 mbsf), 107-652A-58R and -59R (546.60–566.0 mbsf); they are tentatively attributed to eolian material. Scattered plant debris are present in Cores 107-652A-49R, -50R and -51R (between 460.30 and 489.20 mbsf). Numerous sam-

ples from the pre-Pliocene sequence showed a significant amount of organic carbon (i.e., $\%C_{org} > 0.1\%$) (see "Geochemistry" section, this chapter). Core 107-652A-63R (base) and -64R (between 594.90 and 614.20 mbsf) show finely-laminated, brownish black organic-carbon-rich clays as much as $11.4\%C_{org}$, which have the appearance of "black shales." Within this interval, there are two (2.5 cm thick) horizons containing remnants of algae (Fig. 14). The whole formation shows frequent slumps and microfaults (see "Sedimentary Instability" section below).

The rhythmic repetition of numerous centimeter-thick sequences in Subunit Va is tentatively interpreted as reflecting tempestite deposition and bottom current reworking of sediments. The environment was apparently characterized by variable salinity and periods of high productivity, as suggested by the algal blooms.

Subunit Vb: 683.50–721.10 mbsf (Cores 107-652A-72R-2 to -75R). The main characteristic of Subunit Vb is the extreme induration of the sediments and the different composition of the coarse fraction. This subunit comprises alternations of dark grey calcareous siltstones, calcareous sandy siltstones, and calcareous sandstones. Convolute laminations, slumps, and reverse and normal grading are common features. The coarser fraction shows various reworked elements: pelagic micrite, platform carbonates, metamorphic rocks and minerals, quartz with undulating extinction, polycrystalline quartz, feldspar, volcanic rocks, detritic dolomite, calcite, and calcium sulfates, as well as rare planktonic foraminifers, possibly of pre-Miocene age.

Sedimentation Rate

The sediment depth versus age curve for Site 652 (Fig. 15) was constructed using paleomagnetic and biostratigraphic data. This curve cannot be considered as an accurate graph of sedimentation rate, since no correction has been applied for sediment compaction. Within the Pliocene-Pleistocene section, porosity decreases linearly downsection from about 80% to about 60%, suggesting that the slope of the age vs. depth curve underestimates the sedimentation rate at the base of the Pliocene by a factor of two relative to the rate at the seafloor. In spite of this, geological significance can still be extracted from this curve; the timing and direction of breaks in slope are inferred to indicate marked changes in sedimentation rate.

Within the Pliocene-Pleistocene sequence two different general trends in the sedimentation rate can be recognized. In the lower Pliocene, about the top of the Kaena (2.92 m.y.), the sedimentation rate averages 10 mm/1000 yr. Above the top of Kaena until the base of Olduvai a slight increase is recognized with an average sedimentation rate of 14 mm/1000 yr. Above the base of Olduvai the average sedimentation rate is 54 mm/1000 yr partly explained by the amount of coarse-grained volcanic glass and pumice.

Sapropels

In total, eight sapropel intervals were recognized in Units I and II based on their distinctive very dark gray color and organic-carbon content (Table 2). Each of the recognized sapropels is designated by ST (for Sapropel Tyrrhenian) plus a chronologic number according to their appearance downcore at Site 652A. The age of each is also roughly estimated based on the paleomagnetic and biostratigraphic criteria; the youngest, ST-1, is late Pleistocene, while the oldest, ST-8, early Pleistocene. As core recovery was not always continuous, sapropels younger than late Pleistocene and possibly in other intervals could well have been missed. The preliminary organic carbon content for all of the sapropels, except ST-5, are nearly equal to or greater than 2.0%. Using the definition of Kidd et al. (1978), the studied in-

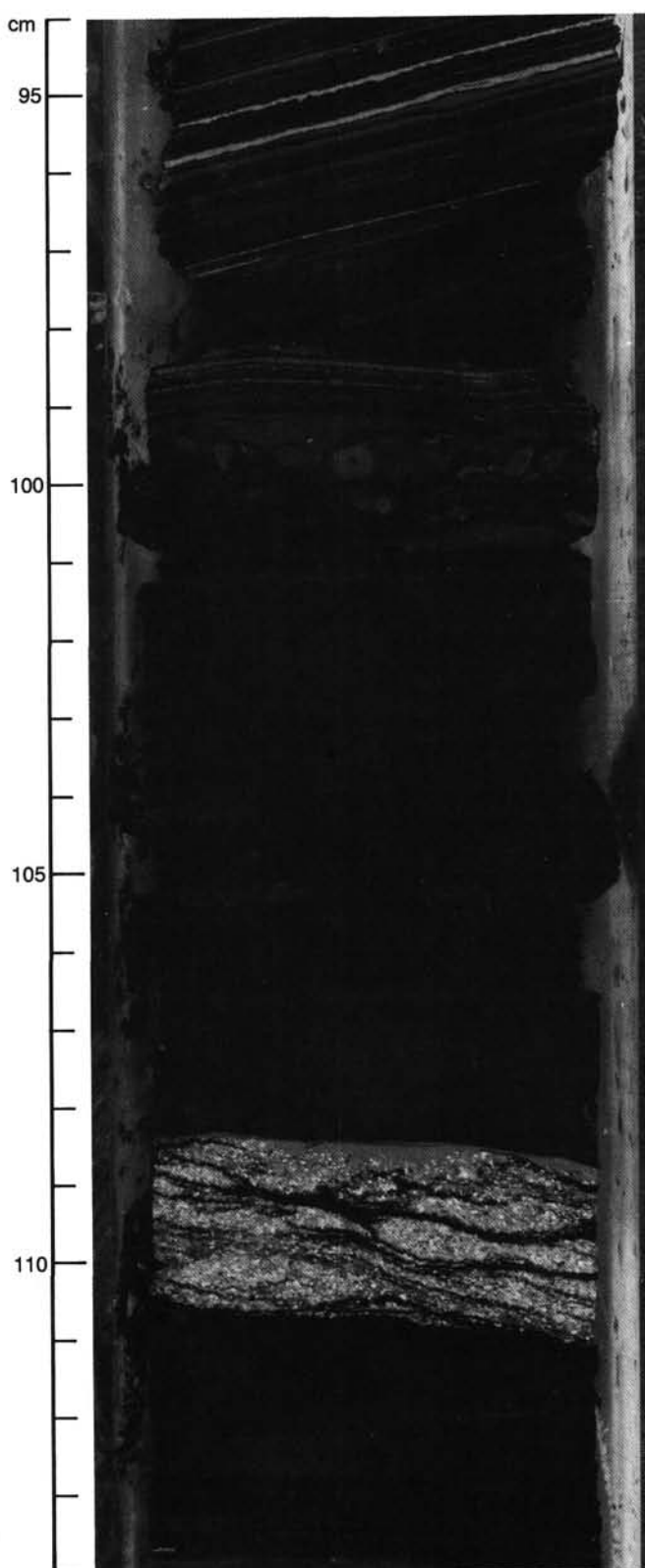


Figure 14. Very finely laminated, brownish black, organic-carbon-rich calcareous mudstones are interbedded with an iridescent, bluish gray sediment composed of algal matter (108.5–110.5 cm). The interval between 101 and 106 cm contains a paper-thin black shale with an organic carbon content of 11.4%. See "Geochemistry" section, this chapter, for further discussion. Core 107-652A-64R-1, 94–114 cm.

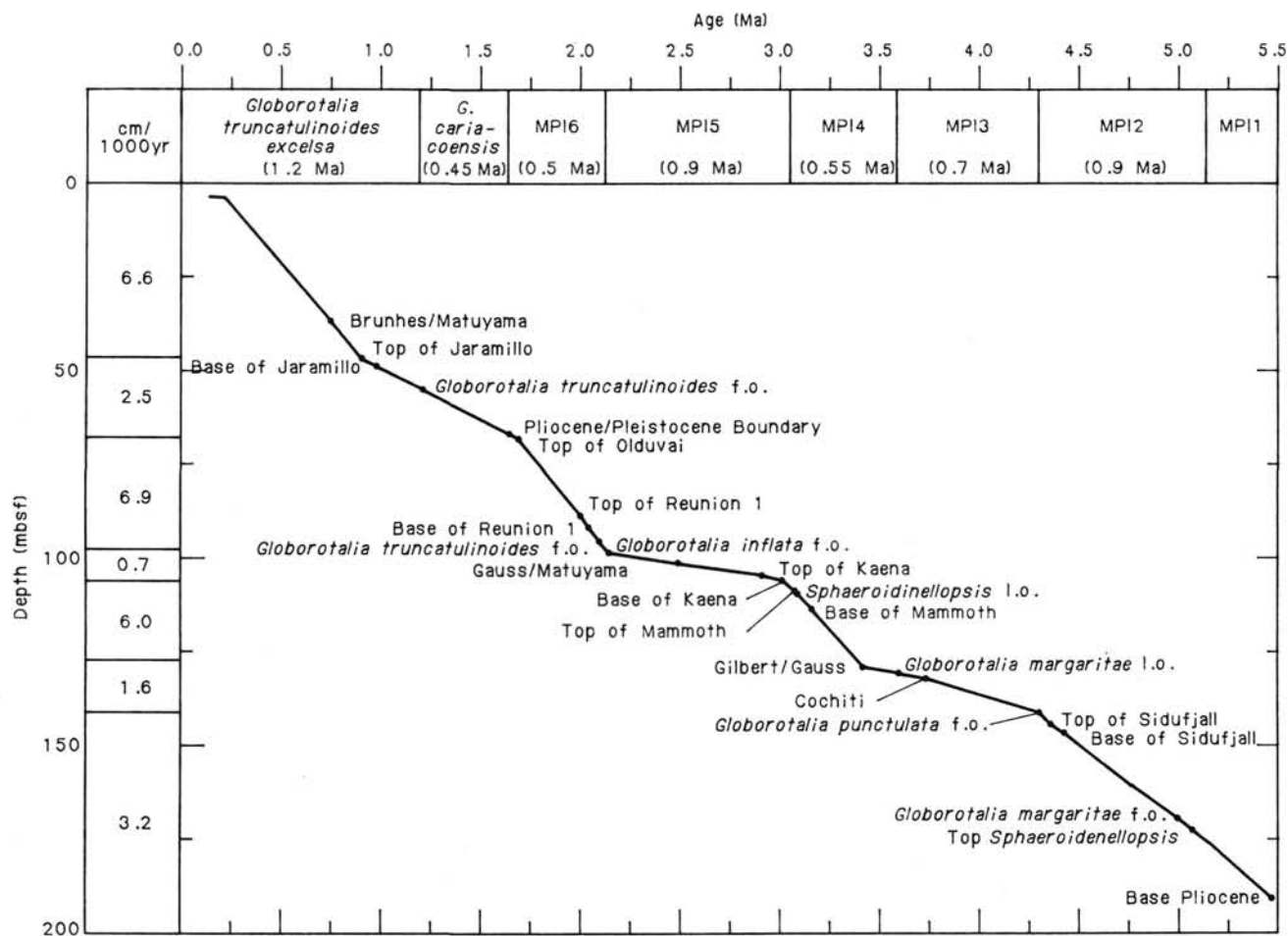


Figure 15. Sediment depth vs. age curve for Site 652 as determined from paleomagnetic and biostratigraphic studies.

Table 2. Sapropels and sapropelic layers for Hole 652A.

Number ^a	Depth (mbsf)	Core interval (cm) ^b	C _{org} %	Age (m.y.b.p.)
ST-1	18.41-18.54	3R-1, 141-150 cm to 3R-2, 0-4 cm	1.91	~0.3
ST-2	24.14-24.30	4R-5, 114-130 cm	3.36	~0.4
ST-3	24.48-24.83	4R-5, 148-150 cm to 4R-6, 0-33 cm	2.31	~0.4
ST-4	46.17-46.32	6R-1, 37-52 cm	3.50-4.18	~0.8
ST-5	60.10-60.25	7R-4, 20-35 cm	0.96	~1.1
ST-6	66.04-66.06	8R-1, 114-116 cm	3.30	~1.2
ST-7	76.36-76.41	9R-2, 36-41 cm	2.77	~1.4
ST-8	76.93-76.96	9R-2, 93-99 cm	3.11	~1.4

^a ST = Sapropel Tyrrhenian.

^b Measured interval of darkest color.

tervals are, indeed, sapropels, exclusive of ST-1 and ST-5 which would be classified as sapropelic layers (0.5% to 2.0% organic carbon).

The discovery of these sapropels is significant in that lower Pleistocene sapropels have not been previously recognized in the western Mediterranean, and no unambiguous sapropels were recovered at DSDP Sites 132 and 373 in the Tyrrhenian Sea (Cita et al., 1973; Kidd et al., 1978). Sapropel development was believed to be basically restricted to the eastern Mediterranean since the termination of the Messinian salinity crisis (Cita and Grignani, 1982; Thunell et al., 1984). Climatically controlled mechanisms were thought to have enhanced vertical stratification of

the eastern Mediterranean waters, while inhibiting bottom-water formation. The resulting oxygen-deficient bottom waters would have promoted sapropel formation. In the western Mediterranean on the other hand, active bottom-water was thought to have been sufficient to keep the depths at least moderately well oxygenated. The recognition of lower Pleistocene sapropels at Hole 652A signifies periods of enhanced preservation of organic matter in the central as well as the eastern Mediterranean. This observation adds a new constraint to the hotly debated question of what climatic and oceanographic conditions are necessary for sapropel development.

The best developed of the sapropels (ST-4), which occurred in Unit I at 46.17-46.32 mbsf (Core 107-652A-6R-1, 37-52 cm), illustrates our shipboard observations. Based on our preliminary data, Figure 16 depicts changes in color, percentage carbonate, and percentage organic matter through this interval. The upper and lower boundaries between the dark gray and gray muds are gradational. The upper boundary shows a slight amount of bioturbation. Sedimentary structures in the middle of the sapropel have been disturbed during drilling, but discontinuous parallel laminations can still be distinguished between 44 and 48 cm. Two organic-carbon-rich samples with different colors were analysed from ST-4. It is interesting to note that the gray interval beneath the darker gray has an organic carbon content of 3.50%, a value greater than many eastern Mediterranean sapropels (Cita and Grignani, 1982). The preliminary shipboard organic geochemical data suggest that the organic matter in the gray interval (107-652A-6R-1, 53-55 cm) was of marine origin deposited under oxic conditions. The organic carbon con-

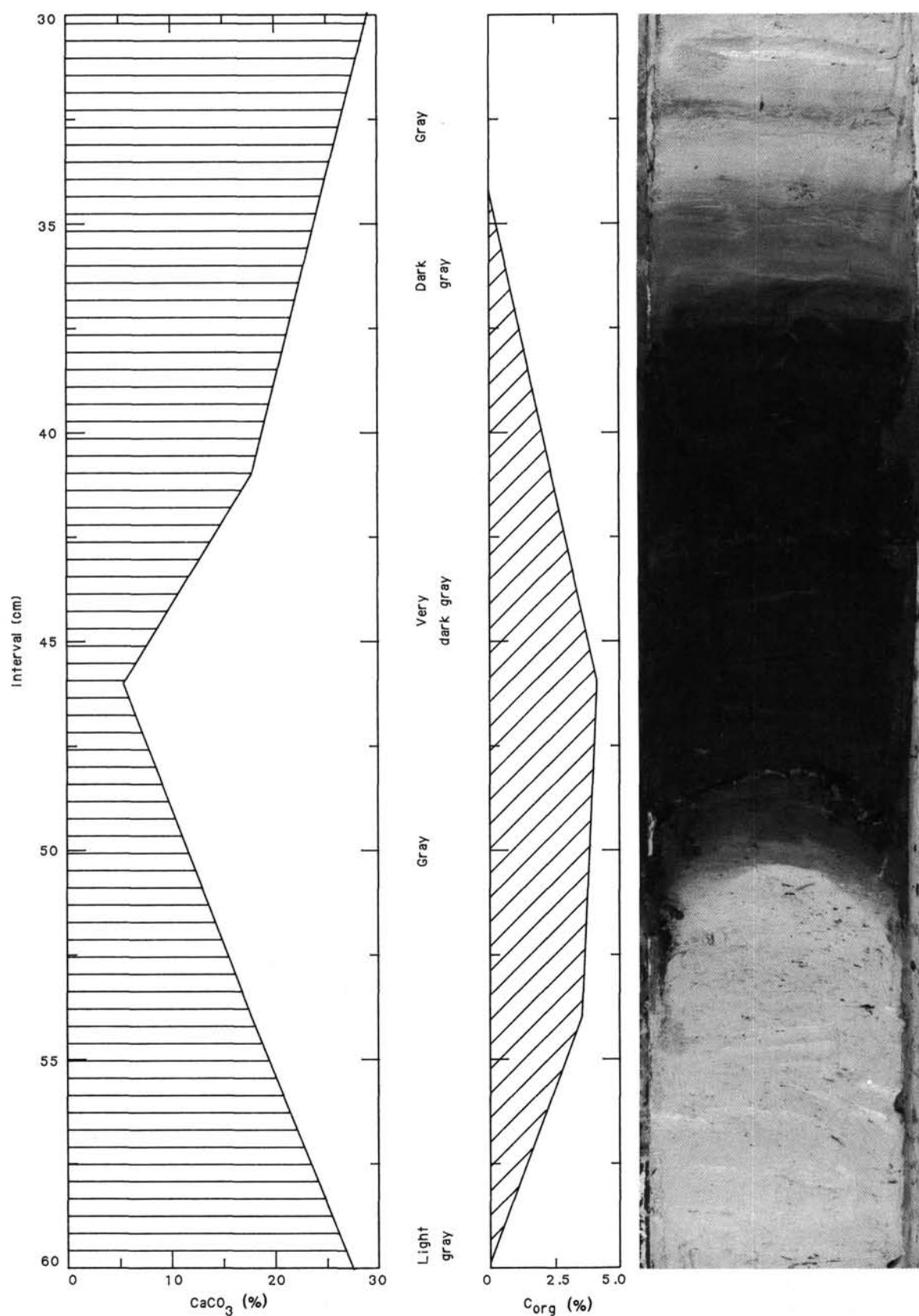


Figure 16. A core photograph of sapropel ST-4 (Core 107-652A-6R-1, 30–60 cm) showing the percentage carbonate, percentage organic carbon, and color changes with depth. Note the diffuse contacts between the lighter and darker boundaries and the apparent burrowing traces in the dark gray zone of the upper boundary.

tent of the sample from the very dark gray interval (107-652A-6R-1, 45–47 cm) is 4.18%. Geochemical data (see “Geochemistry” section, this chapter) suggest both a marine and continental origin for this organic matter, which was apparently deposited under anoxic conditions. The carbonate content of the darkest interval drops to a value of 5.15%, suggesting either dissolution or decreased carbonate input to the sediment. Above and below this point, the carbonate content of the light gray to gray muds progressively approaches values slightly greater than the average value for Unit I calcareous muds (22%). The geochemical and color patterns of individual sapropels in the eastern Mediterranean are generally very characteristic (Sigl and Müller, 1975); further studies will confirm or not if this is also the case for the western Mediterranean sapropels.

Sedimentary Instability

Excellent examples of all types of the structures considered to be typical of sedimentary instability are observed within the pre-Pliocene formations (Units IV and V). Only one somewhat dubious example was observed in the Pliocene-Pleistocene section, in Core 107-652A-15R-4, 80–95 cm.

Extensional microfaults are numerous and widespread in Cores 107-652A-31R to -34R (286.3–325.0 mbsf), 107-652A-37R (344.3–354.0 mbsf), 107-652A-47R to -54R (441.1–518.1 mbsf), 107-652A-56R and -57R (527.8–546.6 mbsf), 107-652A-62R to -65R (585.2–624.5 mbsf) and 107-652A-67R (634.2–643.8 mbsf) (Fig. 17). Apparent reverse faults exist in the Cores 107-652A-32R (295.9–305.6 mbsf), 107-652A-54R (508.5–518.1 mbsf), 107-652A-57R (537.4–546.6 mbsf), 107-652A-63R (594.9–604.5 mbsf) and 107-652A-65R (614.2–624.5 mbsf).

Some microtectonic measurements have been performed. In order to avoid faults produced by drilling disturbance, we have chosen only those faults overlain by unfaulted sediments, and we have separated the two fault sides and measured the pitch of slickensides on the frontal plane (Figs. 18 and 19). Measurements have been performed on Cores 107-652A-49R, -54R, -56R, -62R, and -64R (Table 3).

The different observations indicate that the intersection line between the fault plane and the bedding plane is generally more or less horizontal, demonstrating that the strike of the fault plane is approximately parallel to the strike of the bedding planes. The dip direction of the fault plane is similar to the dip direction of the bedding planes; however, the dip of the fault plane is typically steeper than the dip of the bedding planes. Most microfaults examined show a normal sense of motion. Slickensides on some fault surfaces indicate a slight strike-slip component of motion. If we assume that the regional dip of bedding is to the west or west-northwest, as shown on seismic profiles, the direction of fault planes should be about N 0° to N 30°. Using the “diedre droit” method (Angelier and Mechler, 1977), the construction of fault motions indicates a tensional paleostress field oriented N 100° to N 130°, with a small strike-slip component (right lateral with respect to the north-south direction and left lateral to the east-west direction).

Slumps are frequent within the Cores 107-652A-34R (315.3–325.0 mbsf), 107-652A-45R and -46R (421.8–441.1 mbsf), 107-652A-52R to -56 R (489.2–537.4 mbsf), 107-652A-61R to -64R (575.6–614.2 mbsf) and 107-652A-67R to -68R (634.2–653.4 mbsf). In some cases (107-652A-56R and -57R, 527.8–546.6 mbsf; 107-652A-62R, 585.2–594.9 mbsf) the minerals are reoriented parallel to the flanks of the minor folds; these give way to a well-expressed axial plane cleavage (Fig. 20). This implies that the deformation (i.e., the slump formation) occurred under a rather thick sedimentary load. We also observed minor structures, such as convolutions and breccias, in the same intervals and also in 107-652A-33R (305.6–315.3 mbsf), 107-652A-51R (479.6 to 489.2 mbsf) and 107-652A-73R and -74R (692.2 to 710.5 mbsf).

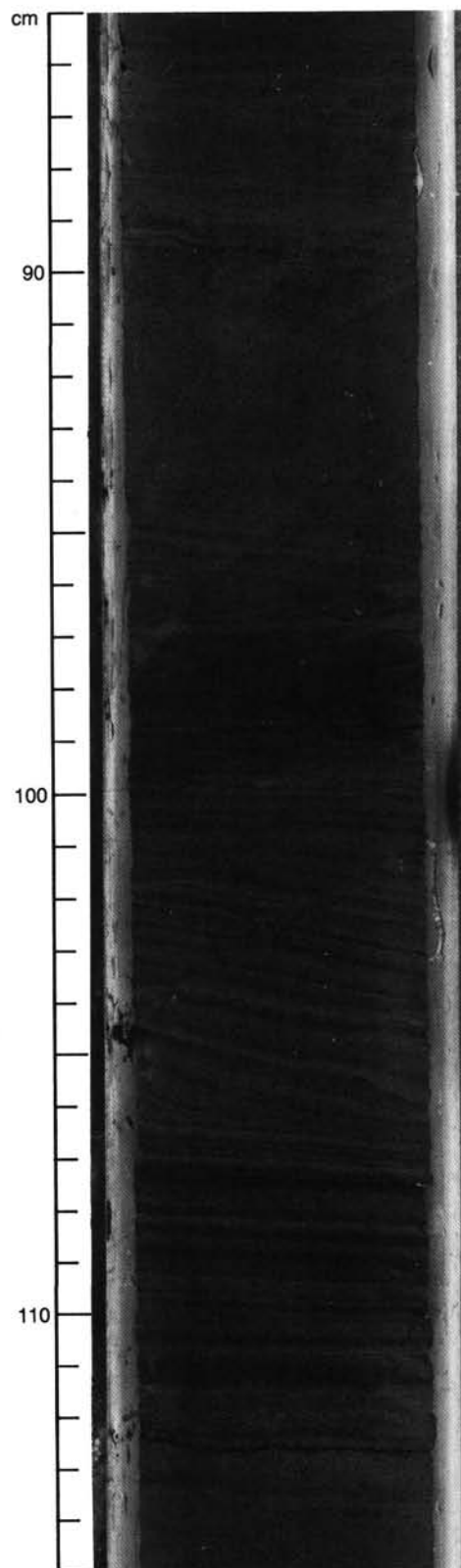


Figure 17. Example of synsedimentary microfaults (Core 107-652A-62R-1, 85–115 cm, 585.2–594.9 mbsf). Numerous synsedimentary microfaults are present between 95 and 112 cm; between 95 and 99 cm they are very flat (angle with bedding below 20°) and synthetic; below 100 cm they are steeper and antithetic, two well-expressed planes (at 104–105 cm) show a small angle (15°); this “Riedel R” pattern confirms the normal sense of motion also shown by throw.

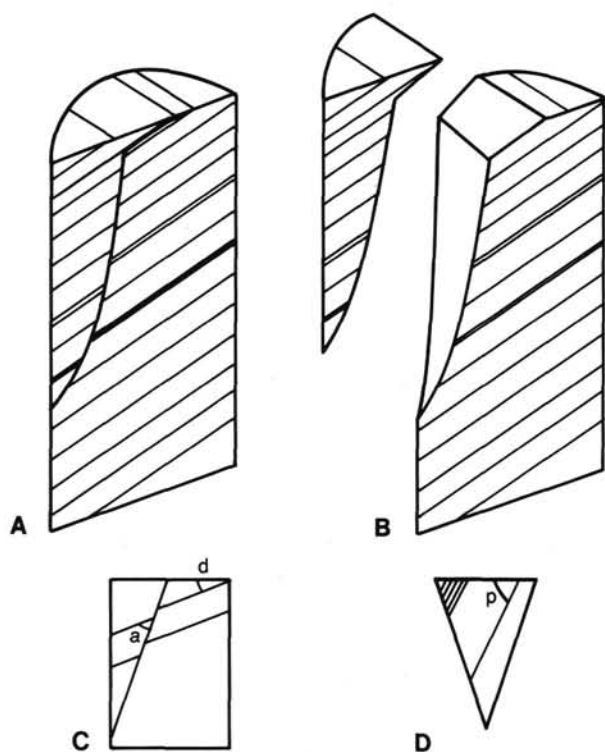


Figure 18. Conditions of measurement and definition of measured fault parameters. A. Piece of core before measurement. B. Piece of core after measurement. C. Lateral section: d = dip of bedding, a = angle between bedding and fault plane. D. Frontal view: p = pitch of slickensides.

Conclusions

The Pliocene-Pleistocene formations are characterized by open marine conditions with a small influx of volcanic material. The change in calcium carbonate concentration from Units I to II is probably due to an increase in allochthonous material during Pleistocene time as there is an increase in the sedimentation rate from about 3.2 cm/1000 yr in Unit II to an average of 6.1 cm/1000 yr in Unit I. The boundary between upper Pliocene and lower Pliocene corresponds to a maximum in the carbonate content of the pelagic sequence. The repeated occurrence of sapropels possibly reflects the recurrence of anoxic conditions during the Pleistocene.

The colorful, iron-oxide-rich sediments in the 40-cm-thick transitional formation indicate a probable strong subaerial weathering of the emerged land during the Messinian drawdown with subsequent erosion into the filling basin.

The pre-Pliocene formations are characterized by periods of variable salinity culminating with the precipitation of evaporites and by possible periods of high productivity, as suggested by the algal blooms and the high organic-carbon content of the anoxic sediments. The pebble horizon may indicate a temporary fluvial or beach environment. The most probable sedimentary environment for the pre-Pliocene units is a closed lake. The sediments are considered to have been deposited during the Messinian. The sedimentation rate would have been quite high, on the order of 50 cm/1000 yr based on the entire Messinian or 100 cm/1000 yr based only on the evaporitic part of the Messinian. The pre-Pliocene formations are clearly contemporaneous with strong extensional activity.

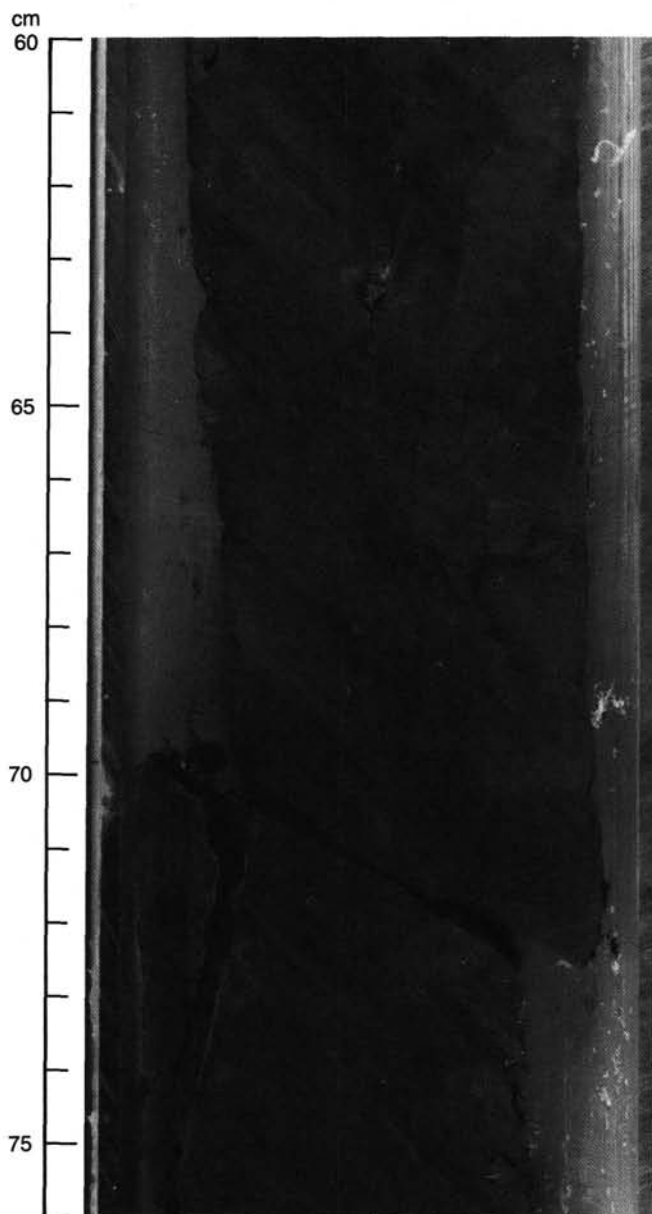


Figure 19. Example of a measured synsedimentary fault plane (107-652A-54R-5, 60-76 cm, 508.5-518.1 mbsf). In the lower part of the segment the two sides of the fault plane have been separated to observe and measure the slickensides (see Table 3).

Table 3. Measured fault planes for Site 652.

Core, interval	Dip So	Angle So/F	Pitch of slicken- sides	Orientation F/So	Sense of motion	Throw (mm)
107-652A-49R-1, 34 cm	27	37	65 l	S	N	9
107-652A-54R-5, 65 cm	10	70	75 r	A	I	5
107-652A-56R-5, 95 cm	5	40	75 l	A	N	25
107-652A-62R-3, 120 cm	20	0	50 l	S	N	?
107-652A-62R-3, 120 cm	20	60	80 l	S	N	3
107-652A-62R-3, 120 cm	20	50	80 l	S	N	sm
107-652A-62R-3, 120 cm	20	120	70 l	A	N	sm
107-652A-64R-1, 125 cm	12	63	80 r	S	N	3

l = left; r = right; N = normal; I = reverse; A = antithetic; S = synthetic; So = stratification bedding plane; F = fault plane; sm = small.

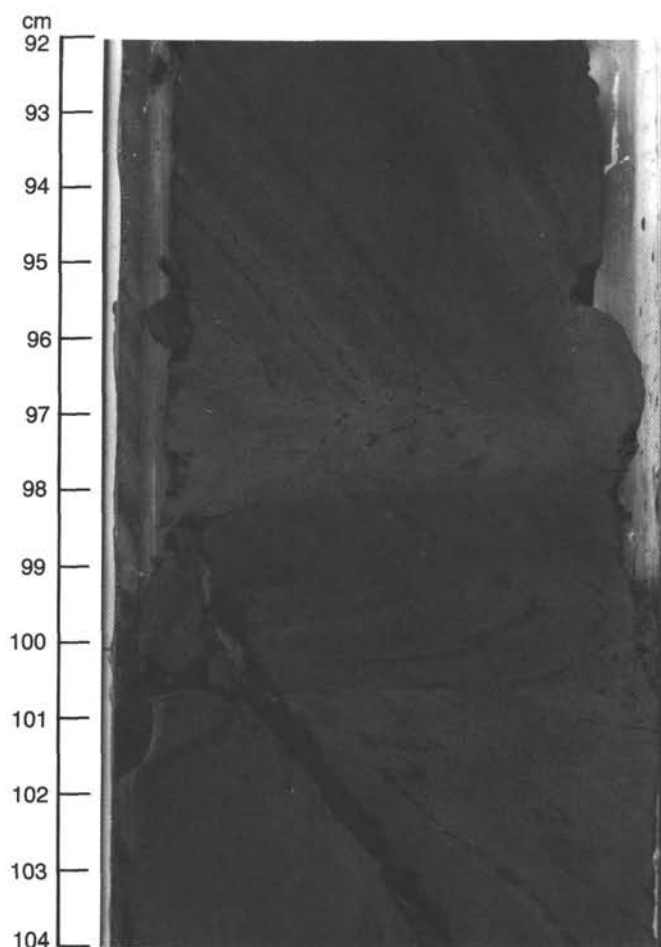


Figure 20. Example of microfolds with the development of an axial plane cleavage within a slump zone (Core 107-652A-55R-4, 92–104 cm, 518.1–527.8 mbsf).

BIOSTRATIGRAPHY

Summary

A Pliocene-Pleistocene sequence of hemipelagic sediments, 188 m thick, was recovered at Site 652. It is underlain by non-marine sediments most probably belonging to the Messinian. The age at the base of this series is unknown.

The Pleistocene is very condensed (85 m). Volcanic ashes occur within nannoplankton zone NN19. Several sapropel layers are present throughout the Pleistocene. Micro- and nannofossils are generally abundant and well preserved. Climatic fluctuations can be recognized throughout the Pliocene-Pleistocene by use of foraminiferal and nannoplankton assemblages.

Good agreement exists between biostratigraphic datings and the paleomagnetic results. The Pliocene-Pleistocene boundary is determined at 85 mbsf by means of planktonic foraminifers just above the top of the Olduvai event.

The *Sphaeroidinellops* MP11 acme zone representing the base of the Pliocene is present in Core 107-652A-20R. Below this there is a marked decrease of autochthonous fossils. At the same time, the abundance of detrital material and reworked Cretaceous and Paleogene nannofossils increases downsection.

The species diversity of benthic foraminifers per sample gradually increases upsection in the lower part of the Pliocene until 112–122 mbsf. Above this level, species diversity decreases until at 84 mbsf many species have disappeared. The base of *Articu-*

lina tuberosa is found at 74.5 mbsf in Sample 652A-8R, CC, just above the Pliocene-Pleistocene boundary.

The sediments recovered from 190 to 720 mbsf are barren of autochthonous micro- and nannofossils, and were apparently deposited in a nonmarine environment.

The biostratigraphic results are summarized in Figure 21.

Planktonic Foraminifers

Pleistocene

The Pleistocene interval was recovered from Core 107-652A-1R to about 85 mbsf (Sample 107-652A-10R-1, 75–77 cm). Two planktonic biozones (Ruggieri and Sprovieri, 1983; Ruggieri et al., 1984) are recognized. The *Globorotalia truncatulinoides excelsa* biozone is present from the top down to 55.40 mbsf (Sample 107-652A-6R, CC). The *Globigerina cariacensis* biozone is present from 55.40 to 85 mbsf. According to the stratotype boundary section (Vrica section, Calabria, Italy) the Pliocene/Pleistocene boundary was recognized by the first presence of abundant specimens of left-coiling *Neogloboquadrina pachyderma* (Colalongo et al., 1982; Tauxe et al., 1983). *Globigerinoides obliquus* disappears above the boundary at about 67.15 mbsf (Sample 107-652A-8R-2, 65–67 cm). The Emilian-Sicilian boundary was recognized at the base of the *Globorotalia truncatulinoides excelsa* biozone (55.40 mbsf). As in the Sicilian stratotype, a level with frequent specimens of *Globorotalia crassaformis*, *Globorotalia viola*, and *Globorotalia hessi* is present just below the *Globorotalia truncatulinoides excelsa* f.o. On the basis of the studied samples, it was not possible to recognize the top of the Sicilian.

Pliocene

The Pliocene interval was completely recovered between about 85 and about 188 mbsf. The six foraminiferal biozones (Cita, 1975; Rio et al., 1984b) were recognized. MP16 biozone is present from 85 to about 100 mbsf (Sample 107-652A-11R-5, 18–20 cm). At the very base of the biozone the zonal marker (*Globorotalia inflata*) is rare; it is not present in the upper part of Section 4 and in the lower part of Section 3 of Core 107-652A-11R and is common to abundant from the top of Section 2 of Core 107-652-11R. In the segment between about 97 and 94.5 mbsf *Globorotalia truncatulinoides*, *Globorotalia tosaensis*, *Globorotalia tosaensis tenuithec*, and *Sphaeroidinella dehiscens* are common. MP15 (*Globigerinodes elongatus*) biozone was recognized between 100 and 109.70 mbsf (Sample 107-652A-12R-5, 68–70 cm) where the *Sphaeroidinellops* spp. l.o. was detected. *Globorotalia crassaformis* s.l. is more or less frequent in this interval. *Globorotalia bononiensis*, which appears at the top of MP14, in Sample 107-652A-13R-2, 9–11 cm (114.30 mbsf) disappears in Sample 107-652A-11R-5, 145–147 cm, (101.2 mbsf). We note that the thickness of sediments referable to this biozone, approximately one million years long (from about 3.0 to about 2.0 m.y.b.p.), is very thin in Site 652 and a sharp reduction in the sedimentation rate is detectable. MP14 was identified between 109.70 and 132.5 mbsf, in coincidence with the *Globorotalia margaritae* l.o. (Sample 107-652A-15R, 57–59 cm). Within this biozone (*Sphaeroidinellops subdehiscens* biozone) the extinction level of *Globorotalia puncticulata* s.s. occurs at 122.3 mbsf (Sample 107-652A-13R, CC). MP13 was recognized from 132.5 to 147 mbsf (Sample 107-652A-16R-4, 80–86 cm) where the appearance of *Globorotalia puncticulata* was detected. Again, the thickness of this biozone is quite thin and a decrease in the sedimentation rate is detected along this interval. MP12 was recognized between 147 and 177.1 mbsf (Sample 107-652A-19R-5, 112–116 cm). *Globorotalia margaritae* is never abundant and is only continuously present in the samples from Sample 107-652A-18R, CC (170.5 mbsf) upward. MP11, characterized by abun-

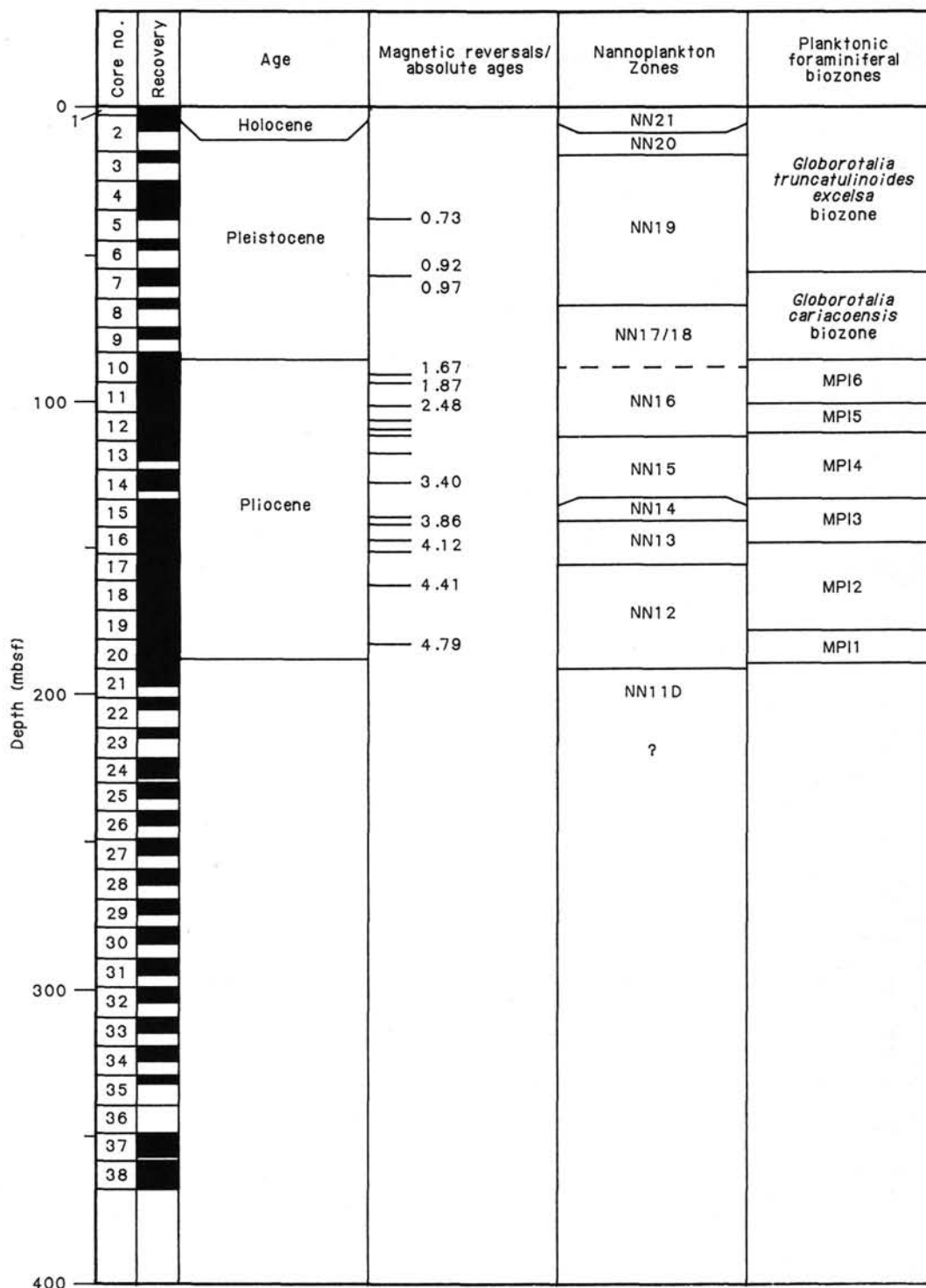


Figure 21. Summary of biostratigraphic results at Site 652.

dant specimens of *Sphaeroidinellopsis* spp., has been recognized from 177.1 mbsf to the base of the Pliocene, at about 188 mbsf. At the very base and top of this biozone *Sphaeroidinellopsis* spp. specimens are not present. At the base the planktonic assemblage is dominated here by *Globigerinoides obliquus*, *Globigerina* spp., and *Globigerinita quinqueloba*.

Pre-Pliocene

From the base of the Pliocene to the base of the drilled interval of Site 652 (720 mbsf), the sequence recovered was generally

barren of planktonic foraminifers. In Sample 107-652A-28R, CC (267 mbsf) a few black spheres, about 0.2 mm in diameter, tentatively referred to micrometeorites (Fig. 22) were recovered. Further studies from thin sections and SEM microscope analyses will define the nature of these findings.

Benthic Foraminifers

Benthic foraminifers occurred in almost all the samples from the top, down to 188 mbsf of Hole 652A. In the top sample of Core 107-652A-1R, several specimens are present. *Glomospira*



Figure 22. SEM photo of black sphere (approximately 0.2 mm diameter), tentatively identified as a micrometeorite. Sample is from 107-652A-28R, CC.

charoides is relatively frequent, and is associated with *Rhabamina* sp., *Ammolagena clavata*, and a few calcareous species. Such species association corresponds to the Recent *Glomospira haroides* assemblage which has been found below 1800 m in the eastern Mediterranean and below 2500 m in the western Mediterranean (Cita and Zocchi, 1978).

The samples of Core 107-652A-1R (3.6 mbsf) yield many species including *Articulina tubulosa*, *Ammonia beccarii*, *Cibicides refulgens*, *Cibicides lobatulus*, *Elphidium crispum*, *Gyroidina* spp., *Melonis pompilioides*, *Neoconorbina* spp., and *Rosalina* spp. In the sample most specimens are broken, and many shallow water species are included. They are considered as displaced. In the interval between 17 mbsf (Core 107-652A-2R, CC) and 58 mbsf (107-652A-7R-2, 116–119 cm), only a few specimens occur. Among them, *A. tubulosa*, *Oridorsalis stellatus*, *Chilostomella mediterraneensis*, and *Gyroidina neosoldanii* are regarded as autochthonous, and suggest mesobathyal or deeper environment. In some horizons, they accompany a small number of displaced specimens.

Between 59.5 mbsf (Core 107-652A-7R-3, 116–119 cm) and 188 mbsf (Core 107-652A-20R-6, 45–46 cm), many species are found, and displaced specimens are very rare. Throughout the interval, a remarkable trend in the species diversity can be recognized. The diversity value increases from 188 mbsf upsection, and attains a maximum around Core 107-652A-13R (112.7–122.3 mbsf). Between the top of this interval and about 84 mbsf (Core 107-652A-9R, CC), many species disappear.

Between 65 mbsf (Core 107-652A-7R, CC) and 77 mbsf (Core 107-652A-9R-2, 115–119 cm) *A. tubulosa*, *O. stellatus*, *Quinqueloculina* spp., *Gyroidina* spp., and *Parafissurina* spp. are frequent. In this interval, the first occurrence of *A. tubulosa* is found at 74.5 mbsf (Core 107-652A-8R, CC) in lower Pleistocene.

In the interval between 84 mbsf (Core 107-652A-9R, CC) and 188 mbsf, *Nuttallides rugosus convexus*, *O. stellatus*, *Bolivina* spp., *Gyroidina* spp., *Silicosigmoilina tenuis*, *Pleurostomella* spp., *Stilostomella* spp., *Karreriella bradyi*, *Cibicoides italicus*, *C. cf. robertsonianus*, *Pullenia* spp., *Q. venusta*, and *Siphonina reticulata* are characteristic. The last occurrence of *C.*

italicus is recognized at 107.2 mbsf (Core 107-652A-12R-3, 120–124 cm) in the lower part of MPI5 zone. It is concordant with some data from the land sections (AGIP, 1982; Sprovieri and Barone, 1984).

Below 190 mbsf (Core 107-652A-20R, CC), down to 335 mbsf (Core 107-652A-35R, CC), some specimens can be found among the well sorted very fine sand grains. They consist of only broken specimens, and seem to be reworked or displaced from the pre-Pliocene sequences. In Sample 107-652A-29R, CC (277 mbsf) three specimens of *Ammonia beccarii tepida* and two fragments that can possibly be referred to the brackish-water ostracod *Cyprideis* sp. were found.

A limestone among the pebbles at 335 mbsf (Core 107-652A-36R) includes several larger foraminifers with smaller benthic and planktonic forms, bryozoans, and calcareous algae. Among them, *Lepidocyclina* (s. l.) sp., *Pseudolepidina*? sp., and *Nummulites* spp. can be identified.

Paleoclimatic Approach

At Site 652, the Pleistocene is only about 85 m thick and therefore needs very close sampling to apply this method; this sampling has not yet been done. Furthermore, the upper part of the sediments has been strongly disturbed by drilling.

Top of Core 107-652A-1R is late Holocene in age with sinistral *Globorotalia truncatulinoides excelsa* and abundant well preserved Pteropods but without living benthic foraminifers. Core 107-652A-4R, CC (36 mbsf) is detrital with dominant dextral *G. truncatulinoides excelsa*. Occurrence of large *Globigerinoides conglobatus* (diameter more than 400 μ m) is noted. By comparing with other Tyrrhenian and Ionian sites we propose an age of about 72,000 years (stage 4/5). The isotopic stage 11 (347,000–421,000 yr) was recorded in Core 107-652A-3R, CC.

Nannoplankton

At Site 652, the sequence of hemipelagic Pliocene-Pleistocene sediments reaches a thickness of 188 m. It is underlain by nonmarine sediments most probably belonging to the Messinian. However, the base of this sequence is of unknown age.

The Pleistocene is very condensed or reduced by erosion (85 m). The *Emiliania huxleyi* Zone (NN21) is present from the top to Sample 107-652A-2R-1, 25 cm, underlain by the *Gephyrocapsa oceanica* Zone (NN20) from Sample 107-652A-2R-1, 70 cm, to Sample 107-652A-2R, CC. Nannoplankton are generally abundant. There are few detrital carbonate and reworked species in several layers.

Helicosphaera sp. (with two large pores) is present just above the boundary NN20/NN19 (Samples 107-652A-2R, CC, 4 cm, and 107-652A-2R, CC). However, at Site 652 this species is present also within Zone NN19 (Sample 107-652A-4R-1, 10 cm). It seems that the lowermost part of Zone NN20 is missing.

The interval from Core 107-652A-3R to Sample 107-652A-8R-2, 60 cm (17.0–67.0 mbsf) belongs to the *Pseudoemiliania lacunosa* Zone (NN19). In several levels nannoplankton are strongly diluted by the high input of volcanic ash.

The acme of the small *Gephyrocapsa* was recognized from Sample 107-652A-6R-1, 53 cm, to Sample 107-652A-6R-1, 138 cm (about 47.0 mbsf). The last *Helicosphaera sellii* was observed in Sample 107-652A-6R, CC.

Very short intervals with abundant small *Gephyrocapsa* were also found within Zone NN20 (Sample 107-652A-2R-1, 125 cm) and in Zone NN21 (Sample 107-652A-3R, 30 cm).

Sapropel layers occur within Zone NN19 concentrated around the Jaramillo magnetic event and the Pliocene/Pleistocene boundary. They are very rich in pyrite and organic matter of marine origin; plant fragments are rare. Nannoplankton are dissolved within the sapropel of Sample 107-652A-6R-1, 45 cm, and they are etched in the Pliocene sapropels.

The level characterized by the abundance of large specimens of *Braarudosphaera bigelowi* is restricted to Sample 107-652A-8R-1, 114 cm, within the lowermost part of Zone NN19, which is in good agreement with results obtained from the other sites.

The Pliocene/Pleistocene boundary was determined by the last occurrence of *Cyclococcolithus macintyreii* and *Discoaster brouweri* between Samples 107-652A-8R-2, 60 cm, and 107-652A-8R-2, 70 cm (85.0 mbsf). The first appearance of *Gephyrocapsa oceanica* corresponds with this boundary.

The Pliocene sequence (85.0–189.0 mbsf) seems to be complete. All nannoplankton zones were determined with the exception of Zone NN17. This zone is always extremely short and in most cases it is impossible to recognize it. The extinction levels of *Discoaster surculus* and *Discoaster pentaradiatus* fall almost together. Furthermore the scarcity or absence of discoasters within the upper part of the Pliocene in the western Mediterranean makes it even more difficult. Fluctuations in the abundance of discoasters as well as differences in the abundance of certain species make it possible to recognize climatic changes within the Pliocene. A very distinct decrease in surface water temperature occurs within the upper part of Zone NN16 at about 2.5–2.6 Ma (Müller, 1978) which reflects the onset of the northern hemisphere glaciation. Changes of surface water temperature within the western Mediterranean are comparable with those in the northeast Atlantic (Bizon and Müller, 1977) and are related to global climatic fluctuations.

Nannoplankton Zone NN18 (*Discoaster brouweri* Zone) was encountered from Samples 107-652A-8R-2, 70 cm, to 107-652A-10R-2, 5 cm. Discoasters are absent from the uppermost part; *Discoaster brouweri* and *Discoaster triradiatus* were found from Core 107-652A-9R.

There are two sapropel layers within this interval (Core 107-652A-9R-2, 36–41 cm and 93–99 cm).

Nannofossils are strongly etched in the sapropel layers. Certain levels within Zone NN18 are characterized by a decrease of nannoplankton and the abundance of tiny carbonate fragments that might originate from broken small coccoliths. This phenomenon was observed in all holes drilled in the Tyrrhenian Sea and might reflect stronger climatic changes within the uppermost Pliocene. They are also expressed in the lithology by alternating marly foraminifer-nannofossil ooze and silt layers. Below this interval the lithology is more homogeneous.

Zone NN16 (*Discoaster surculus*) is determined from Samples 107-652A-10R-2, 107 cm, to 107-652A-12R-4, 47 cm (86.2–108.0 mbsf) underlain by the *Reticulofenestra pseudumbilica* Zone (NN15) from Samples 107-652A-12R-5, 47 cm, to 107-652A-15R-1, 10 cm (109.0–132.0 mbsf). Discoasters are very rare within the upper part of Zone NN16 (Core 107-652A-10R); they are more common from Core 107-652A-11R. The last occurrence of *Discoaster tamalis* was observed in Sample 107-652A-10R-4, 100 cm.

The top of Zone NN15 is not easy to recognize. The specimens of *Reticulofenestra pseudumbilica* are smaller and often they disappear. Also *Sphenolithus abies* which normally can be used also to determine the top of Zone NN15 is very rare or absent within the uppermost part of this zone. Very large specimens of *Reticulofenestra pseudumbilica* occur from Core 107-652A-15R downsection.

The *Discoaster asymmetricus* Zone (NN14) defined by the first occurrence of *Discoaster asymmetricus* at the base and the extinction of *Amaurolithus tricoraniculatus* at its top represents a short time interval (Samples 107-652A-15R-1, 80 cm, to 107-652A-15R-3, 130 cm; 132.8–138.3 mbsf). It is underlain by Zone NN13 (*Ceratolithus rugosus* Zone) recognized from Samples 107-652A-15R-4, 41 cm, to 107-652A-17R-1, 120 cm (137.0–153.4 mbsf), and Zone NN12 (*Amaurolithus tricoraniculatus* Zone) from Samples 107-652A-17R-2, 120 cm to 107-652A-20R-6, 120

cm (154.0–189.5 mbsf). The abundance of the discoasters and the distribution pattern of the different species throughout the Pliocene seems to be comparable with those from other sites drilled in the Tyrrhenian Sea. Discoasters are absent or extremely rare within the uppermost Pliocene, upper NN16 to NN18 (Core 107-652A-9R to Section 107-652A-11R-5). They are few in several levels within Zone NN18 and upper part of NN16. They are common from Section 107-652A-11R-6 (lower part of Zone NN16) represented predominantly by *Discoaster brouweri* and *Discoaster surculus*.

Discoaster tamalis (large size) and *Discoaster asymmetricus* are common around the boundary NN15/NN16 and within the upper part of Zone NN15. *Discoaster variabilis* occurs near the base of Zone NN14 and within the upper NN13 which falls together with a decrease of discoasters (Samples 107-652A-15R-3, 70 cm, to 107-652A-16R-2, 50 cm). The presence of this species is interpreted as indicator of lower surface-water temperature which has been mentioned also from Leg 42A (Müller, 1978). The lower part of Zone NN13 is characterized by the dominance of *Discoaster surculus* and *Discoaster pentaradiatus*, and Zone NN12 by *Discoaster brouweri* and *Discoaster pentaradiatus*. *Discoaster surculus* becomes more common again within the lower part of Zone NN12. However, throughout the whole sequence there are always some horizons poor in discoasters.

The small species of the genus *Gephyrocapsa* has its first occurrence within the upper part of Zone NN14. The Pliocene sediments are generally rich in well-preserved nannoplankton. In some samples a slight overgrowth of the discoasters can be observed. Reworked species are rare. Within the lowermost part of Zone NN12 detrital material increases as well as reworked Cretaceous and Eocene nannoplankton species. There is also formation of secondary dolomite.

In Sample 107-652A-20R, CC one specimen of *Discoaster quinqueramus* was found together with *Amaurolithus tricoraniculatus* indicating the top of the Messinian (NN11b).

The Miocene sediments (189.0–720.0 mbsf) are barren of autochthonous nannofossils. Reworked Cretaceous and Paleogene species are common throughout the sequence indicating deposition of these sediments in a nonmarine environment.

PALEOMAGNETISM

The principal features of the Pliocene/Pleistocene magnetic polarity time scale were resolved at Site 652. The Pliocene/Pleistocene sediments responded well to alternating field demagnetization except in the 100–120 mbsf interval. The correlation of the magnetozone pattern to the magnetic polarity time scale was severely hindered by the poor recovery, and to some extent by core deformation, such that the correlation could not be made solely on the basis of pattern fit. We rely on the paleontological datums to tell approximately where we are in the magnetic polarity time scale; the reversal boundaries then give the precise correlation.

Five hundred twenty-three discrete 7-cm³ "cubic" samples were collected at this site. Two hundred fourteen of these were measured and demagnetized in an alternating field (AF) on board. Nearly all these on-board measurements were from the Pliocene/Pleistocene part of the section. The Messinian samples were often too weakly magnetized for Molspin fluxgate magnetometer and have been analyzed on shore using a cryogenic magnetometer and thermal demagnetization techniques.

Natural remanent magnetization (NRM) intensities in the Pliocene/Pleistocene section were generally about 10⁻⁶ G/cm³ whereas those in the Messinian deposits were often about 10⁻⁷ G/cm³. Alternating fields of 100–200 Oe were usually sufficient to eliminate a low coercivity component with steep positive inclination, probably acquired as a viscous remanence (VRM) from the drill-string. Samples with a reversed characteristic component

often show an increase in intensity as this VRM is removed. In some intervals (namely, 100–120 mbsf), the AF cleaning does not seem to be very efficient at isolating the characteristic component. The presence of low and fluctuating inclination values indicates that mixed components are still present after AF cleaning. Thermal cleaning on shore has improved the data quality in these intervals.

The interpretation of polarity is based on the inclination of the component isolated after AF and thermal demagnetization (Table 4). The poor recovery in Cores 107-652A-5R to 107-652A-9R and the drilling deformation of Cores 107-652A-4R, 107-652A-10R, and 107-652A-13R leave gaps in the data, which make it difficult to observe a polarity pattern correlative to the magnetic polarity time scale. However, we make the following tentative correlations, which are consistent with magnetobiostratigraphic correlations at Sites 650 and 651. The base of the Thvera (C_2) subchron is well defined at Site 652. We observe reversed characteristic magnetizations from Core 107-652A-20R-2 downward to the base of the recovered section, and believe that the entire 500 m of sediments were deposited in a reversed field, part of which corresponds to the basal reversed interval in the Gilbert chron. The Miocene/Pliocene boundary occurs in Core 107-652A-20R-6, and is therefore within this reversed interval.

PHYSICAL PROPERTIES

Introduction

Site 652 on the lower Sardinian margin sampled an 721.1-m-thick sedimentary sequence, ranging from Recent to probably

Table 4. Preliminary determination of magnetozon boundaries for Site 652. The samples which bracket the magnetozon boundaries are given.

Magnetozon boundary	Core	Section	Interval (cm)	Depth (mbsf)
Base of Brunhes	between 4R and 5R	7	34–36	36.05
Top of Jaramillo	between 7R and 7R	1	92–94	56.33
Base of Jaramillo	between 7R and 7R	2	142–144	56.83
Top of Olduvai	between 10R and 10R	4	134–136	90.05
Base of Olduvai	between 10R and 10R	7	10–12	93.31
Top of Gauss	between 11R and 11R	6	26–28	101.57
Top of Kaena	between 12R and 12R	3	120–122	105.71
Base of Kaena	between 12R and 12R	4	139–141	108.90
Top of Mammoth	between 12R and 12R	5	70–72	109.71
Base of Mammoth	between 13R and 13R	3	108–110	116.79
Top of Gilbert	between 14R and 15R	4	83–85	127.64
Top of Cochiti	between 15R and 15R	5	145–147	139.36
Base of Cochiti	between 15R and 16R	6	81–83	140.22
Top of Nunivak	between 16R and 16R	4	64–66	142.15
Base of Nunivak	between 16R and 17R	5	75–77	146.76
Top of Sidufjall (C_1)	between 18R and 18R	2	142–144	147.43
Base of Sidufjall (C_1)	between 18R and 18R	2	124–126	148.75
Top of Thvera (C_2)	between 18R and 18R	4	71–73	151.92
Base of Thvera (C_2)	between 20R and 20R	2	18–20	162.49
	and 18R	2	82–84	163.13
	and 18R	4	89–91	166.20
	and 18R	4	142–144	166.73
	and 18R	5	33–35	167.14
	and 18R	5	52–54	167.33
	and 20R	2	11–13	181.82
	and 20R	2	59–61	182.30

Messinian in age. Routine physical properties measured on the sediments included GRAPE density and thermal conductivity from full round core sections, vane shear strength, compressional-wave velocity, and index properties (porosity, bulk density, and grain density) from split sections.

Tables 5, 6, 7, and 8 list Site 652 physical-properties measurements which are also summarized in Figures 23 and 24.

Table 5. Physical properties index for Site 652.

Core section	Interval (cm) or piece no.	Depth sub-bottom (m)	Bulk density (g/cm^3)	Porosity (%)	Grain density (g/cm^3)
1R-1	0–2	0.00	1.40	79.9	2.73
1R-2	0–2	1.40	1.56	70.3	2.66
1R-2	115–117	2.55	1.32	82.2	2.65
2R-1	100–103	4.06	1.35	81.8	2.57
2R-4	27–30	8.07	1.47	76.8	2.51
3R-1	82–85	17.82	1.56	74.6	2.88
4R-5	40–43	33.13	1.62	73.5	2.88
4R-6	17–20	34.37	1.58	72.4	2.59
6R-1	111–114	46.91	1.69	64.5	2.78
7R-3	124–127	59.55	1.59	56.0	2.87
8R-1	61–65	65.53	1.91	66.1	2.90
9R-1	80–83	75.31	1.86	63.9	2.92
10R-3	100–103	86.72	1.80	62.7	2.75
12R-5	105–108	110.06	1.86	61.5	2.81
13R-4	20–23	117.41	1.90	60.7	2.78
14R-4	64–67	127.45	1.72	62.6	2.76
16R-3	70–73	145.21	1.80	57.3	2.76
17R-4	105–107	156.76	1.85	57.6	2.86
18R-4	93–96	165.85	1.86	55.1	2.80
19R-2	95–98	172.97	1.78	54.4	2.51
19R-6	137–140	179.39	1.79	59.6	2.75
20R-1	71–74	180.92	1.75	63.9	2.73
20R-5	135–138	187.56	1.74	63.3	2.73
21R-2	15–18	191.46	2.03	44.2	2.81
21R-2	134–137	192.66	1.99	48.3	2.76
22R-2	25–28	201.46	2.02	45.3	2.66
23R-2	27–30	210.88	2.04	48.3	2.85
24R-3	63–66	222.35	2.08	42.5	2.79
24R-4	77–80	223.98	2.12	40.7	2.79
25R-2	14–18	230.05	2.08	41.5	2.72
26R-2	113–117	240.75	2.15	37.5	2.76
27R-3	10–13	250.82	2.23	37.5	2.82
28R-1	28–31	257.70	2.31	40.3	2.80
28R-2	8–10	258.99	2.27	35.5	2.77
29R-2	8–11	268.70	2.17	38.5	2.76
30R-1	14–17	276.85	2.25	34.3	2.79
30R-3	55–58	280.25	2.18	37.2	2.76
31R-1	143–146	287.75	2.25	36.1	2.74
31R-3	89–91	290.20	2.28	32.9	2.76
32R-2	70–72	298.12	2.33	28.9	2.80
32R-2	124–126	298.75	2.26	32.1	2.79
33R-2	146–148	308.56	2.28	28.4	2.71
33R-3	101–103	309.64	2.29	30.1	2.75
35R-1	44–46	325.44	2.19	34.8	2.70
37R-2	94–96	346.76	2.45	24.6	2.77
37R-6	6–8	351.87	2.23	36.7	2.74
38R-1	21–23	354.22	2.28	32.3	2.76
38R-3	111–115	358.13	2.88	05.2	2.88
38R-5	9–12	360.10	2.32	29.6	2.77
39R-1	26–29	364.00	2.22	33.8	2.74
39R-7	6–8	372.77	2.22	36.5	2.69
40R-1	72–74	374.13	2.24	34.1	2.74
40R-7	33–35	382.74	2.23	36.7	2.71
41R-2	50–52	385.00	2.22	35.3	2.78
41R-6	30–33	392.32	2.27	32.9	2.73
42R-2	24–27	394.45	2.30	34.7	2.87
42R-5	144–147	400.15	2.27	32.0	2.73
43R-1	93–96	403.35	2.30	31.0	2.75
43R-4	39–41	407.30	2.52	19.4	2.76
44R-1	96–99	413.08	2.23	35.0	2.69
44R-3	75–77	415.86	2.81	08.9	2.85
45R-1	137–139	423.18	2.54	22.2	2.86
45R-2	62–64	423.93	2.32	32.8	2.88
46R-1	60–62	433.13	2.39	30.7	2.73
46R-3	100–102	435.51	2.35	29.3	2.68
47R-1	64–66	441.75	2.36	29.0	2.68

Table 5 (Continued).

Core section	Interval (cm) or piece no.	Depth sub-bottom (m)	Bulk density (g/cm ³)	Porosity (%)	Grain density (g/cm ³)
47R-5	32-34	447.43	2.48	23.7	2.74
48R-1	8-10	450.79	2.36	31.7	2.72
48R-3	130-133	455.02	2.46	24.6	2.79
49R-1	23-25	460.54	2.40	27.4	2.84
49R-2	95-97	462.72	2.56	18.9	2.88
50R-1	59-62	470.62	2.29	35.9	2.92
50R-2	90-113	472.63	2.36	30.4	2.86
50R-3	9-11	472.81	2.34	25.8	2.76
51R-1	13-15	479.75	2.41	25.6	2.73
51R-5	126-128	486.78	2.34	30.0	2.77
51R-6	44-46	487.46	2.36	28.2	2.79
52R-1	78-80	490.00	2.42	28.2	2.87
52R-3	138-140	493.60	2.42	23.1	2.45
53R-3	146-148	503.28	2.38	29.1	2.74
53R-4	14-16	503.46	2.49	26.3	2.89
54R-1	96-98	509.48	2.41	27.7	2.78
54R-3	132-135	512.85	2.46	23.6	2.80
55R-3	30-32	521.42	2.40	27.0	2.80
55R-5	106-117	525.27	2.41	25.4	2.75
55R-5	145-148	525.58	2.47	27.4	2.93
56R-2	32-34	529.64	2.42	23.7	2.73
57R-1	26-28	537.68	2.39	25.7	2.78
57R-3	62-64	541.04	2.60	18.7	2.79
58R-1	48-50	547.10	2.35	28.5	2.72
58R-6	30-32	554.42	2.12	37.4	2.59
59R-1	7-9	556.39	2.40	30.1	2.91
59R-4	18-20	560.90	2.43	24.1	2.83
60R-1	16-18	566.18	2.38	26.5	2.79
60R-5	106-108	573.08	2.42	22.2	2.83
61R-2	2-4	577.14	2.49	26.2	2.78
61R-4	146-148	581.58	2.45	31.7	2.76
62R-3	91-93	589.13	2.44	25.9	2.79
62R-4	112-114	590.84	2.52	23.2	2.77
63R-1	114-116	596.06	2.48	26.5	2.70
63R-3	75-77	598.67	2.51	22.9	2.85
64R-1	105-107	610.57	2.30	29.7	2.53
64R-3	59-61	613.01	2.82	05.7	3.03
65R-1	70-72	614.92	2.25	29.6	2.53
65R-4	2-4	618.73	2.77	30.6	2.90
66R-1	90-92	625.41	2.59	19.2	2.80
66R-3	74-76	628.25	2.52	21.8	2.77
67R-1	107-109	635.28	2.69	13.7	2.85
67R-3	144-146	628.49	2.56	22.6	2.76
67R-5	144-146	641.65	2.57	24.0	2.69
68R-1	146-148	645.26	2.55	22.1	2.83
68R-6	51-53	651.82	2.57	21.7	2.71
69R-1	2-4	653.43	2.56	21.8	2.74
69R-4	70-72	658.61	2.54	21.0	2.70
70R-2	64-66	665.26	2.51	20.9	2.71
70R-4	24-26	667.86	2.58	21.3	2.73
71R-1	78-80	673.59	2.58	20.1	2.71
71R-2	45-47	674.76	2.58	20.9	2.78
72R-1	54-56	683.05	2.59	15.3	2.78
72R-2	80-82	684.81	2.58	16.9	2.76
73R-1	4-6	692.23	2.77	19.7	2.92
73R-3	8-10	695.29	2.69	15.6	2.76
73R-3	99-101	696.20	2.51	18.4	2.70
74R-1	4-6	701.95	2.59	19.1	2.68
74R-2	54-56	703.95	2.75	12.6	2.82
74R-5	52-54	708.43	2.69	16.4	2.68
75R-4	23-25	715.24	2.57	19.3	2.72
75R-6	111-113	719.14	2.89	13.1	2.75

Results

GRAPE Density

Bulk density was determined by gamma ray attenuation porosity evaluation (GRAPE) for the entire length of every core. The GRAPE density appears constant in the upper part of the hole (0-60 mbsf) at about 1.5 g/cm³. It increases progressively to 2.0 g/cm³ between 60 and 190 mbsf and seems to be fixed at

Table 6. Compressional velocity for Site 652.

Core section	Interval (cm)	Depth sub-bottom (m)	Compressional velocity (km/s)
3R-1	82-85	17.82	1.522
4R-6	17-20	34.37	1.627
6R-1	111-114	46.91	1.570
8R-1	61-65	65.53	1.560
9R-1	80-83	75.31	1.673
10R-3	100-103	86.72	1.545
10R-6	140-143	93.12	1.626
11R-5	105-108	100.86	1.615
12R-5	105-108	110.06	1.560
13R-4	20-23	117.41	1.624
14R-4	64-67	127.45	1.559
15R-1	134-137	133.25	1.607
16R-3	70-73	145.21	1.652
17R-4	105-107	156.76	1.736
18R-4	93-96	165.85	1.675
19R-2	95-98	172.97	1.602
20R-1	71-74	180.92	1.612
21R-2	15-18	191.46	1.754
21R-2	134-137	192.66	1.734
22R-2	25-28	201.46	1.712
23R-2	27-30	210.88	1.657
24R-3	63-66	222.35	1.776
24R-4	77-80	223.98	1.819
25R-2	14-18	230.05	1.981
26R-2	113-117	240.75	1.900
27R-3	10-13	250.82	1.864
28R-1	28-31	257.65	1.933
28R-2	8-10	258.99	1.903
29R-2	8-11	269.90	1.852
30R-1	14-17	276.85	1.935
30R-3	55-58	280.26	1.784
31R-1	143-146	287.75	1.819
31R-3	89-91	290.20	1.991
32R-2	70-72	298.12	2.130
32R-2	124-126	298.75	1.986
33R-2	146-148	308.56	2.606
33R-3	101-103	309.64	4.220
35R-1	44-46	325.44	2.022
37R-2	94-96	346.76	3.009
37R-6	6-8	351.87	1.856
38R-1	21-23	354.22	1.984
38R-3	111-115	358.13	5.212
38R-5	9-12	360.10	2.040
39R-1	26-29	364.00	1.905
39R-7	6-8	372.77	1.823
40R-1	72-74	374.13	1.974
40R-7	33-35	382.74	1.933
41R-2	50-52	385.00	1.903
41R-6	30-33	392.32	1.963
42R-2	24-27	394.45	2.095
42R-5	144-147	400.15	1.961
43R-1	93-96	403.35	1.970
43R-4	39-41	407.30	3.376
44R-1	96-99	413.08	1.948
44R-3	75-77	415.86	4.820
45R-1	137-139	423.18	3.080
45R-2	62-64	423.93	2.100
46R-1	60-62	432.11	2.067
46R-3	100-102	435.51	2.025
47R-1	64-66	441.75	2.197

about 2.0 g/cm³, below 190 mbsf to the bottom of the hole at 721.1 mbsf.

Index Properties and Compressional Velocity

Porosity, bulk density, compressional velocity, and grain density are plotted relative to sub-bottom depth in Figures 23 and 24 and are listed in Tables 5 and 6.

The bulk density values are in good agreement with the porosity values and reflect the same trend changes along the cores. To a first approach, two main physical property units can be

Table 6 (Continued).

Core section	Interval (cm)	Depth sub-bottom (m)	Compressional velocity (km/s)
47R-5	32-34	447.43	2.578
48R-1	8-10	450.79	2.301
48R-3	130-133	455.02	2.078
49R-1	23-25	460.54	2.503
49R-2	95-98	462.76	4.275
50R-1	60-63	470.62	2.400
50R-3	9-11	473.10	2.871
51R-1	13-15	479.74	2.165
51R-5	126-128	486.87	2.473
51R-6	44-46	487.55	2.246
52R-2	78-80	491.49	2.476
52R-3	138-140	493.59	2.846
53R-3	146-148	503.19	2.323
53R-4	14-16	503.45	2.622
54R-1	96-98	509.47	2.228
54R-3	132-135	512.92	2.320
55R-3	30-32	521.41	2.316
55R-5	145-148	525.56	2.401
56R-2	32-34	529.23	2.368
56R-6	11-13	535.42	2.485
57R-1	26-28	537.67	2.508
57R-3	62-64	541.03	2.972
58R-1	48-50	547.09	2.191
58R-6	30-32	554.41	2.175
59R-1	7-9	556.38	2.025
59R-4	18-20	560.99	2.467
60R-1	16-18	566.77	2.303
60R-5	106-108	573.67	2.666
61R-2	2-4	577.13	2.433
61R-4	146-148	581.57	2.309
62R-3	91-93	589.12	2.411
62R-4	112-114	590.83	2.543
63R-1	114-116	596.05	2.695
63R-3	75-77	598.66	2.875
64R-1	105-107	610.56	2.246
64R-3	59-61	613.10	3.330
65R-1	70-72	614.91	2.230
65R-4	2-4	618.73	3.960
66R-1	90-92	625.41	3.322
66R-3	74-76	628.25	2.764
67R-1	107-109	635.28	4.284
67R-5	114-146	641.65	2.745
68R-1	146-148	645.25	2.508
68R-6	51-53	651.82	2.910
69R-1	2-4	653.43	2.414
69R-4	70-72	658.61	2.898
70R-2	64-66	665.25	2.970
70R-4	24-26	667.85	2.963
71R-1	78-80	673.59	2.491
71R-2	45-47	674.76	2.933
72R-1	54-56	683.05	3.338
72R-2	80-82	684.81	3.325
73R-1	4-6	692.23	3.263
73R-3	8-10	695.29	3.596
73R-3	99-101	696.20	3.208
74R-1	4-6	701.95	2.772
74R-2	54-56	703.95	3.608
74R-5	52-54	708.43	3.202
75R-4	23-25	715.24	2.680
75R-6	111-113	719.14	3.506

distinguished in Hole 652A: Unit 1 from the seafloor to about 330 mbsf and Unit 2 below this depth to the bottom of the hole.

A more detailed study allows the definition of several sub-units which are as follows:

1. Physical Properties Unit 1-A: From the seafloor to about 60 mbsf showing a downsection decreasing porosity (80%-56%) and density values increasing from 1.40 g/cm³ at the mud line to 1.70 g/cm³.

2. Physical Properties Unit 1-B: From 66 to about 187 mbsf with a downsection decreasing porosity (66%-54%) and density values decreasing from 1.91 to 1.74 g/cm³. This decrease of density is interesting and atypical.

Table 7. Thermal conductivity for Site 652.

Core section	Interval (cm)	Depth sub-bottom (m)	Thermal conductivity (10 ⁻³ /cal·cm ² ·s·deg)
1R-1	100	1.00	2.1931
1R-2	75	2.15	2.5235
1R-3	32	3.22	2.2874
2R-2	75	5.85	2.2851
2R-3	60	7.20	2.6187
3R-1	85	17.85	2.3354
4R-3	80	30.50	1.8760
4R-4	80	32.00	2.6028
4R-5	80	33.50	2.6626
5R-1	23	36.63	2.9070
6R-1	111	46.91	2.9073
7R-1	63	56.03	2.8040
7R-2	26	57.16	2.7608
7R-3	76	58.86	2.8360
7R-4	29	59.89	2.4904
8R-1	75	65.65	2.7799
8R-2	75	68.15	2.8873
10R-1	75	84.95	2.5366
11R-1	75	94.55	3.1060
12R-2	75	105.25	2.9908
13R-1	70	113.40	3.3415
13R-2	70	114.90	3.1699
14R-2	77	124.97	3.0303
14R-4	75	127.15	3.0532
15R-2	77	134.17	3.0474
15R-4	77	137.17	3.2152
17R-2	77	153.47	3.2830
19R-2	73	172.73	3.1178
19R-3	72	174.23	3.1061
21R-1	79	190.59	3.2355
24R-4	94	224.14	4.2228
25R-2	75	230.65	4.2418
27R-2	80	250.00	3.8879
28R-2	75	259.65	3.6629

Table 8. Shear strength measurements for Site 652.

Core section	Interval (cm)	Depth sub-bottom (m)	Shear strength (kPa)
8R-1	69	65.59	24.7608
8R-2	58	66.98	25.6612
9R-1	77	75.27	26.5616
10R-4	81	89.51	45.9200
11R-4	94	99.24	48.8204
12R-4	66	108.16	33.3145
12R-4	100	108.60	152.4820
13R-4	76	117.95	58.0342
14R-4	54	127.34	58.0342
15R-1	104	132.94	26.1723
16R-3	79	145.29	85.3445
17R-4	120	156.90	83.0686
18R-4	102	166.32	89.8962
19R-3	120	174.70	69.4135
19R-6	130	179.30	61.4480
20R-1	67	180.87	72.8273
20R-5	112	187.32	79.6548
20R-CC	7	189.60	72.8273
21R-1	100	190.80	87.6203
21R-3	113	193.93	52.3446
22R-2	36	201.56	73.9652
23R-2	29	210.89	47.7929
24R-3	66	222.36	136.5510
25R-3	10	231.50	73.9652

3. Physical Properties Unit 1-C: From 187 to 330 mbsf, the porosity decreases from 44% to 28.5% and the density increases from 1.99 to 2.29 g/cm³.

4. Physical Properties Unit 2 ranges from about 330 m to the bottom of the hole. It was not possible to distinguish clear sub-units. This unit is characterized by well-marked and constant

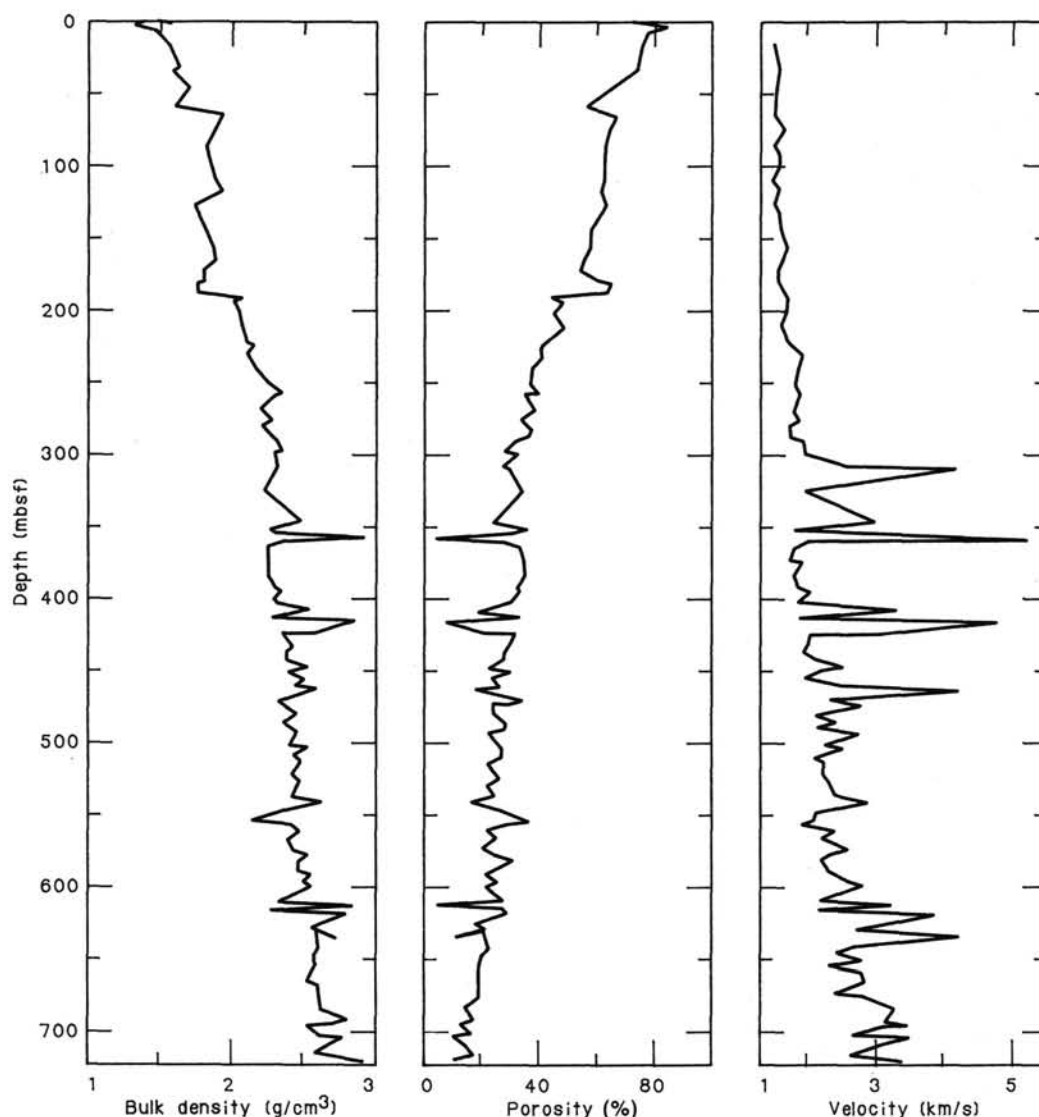


Figure 23. Bulk density, porosity, and velocity vs. depth at Site 652.

porosity and density trends, interrupted by isolated high and low data points. The porosity values range from about 36% at 330 mbsf to 13% at the bottom of the hole. The mean values are associated with clays. The low values (5%–15%) are associated with well-cemented sandstone, gypsum samples, and to one sample (at 610 mbsf) containing a high percentage (11%) of organic matter. The bulk density curve is symmetrical to the porosity curve; the mean values range from 2.19 to 2.60 g/cm³ and represent the clays. Here again, five to eight peaks correspond to measurements done on sandstone and gypsum samples. It has to be noted that the deepest measurements (between 680 and 721.1 mbsf) could define a third unit characterized by a variability of density and porosity.

The compressional-wave velocity plot shows also two main trends:

1. From the seafloor to about 300 mbsf the velocities measured on samples show a constant increase from 1.52 km/s at the mud line to 2.00 km/s at 298 mbsf.

2. Between 300 mbsf and the bottom of the hole; this trend is characterized by a steeper gradient. The measured velocities range from 2.0 to 3.3 km/s vs. depth. This interval is complex. We can

observe a majority of low values which were measured on clay-rich samples; these data constitute the body of the trend. A set of high values is superimposed to the trend and includes about 10 data points. These measurements correspond to cemented sandstones (as high as 4.2 km/s) and/or gypsum samples (as high as 5.2 km/s). Here again the deepest values, between 660 and 721.1 mbsf, suggest a possible third unit.

Shear Strength Measurements

Measurements were done between 65.6 and 231.5 mbsf (Fig. 24). The sediments were too disturbed and soft above 65.6 mbsf, and too indurated below 231.5 mbsf. The few data we have show an increase of shear strength vs. depth from 24.76 to 73.96 kPa. The two anomalously high values (152.48 kPa at 108.6 mbsf and 136.55 kPa at 222.4 mbsf) correspond to measurements on ash layers.

Thermal Conductivity

Thermal conductivity curve is plotted on Figure 24. Extensive discussion of these data will be found in the "Downhole Measurements" section, this chapter.

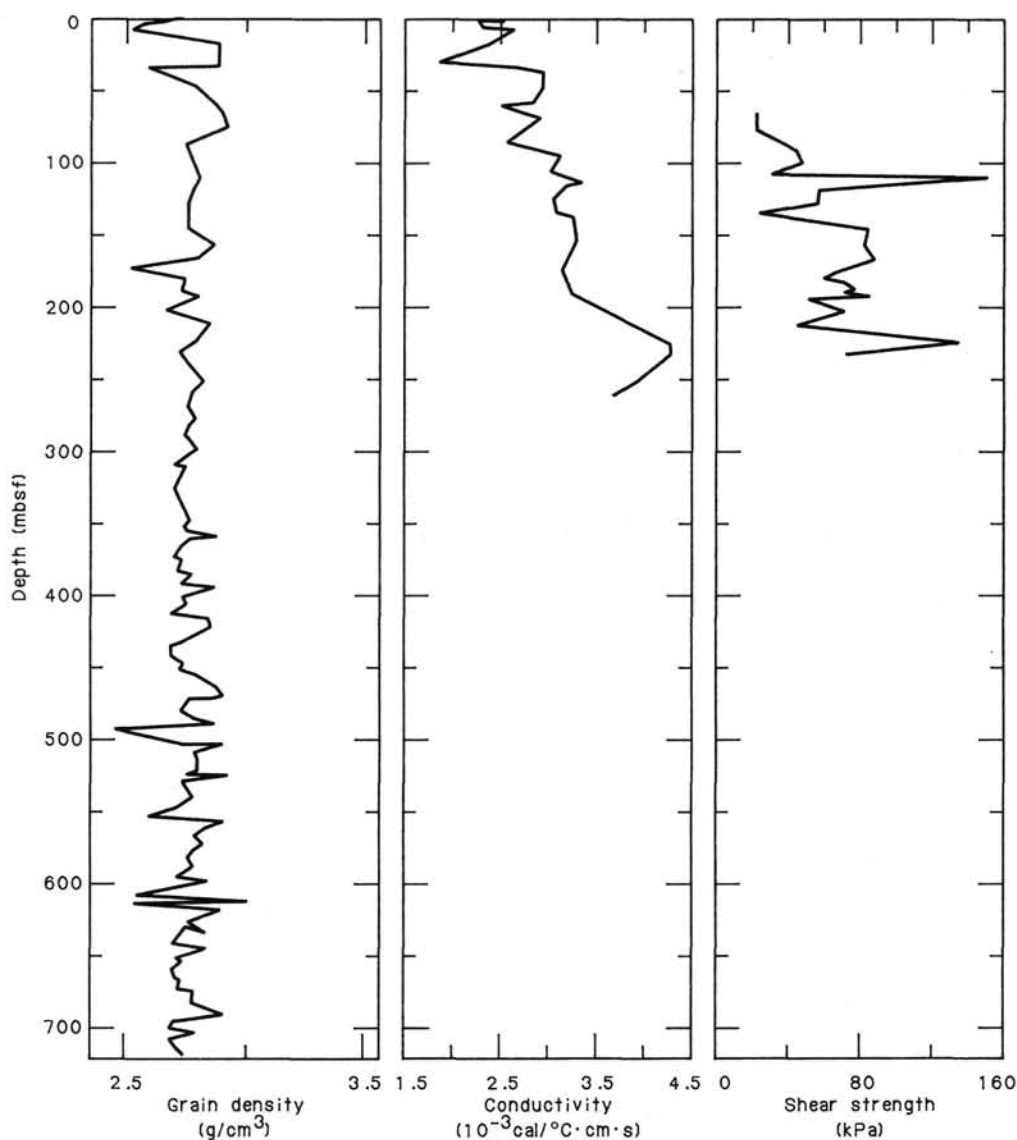


Figure 24. Grain density, thermal conductivity, and shear strength vs. depth at Site 652.

Discussion — Conclusion

The physical property measurements at Site 652 show a set of trends, units, and subunits which are in good agreement with both the lithology and acoustic stratigraphy.

Correlation with Lithostratigraphy

The physical properties analysis at Site 652 underlines the main lithologic units and their boundaries as follows:

1. Lithostratigraphic Unit I, from 0 to 55.4 mbsf (see "Lithostratigraphy" section, this chapter), correlates with a clear gradient of downhole decreasing porosity and increasing density.
2. Lithostratigraphic Unit II (55.4–188.2 mbsf) can be approximately correlated with our physical properties Unit 1-B. This unit is characterized by a decrease of density and of porosity. The base of this unit is underlined by a high porosity (64%).
3. The transition between lithostratigraphic Units II and IV is marked by an important change of density and porosity at about 190 mbsf which correlates well with the appearance of barren pre-Pliocene sediments ("Lithostratigraphy" section).

4. Lithostratigraphic Unit IV (188.6–344.8 mbsf) shows well defined porosity and density trends. The first important change of velocity also occurs near the base of this unit.

5. Lithostratigraphic Unit Va (344.8–721.1 mbsf) appears complex on the density, porosity, and velocity curves. Tentatively, seven or eight cycles could be identified. Each of them starts with a high velocity peak at 309.6, 358.1, 407.3, 415.8, 462.7, 541, 625.4, and 635.3 mbsf. The porosity and density also identify some of these levels. In a first interpretation, the physical properties seem to correlate with the second-order cycles observed in the lithology. The rich organic matter level (610 mbsf) is characterized by a low velocity, a low density, and a low porosity.

6. Lithostratigraphic Unit Vb (683.5–721.1 mbsf) is clearly observed in the physical properties and shows alternation of high and low values of porosity, density, and velocity. This can be explained by the diversified lithology observed in this unit.

Correlation with the Seismic Data

It is interesting to compare the velocity of each main interval defined in the site survey seismic lines with the average velocity measured on the cores:

1. The average laboratory-measured compressional velocity between the mud line and 215 mbsf is 1.636 km/s. This is 0.122 km/s higher than the 1.514 km/s velocity computed from the seismic data for Seismic Unit 1.

2. The velocities measured between 215 and 340 mbsf have an average of 2.089 km/s, which is comparable to the seismic velocity of Seismic Unit 2 (1.914 km/s).

3. The measured average velocity between 340 and 700 mbsf is 2.654 km/s, nearly the same as the computed velocities from the site survey seismic line (2.61 km/s) for Seismic Unit 3.

4. The deepest measurements (between 660 and 719 mbsf) have an average velocity of 3.315 km/s. This interval was not identified by the velocity analysis: Seismic Unit 4 is characterized, on the site survey line, by a low interval velocity (2.3 km/s). According to the correlations between the sedimentary units and the seismic line, this deepest unit was sampled at the site. The discrepancy, between computed velocities on the site survey line and measured velocities on discrete samples, has important consequences: either the computed velocity is right and the pre-rift unit was not sampled by Hole 652A, or, more likely, the pre-rift unit was sampled and the computed velocity will have to be re-evaluated.

GEOCHEMISTRY

Introduction

Using methods outlined in the explanatory notes, numerous carbonate and interstitial water analyses were performed on sediments of Site 652. These investigations cover all sedimentary units and nicely corroborate results obtained by other lines of investigation.

Carbonate Analyses

Data on carbonate content of sample splits are listed in Table 9 and displayed as depth curves in Figure 25.

In this plot two major units correspond to the Pliocene/Pleistocene succession (Cores 1R through 20R-6, 50 cm, 188.2 mbsf) and the Messinian(?) series in the underlying sediments down to a total depth of 720 mbsf: whereas the older, nonmarine facies of the Messinian average 20–30 weight % of CaCO_3 , the onset of fully marine conditions in the lower Pliocene led to the deposition of hemipelagic biogenic oozes averaging 50 weight % CaCO_3 . The contact between these units is fairly abrupt.

In the Pleistocene/Pliocene succession (Fig. 26) several second-order phases of carbonate sedimentation can be discerned. Most of these are of relatively short (less than 1 m.y.) duration, and in some instances correspond to coeval sediments exposed in classical land section in Sicily. Duration and interval have been specified by paleontological methods.

In land section in Sicily, sediments overlying the Messinian/Pliocene boundary are nannofossil chalks of the Trubi Formation (Decima and Wezel, 1973). In Hole 652, the equivalent time is represented by calcareous sediments in the depth interval of 110–188 mbsf. Sandwiched between two homogeneous layers of about 56% CaCO_3 , we found a thin layer between 136 and 144 mbsf, averaging only 35% CaCO_3 . This layer corresponds to a period of reduced sedimentation rate inferred from paleontological investigation (Fig. 26; see also "Biostratigraphy" section, this chapter). This observation implies that carbonate sedimentation is the determining factor in sedimentation rate for the Pliocene. In contrast, fluctuations in Pleistocene sedimentation rates appear to be unaffected by variability in carbonate sedimentation. Carbonate concentrations gradually decline from values around 50% to well below 30% in younger sediments with no apparent correlation with changes in sedimentation rate. Throughout the Pleistocene, the input of siliciclastic and volcanogenic components is the determining factor for sedimentation rates, as was the case for Sites 650 and 651.

Table 9. Carbonate and organic carbon at Site 652.

Sample	Depth (m)	CaCO_3 (%)	C_{org} (%)	Total N (%)	C/N
1-1, 0-2	0.0	25.30			
1-2, 0-2	1.5	26.64			
1-2, 51-52	2.0	25.42			
1-2, 115-117	2.6	23.89			
2-2, 41-47	5.5	19.55	0.01	0.00	—
2-2, 98-100	6.1	31.06	0.00	0.01	—
2-3, 30-31	6.9	30.51			
2-3, 119-120	7.8	6.65	0.43	0.08	5.4
2-4, 27-30	8.4	9.52			
3-1, 83-84	17.8	31.67			
3-1, 118-119	18.2	21.68			
3-2, 0-1	18.5	21.69			
3-2, 1-2	18.51	18.38	1.91	0.13	14.7
3-2, 18-19	18.7	8.29			
4-4, 80-81	32.0	26.98			
4-5, 40-43	33.1	32.28	0.03	0.07	—
4-6, 17-20	34.4	24.24	2.31	0.27	8.6
4-6, 22-24	34.45	24.62	1.72	0.13	13.2
5-1, 6-7	36.5	25.11	0.09	0.00	—
5-1, 27-28	36.7	42.77			
6-1, 33-35	46.1	24.80	0.02	0.09	—
6-1, 40-42	46.2	17.81			
6-1, 45-47	46.25	5.15	4.18	0.28	14.9
6-1, 53-55	46.3	17.81	3.50	0.36	9.7
6-1, 99-100	46.8	27.77	0.10	0.03	3.3
6-1, 111-114	46.85	25.65			
6-1, 133-134	47.0	36.11			
7-1, 21-22	55.6	41.99			
7-3, 1-2	58.4	33.99	0.05	0.03	—
7-3, 69-70	59.1	49.20			
7-3, 126-127	59.6	50.86			
7-4, 30-32	60.2	50.05	0.96	0.01	—
8-1, 56-57	65.45	43.89			
8-1, 61-65	65.5	37.60			
8-1, 113-115	66.0	23.23	3.30	0.03	—
8-3, 81-82	68.7	59.33			
9-1, 80-83	75.3	50.39			
9-2, 37-39	76.4	29.66	2.77	0.14	19.8
9-2, 96-99	77.0	28.11	3.11		
10-3, 100-103	88.2	43.28			
10-4, 81-82	89.5	49.31			
10-6, 140-143	93.1	55.78	0.01	0.10	—
11-3, 98-99	97.8	50.18			
11-5, 130-133	101.1	55.35	0.01	0.00	—
12-2, 78-79	105.3	47.80			
12-5, 105-108	110.1	53.03	0.01	0.00	—
13-1, 61-62	113.3	48.75			
13-3, 80-81	116.5	62.08			
13-3, 119-120	116.9	49.38	0.16	0.07	2.7
13-4, 20-23	117.4	55.53	0.00	0.00	—
13-4, 52-53	117.7	51.13			
14-1, 62-63	122.9	67.87			
14-2, 71-72	124.5	58.77			
14-3, 94-95	126.2	61.35	0.04	0.02	—
15-1, 136-137	133.3	53.98			
15-2, 19-20	133.6	54.40			
15-4, 18-19	136.6	62.08	0.09	0.02	4.5
15-4, 39-40	136.8	37.54			
15-5, 99-100	138.9	21.72			
16-2, 82-83	143.8	46.93			
16-3, 10-13	144.6	33.82			
16-4, 1-2	146.0	52.68	0.15	0.05	3.0
16-4, 66-67	146.7	65.86			
16-4, 73-74	146.8	65.78	0.00	0.08	—
16-5, 44-45	147.9	52.71			
17-2, 68-69	153.4	47.10	1.20	0.30	4.0
17-5, 113-114	158.3	57.46			
18-2, 46-47	162.8	53.77			
18-2, 80-81	163.2	58.27	0.06	0.06	—
18-3, 81-82	164.6	57.18			
18-4, 93-96	166.2	54.59			
18-5, 85-86	167.7	47.02			
18-6, 93-96	169.2	52.82			
19-1, 47-48	171.0	54.09			
19-2, 55-58	172.6	52.64			
19-4, 8-9	175.1	39.25	0.17	0.00	—
19-5, 61-62	177.1	44.54			
19-6, 137-140	179.4	59.31			

Table 9 (Continued).

Sample	Depth (m)	CaCO ₃ (%)	C _{org} (%)	Total N (%)	C/N
20-1, 71-74	180.9	45.79			
20-1, 100-101	181.2	46.33	0.45	0.05	9.0
20-5, 135-138	187.5	51.36			
20-6, 129-130	189.0	20.10			
21-1, 100-101	199.8	22.36			
21-2, 15-18	200.4	30.39	0.14	0.04	3.5
22-2, 25-28	201.5	19.82			
23-1, 100-101	219.1	29.18			
24-2, 83-84	221.0	27.65			
24-2, 93-94	221.1	20.91			
24-3, 63-66	222.3	21.69			
24-4, 9-10	223.3	24.17	0.15	0.21	—
24-4, 77-80	224.0	21.90			
24-4, 112-113	224.3	36.03			
25-1, 40-41	228.8	21.24			
25-1, 61-62	229.0	34.57			
25-1, 72-73	229.1	37.40	0.02	0.05	—
25-2, 14-18	230.0	23.13			
26-2, 40-41	240.0	24.14	0.08	0.08	—
26-2, 89-90	240.5	38.53			
26-2, 113-117	240.7	23.46			
26-c, 5-6	247.5	34.07			
27-1, 111-112	248.8	27.32	0.21	0.03	9.1
27-3, 1-2	250.7	23.67	0.19	0.03	6.3
27-3, 10-13	250.8	29.38			
28-1, 28-31	257.7	25.75	0.10	0.00	—
28-2, 7-10	259.0	34.93			
28-2, 99-100	259.9	24.19			
29-1, 121-122	268.3	28.45			
29-c, 8-11	276.4	27.85	0.01	0.00	—
30-1, 8-10	276.8	33.29			
30-3, 55-58	280.3	29.51	0.00	0.12	—
31-1, 143-146	287.7	34.89			
31-3, 89-91	290.2	36.01			
32-1, 66-67	296.6	24.37			
32-1, 97-98	296.9	23.82			
32-1, 98-99	296.95	25.14			
32-1, 112-113	297.0	38.42	0.00	0.00	—
32-2, 40-41	297.4	24.80			
32-2, 70-72	297.7	36.28			
32-2, 125-127	298.3	25.58			
33-1, 33-34	305.9	30.23			
33-3, 49-50	309.1	25.49	1.45	0.09	16.1
34-2, 50-51	309.9	33.31	0.69	0.02	34.5
34-2, 60-61	317.3	27.56			
35-1, 44-46	317.4	24.73	0.08	0.00	—
37-1, 49-50	344.8	12.80			
37-2, 94-96	346.7	22.33	1.10	0.00	—
37-6, 6-8	351.9	18.27			
38-1, 21-23	354.2	18.77			
38-4, 99-100	359.5	18.84			
38-5, 9-12	360.1	16.73	1.30	0.01	13.0
39-1, 28-29	364.0	27.32			
39-2, 6-8	365.3	23.42			
39-3, 81-82	367.7	23.31	0.25	0.05	5.0
40-1, 72-74	374.1	26.82			
40-4, 100-101	378.9	25.47			
40-5, 118-120	380.6	23.11	0.27	0.09	3.0
40-7, 33-35	382.7	22.37	0.26	0.00	—
41-1, 100-101	384.0	24.87	0.16	0.12	—
41-2, 50-52	385.0	20.25			
41-6, 30-33	390.8	23.43			
42-2, 27-29	394.5	12.53			
42-3, 61-62	396.3	29.77			
42-4, 144-146	398.6	37.93			
42-6, 49-50	400.7	16.20			
43-1, 48-52	402.9	39.12	0.00	0.00	—
43-1, 76-77	403.2	40.04			
43-4, 38-40	407.25	30.64			
43-4, 40-41	407.3	36.78			
44-2, 119-120	414.8	26.84	0.11	0.02	5.5
44-3, 93-96	416.0	21.61	0.36	0.02	18.0
45-1, 137-139	423.2	43.10	0.03	0.01	—
45-2, 62-64	423.9	22.08			
46-1, 60-62	432.1	26.72			
46-3, 55-56	435.1	18.87			
46-3, 100-102	435.5	19.29	0.69	0.01	—
47-1, 64-66	441.7	23.62	1.22	0.00	—

Table 9 (Continued).

Sample	Depth (m)	CaCO ₃ (%)	C _{org} (%)	Total N (%)	C/N
47-3, 97-98	445.1	15.24			
47-5, 32-34	447.4	37.50			
48-1, 8-10	450.8	31.63			
48-2, 37-38	452.6	17.53	0.15	0.00	—
48-3, 130-133	455.0	31.10			
49-1, 109-110	461.4	17.68			
49-2, 23-25	462.0	20.99			
49-2, 95-97	462.8	53.50			
50-1, 59-62	470.6	7.79	0.20	0.03	6.7
50-2, 47-48	472.0	24.58			
50-2, 85-86	472.4	5.90			
50-3, 9-11	473.1	24.2			
51-1, 13-15	479.7	34.20	0.09	0.00	—
51-1, 79-80	480.4	14.55			
51-4, 46-47	484.6	12.78			
51-5, 126-128	486.9	33.67			
51-6, 44-46	487.5	26.41			
52-1, 41-42	489.6	30.82			
52-2, 78-80	491.5	30.50			
52-3, 138-140	493.6	37.26			
52-4, 83-84	494.5	19.43			
53-1, 70-71	499.5	6.33			
53-3, 146-148	503.3	22.61	0.36	0.04	9.0
53-4, 14-16	503.4	34.61			
54-1, 39-40	508.9	25.12			
54-1, 96-98	509.5	25.73			
54-3, 119-120	512.7	17.98	0.18	0.08	—
54-3, 132-135	512.8	26.01	0.16	0.03	5.3
55-1, 60-61	518.7	22.65			
55-2, 60-61	520.2	23.98	0.80	0.10	8.0
55-3, 30-32	521.4	30.23			
55-5, 145-148	525.6	17.53			
56-2, 32-34	529.6	29.25			
56-6, 11-13	535.4	23.89	0.16	0.05	3.2
57-1, 26-28	537.7	29.25			
57-3, 62-64	541.0	43.93	0.15	0.03	5.0
57-3, 89-90	541.3	23.30			
57-3, 119-120	541.6	22.37			
58-1, 21-22	546.8	32.80			
58-1, 48-50	547.1	21.71	0.23	0.05	4.6
58-6, 30-32	554.4	3.96			
59-1, 7-9	556.4	27.03			
59-2, 140-150	559.2	7.19	1.00	n.d.	—
59-4, 18-20	561.0	21.57			
60-1, 16-18	566.2	15.60			
60-1, 87-88	566.9	27.1	0.26	0.08	3.2
60-3, 100-101	570.0	23.70			
60-5, 106-108	573.1	3.18			
61-1, 146-148	577.1	12.11			
61-2, 2-4	577.15	21.33			
61-2, 100-101	578.1	26.82			
61-2, 106-107	578.15	37.94	0.00	0.04	—
61-5, 90-91	582.5	26.94			
62-3, 91-92	589.1	24.43	0.14	0.16	—
62-4, 112-114	590.8	12.21			
63-2, 139-140	597.8	25.54	0.13	n.d.	—
63-3, 40-42	598.3	2.07	1.98	0.40	5.0
64-1, 23-24	604.7	37.51	0.55	0.00	—
64-1, 92-94	605.4	17.58	10.22	0.67	15.3
64-1, 103-104	605.5	16.25	11.41	0.39	29.3
64-1, 104-111	605.55	1.21	8.45	0.38	22.2
64-1, 104-107	605.57	18.28	9.57	0.24	39.8
64-3, 0-1	607.5	6.23	0.40	n.d.	—
64-3, 22-23	607.7	30.46	0.00	0.07	—
64-3, 59-61	608.1	44.75	0.14	0.00	—
64-4, 2-4	609.0	50.53			
65-2, 9-11	615.8	19.15			
65-2, 55-57	616.3	16.81			
65-2, 77-79	616.5	35.83			
65-2, 91-94	616.6	10.78			
65-2, 109-111	616.8	16.43			
65-4, 2-4	618.7	9.61			
65-6, 105-108	622.8	17.30			
66-1, 90-92	625.4	37.88	0.60	0.18	3.4
66-3, 24-25	627.7	22.62			
66-3, 119-120	628.7	21.93	0.25	n.d.	—
67-1, 107-109	635.3	18.65	3.58	0.19	18.9
67-2, 77-78	636.5	29.43			

Table 9 (Continued).

Sample	Depth (m)	CaCO ₃ (%)	C _{org} (%)	Total N (%)	C/N
67-5, 144-146	641.6	17.34			
68-1, 2-4	653.4	45.55	0.53	0.11	4.8
68-1, 24-25	644.0	15.18			
68-1, 146-148	645.3	19.69	1.57	0.12	13.0
69-3, 47-48	656.9	14.70			
69-4, 70-72	658.6	24.54			
70-2, 64-66	665.2	20.96	0.39	0.13	3.0
70-3, 119-120	667.3	19.43	0.22	n.d.	—
70-4, 24-26	667.8	37.3			
71-1, 78-80	673.6	21.47	0.19	0.14	—
71-2, 45-47	674.8	23.70			
72-1, 24-25	682.7	12.05			
72-1, 54-56	683.0	31.77			
72-2, 55-57	684.6	34.62			
72-2, 80-82	684.9	9.83	3.51	0.14	25.0
73-1, 70-71	692.9	28.47	0.64	0.22	3.0
73-2, 119-120	694.9	38.01	0.02		
73-3, 99-100	696.2	24.15	0.11	n.d.	—
74-1, 4-6	701.9	17.92			
74-2, 54-56	703.9	33.99			
74-4, 0-1	706.4	16.73	0.78	n.d.	—
74-4, 97-98	707.4	7.87			
74-5, 52-54	708.4	21.95			
75-c, 1-2	720.0	41.28	0.06	n.d.	—

In sediments of inferred Messinian age carbonate concentrations cluster around 20% CaCO₃ with major fluctuations resulting from grain size effects: Coarse grained siltstones and sandstones apparently are more calcareous due perhaps to a higher contribution of allochthonous carbonate (as much as 50%), while mudstones and claystones range from 10% to 20% CaCO₃. The carbonate content of Messinian(?) sediments is further discussed in "Downhole Measurements" section, this chapter.

Interstitial waters

The presence of nonmarine facies underlying the marine series of Pliocene/Pleistocene age leaves a distinct imprint on the chemistry of interstitial waters obtained from sediments of all ages (Table 10, Fig. 27). Whereas in preceding holes of this cruise diagenesis of authigenic and allochthonous minerals determined the composition of the pore fluid, concentration gradients in Hole 652A are best explained by assuming dissolution of evaporitic minerals at depth, and subsequent migration along concentration gradients toward the seawater/sediment interface. In comparison, effects of dolomitization on Mg²⁺ and Ca²⁺ content, of sulfate reduction, and of neoformation of silicates are not readily discernible, and the shapes of the respective curves suggest an almost conservative behavior. In depth plots of major ions, concentrations of salinity-related components (calcium, magnesium, chlorinity, and sulfate) reach a maximum at about 495 mbsf. This interval corresponds to a maximum depth of occurrence of abundant evaporitic sulfate minerals in the recovered sediments. From the shape of the individual curves with depth, we can formulate some preliminary hypotheses about: (1) flux of components from the underlying salts to the deep water body overlying this site, (2) suggest mineral species present in the evaporite-bearing zone, and (3) get some ideas about changes in physical properties at the Messinian/Pliocene boundary. These hypotheses have to be verified by more detailed studies in subsequent investigations.

The most prominent ions are Cl⁻ and Ca²⁺ with concentrations of 1430 mmol/L and 238 mmol/L, respectively, at a depth of approximately 560 mbsf. SO₄²⁻ concentrations deviate little from a mean value of about 26 mmol/L. The most abundant

mineral of evaporite facies is anhydrite at this depth. According to Manheim and Sayles (1974), a reasonably straight gradient of any one ion in concentration/depth curves suggests that time since emplacement of salt was long enough and subsequent sedimentation was slow enough to permit equilibration between diffusion/compaction and dissolution at depth. A simple formula permits calculating the flux of a component along this gradient:

$$F = -K \frac{dc}{dx}$$

where K is the diffusion coefficient of a given component (in the case of Cl⁻, K = 3 × 10⁻⁶ cm²/s), dc is the difference in concentration between seawater and pore water at 560 mbsf (i.e., 230 mmol/L), and dx is the path length, that is the thickness of overlying sediments (56,000 cm). The resulting flux of Cl⁻ to the lower water column overlying the sediments thus amounts to about 1.6 × 10⁻⁸ mmol/L Cl⁻/s/cm².

From the shape of the magnesium depth plot, we may infer that magnesium concentrations also are controlled by dissolution of evaporite minerals and are little affected by diagenetic uptake by carbonates and silicates along the path. Considering the ample supply of magnesium from below, we can expect that dolomitization and smectite formation in the overlying sediments has reached an equilibrium. X-ray diffraction studies may be a suitable means for verifying this. Possible magnesium-bearing candidates for dissolution are the minerals kieserite (MgSO₄ · H₂O) and certain magnesium halides, but their presence in the Messinian sediments of this depth (560 mbsf) has yet to be confirmed. The steady concentration curve for samples underlying sample 652-51R-4, 140-150 cm suggests that this interval indeed corresponds to the peak of evaporite facies evolution in the sequence studied here.

In the case of chlorinity and magnesium, we observe no gradient in samples overlying the Messinian/Pliocene boundary at approximately 180 mbsf. In samples overlying this boundary, straight lines connect the concentrations with that of the seawater/sediment interface.

Organic Geochemistry

Hole 652A provided samples of elevated organic carbon content in the Pleistocene as well as in the Messinian(?) succession. In the first case, sapropels of a few centimeters thickness (see "Lithostratigraphy" section, this chapter) with organic carbon concentrations greater than 2% were encountered in Samples 4R-6, 17-20 cm (34.4 mbsf); 6R-1, 45-55 cm (46.3 mbsf); 8R-1, 113-115 cm (66.9 mbsf); 9R-2, 37-39 cm (76.5 mbsf); and 9R-2, 96-99 cm (77.0 mbsf) (see Table 9). If we assume a linear sedimentation rate on the order of that computed for over- and underlying sediments (about 5 mm/1000 yr), most of these layers must have been deposited over several hundreds of years in an environment of reduced benthic activity.

Invariably, these organic-matter-rich strata are sandwiched between organic-matter-lean sediments. Average values of C_{org} content for hemipelagic background sediment are only 0.1% C_{org} by unit weight, whereas an average of nine sapropelic samples yielded 2.8% C_{org} (see Fig. 28).

The lower contact appears to be gradational in some cases, with reciprocal concentration of mineral carbon and organic carbon accompanying the lithological changes. In other instances, graded bedding and sharp basal contacts are found. Thus, these sapropels are very similar to the ones described from previous DSDP sites throughout the eastern Mediterranean (Kidd et al., 1978).

Using an empirical relationship between organic matter content, benthic consumption, and sedimentation rate (Mueller and

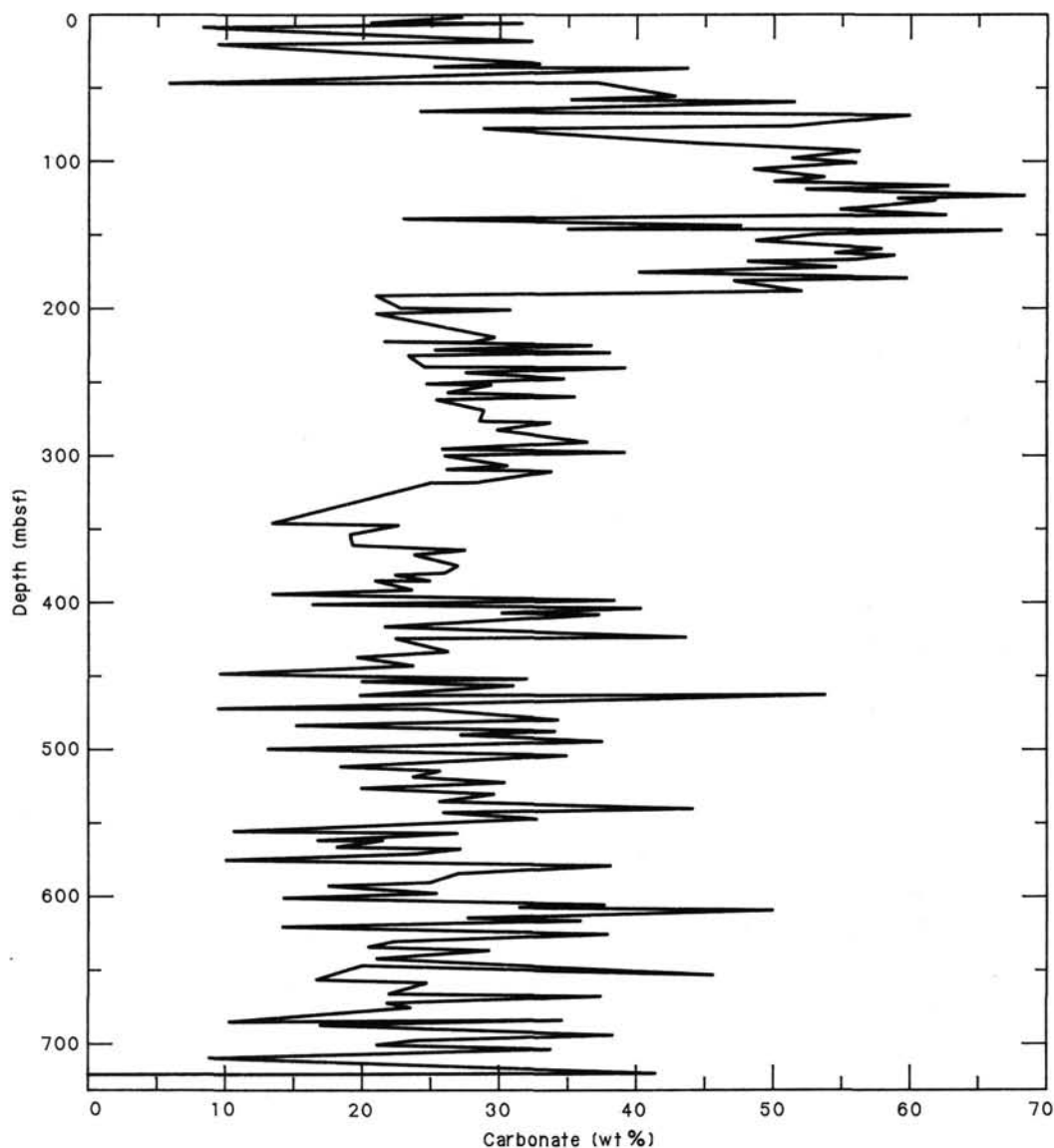


Figure 25. Plot of weight % CaCO_3 vs. depth for Hole 652A.

Suess, 1979), we can roughly estimate the amount of primary production in the euphotic zone of the overlying water column for various times within the Pleistocene and Pliocene: $PP = C \times (D(1-P)/0.003 S^{0.3})$; where PP = primary productivity ($\text{gC}/\text{m}^2/\text{yr}$), C = weight % C_{org} , D = grain density, P = porosity, and s = linear sedimentation rate in $\text{cm}/1000$ yr. This relationship is valid only for hemipelagic sediments.

Values thus computed for the background values of the Pleistocene and Pliocene succession indicate relatively low productivity, ranging from a minimum of $2 \text{ gC}/\text{m}^2/\text{yr}$ at the top of the Pliocene to $86 \text{ gC}/\text{m}^2/\text{yr}$ in the lowermost Pliocene. Recent primary production over the continental margins of the Mediterranean Sea is in the range of $100 \text{ gC}/\text{m}^2/\text{yr}$ (Romankevich, 1984).

Organic carbon concentrations in the pre-Pliocene nonmarine sediments drilled from about 188 mbsf to the total depth of 721 mbsf were found to contain elevated values when compared to the marine succession. An average of 0.34% C_{org} was computed for the background lithology, with a relatively high standard deviation of 0.39. With respect to background lithology, we assume that, in analogy to modern lacustrine or marginal marine sediments, organic carbon concentrations may be as high

as 1% without requiring anaerobic conditions in the lower water column (Demaison and Moore, 1980).

On the other hand, anaerobic conditions were most likely established during the deposition of sediments in Core 64R (604.5–614.2 mbsf). Section 1 of this core contains an approximately 50-cm-thick interval of laminated, petroliferous oil shales with a maximum $\%C_{\text{org}}$ of 11.4% . These “paper shale”-like sediments are laminated on a millimetric scale and consist of alternations of organic and inorganic layers resembling varves or certain bog-head deposits. In these sediments, aquatic euryhaline algae—most notably of colony-forming chlorophyceae related to the genus *Botryococcus braunii*—were deposited as distinct layers and could be indicative of massive blooms in highly productive surface waters. Intercalations of clastic sediments represent times of lower surface productivity or increased input of clastics. The excellent preservation of these fine laminations (Fig. 29), the extremely high organic carbon content, and the nature of the organic matter (see below) suggest a restricted and possibly brackish, highly productive, anoxic basin equivalent to the famous Green River Formation of the Western Interior of the United States and the Messel oil shale in Germany. This kind of envi-

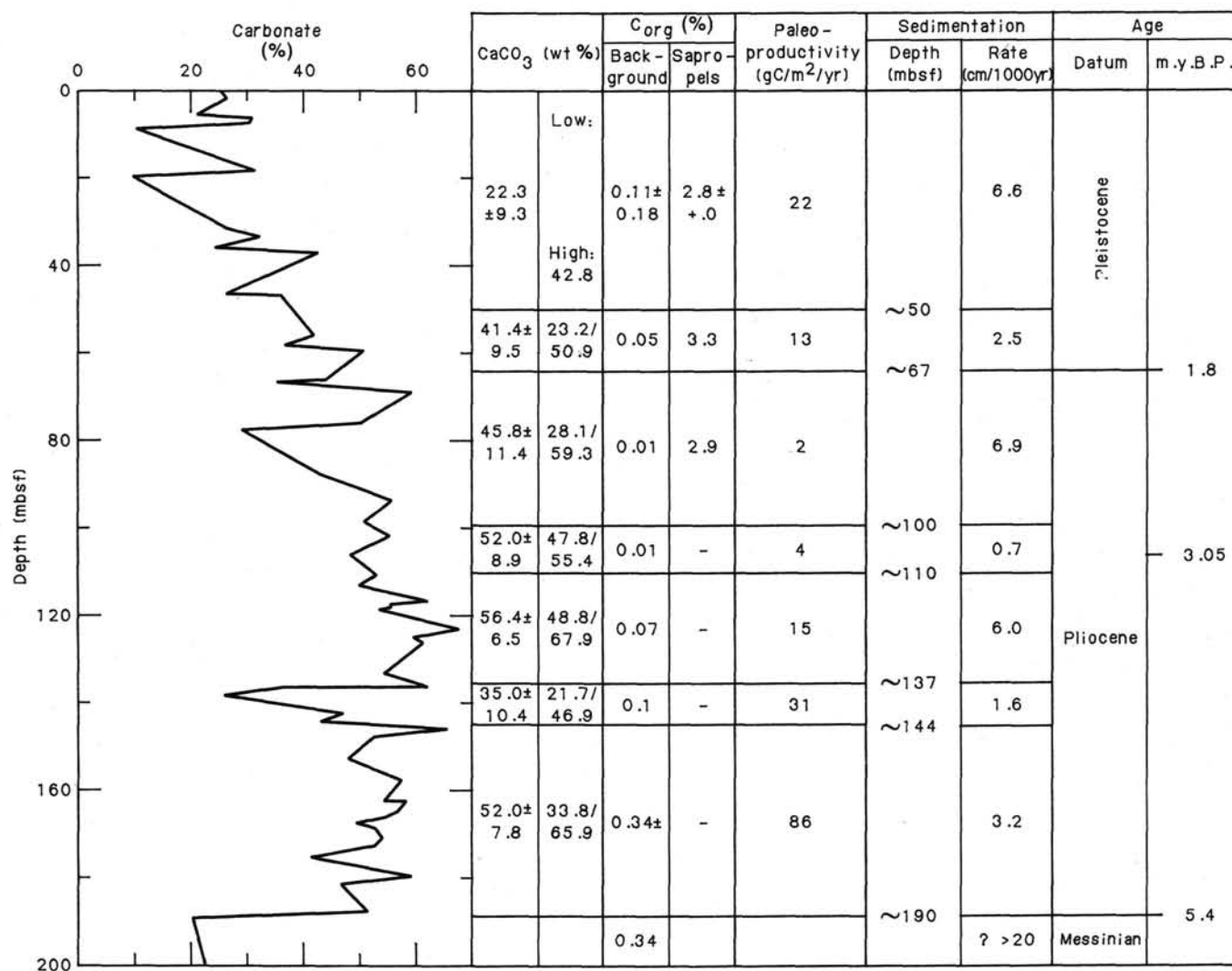


Figure 26. Plot of weight % CaCO₃ vs. depth for the Pliocene/Pleistocene interval of Hole 652A. Average values for individual components were computed for sedimentary units or paleontological units (see Fig. 15). Average C_{org} % were computed without sapropel values to give values of background lithologies. Also given is a computed value for paleoproductivity based on sedimentation rate and organic carbon content (see text for explanation).

Table 10. Summary of interstitial water analyses from Site 652.

Sample no.	Depth	Sal.	Alk.	pH	Cl ⁻	SO ₄ ²⁻	Ca ²⁺	Mg ²⁺	Ca/Mg
Surface	0.0	39.0	2.39	8.19	608	29.7	6.8	64.8	0.11
1R-1, 140-150	1.4	37.9	3.17	7.72	614	30.1	15.4	62.5	0.25
9R-1, 140-150	75.9	38.5	2.89	7.43	645	24.5	17.9	59.0	0.30
14R-3, 140-150	126.7	n.d.	2.33	7.33	625	23.6	26.9	57.8	0.47
20R-5, 140-150	187.6	45.0	1.98	7.35	673	22.6	44.9	56.7	0.79
25R-1, 140-150	229.8	47.0	2.38	7.12	770	25.9	63.1	56.2	1.12
30R-2, 140-150	279.6	n.d.	2.68	7.22	842	28.2	70.7	67.2	1.05
38R-4, 140-150	359.9	65.0	n.d.	7.26	998	27.9	104.9	67.9	1.54
43R-5, 140-150	409.8	70.5	1.72	6.90	1080	26.9	131.4	82.7	1.59
51R-4, 140-150	485.5	95.0	n.d.	n.d.	1428	25.4	237.7	95.2	2.50
59R-2, 140-150	559.2	82.5	2.02	6.87	1368	25.1	176.0	75.9	2.32
64R-2, 140-150	607.4	82.0	2.40	7.21	1323	21.8	171.9	74.0	2.32

Chemical analyses of interstitial water samples, Leg 107/Hole 652A. Sample no.: Hole 652A, Core-Section, Interval. Depth is given in meters below seafloor. Sal.: Salinity in parts per thousand; Alk.: Alkalinity in mmol/L; Cl⁻, SO₄²⁻, Ca²⁺, Mg²⁺ are given in mmol/L. n.d. = not measured.

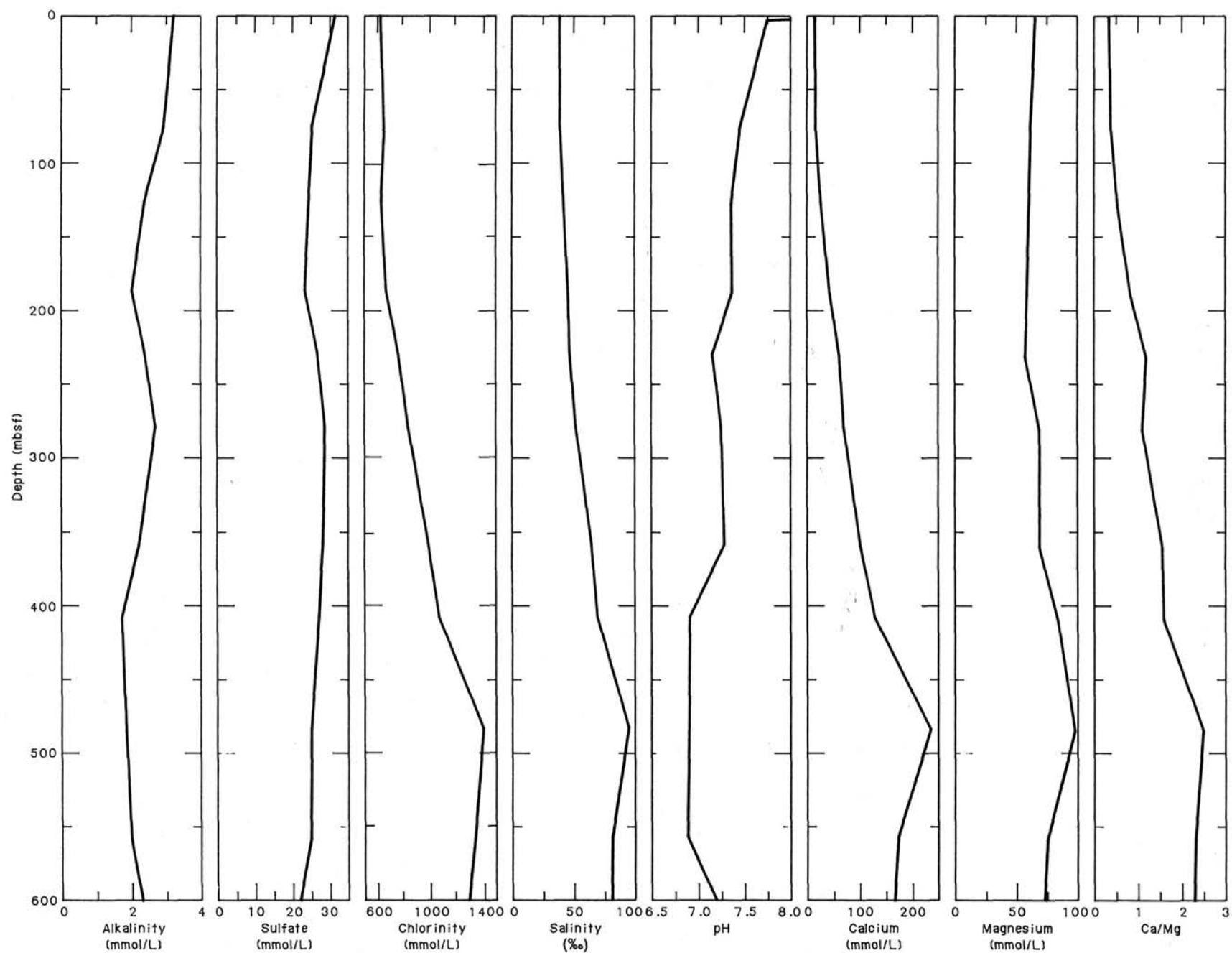


Figure 27. Plot of major ions, pH, salinity, and Ca/Mg ratios vs. depth in interstitial waters of Hole 652A.

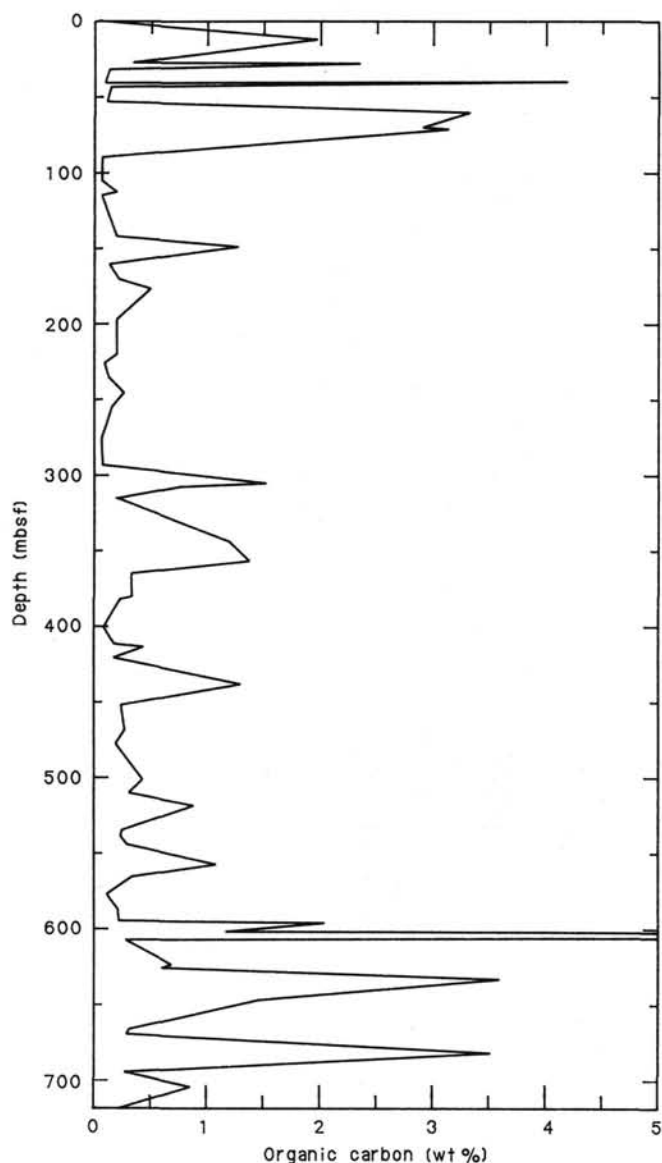


Figure 28. Weight % organic carbon vs. depth, Hole 652A.

ronment, found today in saline lakes like the Great Salt Lake of Utah, is commonly associated with evaporitic facies.

Sediments containing enough kerogen type I, lipid-rich with abundant aliphatic chains, are regarded as excellent oil source rocks. The sediments drilled in this interval may indeed be an ideal oil source rock as verified by the results of downhole gas monitoring and gas chromatography performed on the saturated fraction of a methanol/toluene total extract of this rock. These results are presented and briefly discussed in the following section.

Hydrocarbon Extracts

We extracted the soluble organic matter of seven samples of Pleistocene and Messinian age in order to (1) get an idea of the provenance and the thermal maturity of organic matter in organic-carbon-rich sediments, (2) contrast these organic-carbon-rich sediments with adjacent lean sediments, and (3) reconstruct environments of deposition with the emerging geochemical fingerprints. (Methods used are described in the "Explanatory

Notes" section, this volume.) Results are given in Figure 30 and Table 11.

Preliminary evaluation of geochemical fingerprints suggest that Pleistocene sapropels of Hole 652 are immature and contain a mixture of marine and continental lipids. In the case of Sample 4R-6, 17 cm and 6R-1, 40 cm, anoxic conditions in the environment of deposition are indicated by low pristane/phytane ratios. In contrast, the organic-matter-rich Sample 6R-1, 53 cm, separated by a few centimeters from the latter, suggests dominant preservation of marine derived organic matter under oxic conditions.

Two samples of Messinian age were particularly interesting because a thermal gradient flow of $14^{\circ}\text{C}/100\text{ m}$ (see "Down-hole Measurements" section, this chapter) led to thermal cracking of oil precursors and resulted in the formation of considerable amounts of *n*-alkanes in these sediments. Sample 59R-2, 140 cm at 560 mbsf represents Messinian background lithology in spite of its relatively high C_{org} content of 1%. The saturated hydrocarbons are dominated by medium length *n*-alkanes with a maximum at *n*- C_{22} . Thermal evolution removed all traces of odd-even predominance inherited from organic source material. Judging from the pristane/phytane ratio of 1.4, the environment of deposition was oxic. In contrast to this finding for the background lithology, extracts of Sample 64R-1, 103 cm, are characterized by short chain *n*-alkanes with a maximum at *n*- C_{15} and a low pristane/phytane ratio of 0.3. This suggests an aquatic source of kerogen and pronounced anoxia in the sediment. Safety of the JOIDES Resolution was never at stake during drilling as this oil-shale-bearing interval was only about 50 cm thick.

C_1 – C_5 Hydrocarbons Measured at Site 652

Site 652 was never considered a safety hazard, because of the minor overall quantities of gas recovered. The gas did, however, show a distinct trend which can be related to thermal maturation of the sedimentary organic matter. No gas was found in sediments shallower than 115 mbsf. Analysis of vacutainers yielded extremely minor quantities of gas throughout the entire hole. No gas pockets were observed through the core liner, so the lack of free gas was not surprising. Of more interest were the results of the headspace analysis. At approximately 115 mbsf small amounts of methane (approximately 2–3 ppm/10 cm³ of sample) were measured. Low amounts of C_1 were present in all samples taken below this depth, while hydrocarbon gas of higher molecular weight was not detected until approximately 380 mbsf. At this depth, the amount of C_1 in the sediment began to increase and small amounts of C_2 through C_4 were measured (see Table 12 and Fig. 31). Quantities of C_1 through C_4 continued to increase with depth. At 475 mbsf C_5 became measurable as well.

With regard to safety, a decrease in the ratio of C_1 to the combined quantities of C_{2+} is of more consequence than an increase in overall values with depth. In the safety monitoring procedures of ODP, potential hazards from accumulations of hydrocarbon gases are evaluated by the ratio C_1/C_{2-5} (Emeis and Kvenvolden, 1986). Vacutainer studies have characterized gases with ratios greater than 1000 to be of biogenic origin, and those less than 50 to be of thermogenic origin (Simoneit, 1982). Although the actual delimiting values from vacutainer studies cannot be directly related to the values of the ratios attained from headspace analysis, preliminary investigation of the two methods suggests a higher resolution of the headspace technique in sediments of low overall gas concentration (compare Figs. 31 and 32). While vacutainers contain a comparably higher proportion of volatile methane, thermal heating during the headspace technique desorbs gas of higher molecular weight adsorbed to sediment particles. Further studies are necessary to confirm this finding.

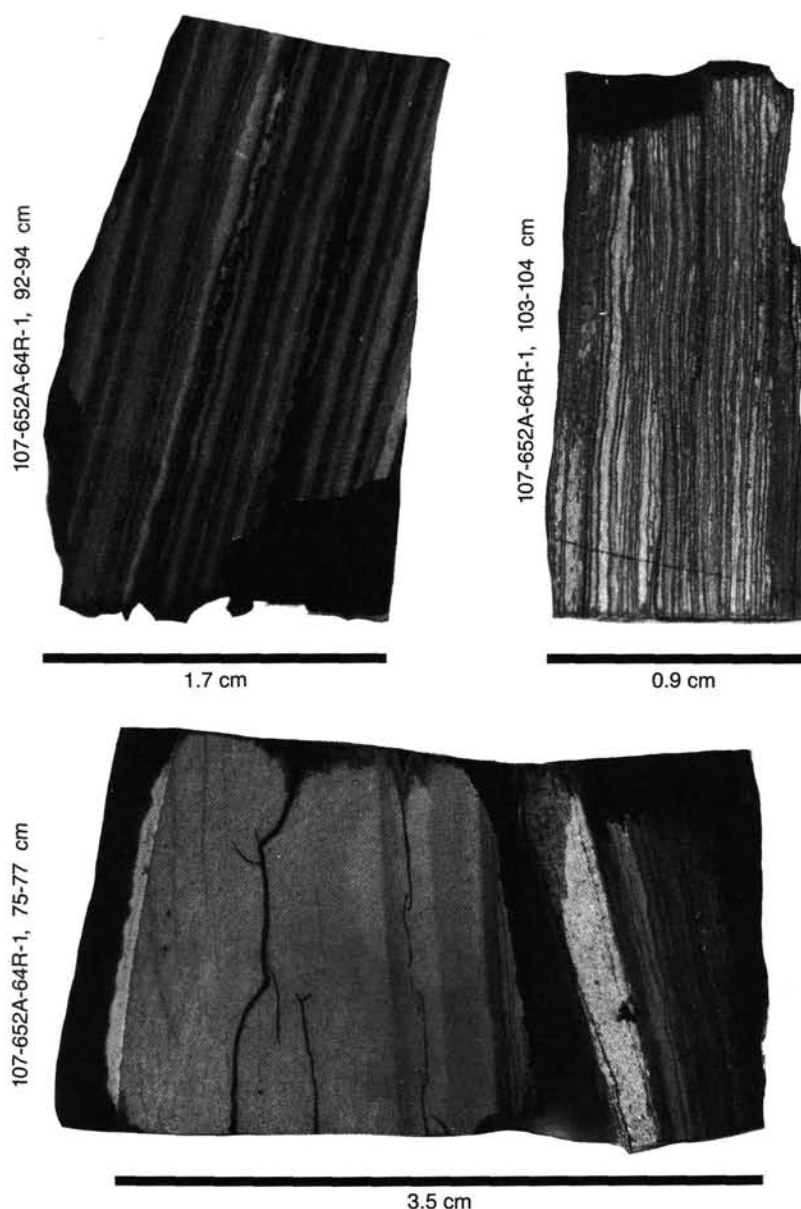


Figure 29. Close-up photographs of Messinian oil shales. Note fine-scale lamination of organic and lithic components.

Once C_{2+} was present, the ratios determined from headspace analysis were always very low and continued to decrease as the highly organic-carbon-rich sequence, beginning at approximately 600 mbsf, was approached (Fig. 29). Quantities of the individual gases also increased.

The low quantities of C_1 in the upper sediments, the low, decreasing C_1/C_{2-5} ratio, and the increasing quantities of C_2 through C_5 indicate that these gases were formed thermogenically and migrated away from the source. The largest quantities of C_2 through C_5 and the lowest ratio C_1/C_{2-5} are associated with the high concentration of organic matter at approximately 600 mbsf, suggesting that this material might be the source of the hydrocarbons. Thermal genesis of organic matter begins between 60°C and 100°C and will yield significant amounts of C_2 through C_6 (Hunt, 1979). Furthermore, the rate of generation approximately doubles when the temperature increases by 10°C (Waples, 1982). At Site 652, the *in-situ* temperature at the depth of the organic-rich sediments is close to 100°C and the thermal

gradient was measured at 14°C/100 m. The thermal conditions at Site 652 are well within the requirements for a thermogenic origin of the sampled hydrocarbon gases. Further confirmation for thermal maturation are the increasing $i-C_5/n-C_5$ values. High values of $i-C_5/n-C_5$ have been shown to correlate well with increasing thermal conditions (Whelan and Hunt, 1982).

SEISMIC STRATIGRAPHY

Site 652 is located on the easternmost tilted block of the lower Sardinian continental margin at shotpoint 4250 on MCS line ST01 (Fig. 7, "Background and Objectives" section, this chapter). Line ST01 and previous single-channel seismic lines show a good penetration of about 1.2 s below seafloor. The section comprises a series of acoustic units well differentiated by high-amplitude reflectors (Fig. 7). At Site 652 five seismic units separated by strong reflectors can be distinguished before a basementlike reflector at about 1.2 s bsf (Fig. 33).

Table 11. Characteristics of saturated hydrocarbon extracts, Site 652.

Sample	Depth (m)	T(°C)	C _{org} %	Pr/Ph	Pr/C17	C29/C17	CPI	Remarks
2-2, 40	5.5	13	0.01	11.1	1.0	0.1	1.1	Immature marine OM, oxic
4-6, 17	34.4	16	2.31	0.7	1.1	0.9	2.0	Immature mixed OM, anoxic (?)
6-1, 33	46.1	18	0.02	0.8	0.9	0.3	1.3	Immature marine OM, anoxic (?)
6-1, 40	46.2	18	4.18	0.5	1.2	1.9	0.9	Immature terrigenous/marine, anoxic
6-1, 53	46.3	18	3.50	7.2	0.9	0.2	1.3	Mixed, maturing OM, oxic
59-2, 140	559.2	90	1.00	1.4	0.5	1.2	1.1	Mature, mixed OM, oxic
64-1, 103	605.5	96	11.41	0.3	0.1	0.2	1.3	Mature, aquatic OM, anoxic

T(°C) = *In-situ* temperature, extrapolated from thermal gradient of 14°C/100 m; CPI = Carbon Preference Index = $2(n\text{-}C_{29}) / (n\text{-}C_{28} + n\text{-}C_{30})$; ratios of individual compounds computed by peak integration after manual background correction.

Table 12. Quantities of measured hydrocarbon gases, Site 652.

Depth	C ₁	C ₂	C ₃	n-C ₄	i-C ₄	n-C ₅	i-C ₅
Headspace analysis (ppm/10 cm ³ of sample)							
117.2	3.0	0.0	0.0	0.0	0.0	0.0	0.0
147.5	3.6	0.0	0.0	0.0	0.0	0.0	0.0
178.0	1.8	0.0	0.0	0.0	0.0	0.0	0.0
250.7	3.0	0.0	0.0	0.0	0.0	0.0	0.0
380.9	62.7	9.0	7.9	5.0	4.7	0.0	0.0
473.0	131.5	12.5	8.3	2.9	2.2	0.0	1.0
513.0	159.0	25.0	24.0	5.0	9.4	4.0	4.0
541.9	175.8	33.2	44.4	12.9	12.4	5.1	2.7
559.3	386.0	47.0	87.0	66.0	105.0	28.0	82.7
607.0	513.5	76.6	142.6	95.4	167.5	30.2	107.8
629.0	224.0	54.5	145.6	215.0	129.1	49.7	250.0
667.0	894.0	137.0	209.0	72.0	19.0	2.0	1.0
695.2	297.7	40.3	42.2	12.7	23.1	4.1	6.5
705.0	977.7	105.1	77.3	17.9	32.3	5.3	7.6
Vacutainer analysis (ppm per volume)							
378.0	5.0	0.0	0.0	0.0	0.0	0.0	0.0
385.0	0.8	0.0	0.0	0.0	0.0	0.0	0.0
405.0	5.0	0.0	0.0	0.0	0.0	0.0	0.0
415.0	3.0	0.0	0.0	0.0	0.0	0.0	0.0
483.0	16.8	1.1	0.0	0.0	0.0	0.0	0.0
493.0	2.5	0.0	0.0	0.0	0.0	0.0	0.0
511.0	6.5	0.0	0.0	0.0	0.0	0.0	0.0
549.0	27.7	6.0	5.9	1.3	0.8	0.9	0.3
618.0	205.6	10.5	9.1	7.1	3.9	0.0	5.9
627.0	208.5	12.9	13.4	0.0	9.5	3.8	4.0
637.0	171.6	5.2	3.7	1.4	2.1	0.0	0.0
647.0	184.0	5.8	4.4	1.8	2.3	0.0	0.0
696.0	160.0	7.2	5.5	0.0	1.8	0.0	0.0
705.0	198.5	5.6	3.9	0.0	1.6	2.4	0.0

Seismic Unit One

Seismic Unit One extends from the seafloor to the top of a series of high-amplitude reflectors. Numerous small vertical displacements are seen at the bottom of the unit. Unit One is about 0.29 s thick at Site 652. Interval velocity is 1.514 km/s. This indicates that the base of Unit One should be at about 215 mbsf. Toward the west Unit One thickens slightly. Maximum thickness is 325 m. Unit One contains a few discontinuous high-amplitude reflectors indicating probable coarser layers. Several small unconformities can also be detected within Unit One. The most obvious lies at about 115 mbsf.

Seismic Unit Two

This unit is bounded by two high-amplitude reflectors. The thickness maintains an average value of 0.13 s. The interval velocity is 1.914 km/s; thickness should therefore be about 125 m. This indicates that the base of Unit Two lies at 340 mbsf. The basal reflectors of Unit Two, like those of Unit One, show numerous small vertical displacements (with an average offset of 15–20 m). This indicates probable tectonic activity or a slightly flowing underlying layer. Laterally toward the west, Unit Two changes its acoustic character and thickens.

Seismic Unit Three

At Site 652 this unit shows a thickness of 0.28 s. Assuming an interval velocity of 2.61 km/s, the total thickness of the unit should be about 360 mbsf. Its base lies at about 700 mbsf. The basal reflectors of Unit Two as well as the uppermost reflectors of Unit Three have very high amplitudes and show an irregular surface, possibly indicating erosion. Toward the west, Unit Three thickens and changes in seismic characteristics (Figs. 7 and 33). In the axis of the half-graben, seismic Unit Three contains a feature which can be considered typical of flowing material. The interval velocity gives a value of 3.4 km/s in this sedimentary body which could reflect the presence of evaporites.

Seismic Unit Four

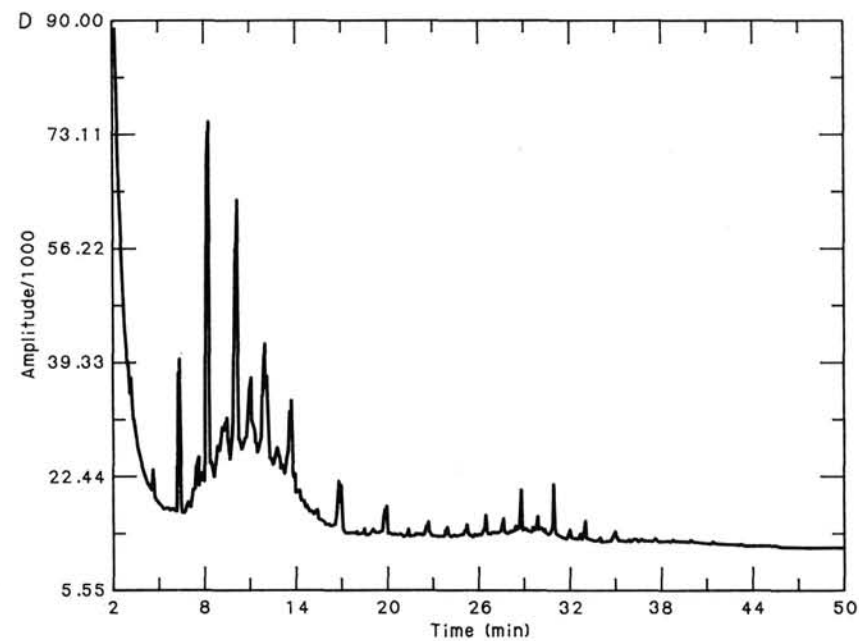
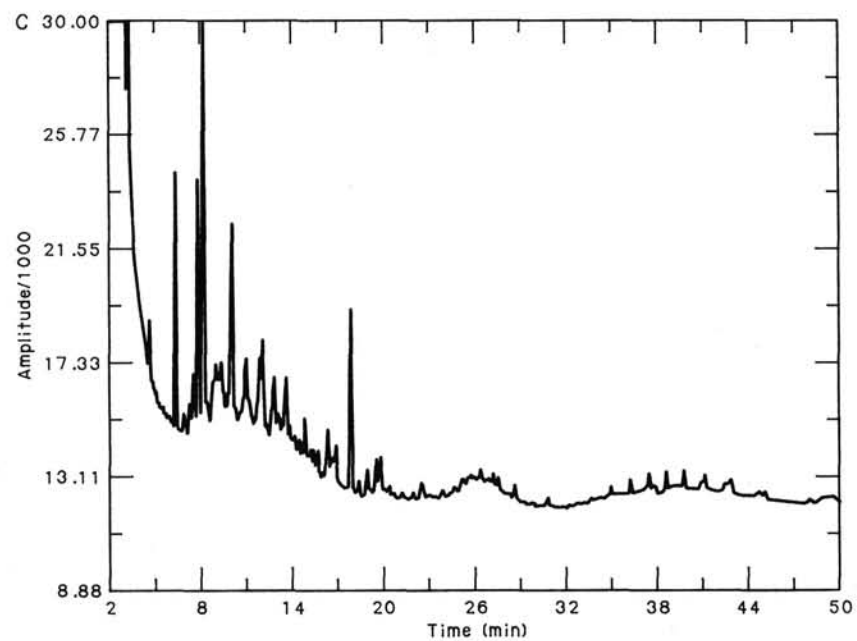
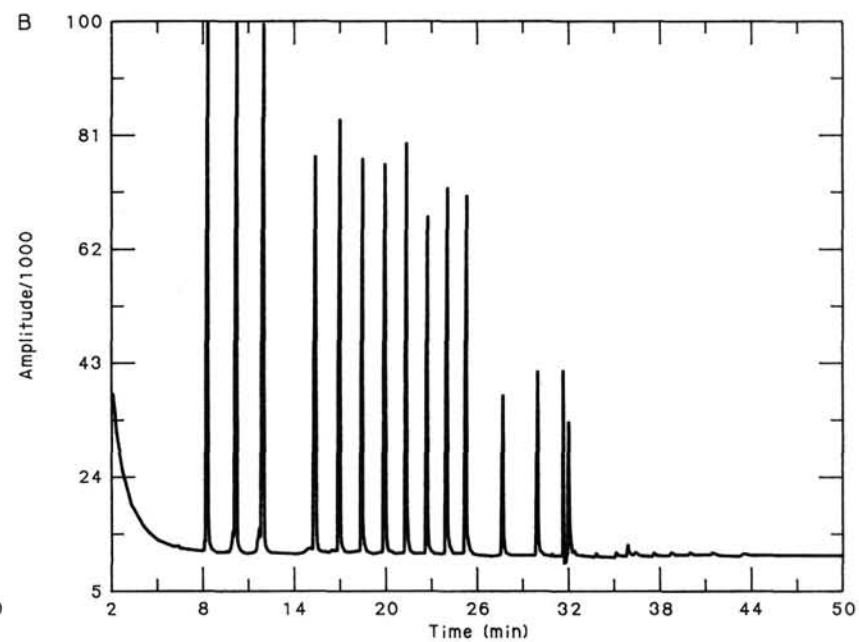
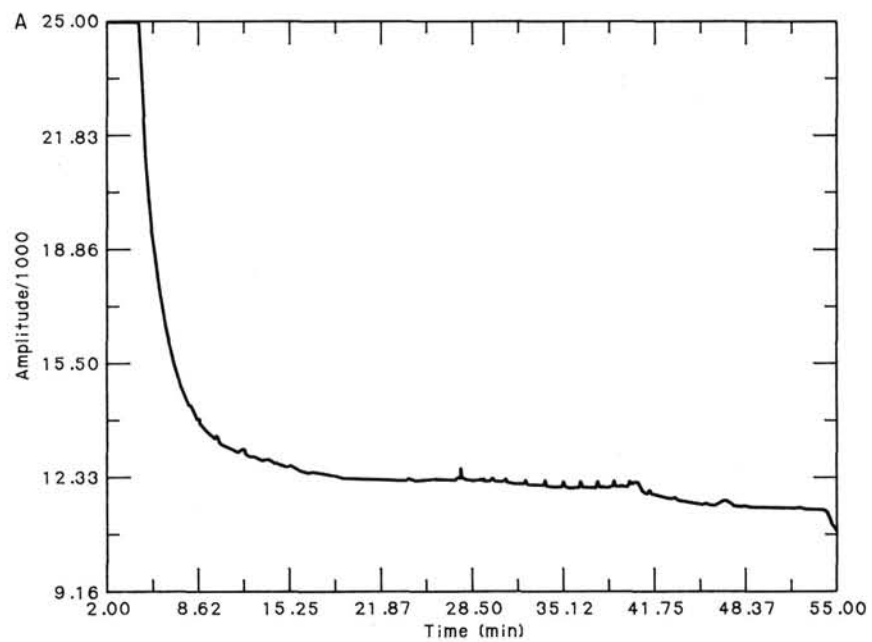
Seismic Unit Four consists of mainly discontinuous and high-amplitude reflectors. The seismic characteristics indicate either dislocated material or erosional events. At the site this unit has a thickness of about 0.2 s. The computed interval velocity for this unit is 2.3 km/s, giving a thickness on the order of 230 m and a depth for its base at about 900–930 mbsf.

Seismic Unit Five and Pseudobasement

An acoustic sequence almost free of internal reflectors is detected beneath Unit Four. This last unit is bounded at its base by an irregular basement surface. The thickness of Unit Five is 0.24 s. Its thickness is 400 m assuming an interval velocity of 3.2 km/s. The top of the basementlike reflector lies at about 1300–1350 mbsf.

Previous Lithologic and Stratigraphic Interpretations

The prominent reflectors bounding the different seismic units have been identified and tentatively dated by Fabbri and Curzi (1979) and by Moussat (1983). The proposed dating indi-



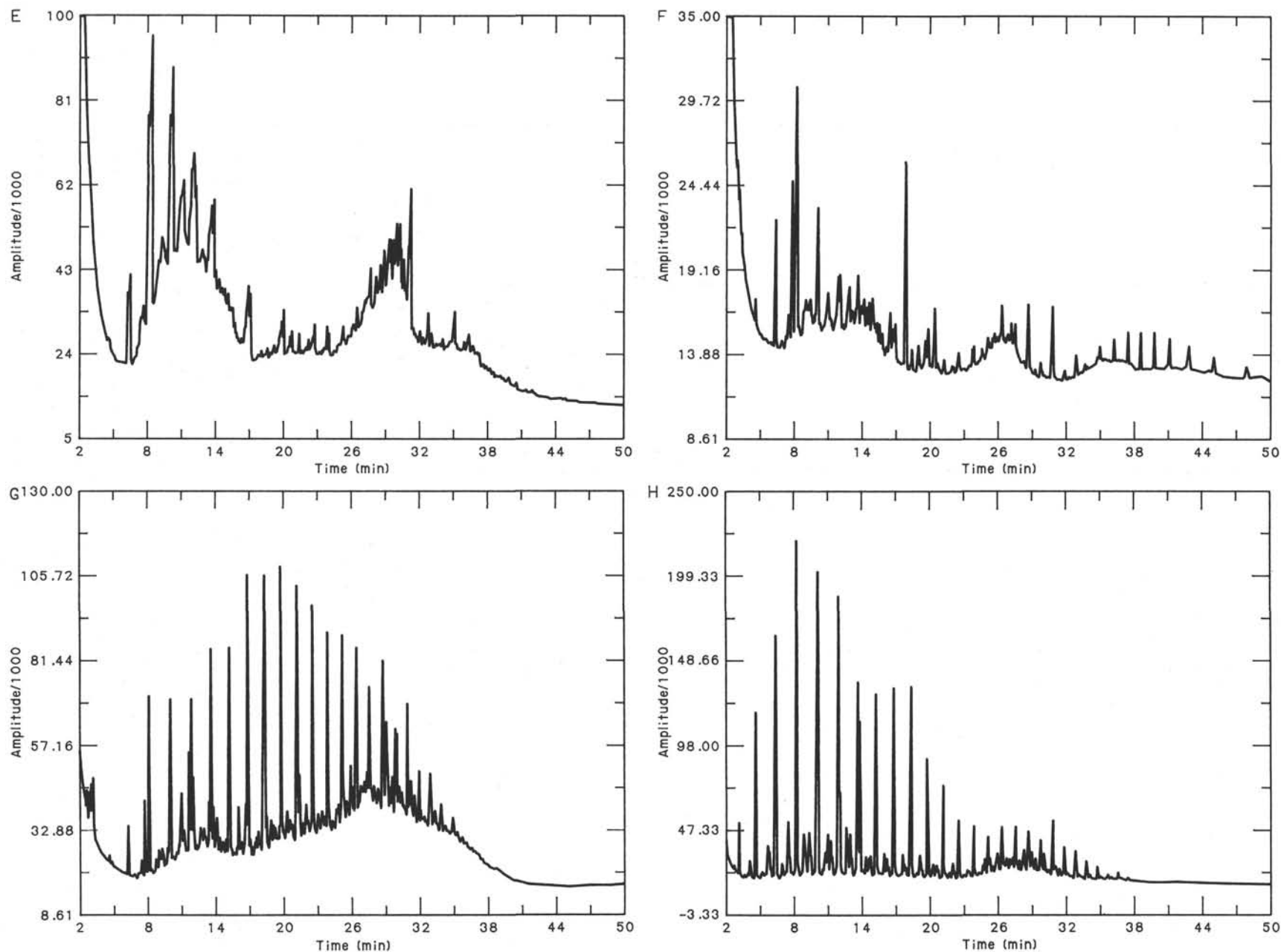


Figure 30. Gas chromatography traces of saturated hydrocarbons extracted from sediments of various lithologies encountered in Hole 652A. A. Flame ionization detector hexane blank. B. Standard high molecular weight *n*-alkane test. C. Sample 2R-2, 40–45 cm. D. Sample 4R-6, 17–20 cm. E. Sample 6R-1, 40 cm. F. Sample 6R-1, 53–55 cm. G. Sample 59R-2, 140 cm. H. Sample 64R-1, 103 cm. See text for explanation.

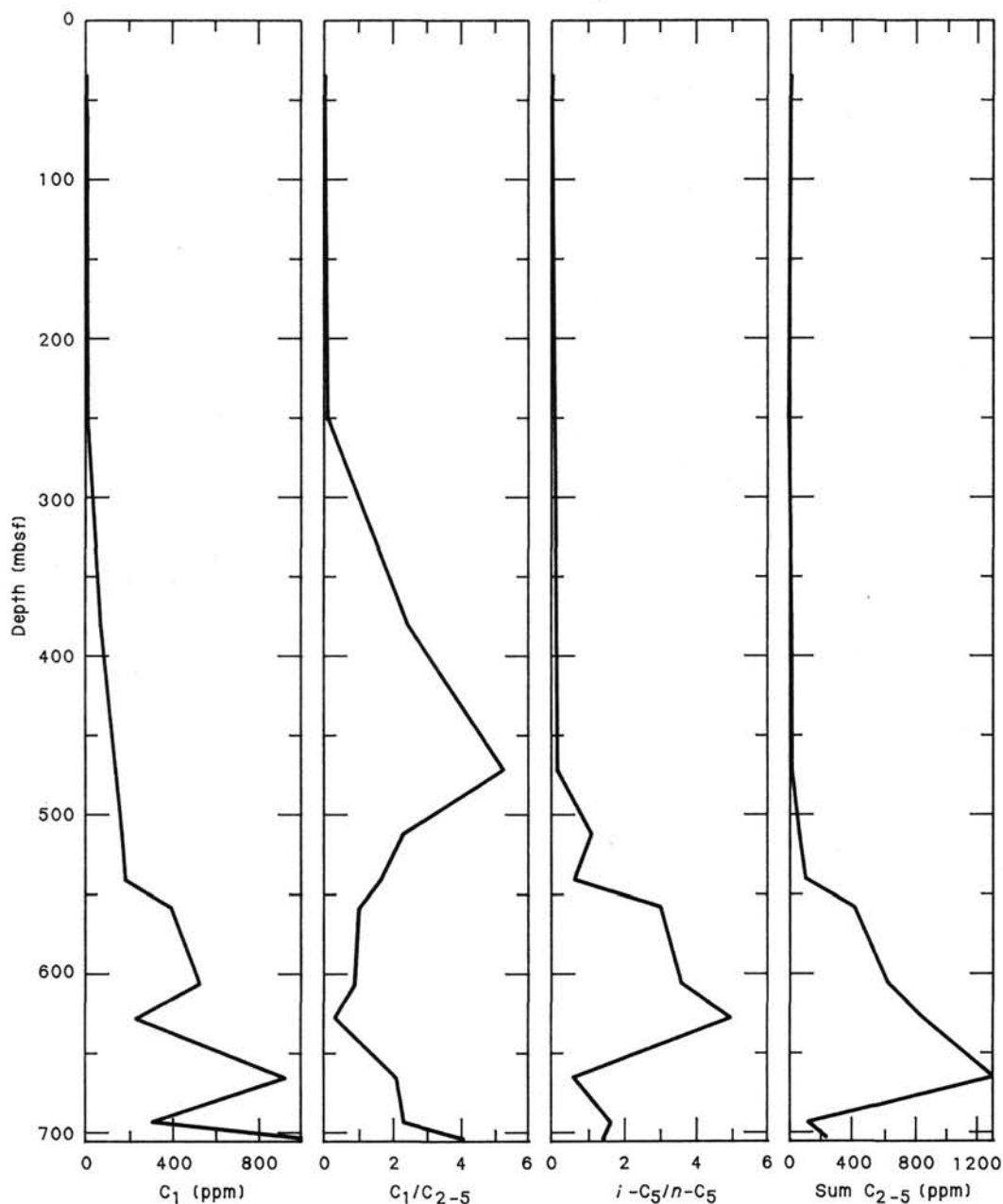


Figure 31. Headspace analysis of hydrocarbons, Site 652.

cates a Pliocene to Quaternary age for Seismic Unit One; the top of our Seismic Unit Two is referred as the "Y" unconformity, interpreted as the top of the Messinian. Neither Fabbri and Curzi (1979) nor Moussat (1983) indicate the presence of the B₂ sequence, representing the Messinian evaporites, below the "Y" unconformity. Moussat (1983) indicates however the presence of the B₃ sequence and of a "Z" sequence, interpreted respectively as pre-evaporitic Miocene sequence and the top of the acoustic basement (Fabbri and Curzi, 1979). The "Z" reflector correlates well with the pseudobasement of MCS line ST01. The B₃ sequence would then represent Seismic Units Three to Five. Rehault et al. (1986) more recently proposed a tentative stratigraphic interpretation of line ST01. Below thin upper Messinian (Seismic Unit Two), these authors note the presence of a sequence inferred to be Messinian (unknown facies) or possibly Tortonian.

Synthetic *P*-wave Seismogram

The synthetic *P*-wave seismogram (Fig. 34) was generated using laboratory measurements of compressional wave velocity and bulk density (see "Physical Properties" section, this chapter). The data were linearly interpolated into an evenly-spaced 1-m grid and input to a single one-dimensional conventional synthetic seismogram as in previous Leg 107 holes. The synthetic seismogram is briefly compared with both a section of Site survey MCS line ST01, near Site 652 (Fig. 32) and the lithology.

The following points should be noted:

1. The base of Seismic Unit One corresponds to a prominent reflector on the seismogram at about 220 mbsf. There is a 32-m discrepancy between the predicted base of Pliocene-Pleistocene

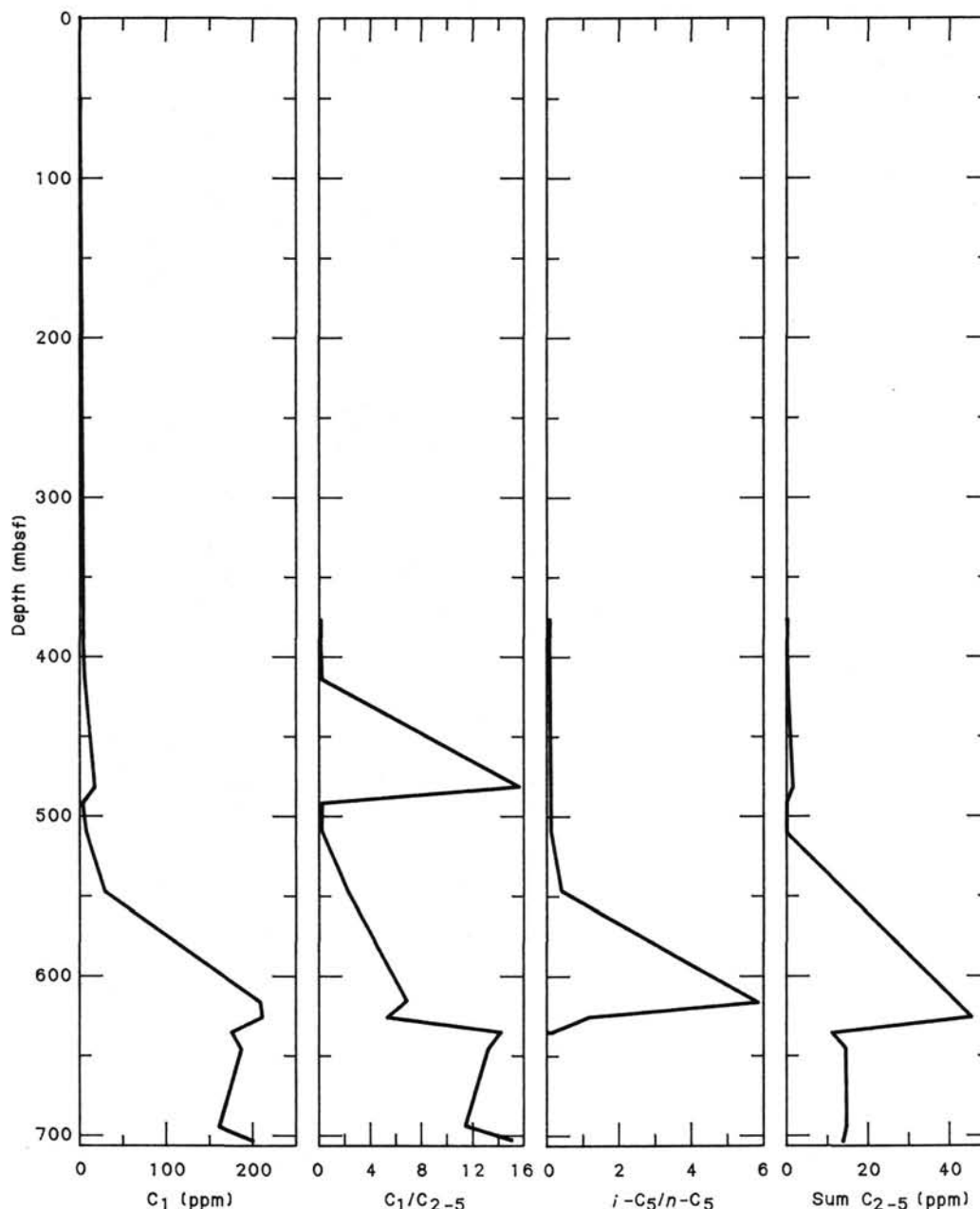


Figure 32. Vacutainer analysis of hydrocarbons, Site 652.

sediments as deduced from the MCS line and the drilling results. However lithologic descriptions indicate that the uppermost Messinian, between 189 and 220 mbsf, is made of rather homogeneous calcareous clay. The high amplitude-reflector that lies at about 220 mbsf corresponds to the first occurrence of gypsiferous layers in the upper Messinian while the boundary between lower Pliocene and latest Messinian is well expressed on the seismogram by a high-amplitude reflector at 190 mbsf.

2. The base of Seismic Unit Two corresponds to a conglomeratic layer recovered between 334.70 and 344.80 mbsf.

3. Seismic Unit Three contains a series of high-amplitude reflectors. These correlate with gypsiferous layers and/or with sandstones interbedded within siltstones and shales.

4. The boundary between Units Three and Four is not very well expressed on the seismogram. Actually the lithology shows

a progressive increase of sandstone layers, still interbedded within siltstones, shales, and thin anhydrites.

Drilling at Site 652 established the following points:

1. Seismic Unit One clearly correlates with Pliocene and Pleistocene hemipelagic sediments but also includes the uppermost Messinian sediments made mostly of calcareous clay.

2. Seismic Unit Two corresponds to alternations of gypsum, carbonate-bearing sandy silts, and calcareous clays and muds (most of lithostratigraphic Unit IV). The bottom of the unit correlates strictly with the base of lithostratigraphic Unit IV (pebble layer).

3. Seismic Units Three and Four correlate with a monotonous succession (gypsiferous thin layers, carbonate-bearing sand,

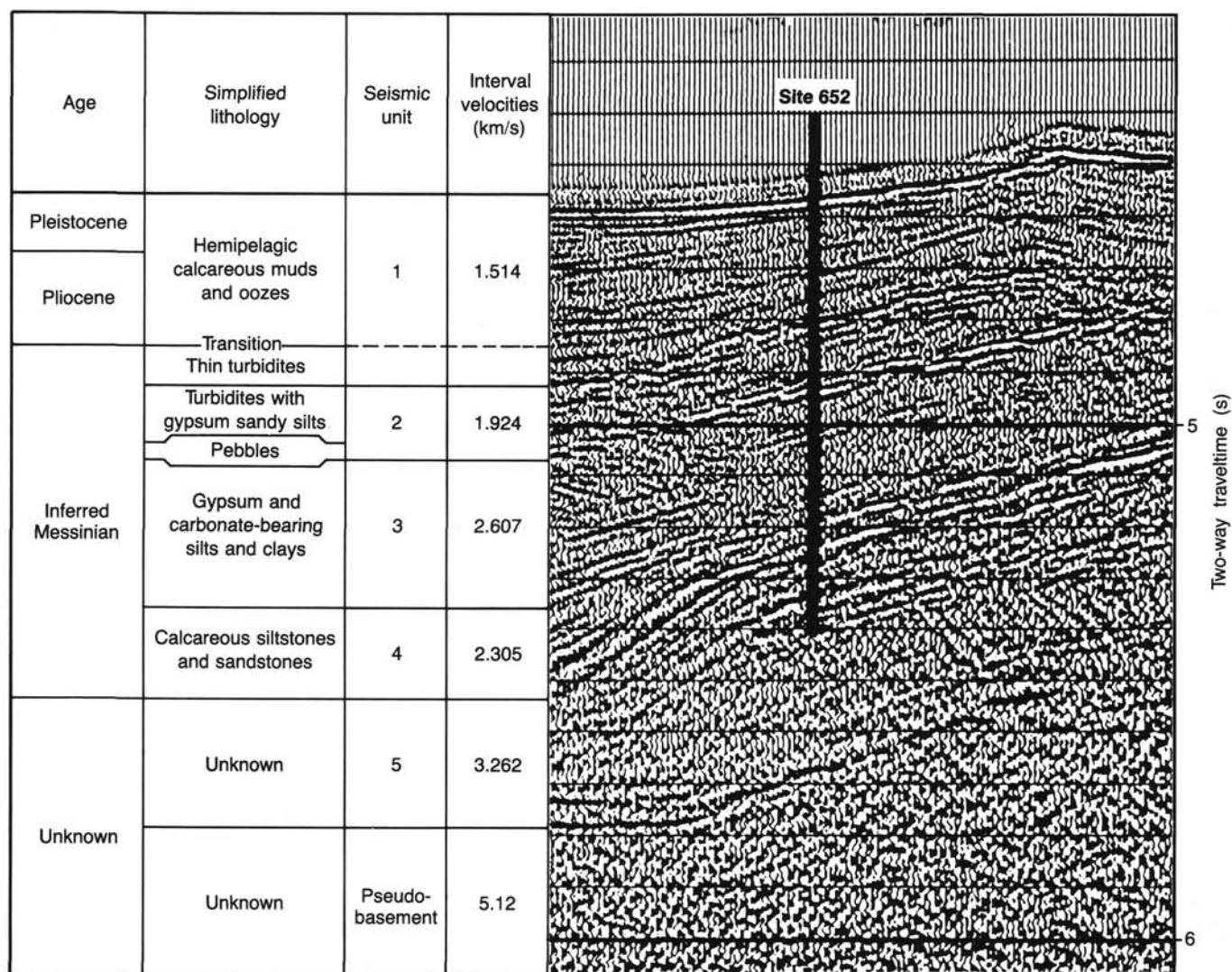


Figure 33. Seismic units at Site 652 (From MCS Site survey line ST01), including correlations with interval velocities, main lithologic units, and time scale.

sandy silt, clays, and thin anhydrites) which corresponds to lithostratigraphic Unit V. The transition from Seismic Unit Three to Four is characterized by a progressive increase and thickening of indurated calcareous siltstones and sandstones.

4. Site 652 bottomed at 721 mbsf in indurated dark gray shale and siltstone, considered to be part of the upper levels of Seismic Unit Four.

5. Seismic Unit One (Pliocene and Pleistocene) can be interpreted as a post-rift sequence, even if minor faulting and unconformities are detected at this level. Seismic Units Two and Three show a marked thickening toward the west (Fig. 7). They are considered as sedimentary sequences deposited during the progressive block rotation (syn-rift sequences). Seismic Unit Three also shows a lateral change in acoustic facies. In the thickest section (toward the west) the unit contains a lens of acoustically transparent material, characterized by an interval velocity of 3.4 km/s. This layer may indicate the presence of an evaporitic body, which could represent the lateral equivalent of lithostratigraphic Units IV and V (essentially made of alternations of gypsum, carbonate-bearing sandy silts, and calcareous clays and muds). The upper levels of Seismic Unit Four correlate with indurated continental sediments which can pertain to the tip of the pre-rift sequence, according to the geometry seen on the seismic line.

DOWNHOLE MEASUREMENTS

Summary of Logging Operations

Logging operations at Site 652 began at 0330 on 27 January 1986. No difficulties were experienced during drilling, and everyone anticipated an excellent hole for logging; such optimism, however, proved to be unfounded. After standing up at 259.5, 269.5, and 349.5 mbsf, the velocity-resistivity-gamma ray-caliper (LSS-DIL-GR-CALI) tool string would not pass below 371.5 mbsf, and logs were recorded up from that depth. On the second run in the hole the induced gamma ray spectrometry tool (GST) was run in place of the lithodensity tool (LDT) in the nuclear combination, because of its additional weight and lack of centralizer springs. The tool string would not pass below 269.5 mbsf and logs were recorded up from that depth.

At 2300 on 27 January, pipe was run down to 429.5 mbsf in an attempt to reopen the hole. Although 8000 lb weight on bit was needed to clear a bridge at 271.5 mbsf, the top drive was never picked up and only minimal circulation of sea water was used. The NGT-CNT-GST combination was again run into the hole and stood up at 371.5 mbsf. Logs were recorded up to 269.5 mbsf, to overlap with the previous run. No log could be recorded below 371.5 mbsf.

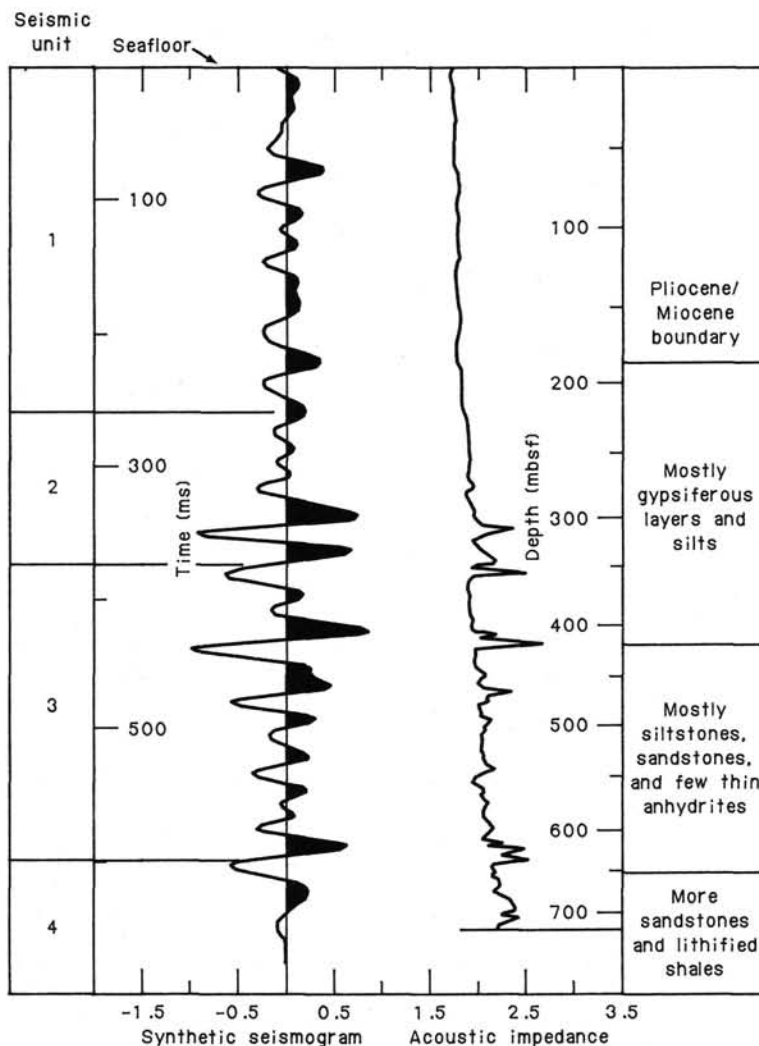


Figure 34. Synthetic seismogram, calculated from shipboard physical properties measurements, allows correlations of core features with seismic reflectors. Correlations with seismic units are shown.

A description of the logging tools used at Site 652 is given in the "Explanatory Notes" section, this volume. Table 13 summarizes the recorded logs.

Discussion of Results

Log Data Quality

Log data quality may be seriously degraded in excessively large sections of the borehole or by rapid changes in the hole diameter. These effects are seen clearly at Hole 652A and limit the accuracy of the log data. Resistivity and velocity measurements are the least sensitive to borehole conditions, while nuclear measurements (neutron porosity and natural and induced spectral gamma ray) are most seriously impaired. A brief description of the applied corrections is presented below.

The velocity log, which was initially affected by noise in the 260–275 mbsf and 320–340 mbsf intervals, has been recomputed from the four original traveltimes curves to produce a more reliable result (Fig. 35). The algorithm makes use of the redundancy of traveltimes measurements to calculate a log uncompensated for hole enlargement or sonde tilt (even for hole enlargements greater than 24 in., velocity errors are quite small, because of the large source-receiver separations used). The resulting log shows a general increase of velocity with depth up to 3.5 km/s

at 331.5 mbsf, and good correlation with electrical and nuclear logs.

The response of resistivity logs is less influenced by hole enlargements. According to the tool manufacturer, corrections of the spherically focused resistivity are required when the hole size exceeds 12 in. (30.48 cm; Schlumberger, 1972); at Hole 652A the caliper log is saturated at its maximum reading (13.5 in.) down to 169 mbsf, and shows variable values (6 in.–13.4 in.; 15.2–34.0 cm) throughout the rest of the hole. The average computed correction, however, is less than 13%, the average resistivity being $0.72 \Omega \cdot \text{m}$. As far as the induction log is concerned, correction is necessary only when there are large contributions to the signal by the borehole fluid, i.e., when the salinity of the drilling fluid exceeds 70,000 ppm. Since seawater was used as the drilling fluid, the correction was less than 3%, the average resistivity being $0.7 \Omega \cdot \text{m}$.

In general the induction deep resistivity is less than the medium or shallow resistivities, suggesting invasion of seawater into the sediments during the time between drilling and logging. This is supported by chemical analyses made aboard ship shortly after drilling which also indicate saline (low resistivity) pore waters (see "Geochemistry" section, this chapter). Resistivity data are not completely reliable in the 259.5–286.5 mbsf interval, due to frequent sticking of the tool during the recording.

Table 13. Summary of log measurements at Hole 652A.

Mnemonic	Tool	Measurement	Unit	Depth (mbsf)
CALI	Caliper	Hole size	inches	73.0–354.5
GR	Natural Gamma Ray	Natural radioactivity	GAPI	73.0–356.5
DIL	Dual Induction	Deep, medium, and focused resistivity	Ω -m	73.0–364.5
LSS	Long Spacing Sonic	Sonic transit time (short and long spacing)	μ s/ft	73.0–352.0
CNT	Compensated Neutron	Porosity	%	73.0–353.0
NGT	Natural Gamma Spectrometry	Total (Th + U + K) and computed (Th + K) natural radioactivity uranium, thorium, potassium	GAPI ppm weight %	73.0–345.5
GST	Induced Gamma Spectrometry	Elemental yields (Ca, Cl, H, Fe, S, Si)		73.0–363.5

The influence of hole enlargements on the nuclear logs is very clear opposite the large washout between 73 and 145 mbsf (see log section following the barrel sheets); the lower gamma ray and higher neutron porosity values indicate attenuation by the borehole fluid, particularly from 107 to 144 mbsf. The same effect is also observed on the curves of the elemental yields. Therefore, natural gamma ray has been corrected for hole size and neutron porosity for hole size, standoff, and pressure according to Schlumberger's (1985) correction charts. No correction algorithm is available to correct natural and induced spectral gamma ray. Due to the saturation of the caliper log these corrections partially remove the hole size effect, thus they can be considered reliable only from a qualitative point of view.

Log Interpretation

Due to the extremely poor conditions of the hole in the upper part of the logged interval (73–169.5 mbsf) the interpretation of the logging data was limited to the lower part of the Pliocene and to the Messinian sediments: an improvement of the log quality was observed in this section, related to a change in physical properties (see below). Indication of the better quality of log readings was provided by cross-correlations of the different curves shown in Figure 35.

In addition to the traditional natural radioactivity, velocity, and resistivity curves, the data from the induced gamma ray spectrometry tool (GST) proved to be very useful in developing a more accurate lithostratigraphy (core recovery in the Miocene section was only 29%). This tool indicates the proportions of the total spectrum attributed to the following elements: Ca, Si, H, S, Cl, and Fe. As their sum is always one the yields do not reflect the actual elemental composition. Therefore, the following yield ratios may be computed to detect changes in the macroscopic properties of the formation:

LIR = lithology-indicator ratio	Si/(Ca + Si)
IIR = iron-indicator ratio	Fe/(Ca + Si)
PIR = porosity-indicator ratio	H/(Ca + Si)
GIR = gypsum/anhydrite indicator ratio	S/(Ca + Si)

LIR reads close to 1 in siliceous silts and sands, 0.2 in dolomites, and 0 in limestone. IIR can be used to detect clays, since clay minerals tend to contain iron and pyrite-rich layers. PIR indicates porosity changes: Figure 35 shows the good correlation between the neutron porosity (quantitative) and the PIR (qualitative) curve. Finally, GIR is related to the presence of gypsum or anhydrite.

Logs indicate that the bottom of lithostratigraphic Unit II (169.5–188.2 mbsf) and Unit III (188.2–188.6 mbsf) are marked by a steady increase of iron content; the top of the Messinian corresponds to a 2-m-thick low-carbonate iron-rich clay. The

Messinian sediments from 191 mbsf to the top of the pebble interval (lithostratigraphic Unit IVc; 324 mbsf) are characterized by the presence of layers of gypsiferous claystone-mudstone, 1–2 m thick, cyclically interbedded with gypsiferous sands and silts. The former are distinguished by higher porosity, lower velocity-resistivity, and high iron-silicon content (black bars in Fig. 35). The low carbonate content is also confirmed by the results of shipboard measurements indicating the CaCO_3 ranges from 10% to 20% in claystones and mudstones (see "Geochemistry" section, this chapter).

A plot of thorium vs. potassium concentration (Fig. 36) has been used to identify the major clay minerals in the logged interval. Because the composition of clay minerals is quite variable, each of them is represented by a general area rather than by a single point. The figure shows that most of the values fall in the field of montmorillonite, and subordinately of chlorite and kaolinite. The presence of such minerals and in particular the predominance of montmorillonite is quite common in Messinian sediments of the Tyrrhenian area; the clay fraction of Messinian sediments recovered at DSDP Sites 132 and 373 contains great amounts of well-crystallized smectites (Ryan et al., 1973; Chamley et al., 1978), which represent as much as 100% of the clay mineralogy. In the absence of shipboard XRD/XRF analyses the iron indicator ratio curve indicates a marked enrichment in iron opposite the clay layers, suggesting that these clays may be similar to the nontronites-iron beidellites described by Chamley et al. (1978). These clays may have formed in the soils of higher standing areas exposed as the water level dropped during the Messinian. Their deposition interbedded with carbonatic-gypsiferous sands and silts would be the result of the enhanced continental erosion in combination with tectonic activity.

Gypsiferous carbonatic sands and silts are characterized on logs by higher velocity-resistivity, lower porosity, higher carbonate content (CaCO_3 shipboard measurements range from 20% to 38.5%). A good qualitative calibration of the logging data against cores was performed in the interval 307–325 mbsf, corresponding to Cores 107-652A-33R to 107-652A-34R. The core recovery was only 44%, but the uniformity of log readings allows a tie of logs to cores. According to the LIR-IIR curves this section consists of prevalent gypsiferous carbonatic sands and silts, delimited at the top and bottom by claystone/mudstone. This interpretation is confirmed by the smear slides and CaCO_3 analysis results, which range from 25.5% to 33%. A close examination of cores also reveals that silts and sands are cemented with carbonate, thus explaining the increase of velocity with respect to the clays.

The gypsum-indicator ratio (GIR) does not indicate a preferential distribution of gypsum opposite clay intervals; in the logged section of Unit V, however, it is more abundant than anywhere else in the cores, along with a dramatic increase in the

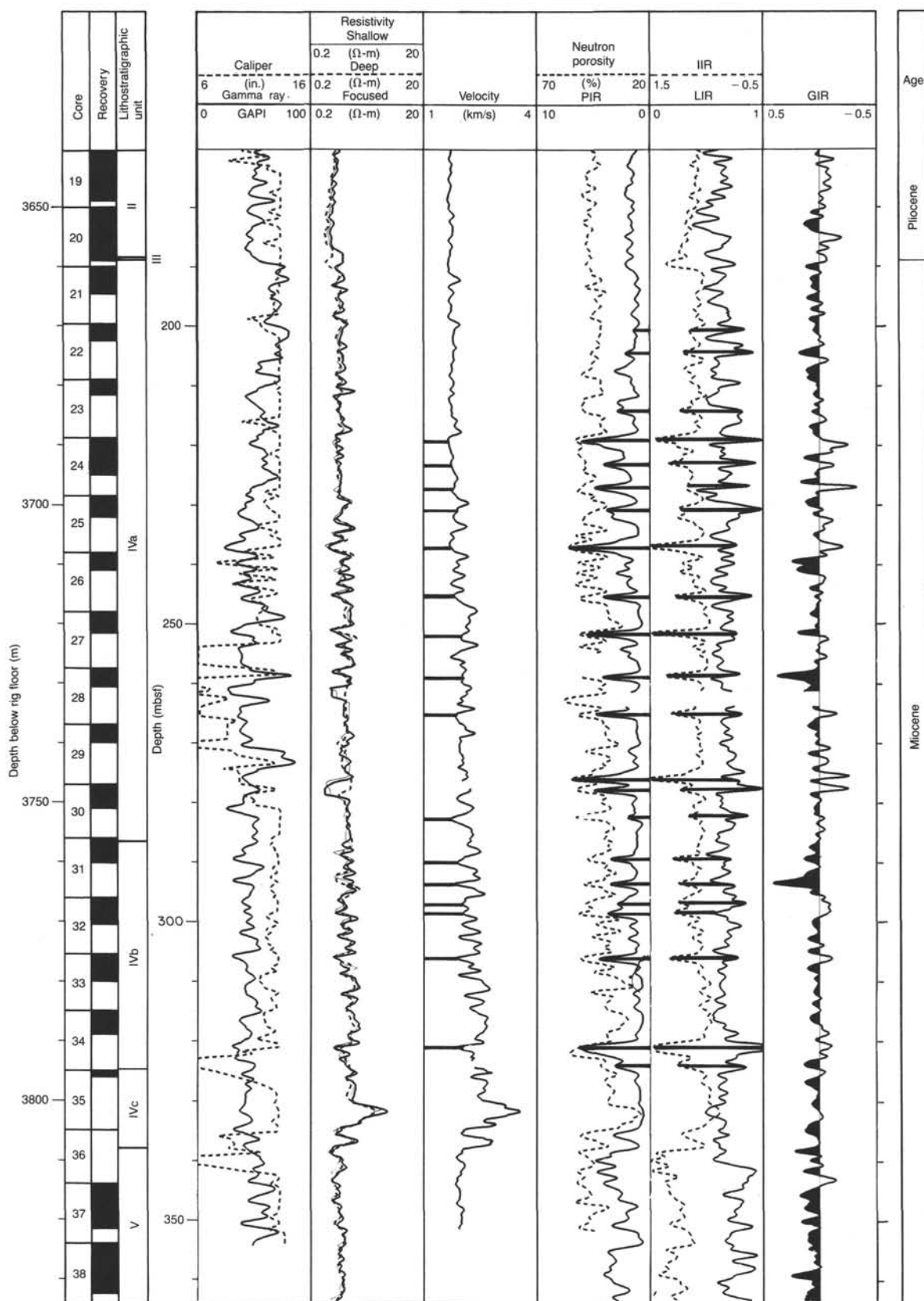


Figure 35. Logging data at Hole 652A. Gamma ray and neutron porosity are corrected for borehole effects; velocity has been re-computed from the original traveltimes. LIR (lithology indicator ratio), IIR (iron indicator ratio), PIR (porosity indicator ratio), GIR (gypsum/anhydrite indicator ratio). Clay-rich levels are indicated by black bars: they correspond to low velocity-resistivity and high porosity values, and to an increase in the silica and iron content.

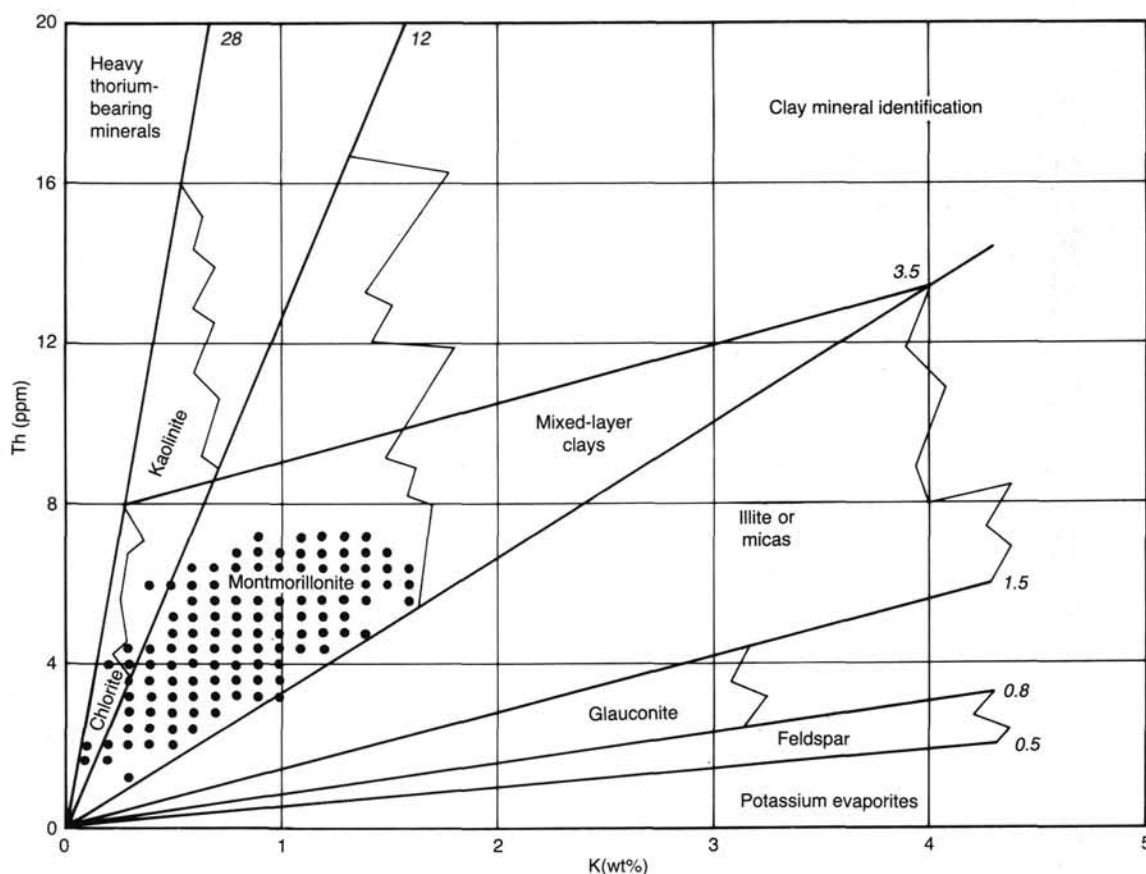


Figure 36. Plot of thorium vs. potassium concentrations for clay-mineral identification in the Miocene sediments of Hole 652A. Because the composition of clay minerals is quite variable, each mineral is represented by a general area rather than by a single point. Lines represent points of constant Th/K ratio. Most of the logged values fall in the field of montmorillonite, but chlorite and kaolinite are also present.

iron content. Both these features are confirmed by Cores 107-652A-37R to 107-652A-38R, which consist primarily of gypsum-bearing clay and mud rich in iron oxides. No sediment was recovered in Core 107-652A-36R, but logs clearly indicate that the top of Unit V occurs at 338 mbsf.

The overlying lithostratigraphic Unit IVc consists of 14 loose pebbles recovered in the core catcher of Core 107-652A-36R. Logs in this interval show a different signature from adjacent sediments that allows the identification of the top of the unit at 324 mbsf. The discrepancy between the depth of this boundary on cores (334.7 mbsf) and logs is explained by the extremely low recovery in Cores 107-652A-35R to 107-652A-36R.

Comparison of Logging and Physical-Property Measurements

Figure 37 shows the physical-properties data from logs and cores. High velocity (3–5 km/s) and low porosity (<5%) samples corresponding to streaks of gypsum or anhydrite have been omitted from the physical-properties data because their thickness (<5 cm) is less than the tool resolution.

Agreement between log and sample velocities is quite good throughout the section. Pliocene sediments to 189 mbsf show a uniform low velocity of 1.6–1.7 km/s. The Pliocene-Miocene boundary at 189 mbsf is not marked by a sharp change in velocity (i.e., by a seismic reflector), but by a gradual and steady increase becoming more evident in the log data below 230 mbsf. This depth marks the onset of gypsum- and carbonate-bearing sands and silts of lithostratigraphic Units IVa and IVb.

The pebble interval, at 324–337.5 mbsf, exhibits the highest velocity values, 2.7–3.5 km/s; the bottom of this unit is indicated by the sudden drop of velocity to 2.0 km/s.

Raw neutron porosity and neutron porosity corrected for hole size, pressure, and standoff are shown plotted against the laboratory porosities in Figure 37. The corrected neutron porosities are considerably lower than the raw porosities. In the Pliocene section (down to 189 mbsf), the corrected neutron porosities are smaller than the sample measurements, probably a reflection of the amount of elastic rebound undergone by these high porosity samples as they are brought to the surface. In the Miocene sediments, the corrected neutron porosities are larger than the corresponding sample values. This is due to (1) less elastic rebound effect in a stiffer (e.g., higher velocity) sediment, (2) bound water in clays “seen” by the neutron tool, and (3) insufficient correction of the neutron response for the borehole effects.

Alternatively, a synthetic porosity curve calculated from the deep induction log is shown plotted along with the core data in Figure 36. This calculation assumes that Archie’s (1942) relationship

$$R(\text{formation}) = R(\text{water}) \times \text{porosity}^{-2}$$

is here applicable. $R(\text{formation})$ was taken to be the measured deep induction resistivity, and $R(\text{water})$ values were calculated from the measured pore-water salinities and temperature data. In high porosity sediments this assumption is often untenable,

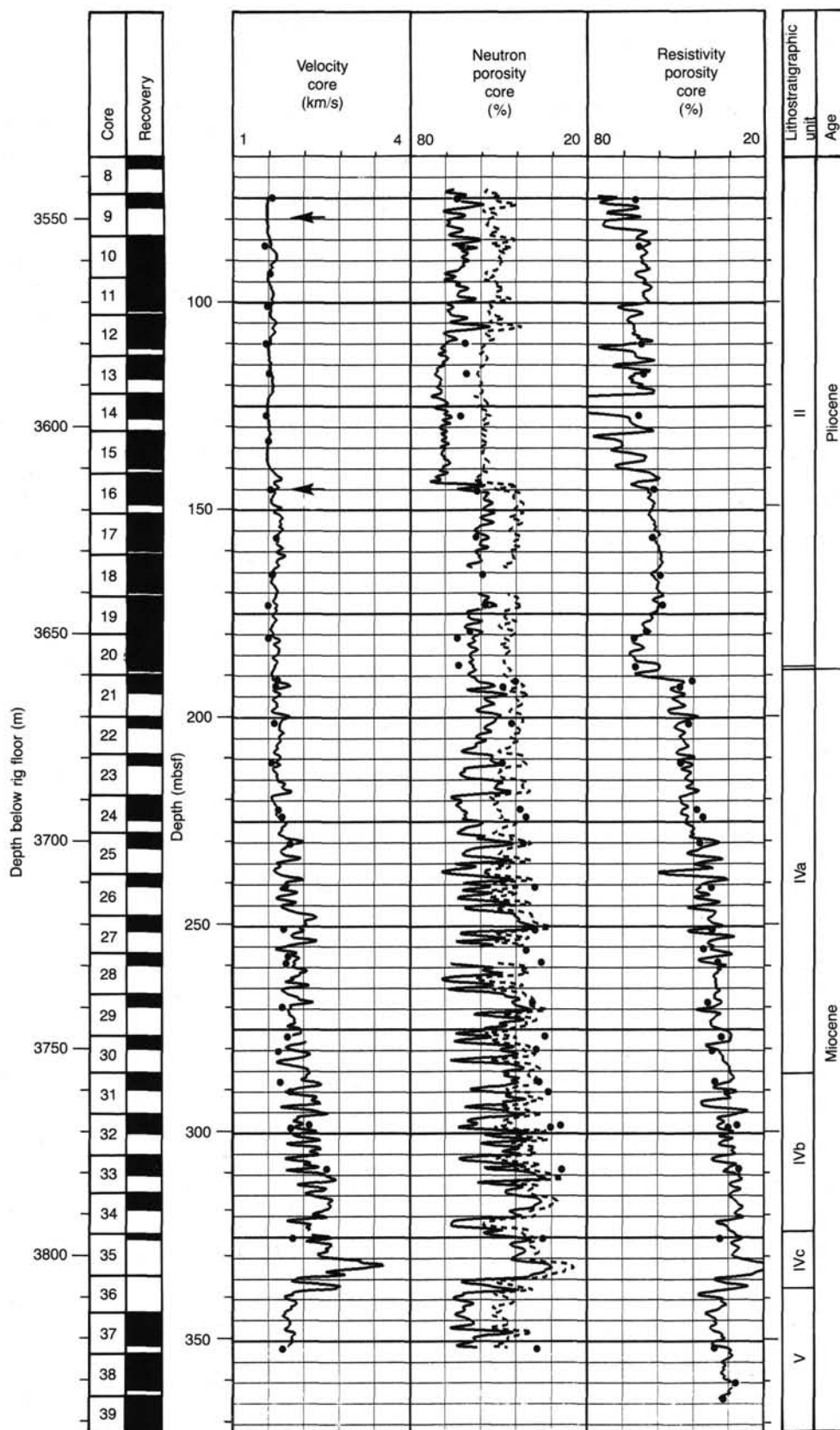


Figure 37. Physical properties from logs (lines) and cores (points) at Hole 652A. The arrows delimit the large washout as detected from caliper and nuclear logs; in this section the original neutron log readings (solid line) are significantly affected by neutron absorption by the borehole fluid (log porosities higher than core porosities). The dashed curve represents porosity values corrected for borehole size. Logs are smoothed using a 5-point running average filter. Data acquired every 0.15 m.

but the agreement between the calculated and measured porosities throughout the interval is striking, even in the washed-out section at the top of the hole. Computed porosities average 63% in the logged Pliocene sediments. In the pre-Pliocene sediments, a rapid decrease in porosity is observed; over a distance of less than 200 m, porosity decreases to an average value of 37%. Further examination of the samples will help to reveal the cause of the rapid reduction of pore space.

HEAT FLOW

Introduction

Site 652 was drilled on one of the easternmost tilted blocks of the Vavilov rift-basin western margin, between the Central Fault zone and de Marchi Seamount (Fig. 38). At this site, reflection seismic data permit recognition of a Pliocene-Pleistocene post-rift sequence and thick syn-rift and pre-rift series below the Upper Messinian unconformity.

Data

Five excellent temperature measurements were obtained at Site 652 with the same Uyeda-T-Probe downhole recorder and sensor (thermistor 14 combination), thus minimizing calibration errors that may arise from the use of different measuring systems. Figure 39 displays the temperature vs. time records of the measurements. An average bottom water temperature of 13.30°C was measured.

The downhole measured temperatures of Hole 652A plotted vs. sub-bottom depth fit a nearly straight line (Fig. 40); a mean gradient of $140^{\circ} \pm 20^{\circ}\text{C}/\text{km}$ can be calculated, taking into account the sea-bottom water temperature. Nevertheless the gradient gradually decreases with depth from $165^{\circ}\text{C}/\text{km}$ in the upper interval (0–36.4 mbsf) to $105^{\circ}\text{C}/\text{km}$ in the lowermost interval (151.2–189.8 mbsf, Table 14).

Thermal conductivities were measured at several depths along recovered cores using the needle-probe method. Unfortunately only a few measurements are available because of technical fail-

ures in the equipment and calibration program. Figure 24 shows the thermal conductivities plotted vs. sub-bottom depth. Table 14 gives the harmonic mean conductivities for several depth intervals. Note the high thermal conductivity over the interval 189.8–267 mbsf giving a harmonic mean of $1.61 \text{ W m}^{-1} \text{ }^{\circ}\text{C}^{-1}$ ($3.85 \cdot 10^{-3} \text{ cal cm}^{-2} \text{ s}^{-1}$) for $n = 5$ measurements. Calculated heat flow determinations for the same intervals are also given in Table 14. The mean heat flow value is $160 \text{ mW/m}^2 \pm 17 \text{ mW/m}^2 = 3.82 \pm 0.4 \text{ HFU}$.

Comments

Assuming a normal constant heat flow with depth, as a first approximation, the decrease in the temperature gradient down-hole is compensated by the increase in the thermal conductivity over the depth interval of measurements of the temperature gradient.

Conclusions

We determined a heat flow value of $160 \pm 17 \text{ mW/m}^2$ at Site 652 based on five temperature and conductivity measurements made on the recovered sediments.

This heat flow value is in the range of those obtained at Site 651 in the Vavilov Basin and at Site 650 in the Marsili Basin (144 and 162 mW/m^2 , respectively). The high heat flow at these three sites is consistent with the inferred presence of hot mantle material at shallow depth beneath or intruding the stretched continental lithosphere. Nevertheless, along surficial profiles, variability and anomalies in the heat flow distribution are recognized in the central Tyrrhenian in conjunction with the regional structural pattern and localized volcanic activity.

A linear extrapolation of the temperature profile obtained at Site 652 in the uppermost 189.8 mbsf to total depth gives a temperature of about 130°C at the bottom of the hole compared with the 60°C critical temperature. This is a high temperature considering the diagenetic evolution of the sediments, in particular clay minerals, and the dolomitic and sulfate crystallization. It is also probable that the high heat flow regime has enhanced

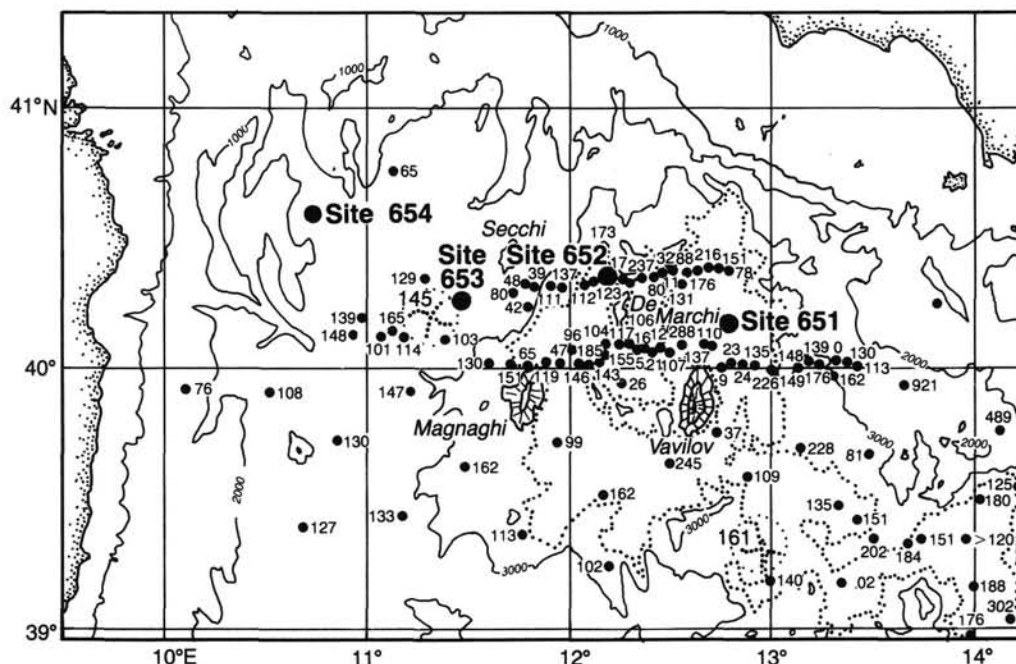


Figure 38. Heat flow distribution across central and western Tyrrhenian Basins (after Della Vedova et al., 1984). Heat units are shown in mW/m^2 .

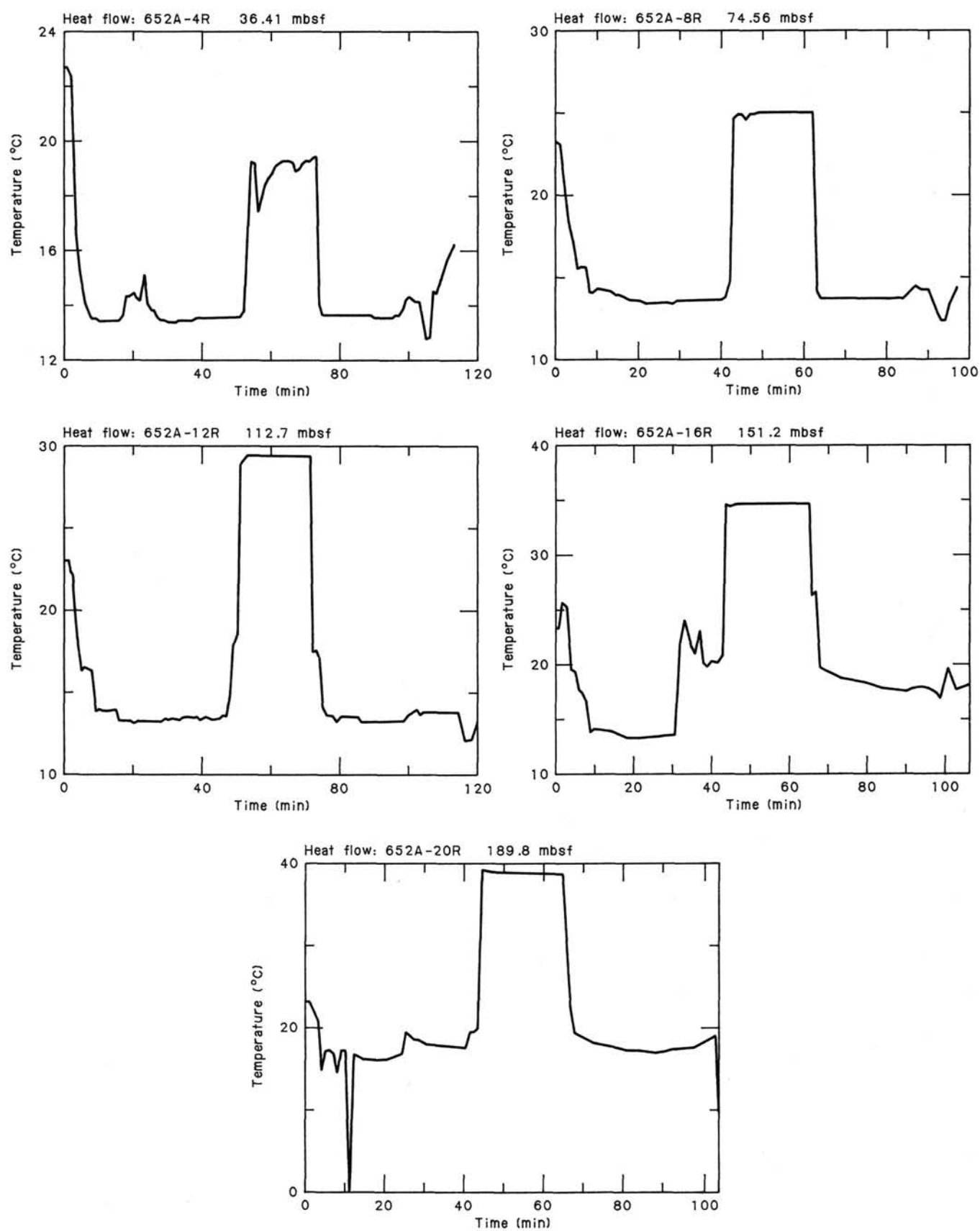


Figure 39. Downhole temperature measurements in Hole 652A at sub-bottom depths of 36.41, 74.56, 112.7, 151.2, and 189.8 m.

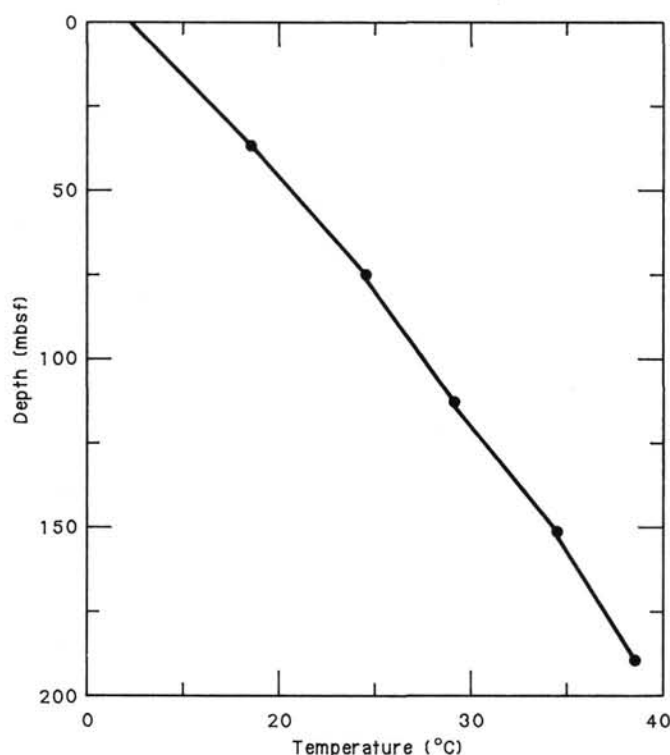


Figure 40. Plot of sediment temperature vs. bottom depth in Hole 652A.

thermal maturation of organic-carbon-rich sediments of the western deep margin of the Vavilov Basin (see "Geochemistry" section, this chapter).

DISCUSSION AND CONCLUSIONS

Overview

Site 652 achieved its primary objective of documenting the sedimentary sequences deposited prior to, during, and after the main episode of stretching of a passive continental margin. Unfortunately, the sediments at the pre-rift/syn-rift contact and within the lower syn-rift sequence were not datable with ship-board techniques. A complete Pliocene/Pleistocene section was obtained, which appears to be suitable for detailed comparisons of biostratigraphy, magnetostratigraphy, and stable isotope strati-

tigraphy. Finally, the lower 540 m of Hole 652A recovered an unusual pre-Pliocene (presumed Messinian) clastic and evaporitic facies which is tentatively interpreted as lacustrine.

Pliocene-Pleistocene Sediments

The Pliocene-Pleistocene sediments are characterized by open marine conditions, with a significant influx of volcanic material, notably in the Pleistocene and upper Pliocene. The Pliocene/Pleistocene boundary has no obvious lithological expression.

Repeated sapropelic intervals incorporate both marine and continental organic carbon. Organic matter has apparently been preferentially preserved under conditions of anoxic bottom water during these brief intervals of the Pleistocene. Prior to the drilling of this site, late Pliocene and early Pleistocene sapropels were mostly viewed as an eastern Mediterranean phenomenon, and explanations for their origin were sought in local processes such as vertical stratification of the water column following increased fresh water input from the Nile and/or Black Sea. The geochemical and color patterns of individual sapropels in the eastern Mediterranean have proved to be quite distinctive, so it should be possible to determine whether individual Tyrrhenian sapropels correlate with Ionian and Levantine Sea sapropels. If so, an explanation must be found for the Pleistocene sapropels which is equally applicable both east and west of the Sicily Channel.

The lowermost Pliocene and the Miocene/Pliocene transition zone are characterized by a strong red-brown coloration which is attributed to iron oxides. The iron oxide component suggests that these sediments had been subaerially weathered during the Messinian drawdown and were reworked during and immediately after the terminal Messinian transgression.

Pre-Pliocene Sediments

The pre-Pliocene sequence at Site 652 is characterized by a thick sequence of subaqueously-deposited, clastic sediments. The entire sequence, from 189 mbsf to the base of the hole at 721 mbsf, is barren of autochthonous fauna.

Environment of Deposition

The environment in which the pre-Pliocene sequence was deposited seems to have been highly variable through time. Frequent, thin evaporitic interbeds indicate periods of higher bottom-water salinity. Algae- and organic-carbon-rich beds suggest periods of higher productivity. The pebble horizon at 335 mbsf may indicate a temporary fluvial or beach environment. The presence of millimetric red and yellow laminae rich in iron oxide

Table 14. Heat flow at Site 652.

Depth (mbsf)	Interval temperature increase °C	Thermal gradient °C/km	Thermal conductivity $Wm^{-1} C^{-1}$	n	Heat flow	
					(mW/m ²)	(HFU)
36.4	6.0 ± 0.1	165 ± 3	0.98 ± 0.06	10	162 ± 10	3.87 ± 0.24
38.16	5.65 ± 0.05	148 ± 1.5	1.17 ± 0.05	8	173 ± 9	4.13 ± 0.21
38.14	4.6 ± 0.05	121 ± 1.5	1.20 ± 0.08	3	145 ± 10	3.46 ± 0.24
38.5	5.2 ± 0.05	135 ± 1.5	1.32 ± 0.1	6	178 ± 10	4.25 ± 0.24
38.6	4.05 ± 0.05	105 ± 1.5	1.33 ± 0.1	4	140 ± 10	3.34 ± 0.24
74.56	11.65 ± 0.08	156 ± 1.5	1.075 ± 0.06	18	167 ± 10	3.99 ± 0.21
112.7	16.25 ± 0.08	144.2 ± 1.5	1.12 ± 0.08	21	161.5 ± 13	3.86 ± 0.31
151.2	21.45 ± 0.08	142 ± 1.5	1.17 ± 0.1	27	166 ± 17	3.96 ± 0.4
189.8	25.5 ± 0.08	134.4 ± 1.5	1.20 ± 0.1	31	161 ± 15	3.84 ± 0.36
76.64	9.8 ± 0.05	128 ± 1.5	1.26 ± 0.1	9	161 ± 13	3.84 ± 0.31
115.24	13.85 ± 0.08	120 ± 1.5	1.283 ± 0.1	13	154 ± 12	3.68 ± 0.28
77.2			1.61 ± 0.08	5		

Note: n = number of conductivity measurements/interval.

To be mentioned: Temperature from logging at 350 mbsf → T = 56.7 ± 2°C;

expected temperature according average 14°C/100 m gradient = 62.3°C.

Water temperature was near equilibrium in the hole at time of measurement.

may indicate that there was land exposed nearby, if the laminae are indeed derived from subaerial weathering and brought to the site by eolian transport. However we found no mudcracks or other direct evidence of subaerial exposure in the cores. We consider that the most probable sedimentary environment for the pre-Pliocene units (other than the pebble horizon) is lacustrine. Evidence for a euryhaline or lacustrine environment includes the total absence of normal marine organisms, the very rare occurrence of *Ammonia beccarii* and *Cypridies*, the presence of *Borystococcus*-type algae, the extreme fluctuations of salinity and productivity inferred from lithologic variability, and the inferred proximity of subaerial source areas for significant input of eolian sediment.

Age of the Pre-Pliocene Sequence

The pre-Pliocene sequence hampered shipboard attempts at stratigraphic control. The only *in-situ* flora or fauna recovered from the pre-Pliocene sequence were three specimens of *Ammonia beccarii tepida*, fragments of ostracodes, and possible algae. The upper 40 m of the pre-Pliocene are reversely magnetized, which taken in context of the magnetostratigraphy of the overlying sediments implies that this interval lies within the lowermost reversed interval in the Gilbert geomagnetic epoch (i.e., between 4.79 and 5.41 m.y.b.p. according to Harland et al., 1982). Below this depth, the natural remnant magnetization was too weak for shipboard measurement. Preliminary shore-based work suggests that this reversed magnetic polarity continues to the base of the drilled section. Additional shore-based paleomagnetic and pollen-stratigraphic studies may further constrain the age of the barren units.

Because of the presence of evaporites, the reversed magnetic polarity, and the position of these barren sediments beneath the Pliocene, a Messinian age has been tentatively assigned to the interval from 189 to 721 mbsf. We speculate that the pebble horizon at approximately 335 mbsf may correlate with the intra-Messinian erosional event which is expressed elsewhere in the Mediterranean as an unconformable contact between the upper and lower evaporites. If so, lithostratigraphic Unit IV between 189 and 330 mbsf would be the lateral equivalent of the upper evaporite, while lithostratigraphic Unit Va (and possibly Vb) would be the lateral equivalent of the lower evaporites. In this context, it is interesting to note that within lithostratigraphic Unit Va, it is possible to distinguish several second-order sedimentary cycles within the sequence of alternating clastic and chemical sediments. Each of these cycles is about 10 m thick, and is characterized by an increase in the abundance of sulfate toward the top of the cycle (see "Lithostratigraphy" section, this chapter). Cyclic sedimentation is also known in the lower evaporites of Sicily (Heimann and Mascle, 1974; Decima and Wezel, 1973; Garrison et al., 1978).

Although we are reasonably confident that most of the barren, evaporite-bearing interval was deposited during the Messinian, we cannot totally exclude the possibility that the base of this sequence was deposited in a pre-Messinian, early-rift continental environment analogous to the modern east African rift valley lakes.

Tectonic Significance

Numerous microstructures indicative of sedimentary instability are found in the pre-Pliocene sequence. These features include numerous synsedimentary normal faults, less common reverse faults, slumps, convoluted bedding, and breccias. In contrast, only one, poorly-developed, possible slump was observed in the Pliocene-Pleistocene section.

Preliminary measurements on microfaults suggest a direction of extension between 100° and 130°. (Note that since the cores were not oriented, this line of reasoning incorporates an as-

sumption that the dip of bedding in the cores is parallel to the regional dip of reflectors in seismic reflection profiles). This inferred east-southeast direction of extension is consistent with seismic reflection data which show north-northeast-striking normal faults (Moussat, 1983), and with an inferred north-northwest/south-southeast direction of opening of the Vavilov Basin (e.g., Moussat, 1983; Moussat et al., 1985; Rehault et al., 1987; Malinverno and Ryan, 1986).

A preliminary comparison between the lithostratigraphy and the seismic reflection data indicates that:

1. The uppermost pre-rift sequence appears to coincide with the highly-indurated lowest 30 or 40 m of sedimentary Unit V. We cannot rule out the possibility that these indurated, barren sediments were deposited in a pre-Messinian continental environment which was situated above modern sea level before the onset of rifting. However, we consider it more likely that the pre-rift to syn-rift transition occurred during the Messinian.

2. Most of the pre-Pliocene section, presumably of Messinian age, can be interpreted as syn-rift deposits. Ages within this interval have not been determined, other than to speculate that the pebble horizon between 335 and 345 mbsf may coincide with the intra-Messinian erosional event.

3. The transition from syn-rift to post-rift sedimentation occurred during Pliocene time.

4. Minor tectonic activity may have continued or resumed in the Pleistocene. The seaward-dipping fault which bounds the eastern edge of the tilted block at Site 652 has displaced Pleistocene sediments as well as the seafloor; however, the sense of motion in the Quaternary has been reverse rather than normal, suggesting reactivation of the fault in a new stress regime rather than continued motion.

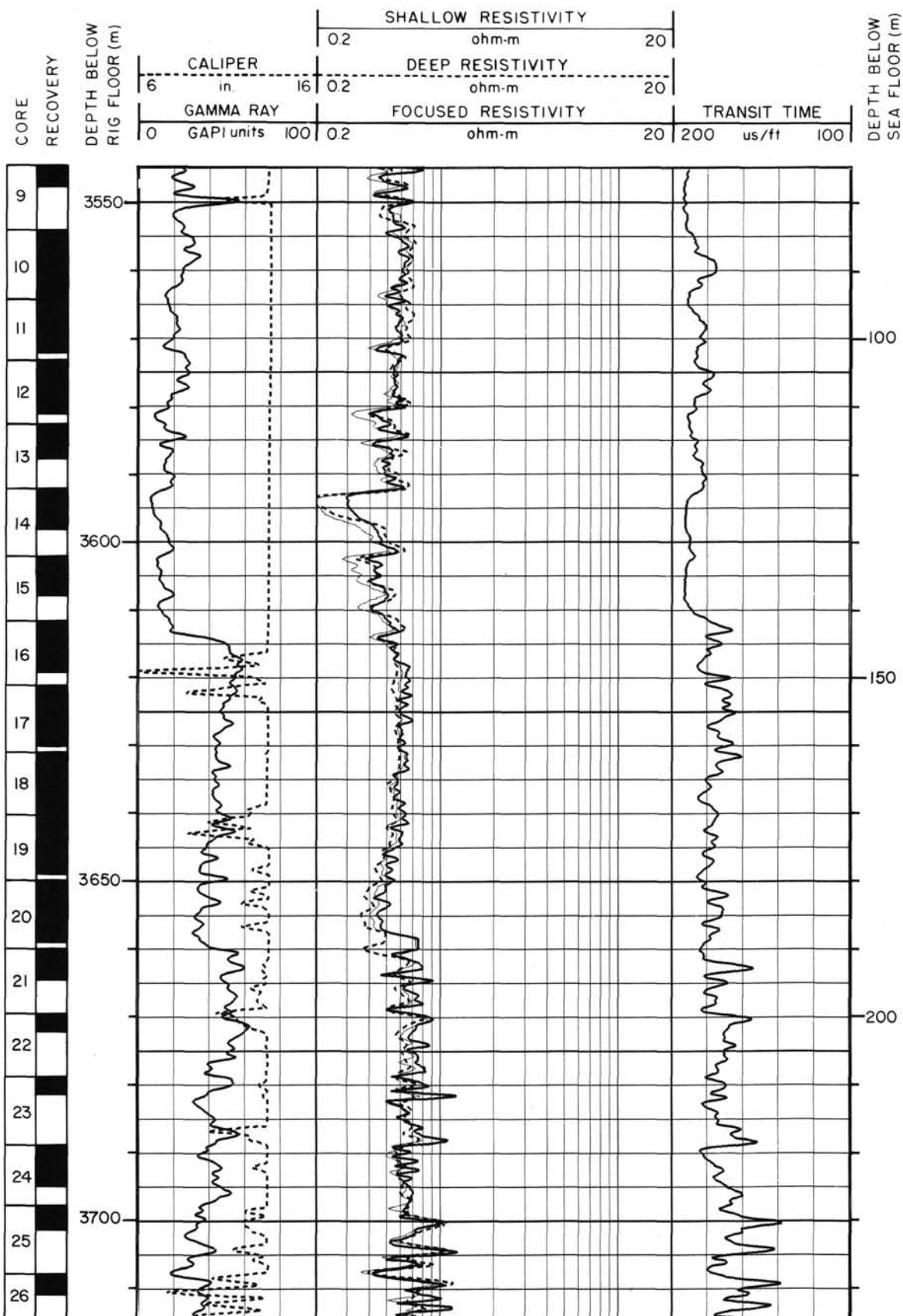
REFERENCES

- AGIP, 1982. Foraminiferi Padani—Atlante iconografico e distribuzione, (2nd ed.): Milano (AGIP).
- Amodio-Morelli, L., et al., 1976. L'arco calabro-peloritano nell'orogene appenninico-maghrebide. *Mem. Soc. Geol. Ital.* 17:1-60.
- Angelier, J., and Mechler, P., 1977. Sur une méthode graphique de recherche des contraintes principales, également utilisables en tectonique et en séismologie: la méthode des dièdres droits. *Bull. Soc. Geol. France*, 29:6,1309-1318.
- Archie, G. E., 1942. The electrical resistivity log as an aid in determining some reservoir characteristics. *Pet. Technol.*, 5(1).
- Berggren, W. A., Kent, D. V., and van Couvering, J. A., 1984. Neogene chronology and chronostratigraphy. In Snelling (Ed.), *Geochronology and geological record*, *Geol. Soc. London, Spec. Paper*.
- Bizon, G., and Müller, C., 1977. Remarks on some biostratigraphic problems in the Mediterranean Neogene. In Biju-Duval, B., and Montadert, L. (Eds.), *Structural History of the Mediterranean Basins*. Paris (Technip), 381-390.
- Broecker, W. S., and Van Donk, J., 1970. Insolation changes, ice volume, and the ^{18}O record in deep-sea cores. *Rev. Geophys. Space Phys.*, 8:169-198.
- Chamley, H., Dunoyer de Segonzac, G., and Melieres, F., 1978. Clay minerals in Messinian sediments of the Mediterranean area. In Hsü, K. J., Montadert, L., et al., *Init. Repts. DSDP*, 42, Pt. 2: Washington (U.S. Govt. Printing Office), 389-397.
- Cifelli, R., 1974. Planktonic foraminifera from the Mediterranean and adjacent Atlantic waters (cruise of the Atlantic II, 1969). *J. Foraminiferal Res.*, 4:171-183.
- Cita, M. B., 1975. Studi sul Pliocene e le strati di passaggio del Miocene al Pliocene, VIII. Planktonic foraminiferal biozonation of the Mediterranean deep sea record: a revision. *Rev. Ital. Paleontol. Stratigr.*, 81:527-544.
- Cita, M. B., and Zocchi, M., 1978. Distribution patterns of benthic foraminifera on the floor of the Mediterranean sea. *Oceanol. Acta*, 1(4):445-462.
- Cita, M. B., Chierichi, M. A., Cliampo, G., Moncharmont, Z. M., D'Onofrio, S., Ryan, W.B.F., and Scorziello, R., 1973. The Quater-

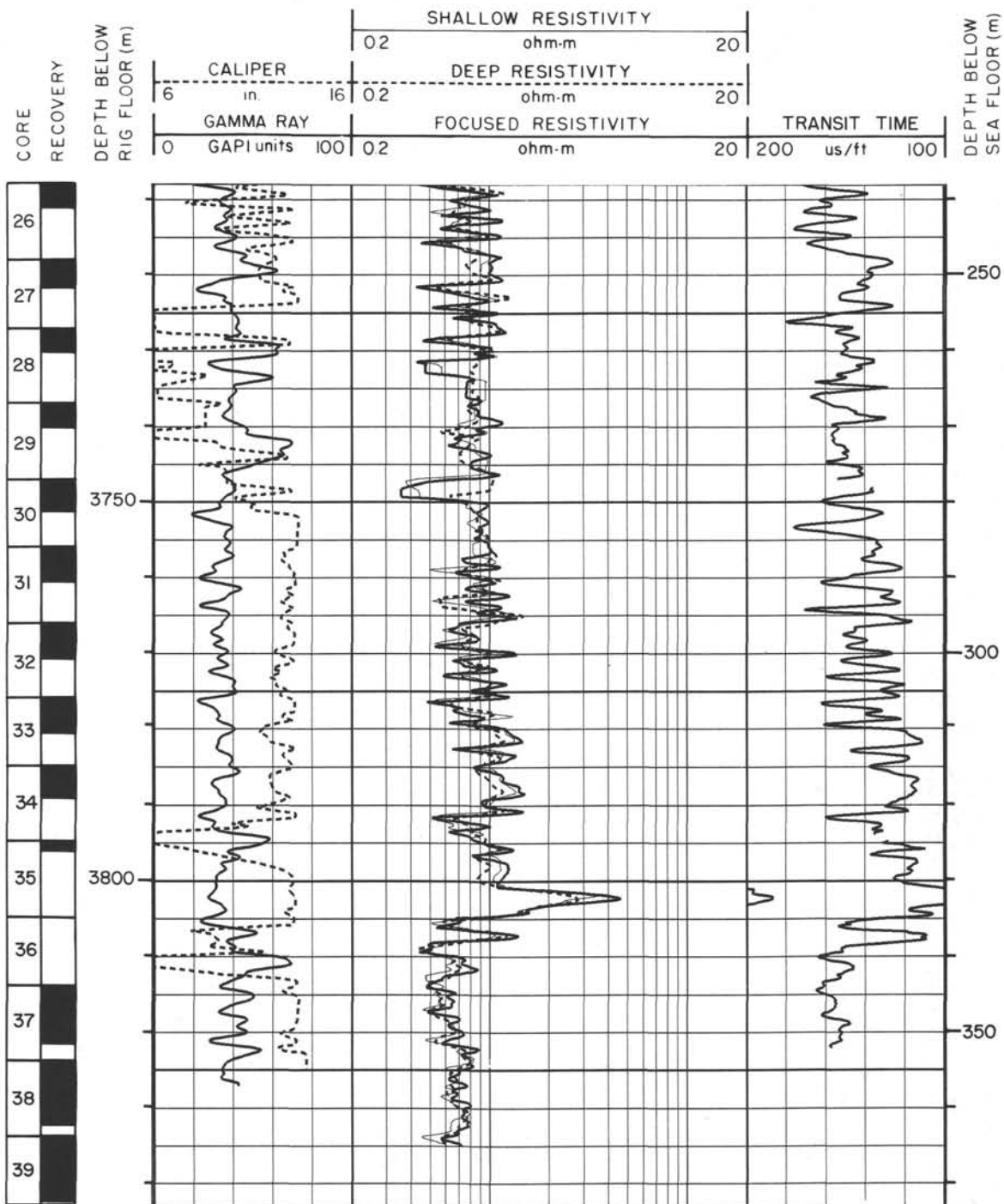
- nary record of the Tyrrhenian and Ionian Basins of the Mediterranean Sea. In Ryan, W.B.F., Hsü, K. J., et al., *Init. Repts. DSDP*, 13: Washington (U.S. Govt. Printing Office), 1405-1415.
- Cita, M. B., and Grignani, D., 1982. Nature and origin of late Neogene Mediterranean Sapropels. In Schlanger, S. O., and Cita, M. B. (Eds.), *Nature and Origin of Cretaceous Carbon-rich Facies*: London (Academic Press), 165-196.
- Colalongo, M. L., Pasini, G., Pelosio, G., Raffi, S., Rio, D., Ruggieri, G., Sartoni, S., Selli, R., and Sprovieri, R., 1982. The Neogene/Quaternary boundary definition: a review and a proposal. *Geogr. Fis. Din. Quat.*, 5:59-68.
- Colantoni, P., Fabbri, A., Gallignani, P., Sartori, R., and Rehault, J. P., 1981. *Carta Litologica e Stratigrafica dei Mari Italiani*. Litografia artistica cartografica, Firenze.
- Decima, A., and Wezel, F. C., 1973. Late Miocene evaporites of the central Sicilian Basin. In Ryan, W.B.F., and Hsü, K., et al., *Init. Repts. DSDP*, 13: Washington (U.S. Govt. Printing Office), 1234-1240.
- Demaision, G. J., and Moore, G. T., 1980. Anoxic environments and oil source bed genesis. *AAPG Bull.* 64:1179-1209.
- Emeis, K. C., and Kvenvolden, K. A., 1986. Shipboard organic geochemistry on JOIDES Resolution. *ODP Tech. Note* 7.
- Emiliani, C., 1978. The cause of the ice ages. *Earth Planet. Sci. Lett.*, 37:349-352.
- Fabbri, A., and Curzi, P., 1979. The Messinian of the Tyrrhenian Sea: seismic evidences and dynamic implications. *G. Geol.*, 43,2:215-248.
- Fabbri, A., Gallignani, P., and Zitellini, N., 1981. Geologic evolution of the Peri-Tyrrhenian sedimentary basins. In Wezel, F.C. (Ed.), *Sedimentary basins of Mediterranean margins*. Bologna (Technoprint), 101-126.
- Finetti, I., and Morelli, C., 1973. Geophysical exploration of the Mediterranean Sea. *Boll. Geofis. Teor. Appl.*, 15:263-340.
- Finetti, I., Morelli, C., and Zarudzki, E., 1970. Reflection seismic study of the Tyrrhenian Sea. *Boll. Geofis. Teor. Appl.*, 12,48:311-346.
- Garrison, R. E., Schreiber, B. C., Bernoulli, D., Fabricius, F., Kidd, R. B., and Melieres, F., 1978. Sedimentary petrology and structures of Messinian evaporitic sediments in the Mediterranean Sea, Leg 42A, Deep Sea Drilling Project, In Hsü, K., and Montadert, L., et al., *Init. Repts. DSDP* 42, Pt. 1: Washington (U.S. Govt. Printing Office), 571-612.
- Genesseeux, M., Rehault, J.-P., Thomas, B., Colantoni, P., Fabbri, A., Lepvrier, C., Mascle, G., Mauffret, A., Polino, R., Robin, C., and Vanney, J., 1986. Resultats de plongées en submersible Cyana sur les blocs basculés de la mer Tyrrhénienne centrale et le volcan sous-marin Vavilov. *C.R. Acad. Sci. Paris Ser. A*, T302,12:785-792.
- Grandjacquet, C., and Mascle, G., 1978. The structure of the Ionian Sea, Sicily and Calabria-Lucania. In Nairn, A.E.M., et al. (Eds.), *The Ocean Basins and Margins*: New York (Plenum Press), 4B,257-329.
- Hardie, L. A., 1967. The gypsum-anhydrite equilibrium at one atmosphere pressure. *Am. Mineralogist*, 52:171-200.
- Harland, W. B., Cox, A., Lewellyn, P. G., Pickton, C.A.G., Smith, A. G., and Walters, R., 1982. *A Geologic Time Scale*: Cambridge (Cambridge Univ. Press).
- Hassan, M., and Hossin, A., 1975. Contributions à l'étude des comportements du Thorium et du Potassium dans les roches sédimentaires. *C.R. Acad. Sci., Paris Ser. A*, T280,533-535.
- Heimann, K. O., and Mascle, G., 1974. Les séquences de la série évaporitique messinienne. *C.R. Acad. Sci. Paris Ser. A*, 279,1967-1970.
- Hunt, J. M., 1979. *Petroleum Geochemistry and Geology*: San Francisco (Freeman and Co.).
- Hutchison, I., Von Herzen, R., Loudon, K., Sclater, J., and Jemsek, J., 1985. Heat flow in the Balearic and Tyrrhenian basins, Western Mediterranean. *J. Geophys. Res.*, 90(B1):685-701.
- Kidd, R. B., Cita, M. B., and Ryan, W.B.F., 1978. Stratigraphy of eastern Mediterranean sapropel sequences recovered during Leg 42A and their paleoenvironmental significance. In Hsü, K. J., Montadert, L., et al., *Init. Repts. DSDP*, 42A: Washington (U.S. Govt. Printing Office), 421-443.
- Malinverno, A., 1981. Quantitative estimates of age and Messinian paleobathymetry of the Tyrrhenian Sea after seismic reflection, heat flow and geophysical models. *Boll. Geofis. Teor. Appl.*, 23,90-91: 159-171.
- Malinverno, A., and Ryan, W.B.F., 1986. Extension in the Tyrrhenian Sea and shortening in the Apenninic as a result of arc migration driven by a sinking of the lithosphere. *Tectonics*, 5,2:227-245.
- Malinverno, A., Cafiero, M., Ryan, W.B.F., and Cita, M. B., 1981. Distribution of Messinian sediments and erosional surfaces beneath the Tyrrhenian Sea: geodynamic implications. *Oceanol. Acta*, 4: 489-496.
- Manheim, F. T., and Sayles, F. L., 1974. Composition and origin of interstitial waters of marine sediments based on deep sea drill cores. In Goldberg, E. D. (Ed.) *The Sea* 5:527-568.
- Mankinen, E. A., and Dalrymple, G. B., 1979. Revised geomagnetic polarity time scale for the interval 1-5 m.y.B.P., *J. Geophys. Res.*, 84:615-626.
- Moussat, E., 1983. Evolution de la Mer Tyrrhénienne centrale et orientale et de ses marges septentrionales en relation avec la neotectonique dans l'Arc Calabrais [Thesis]. Univ. P. et M. Curie, Paris.
- Moussat, E., Rehault, J. P., Fabbri, A., and Mascle, G., 1985. Evolution géologique de la mer Tyrrhénienne. *C.R. Acad. Sci. Paris Ser. A*, 301:491-496.
- Morelli, C., 1970. Physiography and magnetism of Tyrrhenian Sea. *Boll. Geofis. Teor. Appl.*, 12,(48):275-309.
- Mueller, P. J., and Suess, E., 1979. Productivity, sedimentation rate, and sedimentary organic matter in the oceans — I. Organic carbon preservation. *Deep Sea Res.*, 26A:1347-1362.
- Muerdter, D. R., and Kennett, J. P., 1983. Late Quaternary planktonic foraminiferal Biostratigraphy, Strait of Sicily, Mediterranean Sea. *Mar. Micropaleontol.*, 8:339-359.
- Müller, C., 1978. Neogene calcareous nannofossils from the Mediterranean — Leg 42 of the Deep Sea Drilling Project. In Hsü, K. J., Montadert, L., et al., *Init. Repts. DSDP*, 42, Pt.1: Washington (U.S. Govt. Printing Office), 727-752.
- Muller, D. C., 1985. Computer method to detect and correct cycle skipping on sonic logs, In Trans. SPWLA, paper R.
- Murat, A., and Glaçon, G., 1985. In Rapport des campagnes à la mer du Marion Dufresne. T.A.A.F. Campagne Strabon.
- Parker, F. L., 1955. Distribution of planktonic foraminifera in some Mediterranean sediments. *Papers in Marine Biology and Oceanography*, London (Pergamon) 204-241.
- Reca, M., Rehault, J.-P., Steinmetz, L., and Fabbri, A., 1984. Amincissement de la croûte et accretion au centre du bassin Tyrrhénien d'après la sismique refraction. *Mar. Geol.*, 55:411-428.
- Rehault, J.-P., Moussat, E., and Fabbri, A., 1987. Structural evolution of the Tyrrhenian back-arc basin. *Mar. Geol.*, 74:123-150.
- Rehault, J.-P., Tisseau, C., and Foucher, J. P., 1984a. Structure, subsidence et flux thermique de la Mer Tyrrhénienne Centrale: essais de modélisation. CIESM, (29th meeting) 11-19 October 1984, Lucerne.
- Rehault, J.-P., Mascle, J., and Boillot, G., 1984b. Evolution géodynamique de la Méditerranée depuis l'Oligocène. *Mem. Soc. Geol. Ital.*, 27:85-96.
- Rio, D., Sprovieri, R., Di Stefano, I., and Raffi, I., 1984a. *Globorotalia truncatulinoides* (d'Orbigny) in the Mediterranean upper Pliocene geologic record. *Micropaleontology*, 30:12-137.
- Rio, D., Sprovieri, R., and Raffi, I., 1984b. Calcareous plankton biostratigraphy and biochronology of the Pliocene-lower Pleistocene succession of the Capo Rosello area, Sicily. *Mar. Micropaleontol.* 9:135-180.
- Romankevich, E. A., 1984. *Geochemistry of Organic Matter in the Ocean*. Berlin (Springer).
- Ruggieri, G., Rio, D., and Sprovieri, R., 1984. Remarks on the chronostratigraphic classification of Lower Pleistocene. *Boll. Soc. Geol. Ital.*, 103:252-259.
- Ruggieri, G., and Sprovieri, R., 1983. Recenti progressi nella stratigrafia del Pleistocene inferiore. *Boll. Soc. Paleontol. Ital.*, 22(3):315-321.
- Ryan, W.B.F., Hsü, K. D., et al., 1973. Site 132. In Ryan, W.B.F., Hsü, K. D., et al., *Init. Repts. DSDP*, 13: Washington (U.S. Govt. Printing Office), 402-464.
- Schlumberger, 1972. *The Essentials of Log Interpretation Practice*. Paris (Services Techniques Schlumberger).
- , 1985. *Log Interpretation Charts*. New York (Schlumberger Well Services).
- Selli, R., and Fabbri, A., 1971. Tyrrhenian: a Pliocene deep sea. *Rend. Cl. Sci. Fis. Mat. Acc. Naz. Lincei*, 50:104-116.

- Sigl, W., and Muller, J., 1975. Identification and correlation of stagnation layers in cores from the eastern Mediterranean Sea. *Rapports Proces Verbaux CIESM*: 23:277-279.
- Simoneit, B.R.T., 1982. Shipboard organic geochemistry and safety monitoring Leg 64, Gulf of California. In Curry, J. R., Moore, D. G., et al., *Init. Repts. DSDP*, 64 (Pt. 2): Washington (U.S. Govt. Printing Office), 723-727.
- Sprovieri, R., and Barone, G., 1984. I Foraminiferi bentonici della sezione pliocenica di Punta Piccola (Agrigento, Sicilia). *Geol. Rom.*
- Steinmetz, L., Ferricci, F., Hirn, A., Morelli, C., and Nicolich, R., 1983. A 550 km long Moho traverse in the Tyrrhenian Sea from O.B.S record P_n waves. *Geophys. Res. Lett.*, 10:428-431.
- Tauxe, L., Opdyke, N., Pasini, G., and Elmi, C., 1983. Age of the Plio-Pleistocene boundary in the Vrica section, southern Italy. *Nature*, 304:125-129.
- Todd R., 1958. Foraminifera from Western Mediterranean Deep-Sea cores. *Rep. Swed. Deep-Sea Exped.*, 3:169-215.
- Thunnell, R., Williams, D., and Belyea, P., 1984. Anoxic events in the Mediterranean Sea in relation to the evolution of late Neogene climates. *Mar. Geol.*, 59:105-134.
- Van Donk, J., 1976. ^{18}O record of the Atlantic Ocean for the entire Pleistocene Epoch. In Cline, R. M., and Hays, J. D. (Eds.), *Investigation of Late Quaternary paleoceanography and paleoclimatology*. Mem. Geol. Soc. Am. 145:147-163.
- Waples, D., 1982. Organic Geochemistry for Exploration Geologists. Boston (Int. Human Res. Develop. Corp.).
- Whelan, J. K., and Hunt, J. M., 1982. $C_1 - C_8$ Hydrocarbons in Leg 64 Sediments, Gulf of California. In Curran, J. R., Moore, D. G., et al., *Init. Repts. DSDP*, 64 (Pt.2): Washington (U.S. Govt. Printing Office), 763-779.

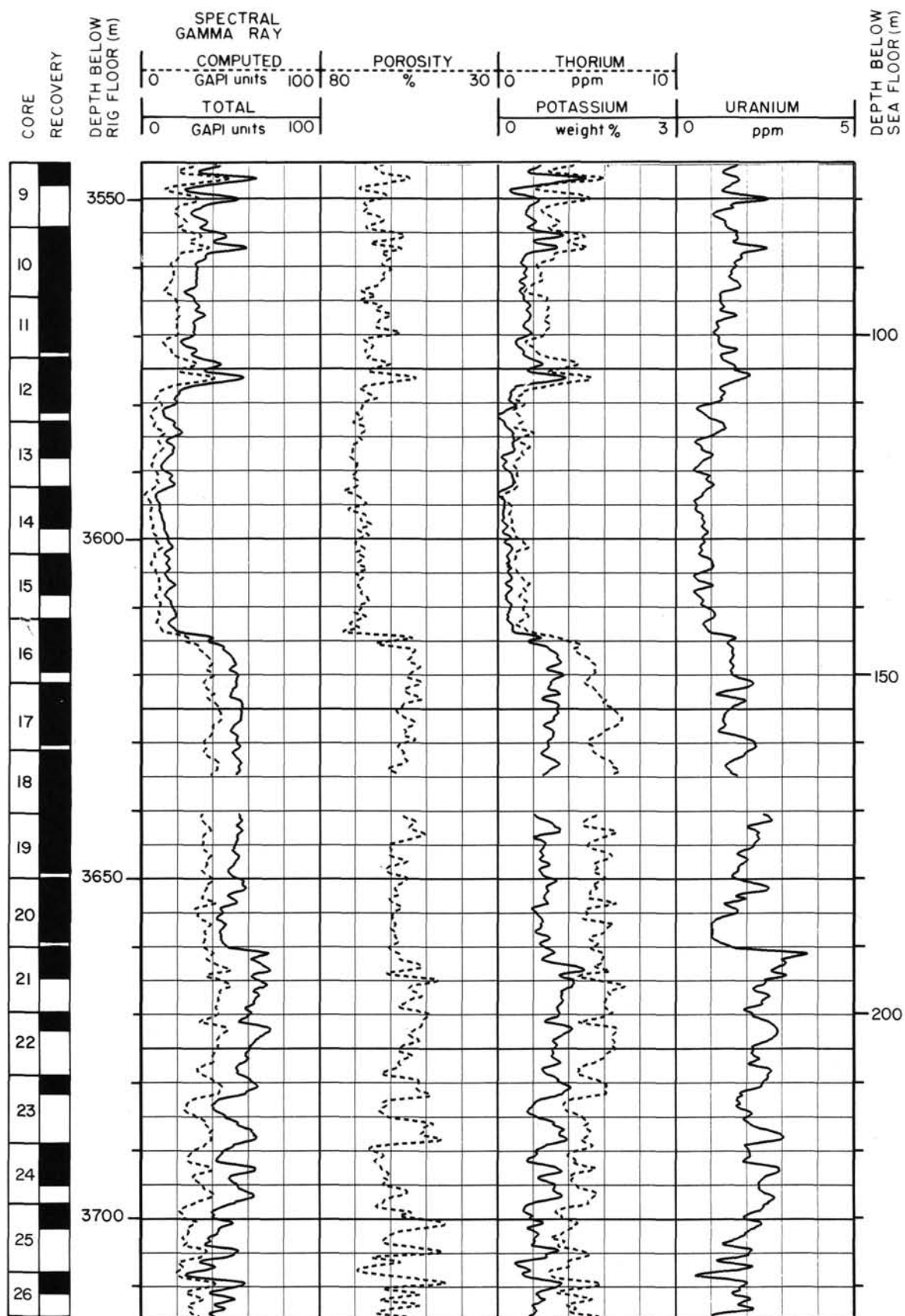
Summary Log for Hole 652A



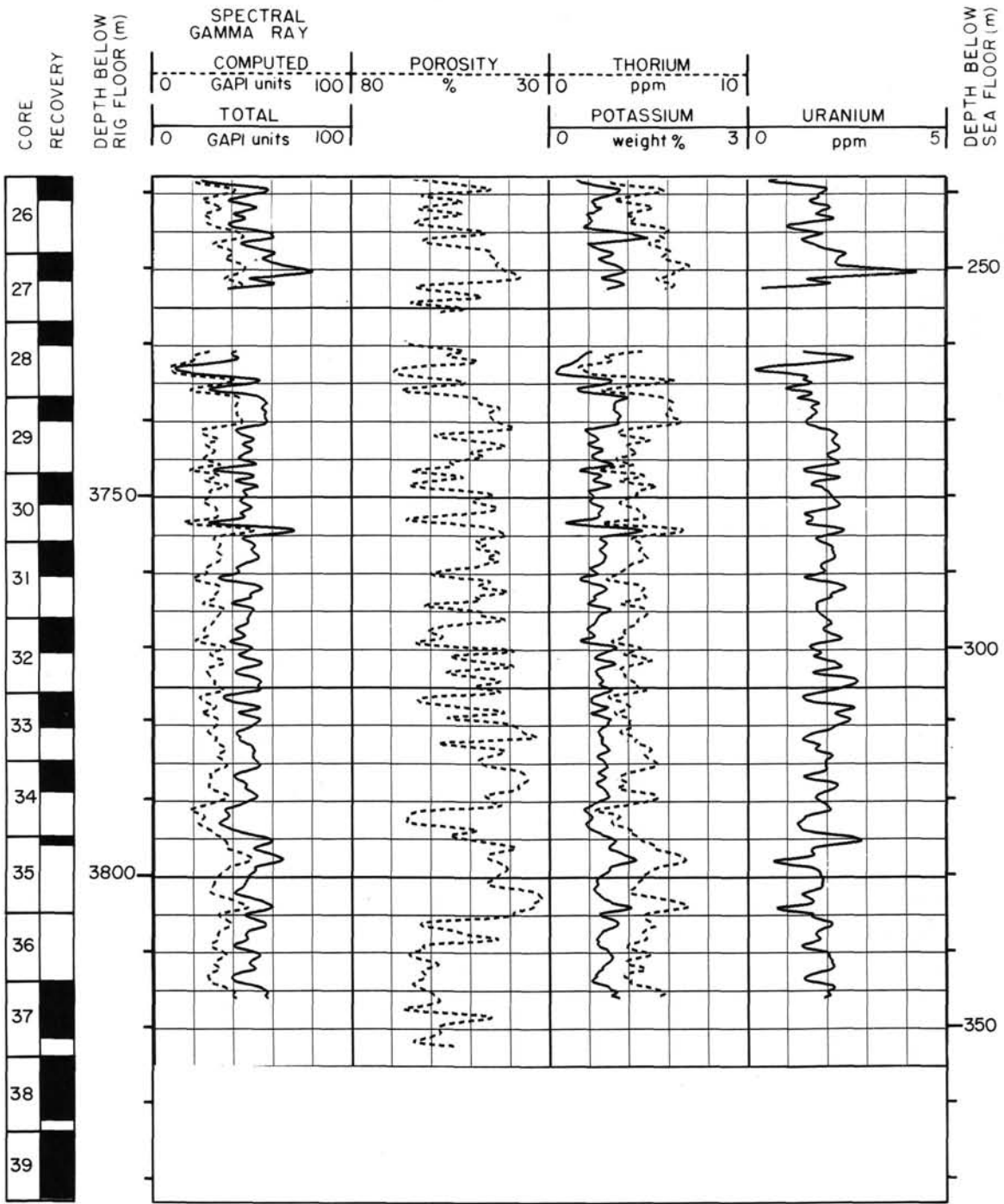
Summary Log for Hole 652A (continued)



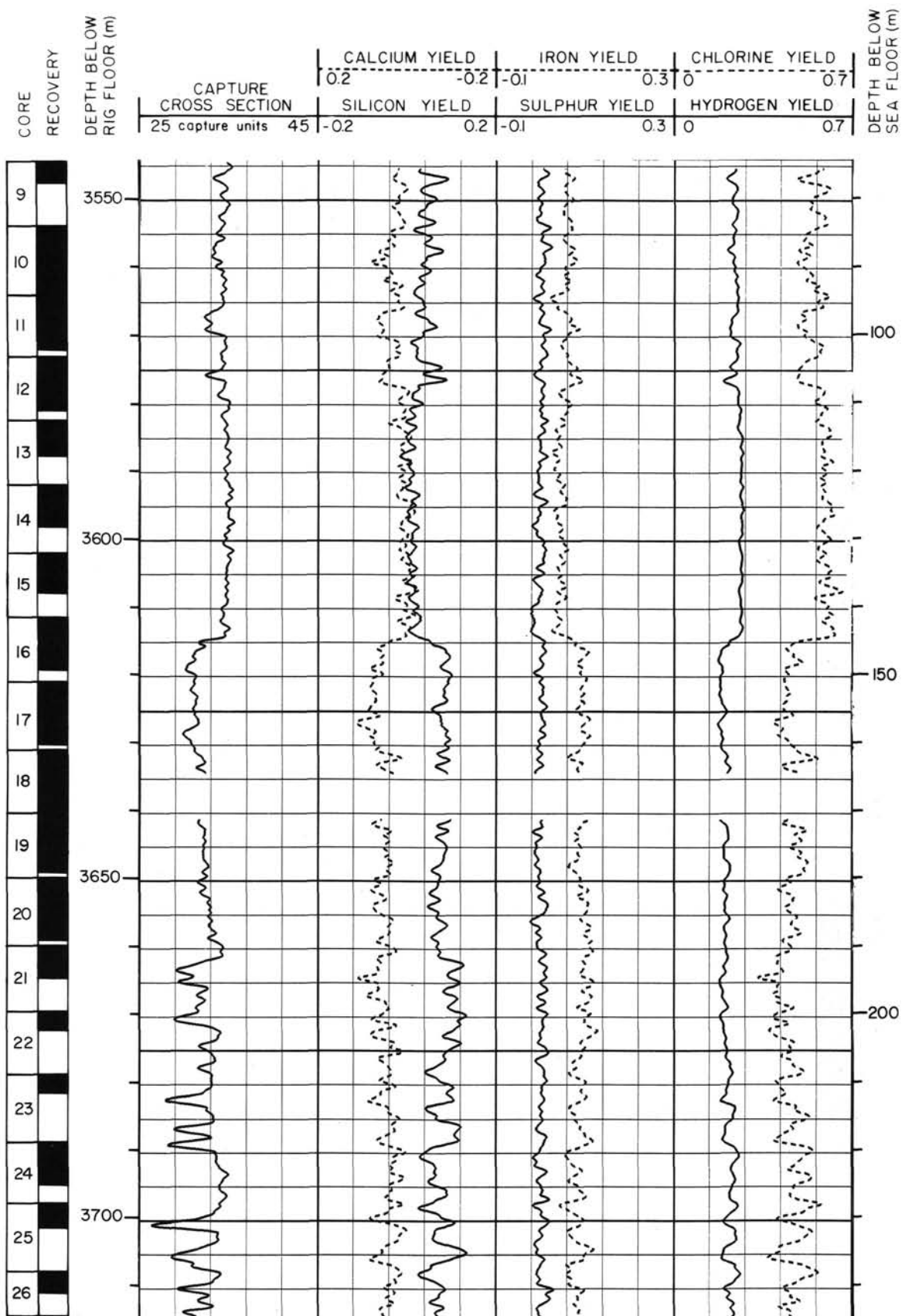
Summary Log for Hole 652A (continued)



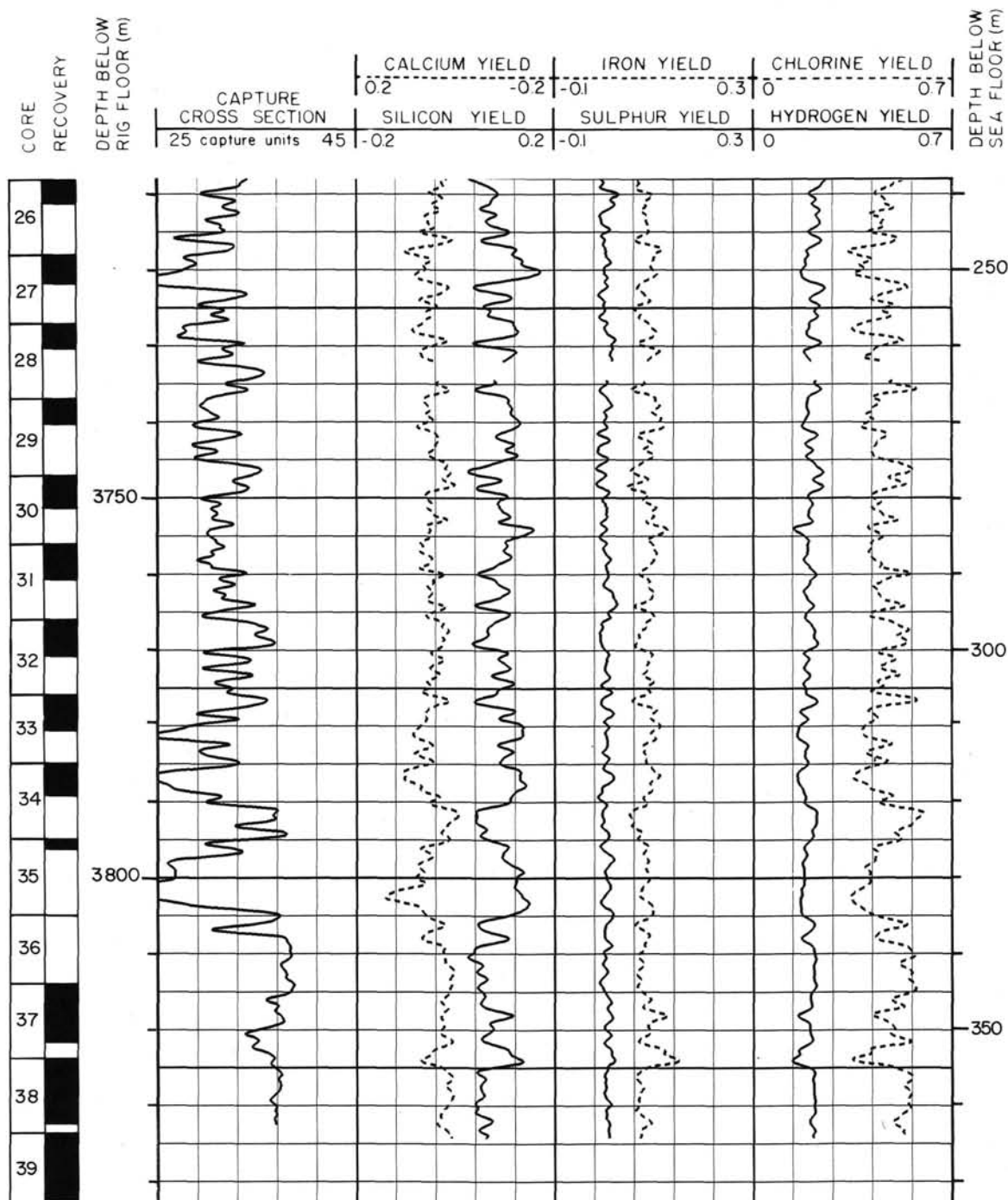
Summary Log for Hole 652A (continued)



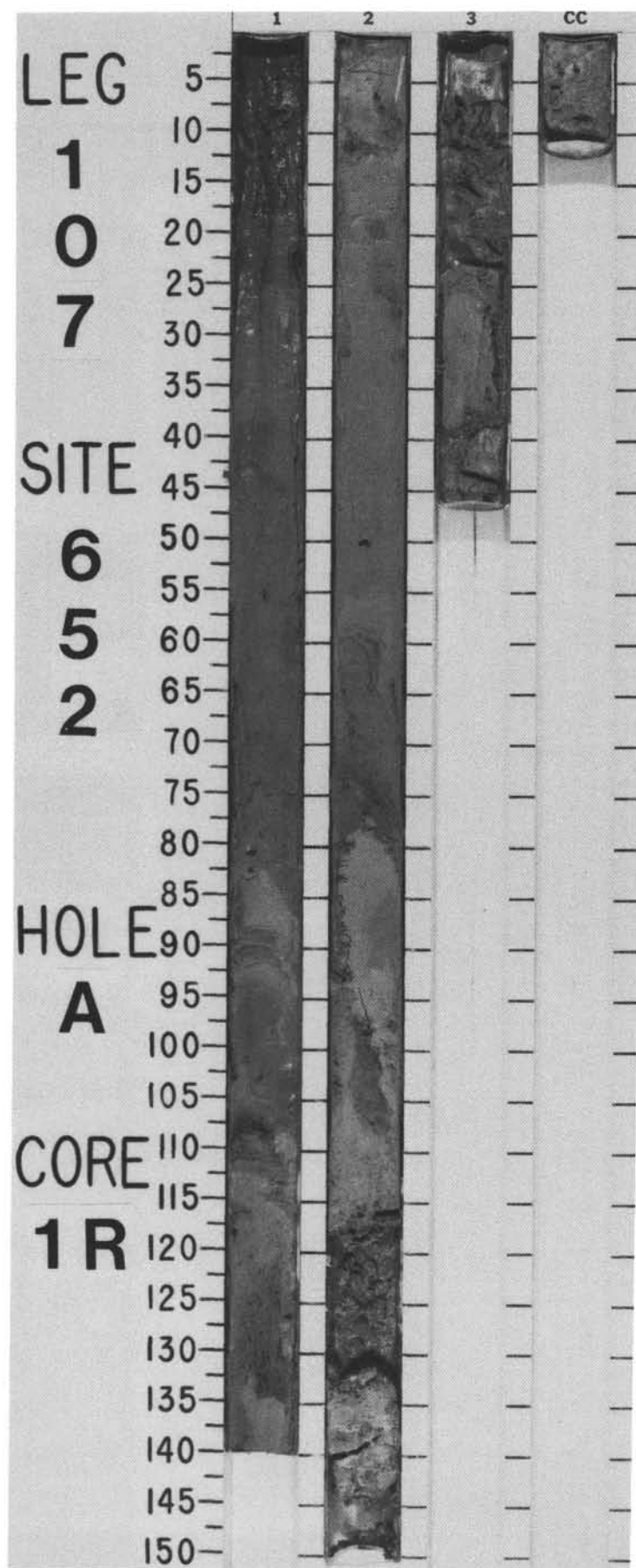
Summary Log for Hole 652A (continued)



Summary Log for Hole 652A (continued)



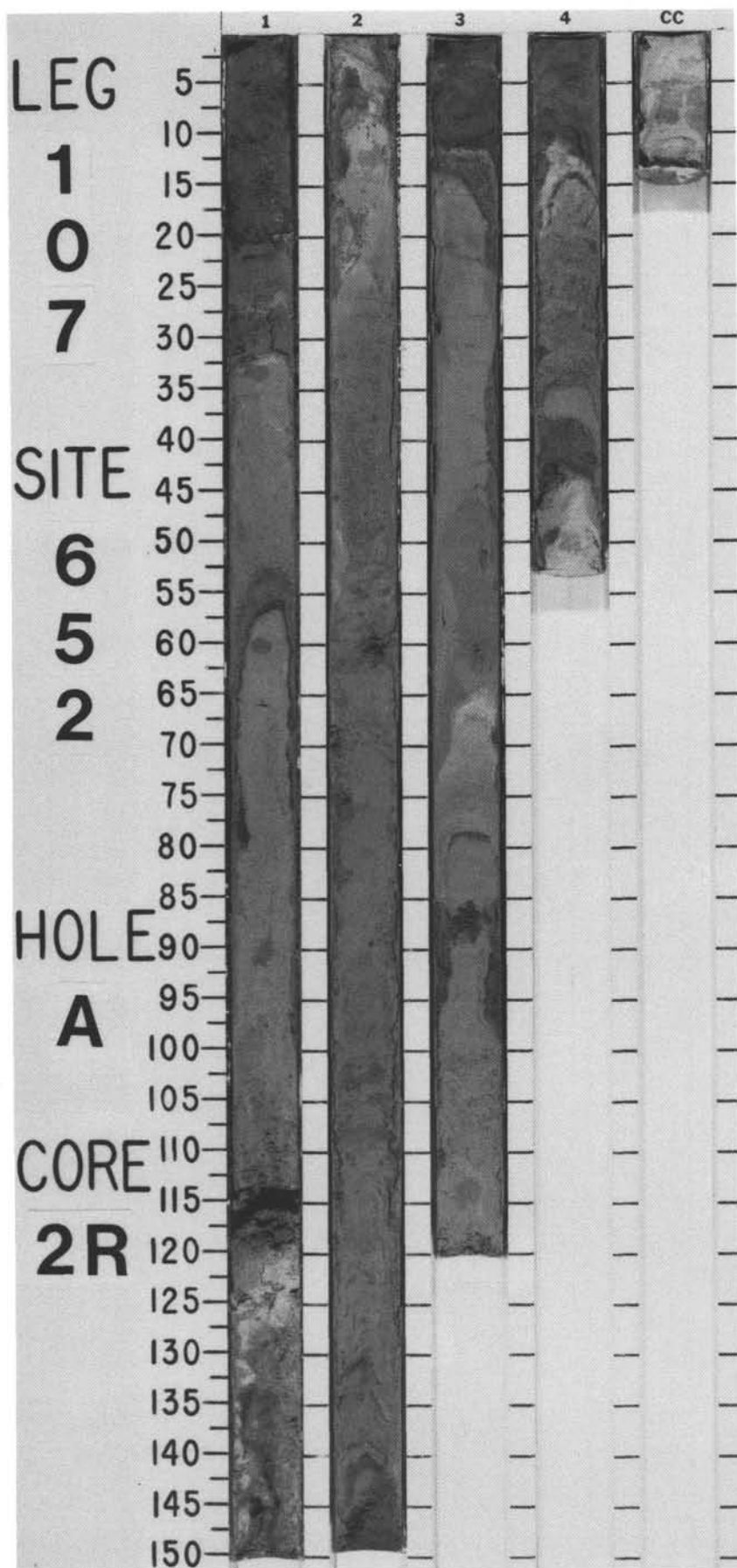
[illegible]



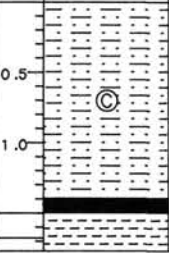

SITE 652 HOLE A CORE 2 R CORED INTERVAL 3449.6-3463.0 mbsl; 3.6-17.0 mbsf

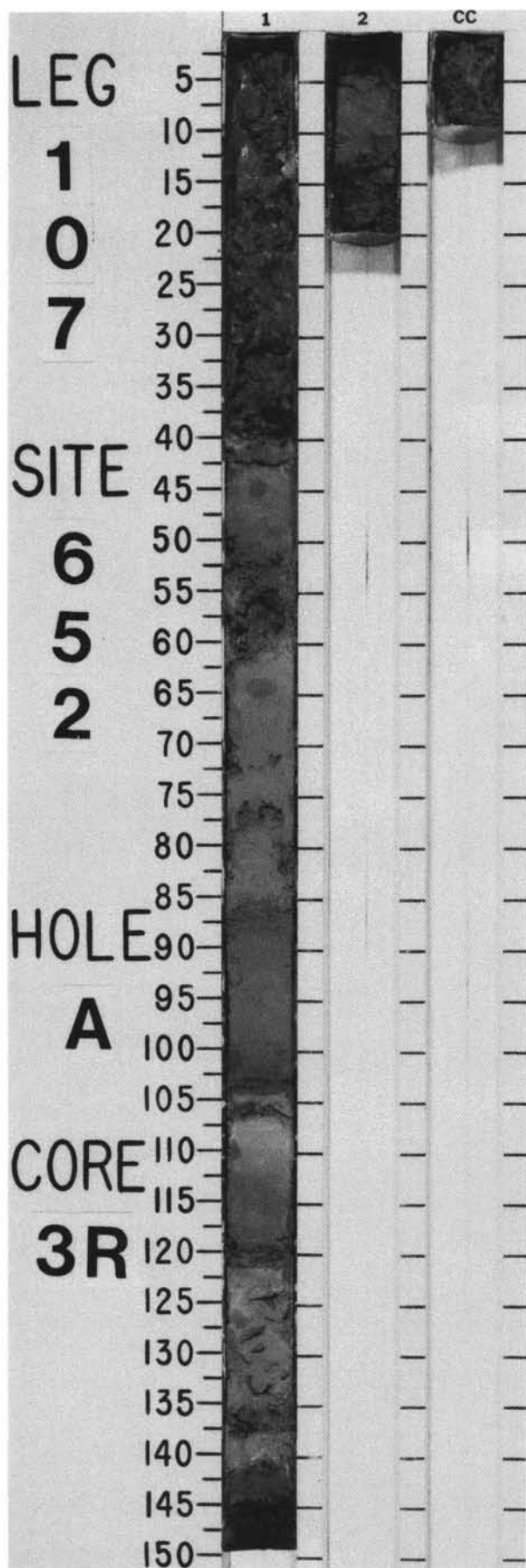
TIME-ROCK UNIT	BIOSTRAT. ZONE/ FOSSIL CHARACTER				PALEOMAGNETICS	PHYS. PROPERTIES	CHEMISTRY	SECTION	METERS	GRAPHIC LITHOLOGY	DRILLING DISTURB.	SED. STRUCTURES	SAMPLES	LITHOLOGIC DESCRIPTION
	FORAMINIFERS	NANNOFOSSILS	RADIOLARIANS	DIATOMS										
PLEISTOCENE	A/G	NN	NN20	NN20	Brunhes	$\gamma = 1.35 \phi = 82$	$\gamma = 1.47 \phi = 77$	1	0.5				*	SANDY CALCAREOUS MUD, CALCAREOUS MUD, and MUD
								2	1.0				*	Sandy calcareous mud (Sections 1 and 2) to calcareous mud (Section 3, 1-70 cm) to mud (Section 3, 70-150 cm, Section 4, and CC), with variable nannofossil content and a few centimeters-thick, fine-grained, sandy layers containing abundant foraminifers; light olive-gray (5Y 6/2) and olive-gray (5Y 5/2) to gray (5Y 6/1), with greenish gray (5GY 5/1) and light brownish gray (2.5Y 6/2); zone of moderate bioturbation in Section 3.
								3					*	
								4					OG	
								CC					*	

SMEAR SLIDE SUMMARY (%):				
	1, 140	3, 30	3, 83	4, 28
	D	D	D	D
TEXTURE:				
Sand	20	—	—	—
Silt	35	15	20	15
Clay	45	85	80	85
COMPOSITION:				
Quartz	10	3	3	1
Feldspar	5	Tr	Tr	2
Mica	2	1	1	—
Clay	31	14	40	72
Volcanic glass	8	2	2	2
Calcite	5	5	—	—
Dolomite	2	5	2	3
Accessory minerals	10	2	—	Tr
Opaque minerals	—	—	1	—
Foraminifers	5	2	2	3
Nannofossils	20	65	44	12
Diatoms	—	Tr	1	2
Radiolarians	1	—	1	—
Sponge spicules	1	1	—	—
Pellets	—	—	3	—
Micrite	—	—	—	3



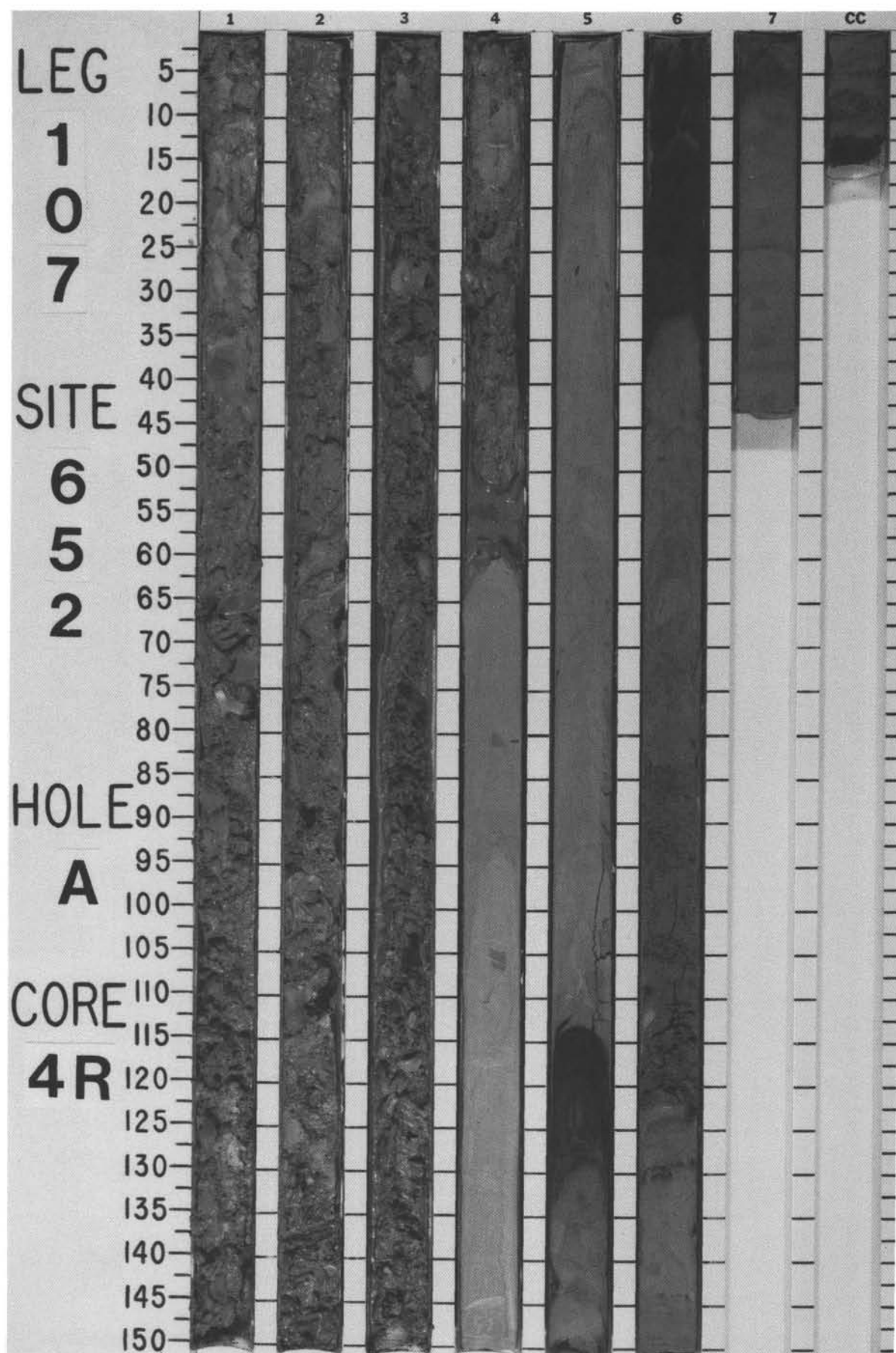
SITE 652 HOLE A CORE 3 R CORED INTERVAL 3463.0-3472.7 mbsl; 17.0-26.7 mbsf

TIME-ROCK UNIT	BIOSTRAT. ZONE/ FOSSIL CHARACTER				PALEOMAGNETICS	PHYS. PROPERTIES	CHEMISTRY	SECTION	METERS	GRAPHIC LITHOLOGY	DRILLING DISTURB.	SED. STRUCTURES	SAMPLES	LITHOLOGIC DESCRIPTION																																																																																															
	FORAMINIFERS	NANNOFOSSILS	RADIOLARIANS	DIATOMS																																																																																																									
PLEISTOCENE	A/G					$\gamma=1.56 \phi=75 \vee-1522$	22 ● ●22 ●32	1	0.5 1.0				* * *	<p>CALCAREOUS MUD</p> <p>Calcareous mud, light olive-gray (5Y 6/2), olive-gray (5Y 5/2), and greenish gray (10Y 5/2, 6/1, 6/2), with rare centimeter-thick, fine-grained, foraminifer-bearing sand layers.</p> <p>Minor lithology: Section 1, 141-150 cm, and Section 2, 0-4 cm, is a very dark gray (5Y 3/1), organic-bearing, calcareous mud (a sapropel), which overlies gray (5Y 5/1) clay. In Section 1, 37-38 cm, a 1.5-cm piece of black (5Y 2.5/1), noncalcareous material, possibly sapropelic or manganese-rich.</p> <p>SMEAR SLIDE SUMMARY (%):</p> <table><tr><td></td><td>1, 83</td><td>1, 118</td><td>2, 1</td><td>2, 17</td></tr><tr><td>D</td><td></td><td>M</td><td>M</td><td>M</td></tr></table> <p>TEXTURE:</p> <table><tr><td>Sand</td><td>5</td><td>5</td><td>7</td><td>—</td></tr><tr><td>Silt</td><td>10</td><td>10</td><td>20</td><td>10</td></tr><tr><td>Clay</td><td>85</td><td>85</td><td>73</td><td>90</td></tr></table> <p>COMPOSITION:</p> <table><tr><td>Quartz</td><td>2</td><td>3</td><td>2</td><td>2</td></tr><tr><td>Feldspar</td><td>Tr</td><td>5</td><td>1</td><td>4</td></tr><tr><td>Clay</td><td>75</td><td>58</td><td>67</td><td>77</td></tr><tr><td>Volcanic glass</td><td>5</td><td>5</td><td>Tr</td><td>2</td></tr><tr><td>Calcite/dolomite</td><td>—</td><td>2</td><td>—</td><td>—</td></tr><tr><td>Accessory minerals</td><td>Tr</td><td>1</td><td>—</td><td>Tr</td></tr><tr><td>Black, undet. (organic?)</td><td>—</td><td>—</td><td>7</td><td>—</td></tr><tr><td>Undetermined opaques</td><td>—</td><td>—</td><td>—</td><td>1</td></tr><tr><td>Foraminifers</td><td>3</td><td>6</td><td>4</td><td>2</td></tr><tr><td>Nannofossils</td><td>8</td><td>8</td><td>15</td><td>7</td></tr><tr><td>Diatoms</td><td>—</td><td>—</td><td>Tr</td><td>1</td></tr><tr><td>Radiolarians</td><td>1</td><td>3</td><td>2</td><td>1</td></tr><tr><td>Sponge spicules</td><td>—</td><td>2</td><td>—</td><td>Tr</td></tr><tr><td>Micrite</td><td>6</td><td>7</td><td>2</td><td>3</td></tr></table>		1, 83	1, 118	2, 1	2, 17	D		M	M	M	Sand	5	5	7	—	Silt	10	10	20	10	Clay	85	85	73	90	Quartz	2	3	2	2	Feldspar	Tr	5	1	4	Clay	75	58	67	77	Volcanic glass	5	5	Tr	2	Calcite/dolomite	—	2	—	—	Accessory minerals	Tr	1	—	Tr	Black, undet. (organic?)	—	—	7	—	Undetermined opaques	—	—	—	1	Foraminifers	3	6	4	2	Nannofossils	8	8	15	7	Diatoms	—	—	Tr	1	Radiolarians	1	3	2	1	Sponge spicules	—	2	—	Tr	Micrite	6	7	2	3
	1, 83	1, 118	2, 1	2, 17																																																																																																									
D		M	M	M																																																																																																									
Sand	5	5	7	—																																																																																																									
Silt	10	10	20	10																																																																																																									
Clay	85	85	73	90																																																																																																									
Quartz	2	3	2	2																																																																																																									
Feldspar	Tr	5	1	4																																																																																																									
Clay	75	58	67	77																																																																																																									
Volcanic glass	5	5	Tr	2																																																																																																									
Calcite/dolomite	—	2	—	—																																																																																																									
Accessory minerals	Tr	1	—	Tr																																																																																																									
Black, undet. (organic?)	—	—	7	—																																																																																																									
Undetermined opaques	—	—	—	1																																																																																																									
Foraminifers	3	6	4	2																																																																																																									
Nannofossils	8	8	15	7																																																																																																									
Diatoms	—	—	Tr	1																																																																																																									
Radiolarians	1	3	2	1																																																																																																									
Sponge spicules	—	2	—	Tr																																																																																																									
Micrite	6	7	2	3																																																																																																									




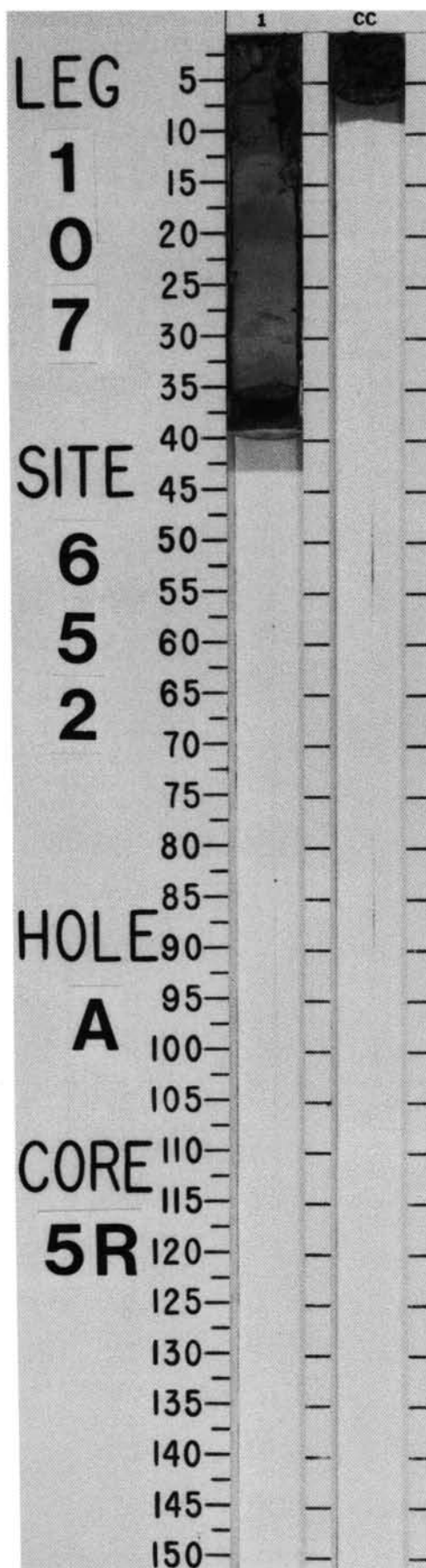
SITE 652 HOLE A CORE 4 R CORED INTERVAL 3472.7-3482.4 mbsl; 26.7-36.4 mbsf

TIME- ROCK UNIT	BIOSTRAT. ZONE/ FOSSIL CHARACTER				PALEOMAGNETICS	PHYS. PROPERTIES	CHEMISTRY	SECTION	METERS	GRAPHIC LITHOLOGY	DRILLING DISTURB.	SED. STRUCTURES	SAMPLES	LITHOLOGIC DESCRIPTION
	FORAMINIFERS	NANNOFOSSILS	RADIOLARIANS	DIATOMS										
PLEISTOCENE	<i>Giborotalia truncatulinoidea excelsa</i> NN19				Brunhes									
F/G														



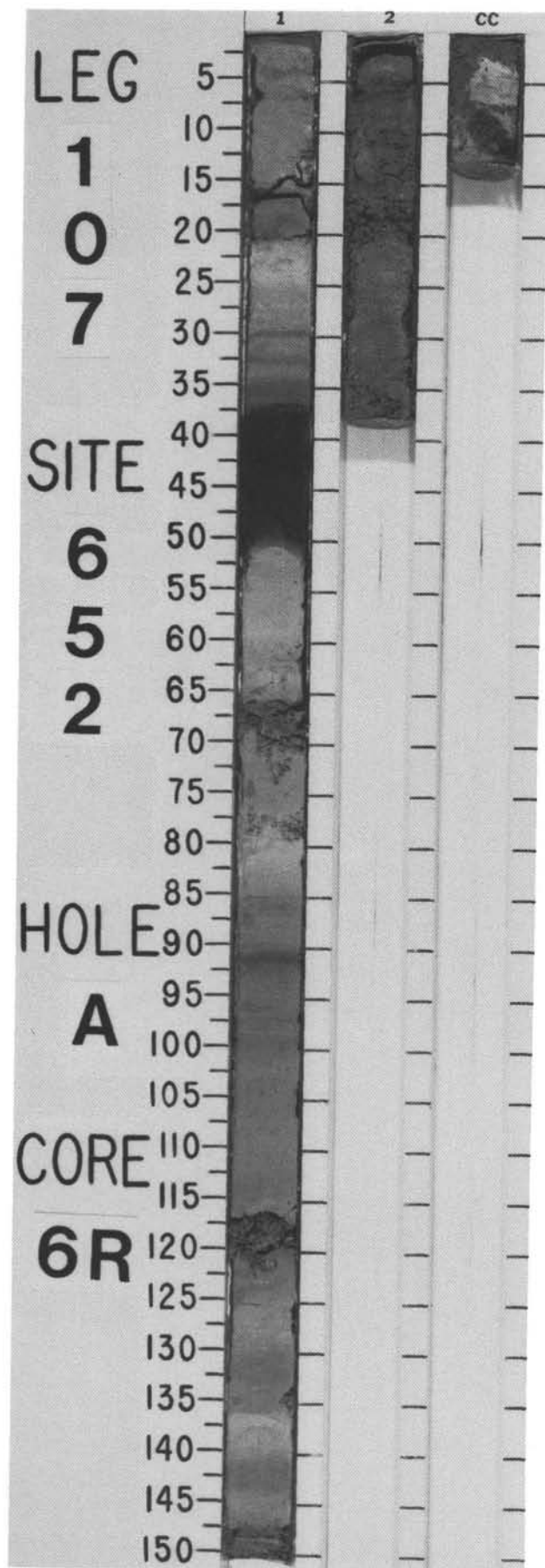
SITE 652 HOLE A CORE 5 R CORED INTERVAL 3482.4-3491.8 mbsl; 36.4-45.8 mbsf

TIME-ROCK UNIT	BIOSTRAT. ZONE/ FOSSIL CHARACTER				PALEOMAGNETICS	PHYS. PROPERTIES	CHEMISTRY	SECTION	METERS	GRAPHIC LITHOLOGY	DRILLING DISTURB.	SED. STRUCTURES	SAMPLES	LITHOLOGIC DESCRIPTION
	FORAMINIFERS	NANNOFOSSILS	RADIOLARIANS	DIATOMS										
PLEISTOCENE	<i>Globorotalia truncatulinoides excelsa</i>	F/G	NN19		Matuyama		25	1			-	-	-	*
							43							



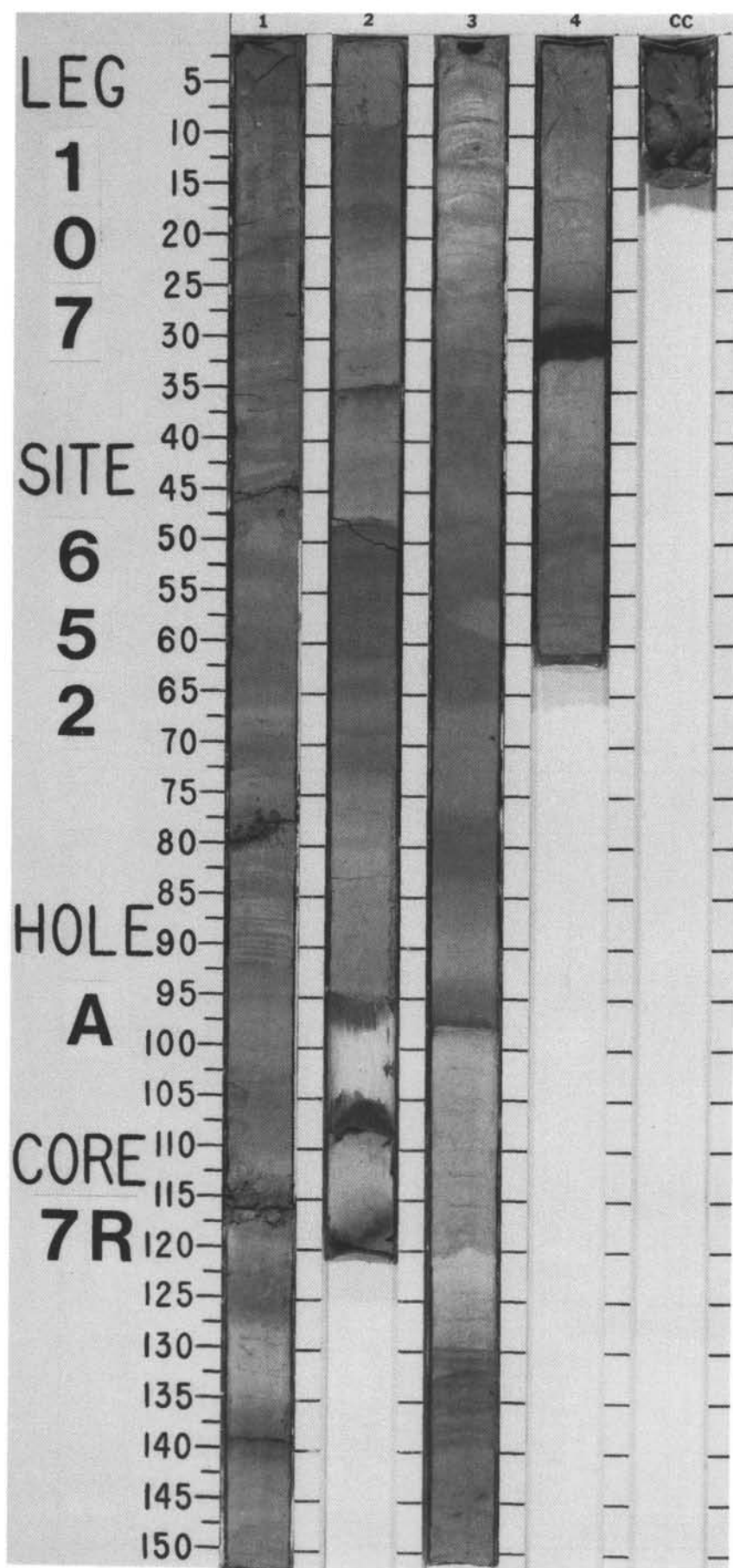
SITE 652 HOLE A CORE 6 R CORED INTERVAL 3491.8-3501.4 mbsl; 45.8-55.4 mbsf

TIME- ROCK UNIT	BIOSTRAT. ZONE/ FOSSIL CHARACTER				PALEOMAGNETICS	PHYS. PROPERTIES	CHEMISTRY	SECTION	METERS	GRAPHIC LITHOLOGY	DRILLING DISTURB.	SED. STRUCTURES	SAMPLES	LITHOLOGIC DESCRIPTION																																																																																																																			
	FORAMINIFERS	NANNOFOSSILS	RADIOLARIANS	DIATOMS																																																																																																																													
PLEISTOCENE	<i>Globorotalia truncatulinoides excelsa</i>				Matuyama	$\gamma = 1.69 \phi = 65 \psi = 1570$	36 ● 28 ● 5 ● 25 ● 18 ● 18 ●	1	0.5 1.0				* * * *	CALCAREOUS MUD, CLAY, and MARLY NANNOFOSSIL OOZE Calcareous mud grading between calcareous clay and marly nannofossil ooze in multi-colored layers, each approximately 15 cm thick; light brownish gray (2.5Y 6/2), light gray (10Y 7/1), and gray (10Y 6/1), to light olive-gray (5Y 6/2), gray (5Y 6/1), and greenish gray (5GY 5/1). Minor lithology: very dark gray (10Y 3/1) to black (10Y 2/1), organic-rich mud occurs in Section 1, 37-52 cm; underlying light gray (10Y 7/1), marly nannofossil ooze is pyrite-bearing.																																																																																																																			
		R/G						2																																																																																																																									
		NN19						CC						<p>SMEAR SLIDE SUMMARY (%):</p> <table><tr><td></td><td>1, 42</td><td>1, 60</td><td>1, 135</td><td>1, 148</td></tr><tr><td></td><td>M</td><td>D</td><td>M</td><td>M</td></tr></table> <p>TEXTURE:</p> <table><tr><td>Sand</td><td>10</td><td>2</td><td>2</td><td>8</td></tr><tr><td>Silt</td><td>25</td><td>8</td><td>20</td><td>15</td></tr><tr><td>Clay</td><td>65</td><td>90</td><td>78</td><td>77</td></tr></table> <p>COMPOSITION:</p> <table><tr><td>Quartz</td><td>1</td><td>2</td><td>2</td><td>1</td></tr><tr><td>Feldspar</td><td>3</td><td>2</td><td>4</td><td>1</td></tr><tr><td>Clay</td><td>53</td><td>22</td><td>26</td><td>36</td></tr><tr><td>Volcanic glass</td><td>—</td><td>2</td><td>Tr</td><td>—</td></tr><tr><td>Calcite</td><td>2</td><td>Tr</td><td>1</td><td>Tr</td></tr><tr><td>Dolomite</td><td>Tr</td><td>Tr</td><td>2</td><td>Tr</td></tr><tr><td>Accessory minerals</td><td>—</td><td>—</td><td>—</td><td>Tr</td></tr><tr><td>Amorphous opaques</td><td>—</td><td>—</td><td>—</td><td>—</td></tr><tr><td>(organic matter?)</td><td>35</td><td>—</td><td>—</td><td>—</td></tr><tr><td>Pyrite (and other crystalline opaques)</td><td>—</td><td>8</td><td>—</td><td>—</td></tr><tr><td>Foraminifers</td><td>—</td><td>2</td><td>4</td><td>5</td></tr><tr><td>Nannofossils</td><td>3</td><td>55</td><td>55</td><td>50</td></tr><tr><td>Diatoms</td><td>—</td><td>1</td><td>1</td><td>2</td></tr><tr><td>Radiolarians</td><td>Tr</td><td>4</td><td>1</td><td>2</td></tr><tr><td>Sponge spicules</td><td>Tr</td><td>—</td><td>—</td><td>Tr</td></tr><tr><td>Fish remains</td><td>1</td><td>—</td><td>—</td><td>—</td></tr><tr><td>Micrite</td><td>2</td><td>2</td><td>1</td><td>3</td></tr><tr><td>Undetermined red and black blebs</td><td>—</td><td>—</td><td>3</td><td>—</td></tr></table>		1, 42	1, 60	1, 135	1, 148		M	D	M	M	Sand	10	2	2	8	Silt	25	8	20	15	Clay	65	90	78	77	Quartz	1	2	2	1	Feldspar	3	2	4	1	Clay	53	22	26	36	Volcanic glass	—	2	Tr	—	Calcite	2	Tr	1	Tr	Dolomite	Tr	Tr	2	Tr	Accessory minerals	—	—	—	Tr	Amorphous opaques	—	—	—	—	(organic matter?)	35	—	—	—	Pyrite (and other crystalline opaques)	—	8	—	—	Foraminifers	—	2	4	5	Nannofossils	3	55	55	50	Diatoms	—	1	1	2	Radiolarians	Tr	4	1	2	Sponge spicules	Tr	—	—	Tr	Fish remains	1	—	—	—	Micrite	2	2	1	3	Undetermined red and black blebs	—	—	3	—
	1, 42	1, 60	1, 135	1, 148																																																																																																																													
	M	D	M	M																																																																																																																													
Sand	10	2	2	8																																																																																																																													
Silt	25	8	20	15																																																																																																																													
Clay	65	90	78	77																																																																																																																													
Quartz	1	2	2	1																																																																																																																													
Feldspar	3	2	4	1																																																																																																																													
Clay	53	22	26	36																																																																																																																													
Volcanic glass	—	2	Tr	—																																																																																																																													
Calcite	2	Tr	1	Tr																																																																																																																													
Dolomite	Tr	Tr	2	Tr																																																																																																																													
Accessory minerals	—	—	—	Tr																																																																																																																													
Amorphous opaques	—	—	—	—																																																																																																																													
(organic matter?)	35	—	—	—																																																																																																																													
Pyrite (and other crystalline opaques)	—	8	—	—																																																																																																																													
Foraminifers	—	2	4	5																																																																																																																													
Nannofossils	3	55	55	50																																																																																																																													
Diatoms	—	1	1	2																																																																																																																													
Radiolarians	Tr	4	1	2																																																																																																																													
Sponge spicules	Tr	—	—	Tr																																																																																																																													
Fish remains	1	—	—	—																																																																																																																													
Micrite	2	2	1	3																																																																																																																													
Undetermined red and black blebs	—	—	3	—																																																																																																																													



SITE 652 HOLE A CORE 7 R CORED INTERVAL 3501.4-3510.9 mbsl; 55.4-64.9 mbsf

TIME-ROCK UNIT	BIOSTRAT. ZONE/ FOSSIL CHARACTER				PALEOMAGNETICS	PHYS. PROPERTIES	CHEMISTRY	SECTION	METERS	GRAPHIC LITHOLOGY	DRILLING DISTURB.	SED. STRUCTURES	SAMPLES	LITHOLOGIC DESCRIPTION																																																																																																																																			
	FORAMINIFERS	NANNOFOSSILS	RADIOLARIANS	DIATOMS																																																																																																																																													
PLEISTOCENE	<i>Globigerina cariacensis</i> NN19	A/G	Jaramillo	Matuyama	● 42 ●	● 34 ●	● 49 ●	● 51 ●	● 50 ●	1	0.5	1.0	* * * OG * *	MARLY NANNOFOSSIL OOZE and FORAMINIFER-RICH SAND Marly nannofossil ooze with a varying amount of CaCO ₃ , light gray (5Y 7/1) to light olive-gray (5Y 6/2), or pale olive (5Y 6/3). Some small diagenetic fronts above thin horizons of gray (5Y 5/1), foraminifer-rich sand with a small amount of volcanic glass in Section 1, 78, 115, and 138 cm; Section 2, 8-35 and 47 cm; and Section 3, 120 cm; and one very dark gray (5Y 3/1), organic-rich sapropelic layer in Section 3. SMEAR SLIDE SUMMARY (%): <table><tr><td></td><td>1, 27</td><td>1, 138</td><td>2, 34</td><td>3, 67</td><td>3, 135</td></tr><tr><td>D</td><td>M</td><td>M</td><td>D</td><td>M</td></tr></table> TEXTURE: <table><tr><td>Sand</td><td>2</td><td>7</td><td>65</td><td>1</td><td>3</td></tr><tr><td>Silt</td><td>10</td><td>20</td><td>10</td><td>12</td><td>7</td></tr><tr><td>Clay</td><td>88</td><td>73</td><td>25</td><td>87</td><td>90</td></tr></table> COMPOSITION: <table><tr><td>Quartz</td><td>1</td><td>Tr</td><td>20</td><td>—</td><td>2</td></tr><tr><td>Feldspar</td><td>3</td><td>4</td><td>30</td><td>1</td><td>4</td></tr><tr><td>Rock fragments</td><td>—</td><td>—</td><td>4</td><td>—</td><td>—</td></tr><tr><td>Mica</td><td>—</td><td>—</td><td>1</td><td>—</td><td>—</td></tr><tr><td>Clay</td><td>20</td><td>36</td><td>5</td><td>20</td><td>34</td></tr><tr><td>Volcanic glass</td><td>1</td><td>Tr</td><td>5</td><td>1</td><td>2</td></tr><tr><td>Calcite</td><td>Tr</td><td>2</td><td>3</td><td>—</td><td>2</td></tr><tr><td>Dolomite</td><td>1</td><td>1</td><td>—</td><td>1</td><td>—</td></tr><tr><td>Accessory minerals</td><td>Tr</td><td>Tr</td><td>4</td><td>—</td><td>Tr</td></tr><tr><td>Reddish amorphous blebs (limonite?)</td><td>—</td><td>15</td><td>—</td><td>—</td><td>3</td></tr><tr><td>Glauconite/celadonite</td><td>—</td><td>—</td><td>3</td><td>—</td><td>—</td></tr><tr><td>Foraminifers</td><td>2</td><td>2</td><td>20</td><td>1</td><td>4</td></tr><tr><td>Nannofossils</td><td>65</td><td>40</td><td>5</td><td>75</td><td>40</td></tr><tr><td>Diatoms</td><td>2</td><td>—</td><td>—</td><td>1</td><td>5</td></tr><tr><td>Radiolarians</td><td>Tr</td><td>—</td><td>—</td><td>—</td><td>—</td></tr><tr><td>Sponge spicules</td><td>1</td><td>—</td><td>Tr</td><td>Tr</td><td>—</td></tr><tr><td>Micrite</td><td>4</td><td>Tr</td><td>Tr</td><td>—</td><td>4</td></tr></table>		1, 27	1, 138	2, 34	3, 67	3, 135	D	M	M	D	M	Sand	2	7	65	1	3	Silt	10	20	10	12	7	Clay	88	73	25	87	90	Quartz	1	Tr	20	—	2	Feldspar	3	4	30	1	4	Rock fragments	—	—	4	—	—	Mica	—	—	1	—	—	Clay	20	36	5	20	34	Volcanic glass	1	Tr	5	1	2	Calcite	Tr	2	3	—	2	Dolomite	1	1	—	1	—	Accessory minerals	Tr	Tr	4	—	Tr	Reddish amorphous blebs (limonite?)	—	15	—	—	3	Glauconite/celadonite	—	—	3	—	—	Foraminifers	2	2	20	1	4	Nannofossils	65	40	5	75	40	Diatoms	2	—	—	1	5	Radiolarians	Tr	—	—	—	—	Sponge spicules	1	—	Tr	Tr	—	Micrite	4	Tr	Tr	—	4
																1, 27	1, 138	2, 34	3, 67	3, 135																																																																																																																													
															D	M	M	D	M																																																																																																																														
															Sand	2	7	65	1	3																																																																																																																													
															Silt	10	20	10	12	7																																																																																																																													
															Clay	88	73	25	87	90																																																																																																																													
															Quartz	1	Tr	20	—	2																																																																																																																													
															Feldspar	3	4	30	1	4																																																																																																																													
															Rock fragments	—	—	4	—	—																																																																																																																													
															Mica	—	—	1	—	—																																																																																																																													
Clay	20	36	5	20	34																																																																																																																																												
Volcanic glass	1	Tr	5	1	2																																																																																																																																												
Calcite	Tr	2	3	—	2																																																																																																																																												
Dolomite	1	1	—	1	—																																																																																																																																												
Accessory minerals	Tr	Tr	4	—	Tr																																																																																																																																												
Reddish amorphous blebs (limonite?)	—	15	—	—	3																																																																																																																																												
Glauconite/celadonite	—	—	3	—	—																																																																																																																																												
Foraminifers	2	2	20	1	4																																																																																																																																												
Nannofossils	65	40	5	75	40																																																																																																																																												
Diatoms	2	—	—	1	5																																																																																																																																												
Radiolarians	Tr	—	—	—	—																																																																																																																																												
Sponge spicules	1	—	Tr	Tr	—																																																																																																																																												
Micrite	4	Tr	Tr	—	4																																																																																																																																												

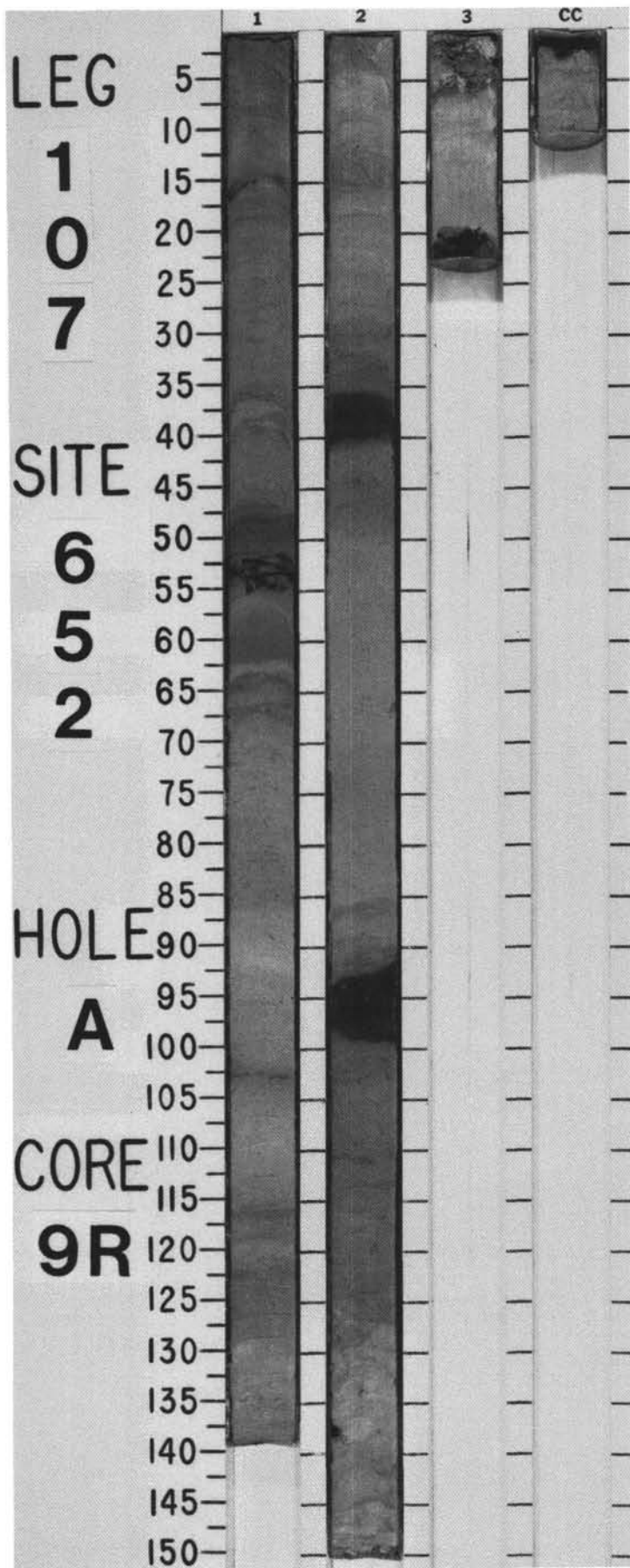
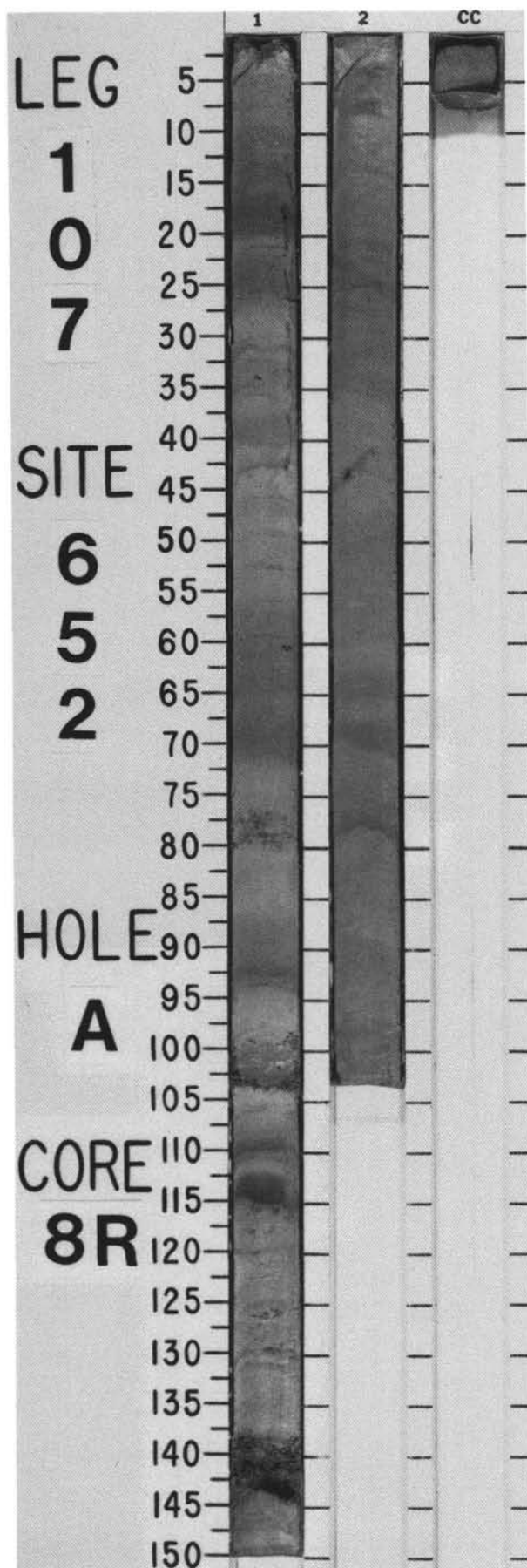


SITE 652 HOLE A CORE 8 R CORED INTERVAL 3510.9-3520.5 mbsl; 64.9-74.5 mbsf

TIME-ROCK UNIT	BIOSTRAT. ZONE/ FOSSIL CHARACTER				PALEOMAGNETICS	PHYS. PROPERTIES	CHEMISTRY	SECTION	METERS	GRAPHIC LITHOLOGY	DRILLING DISTURB.	SED. STRUCTURES	SAMPLES	LITHOLOGIC DESCRIPTION				
	FORAMINIFERS	NANNOFOSSILS	RADIOLARIANS	DIATOMS														
PLEISTOCENE	<i>Globigerina carlinensis</i>					$\gamma = 1.91 \phi = 66 \text{ V} \sim 1560$	23 ● 38 ● 44 ●	1	0.5 1.0	SAP		* * *	MARLY FORAMINIFER-NANNOFOSSIL OOZE and VOLCANIC GLASS-BEARING SILT					
	NN18	C/G	NN19															
								2						Marly foraminifer-nannofossil ooze with minor amounts of nannofossil-foraminifer ooze; pale olive (5Y 6/4) to light olive-gray (5Y 6/2); two thin layers of volcanic glass-bearing silt; some diagenetic fronts in Section 1, 17, 90, and 109 cm; one dark gray (5Y 4/1), organic-rich sapropel horizon in Section 1, 114-116 cm.				
														SMEAR SLIDE SUMMARY (%):				
														1, 33 D	1, 102 D	1, 143 M	2, 44 D	2, 60 D
														TEXTURE:				
														Sand	1	2	—	—
														Silt	39	40	40	40
														Clay	60	60	60	60
														COMPOSITION:				
														Quartz	1	—	2	—
														Feldspar	2	—	5	—
														Mica	—	—	Tr	—
														Clay	29	36	35	23
														Volcanic glass	7	—	30	—
														Calcite/dolomite	1	—	—	2
														Accessory minerals	—	1	8	—
														Zeolites	—	3	Tr	—
														Foraminifers	10	20	Tr	30
														Nannofossils	40	35	20	35
														Bioclasts	10	5	—	10
														Intraclasts	—	—	—	5

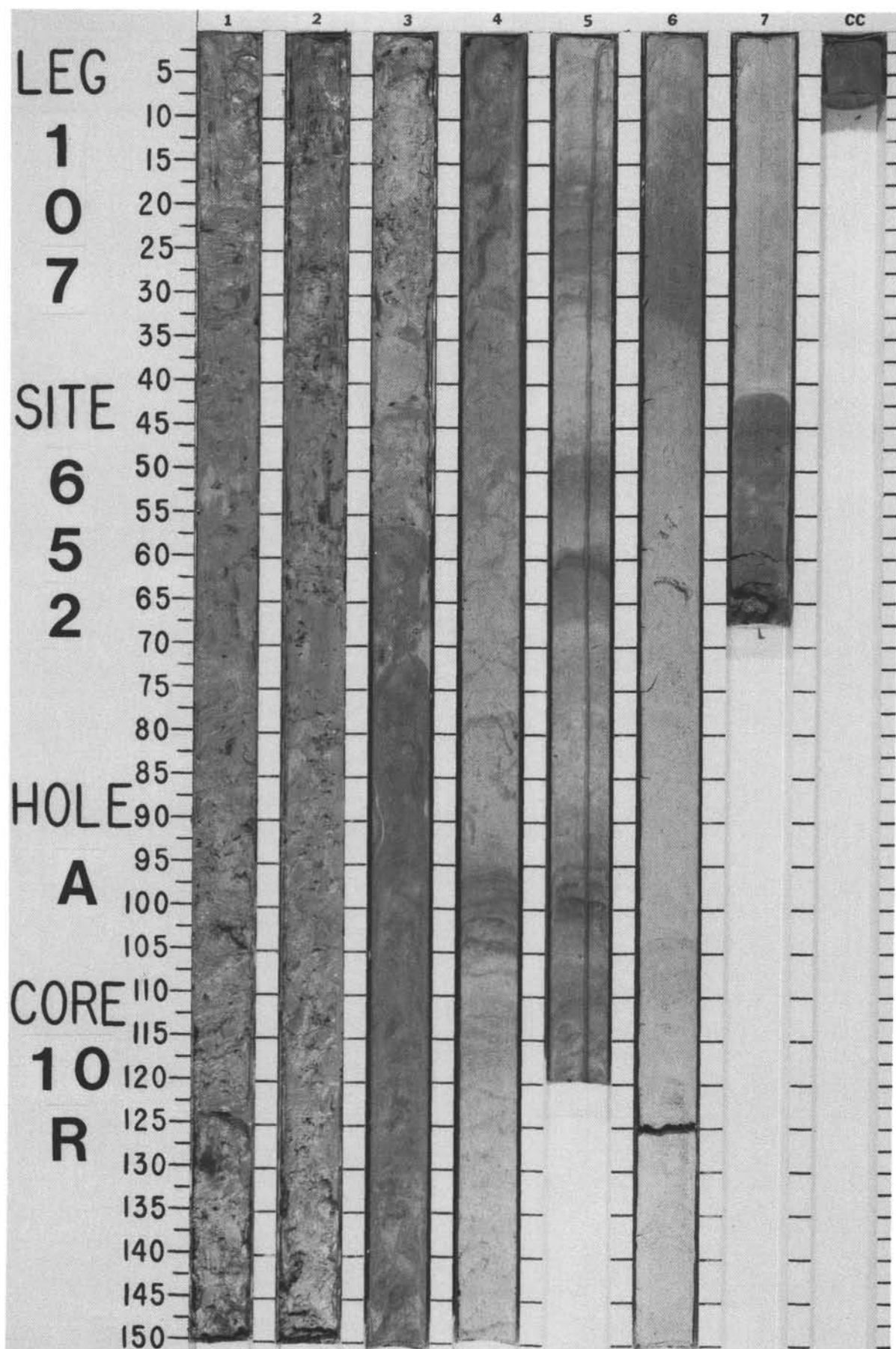
SITE 652 HOLE A CORE 9 R CORED INTERVAL 3520.5-3530.2 mbsl; 74.5-84.2 mbsf

TIME-ROCK UNIT	BIOSTRAT. ZONE/ FOSSIL CHARACTER				PALEOMAGNETICS	PHYS. PROPERTIES	CHEMISTRY	SECTION	METERS	GRAPHIC LITHOLOGY	DRILLING DISTURB.	SED. STRUCTURES	SAMPLES	LITHOLOGIC DESCRIPTION
	FORAMINIFERS	NANNOFOSSILS	RADIOLARIANS	DIATOMS										
PLEISTOCENE	<i>G. carliacoensis</i>	NN18	A/G		Matuyama	$\gamma = 1.86 \phi = 64 \text{ V} = 1673$	● 28 ● 30 ● 50 ●	1	0.5 1.0		—	↑	*	Marly foraminifer-nannofossil ooze, light olive-gray (5Y 6/1 to 6/2); two very thin, olive-gray (5Y 4/2), silt horizons in Section 1; and two black (5Y 3/1) sapropel horizons in Section 2. The silt horizons contain volcanic glass and detrital material.
								2						
								3			—	↑	*	Texture:
														Composition:
														Quartz
														Feldspar
														Mica
														Clay
														Volcanic glass
														Calcite/dolomite
														Accessory minerals
														Zeolites
														Foraminifers
														Nannofossils
														Bioclasts
														Micrite



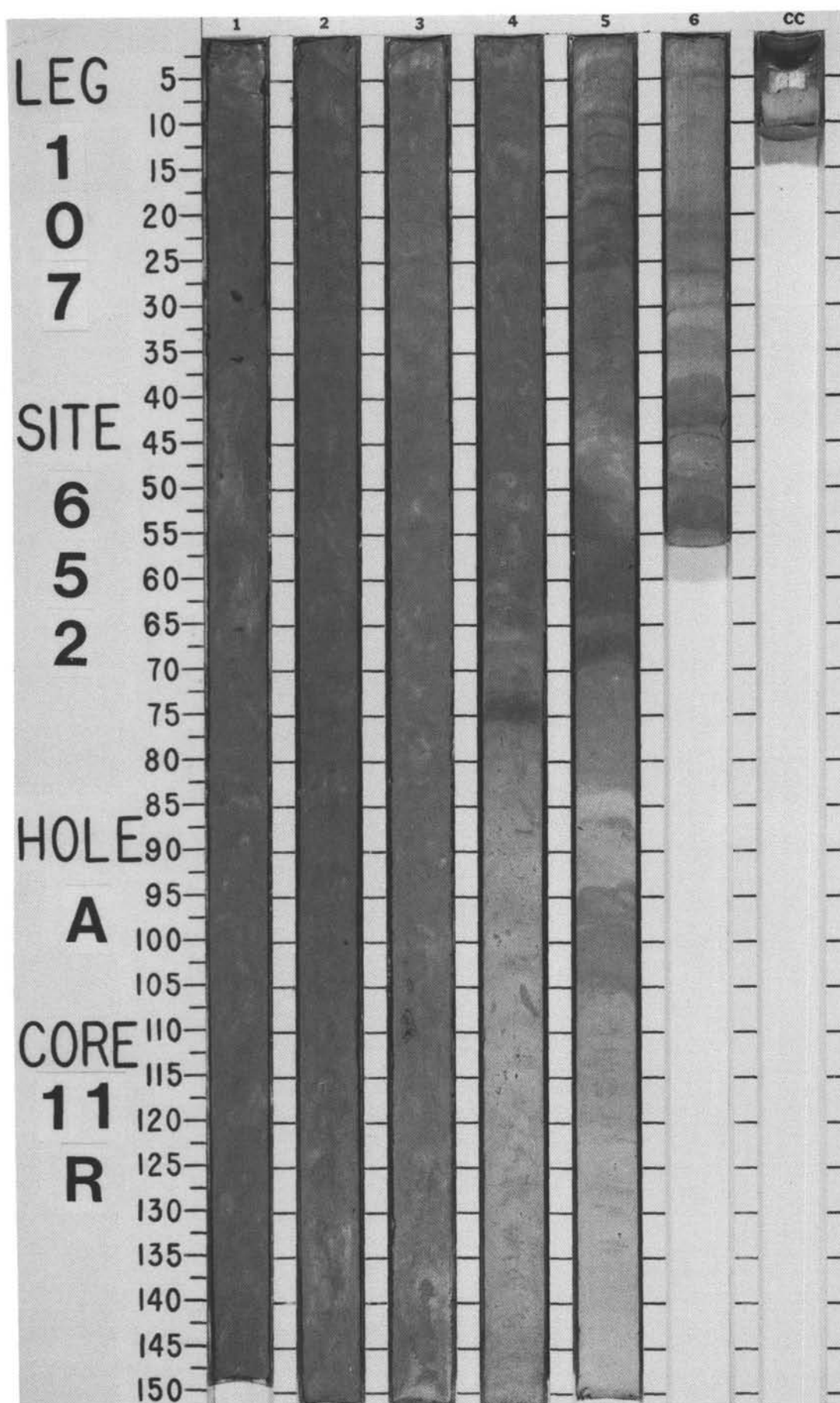
SITE 652 HOLE A CORE 10 R CORED INTERVAL 3530.2-3539.8 mbsl; 84.2-93.8 mbsf

TIME-ROCK UNIT	BIOSTRAT. ZONE/ FOSSIL CHARACTER				PALEOMAGNETICS	PHYS. PROPERTIES	CHEMISTRY	SECTION	METERS	GRAPHIC LITHOLOGY	DRILLING DISTURB.	SED. STRUCTURES	SAMPLES	LITHOLOGIC DESCRIPTION																																																												
	FORAMINIFERS	NANNOFOSSILS	RADIOLARIANS	DIATOMS																																																																						
LATE PLIOCENE	MPI 6				● V-1626	● V-1545	69 ●	4	0.5	+				MARLY NANNOFOSSIL-FORAMINIFER OOZE and FORAMINIFER-NANNOFOSSIL OOZE Marly foraminifer-nannofossil ooze, gray (5Y 6/1), highly disturbed by drilling, in Sections 1, 2, 3 and three-fourths of Section 4; foraminifer-nannofossil ooze, gray (2.5Y 6/1 to 10YR 6/1) to yellowish brown (10YR 6/4) with a minor amount of volcanic glass in Section 7, 40-64 cm, and CC. SMEAR SLIDE SUMMARY (%): <table><tr><td></td><td>4, 80</td><td>6, 56</td><td>7, 45</td></tr><tr><td>D</td><td></td><td>M</td><td>M</td></tr></table> TEXTURE: <table><tr><td>Sand</td><td>—</td><td>—</td><td>—</td></tr><tr><td>Silt</td><td>40</td><td>40</td><td>40</td></tr><tr><td>Clay</td><td>60</td><td>60</td><td>60</td></tr></table> COMPOSITION: <table><tr><td>Quartz</td><td>—</td><td>2</td><td>1</td></tr><tr><td>Feldspar</td><td>2</td><td>3</td><td>3</td></tr><tr><td>Mica</td><td>—</td><td>1</td><td>—</td></tr><tr><td>Clay</td><td>41</td><td>44</td><td>40</td></tr><tr><td>Volcanic glass</td><td>5</td><td>—</td><td>5</td></tr><tr><td>Calcite/dolomite</td><td>—</td><td>6</td><td>—</td></tr><tr><td>Accessory minerals</td><td>2</td><td>4</td><td>1</td></tr><tr><td>Foraminifers</td><td>15</td><td>6</td><td>15</td></tr><tr><td>Nannofossils</td><td>35</td><td>30</td><td>35</td></tr><tr><td>Bioclasts</td><td>—</td><td>4</td><td>—</td></tr></table>		4, 80	6, 56	7, 45	D		M	M	Sand	—	—	—	Silt	40	40	40	Clay	60	60	60	Quartz	—	2	1	Feldspar	2	3	3	Mica	—	1	—	Clay	41	44	40	Volcanic glass	5	—	5	Calcite/dolomite	—	6	—	Accessory minerals	2	4	1	Foraminifers	15	6	15	Nannofossils	35	30	35	Bioclasts	—	4	—
		4, 80	6, 56	7, 45																																																																						
D		M	M																																																																							
Sand	—	—	—																																																																							
Silt	40	40	40																																																																							
Clay	60	60	60																																																																							
Quartz	—	2	1																																																																							
Feldspar	2	3	3																																																																							
Mica	—	1	—																																																																							
Clay	41	44	40																																																																							
Volcanic glass	5	—	5																																																																							
Calcite/dolomite	—	6	—																																																																							
Accessory minerals	2	4	1																																																																							
Foraminifers	15	6	15																																																																							
Nannofossils	35	30	35																																																																							
Bioclasts	—	4	—																																																																							
	NN16																																																																									
PLEISTOCENE	G. cariacensis				● 56	● 43	3	2	1.0	+																																																																
	NN17/18																																																																									
	Matuyama				● 56	● 43	3	2	1.0	+																																																																
	Olduvai																																																																									
	C/G				● 56	● 43	3	2	1.0	+																																																																
					● 56	● 43	3	2	1.0	+																																																																
					● 56	● 43	3	2	1.0	+																																																																
					● 56	● 43	3	2	1.0	+																																																																
					● 56	● 43	3	2	1.0	+																																																																
					● 56	● 43	3	2	1.0	+																																																																
					● 56	● 43	3	2	1.0	+																																																																
					● 56	● 43	3	2	1.0	+																																																																
					● 56	● 43	3	2	1.0	+																																																																
					● 56	● 43	3	2	1.0	+																																																																
					● 56	● 43	3	2	1.0	+																																																																
					● 56	● 43	3	2	1.0	+																																																																
					● 56	● 43	3	2	1.0	+																																																																
					● 56	● 43	3	2	1.0	+																																																																
					● 56	● 43	3	2	1.0	+																																																																
					● 56	● 43	3	2	1.0	+																																																																
					● 56	● 43	3	2	1.0	+																																																																
					● 56	● 43	3	2	1.0	+																																																																
					● 56	● 43	3	2	1.0	+																																																																
					● 56	● 43	3	2	1.0	+																																																																
					● 56	● 43	3	2	1.0	+																																																																
					● 56	● 43	3	2	1.0	+																																																																
					● 56	● 43	3	2	1.0	+																																																																
					● 56	● 43	3	2	1.0	+																																																																
					● 56	● 43	3	2	1.0	+																																																																
					● 56	● 43	3	2	1.0	+																																																																
					● 56	● 43	3	2	1.0	+																																																																
					● 56	● 43	3	2	1.0	+																																																																
					● 56	● 43	3	2	1.0	+																																																																
					● 56	● 43	3	2	1.0	+																																																																
					● 56	● 43	3	2	1.0	+																																																																
					● 56	● 43	3	2	1.0	+																																																																
					● 56	● 43	3	2	1.0	+																																																																
					● 56	● 43	3	2	1.0	+																																																																
					● 56	● 43	3	2	1.0	+																																																																
					● 56	● 43	3	2	1.0	+																																																																
					● 56	● 43	3	2	1.0	+																																																																
					● 56	● 43	3	2	1.0	+																																																																
					● 56	● 43	3	2	1.0	+																																																																
					● 56	● 43	3	2	1.0	+																																																																
					● 56	● 43	3	2	1.0	+																																																																
					● 56	● 43	3	2	1.0	+																																																																
					● 56	● 43	3	2	1.0	+																																																																
					● 56	● 43	3	2	1.0	+																																																																
					● 56	● 43	3	2	1.0	+																																																																
					● 56	● 43	3	2	1.0	+																																																																
					● 56	● 43	3	2	1.0	+																																																																
					● 56	● 43	3	2	1.0	+																																																																
					● 56	● 43	3	2	1.0	+																																																																
					● 56	● 43	3	2	1.0	+																																																																
					● 56	● 43	3	2	1.0	+																																																																
					● 56	● 43	3	2	1.0	+																																																																
					● 56	● 43	3	2	1.0	+																																																																
					● 56	● 43	3	2	1.0	+																																																																
					● 56	● 43	3	2	1.0	+																																																																
					● 56	● 43	3	2	1.0	+																																																																
					● 56	● 43	3	2	1.0	+																																																																
					● 56	● 43	3	2	1.0	+																																																																
					● 56	● 43	3	2	1.0	+																																																																
					● 56	● 43	3	2	1.0	+																																																																
					● 56	● 43	3	2	1.0	+																																																																
					● 56	● 43	3	2	1.0	+																																																																
					● 56	● 43	3	2	1.0	+																																																																
					● 56	● 43	3	2	1.0	+																																																																
					● 56	● 43	3	2	1.0	+																																																																
					● 56	● 43	3	2	1.0	+																																																																
					● 56	● 43	3	2	1.0	+																																																																
					● 56	● 43	3	2	1.0	+																																																																
					● 56	● 43	3	2	1.0	+																																																																
					● 56	● 43	3	2	1.0	+																																																																
					● 56	● 43	3	2	1.0	+																																																																
					● 56	● 43	3	2	1.0	+																																																																
					● 56	● 43	3	2	1.0	+																																																																
					● 56	● 43	3	2	1.0	+																																																																
					● 56	● 43	3	2	1.0	+																																																																
					● 56	● 43	3	2	1.0	+																																																																
					● 56	● 43	3	2	1.0	+																																																																
					● 56	● 43	3	2	1.0	+																																																																
					● 56	● 43	3	2	1.0	+																																																																
					● 56	● 43	3	2	1.0	+																																																																
					● 56	● 43	3	2	1.0	+																																																																
					● 56	● 43	3	2	1.0	+																																																																
					● 56	● 43	3	2	1.0	+																																																																
					● 56	● 43	3	2	1.0	+																																																																
					● 56	● 43	3	2	1.0	+																																																																
					● 56	● 43	3	2	1.0	+																																																																
					● 56	● 43	3	2	1.0	+																																																																
					● 56	● 43	3	2	1.0	+																																																																
					● 56	● 43	3	2	1.0	+																																																																
					● 56	● 43	3	2	1.0	+																																																																
					● 56	● 43	3	2	1.0	+																																																																
					● 56	● 43	3	2	1.0	+																																																																
					● 56	● 43	3	2	1.0	+																																																																
					● 56	● 43	3	2	1.0	+																																																																

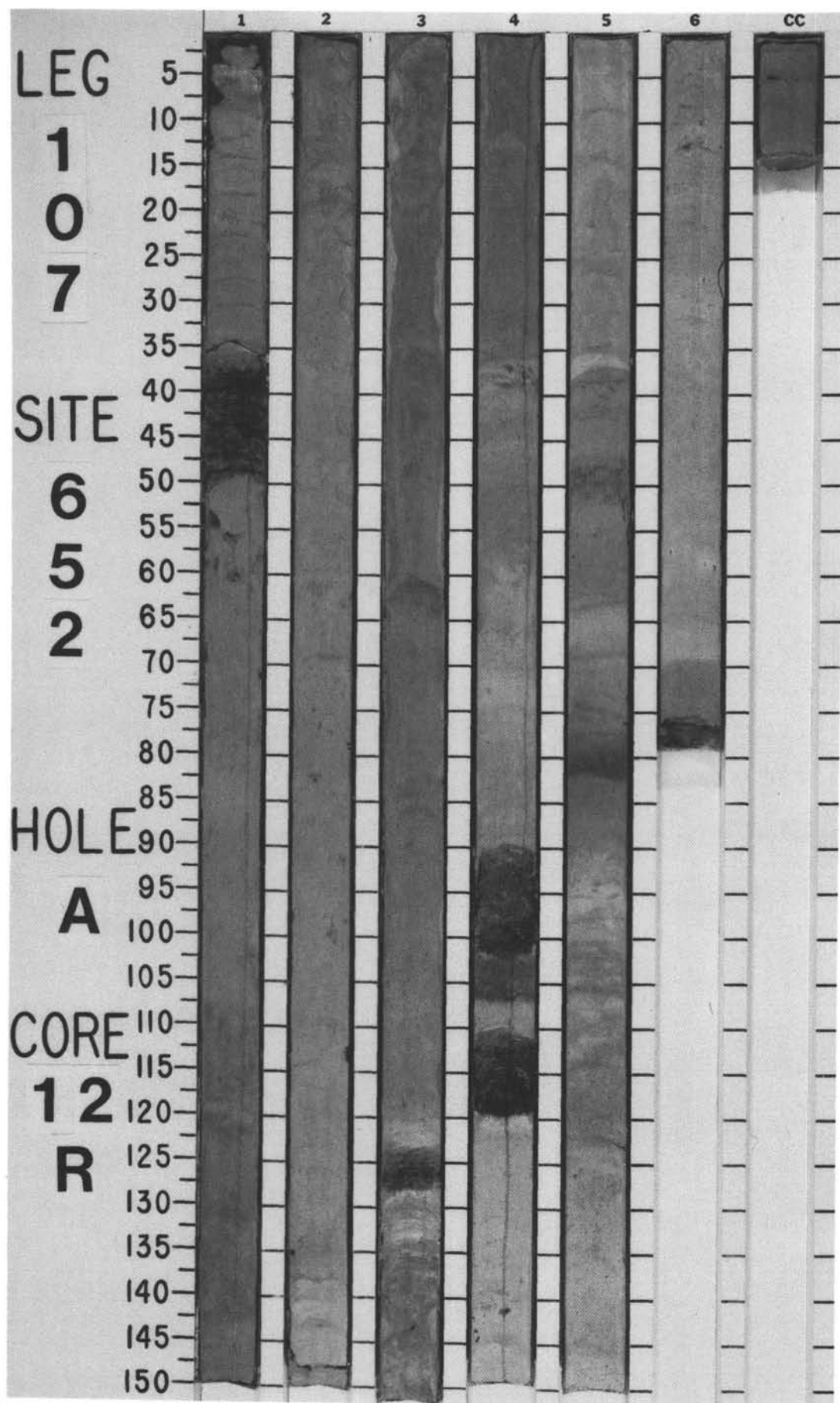


SITE 652 HOLE A CORE 11 R CORED INTERVAL 3539.8-3549.0 mbsl; 93.8-103.0 mbsf

LATE PLIOCENE																																																																						
TIME-ROCK UNIT	BIOSTRAT. ZONE/ FOSSIL CHARACTER				PALEOMAGNETICS	PHYS. PROPERTIES	CHEMISTRY	SECTION	METERS	GRAPHIC LITHOLOGY	DRILLING DISTURB.	SED. STRUCTURES	SAMPLES	LITHOLOGIC DESCRIPTION																																																								
	FORAMINIFERS	NANNOFOSSILS	RADIOLARIANS	DIATOMS																																																																		
MPI 5	MPI 6	NN16	A/G	Matuyama	● 50	● 55	● 1615	1	0.5 1.0			*		MARLY FORAMINIFER-NANNOFOSSIL OOZE Homogeneous, intensely burrowed, marly foraminifer-nannofossil ooze with a small amount of volcanic glass and feldspar, pale brown (10YR 6/3) in Sections 1, 2, 3, and the upper half of Section 4, and light gray (10YR 6/4) in the lower half of Section 4 and Sections 5 and 6. SMEAR SLIDE SUMMARY (%): <table><tr><td></td><td>1, 48</td><td>2, 99</td><td>5, 56</td></tr><tr><td>M</td><td>D</td><td>D</td><td></td></tr></table> TEXTURE: <table><tr><td>Sand</td><td>—</td><td>—</td><td>—</td></tr><tr><td>Silt</td><td>40</td><td>30</td><td>40</td></tr><tr><td>Clay</td><td>60</td><td>70</td><td>60</td></tr></table> COMPOSITION: <table><tr><td>Feldspar</td><td>3</td><td>1</td><td>3</td></tr><tr><td>Clay</td><td>32</td><td>40</td><td>40</td></tr><tr><td>Volcanic glass</td><td>5</td><td>5</td><td>2</td></tr><tr><td>Accessory minerals</td><td>2</td><td>2</td><td>2</td></tr><tr><td>Foraminifers</td><td>20</td><td>5</td><td>10</td></tr><tr><td>Nannofossils</td><td>35</td><td>45</td><td>40</td></tr><tr><td>Sponge spicules</td><td>3</td><td>—</td><td>—</td></tr><tr><td>Micrite</td><td>—</td><td>2</td><td>—</td></tr><tr><td>Bioclasts</td><td>—</td><td>—</td><td>3</td></tr></table>		1, 48	2, 99	5, 56	M	D	D		Sand	—	—	—	Silt	40	30	40	Clay	60	70	60	Feldspar	3	1	3	Clay	32	40	40	Volcanic glass	5	5	2	Accessory minerals	2	2	2	Foraminifers	20	5	10	Nannofossils	35	45	40	Sponge spicules	3	—	—	Micrite	—	2	—	Bioclasts	—	—	3
																1, 48	2, 99	5, 56																																																				
															M	D	D																																																					
															Sand	—	—	—																																																				
															Silt	40	30	40																																																				
															Clay	60	70	60																																																				
Feldspar	3	1	3																																																																			
Clay	32	40	40																																																																			
Volcanic glass	5	5	2																																																																			
Accessory minerals	2	2	2																																																																			
Foraminifers	20	5	10																																																																			
Nannofossils	35	45	40																																																																			
Sponge spicules	3	—	—																																																																			
Micrite	—	2	—																																																																			
Bioclasts	—	—	3																																																																			
Gauss								2				*																																																										
Gauss								3				*																																																										
Gauss								4				*																																																										
Gauss								5				*																																																										
Gauss								6				*																																																										

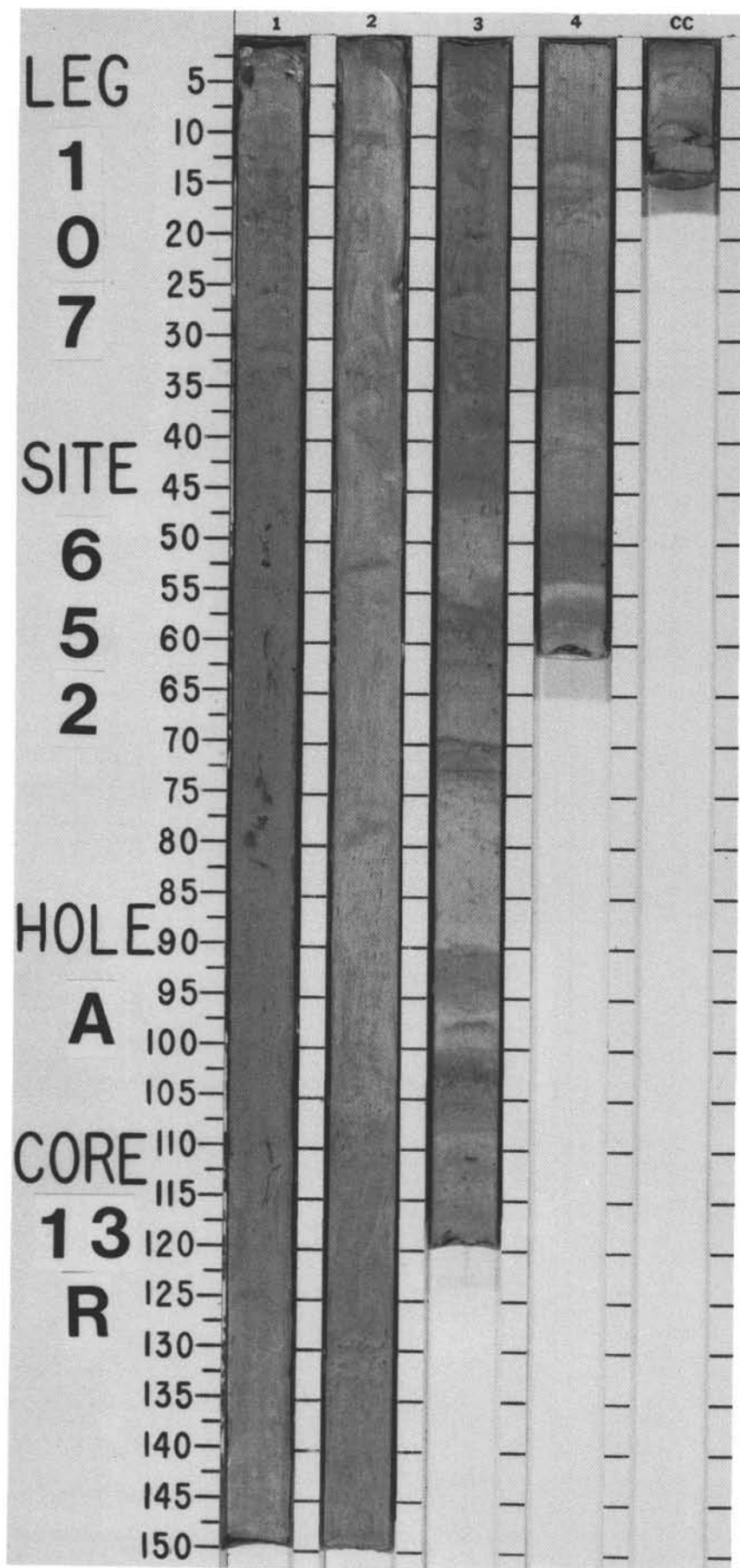


TIME-ROCK UNIT						BIOSTRAT. ZONE/ FOSSIL CHARACTER	PALEOMAGNETICS		PHYS. PROPERTIES		CHEMISTRY	SECTION	METERS	GRAPHIC LITHOLOGY	DRILLING DISTURB.	SED. STRUCTURES	SAMPLES	LITHOLOGIC DESCRIPTION
		FORAMINIFERS	NANNOFOSSILS	RADIOLARIANS	DIAZONES													
LATE PIOCENE							Gauss	Kaena	Gauss	$\gamma = 1.86 \quad \phi = 62^\circ \quad V = 1560$	$\bullet 48$	1	0.5	[+ + +]	- - -	*		MARLY FORAMINIFER-NANNOFOSSIL OOZE and CALCAREOUS MUDSTONE
MPI 4	MPI 5	NN16										2	1.0	[+ + +]	- - -			Randomly burrowed, marly foraminifer-nannofossil ooze, brown gray (2.5Y 6/2) to yellowish brown (2.5Y 6/4), intercalated by dark gray layers (2.5Y 4/0) of calcareous mudstone with some volcanic glass. Calcareous mudstone in Section 1, 38-50 cm, Section 3, 125-128 cm, and Section 4, 90-102 and 111-119 cm, is more indurated than surrounding ooze and was fractured by drilling.
A/G	NN15											3		[+ + +]	- - -			SMEAR SLIDE SUMMARY (%):
												4		[+ + +]	- - -			
												5		[+ + +]	- - -			
												6		[+ + +]	- - -			
												7		[+ + +]	- - -			
												8		[+ + +]	- - -			
												9		[+ + +]	- - -			
												10		[+ + +]	- - -			
												11		[+ + +]	- - -			
												12		[+ + +]	- - -			
												13		[+ + +]	- - -			
												14		[+ + +]	- - -			
												15		[+ + +]	- - -			
												16		[+ + +]	- - -			
												17		[+ + +]	- - -			
												18		[+ + +]	- - -			
												19		[+ + +]	- - -			
												20		[+ + +]	- - -			
												21		[+ + +]	- - -			
												22		[+ + +]	- - -			
												23		[+ + +]	- - -			
												24		[+ + +]	- - -			
												25		[+ + +]	- - -			
												26		[+ + +]	- - -			
												27		[+ + +]	- - -			
												28		[+ + +]	- - -			
												29		[+ + +]	- - -			
												30		[+ + +]	- - -			
												31		[+ + +]	- - -			
												32		[+ + +]	- - -			



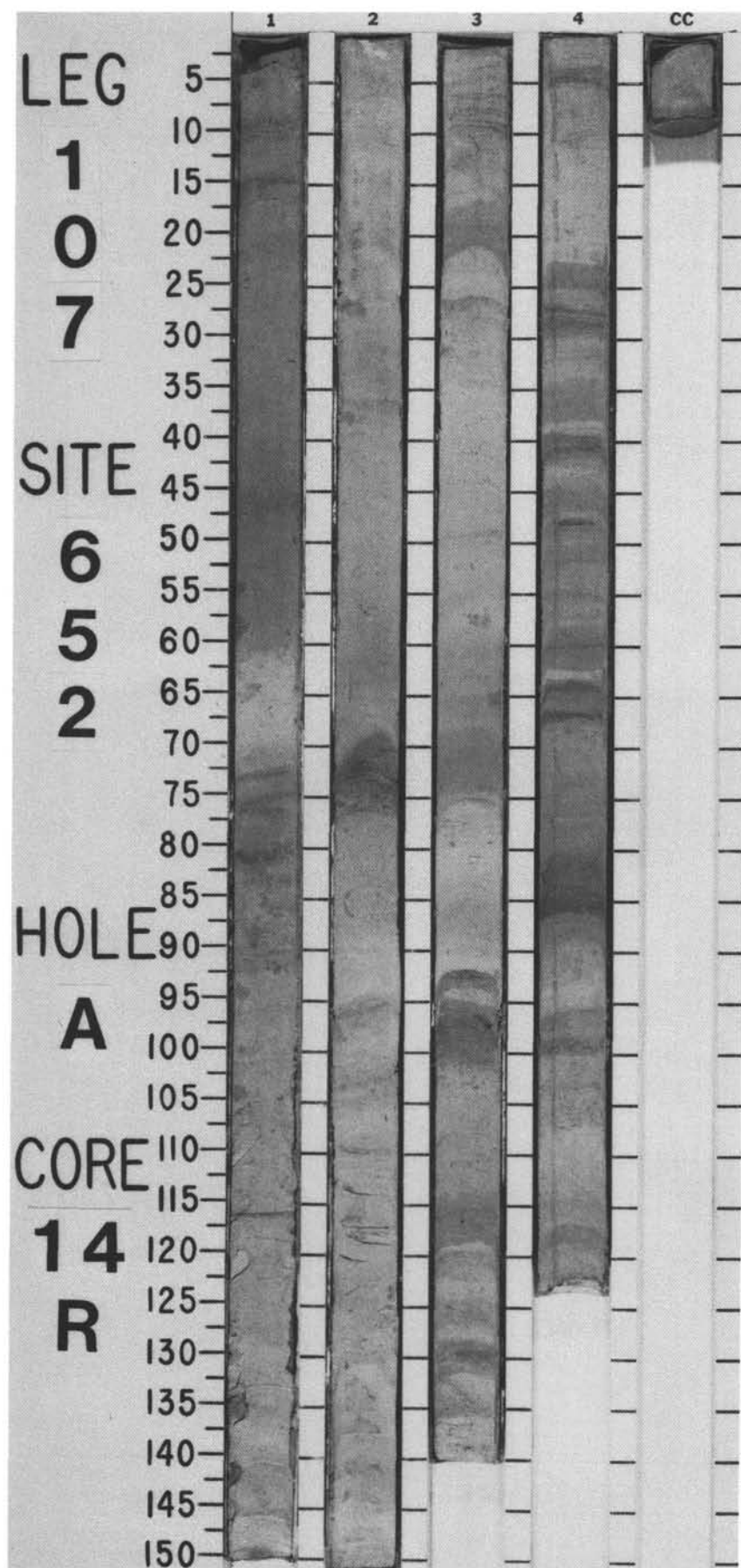
SITE 652 HOLE A CORE 13 R CORED INTERVAL 3558.7-3568.3 mbsl; 112.7-122.3 mbsf

TIME-ROCK UNIT	BIOSTRAT. ZONE/ FOSSIL CHARACTER				PALEOMAGNETICS	PHYS. PROPERTIES	CHEMISTRY	SECTION	METERS	GRAPHIC LITHOLOGY	DRILLING DISTURB.	SED. STRUCTURES	SAMPLES	LITHOLOGIC DESCRIPTION
	FORAMINIFERS	NANNOFOSSILS	RADIOLARIANS	DIATOMS										
LATE PLIOCENE	MPI 4	NN15							0.5	1			*	



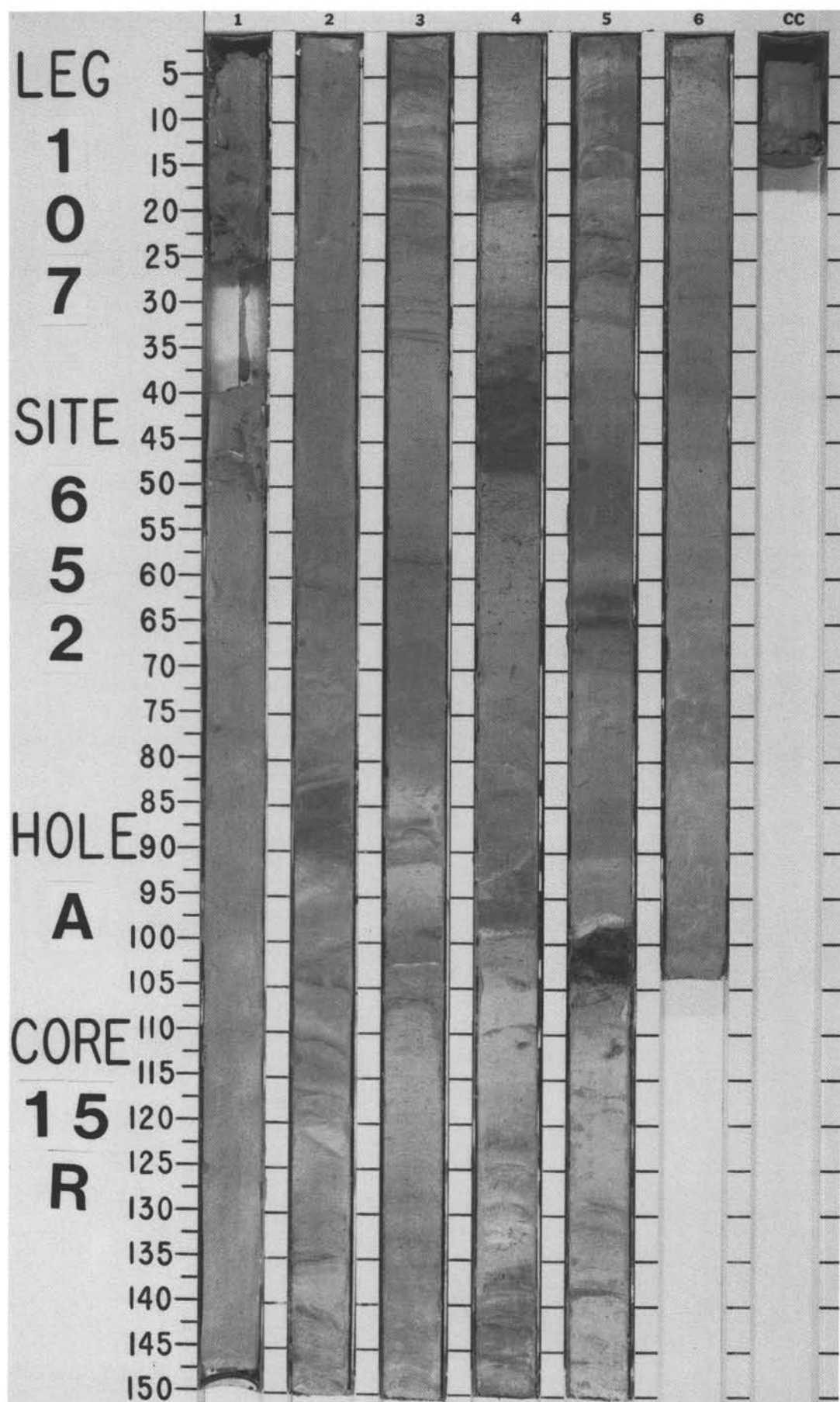
SITE 652 HOLE A CORE 14 R CORED INTERVAL 3568.3-3577.9 mbsl; 122.3-131.9 mbsf

[illegible]



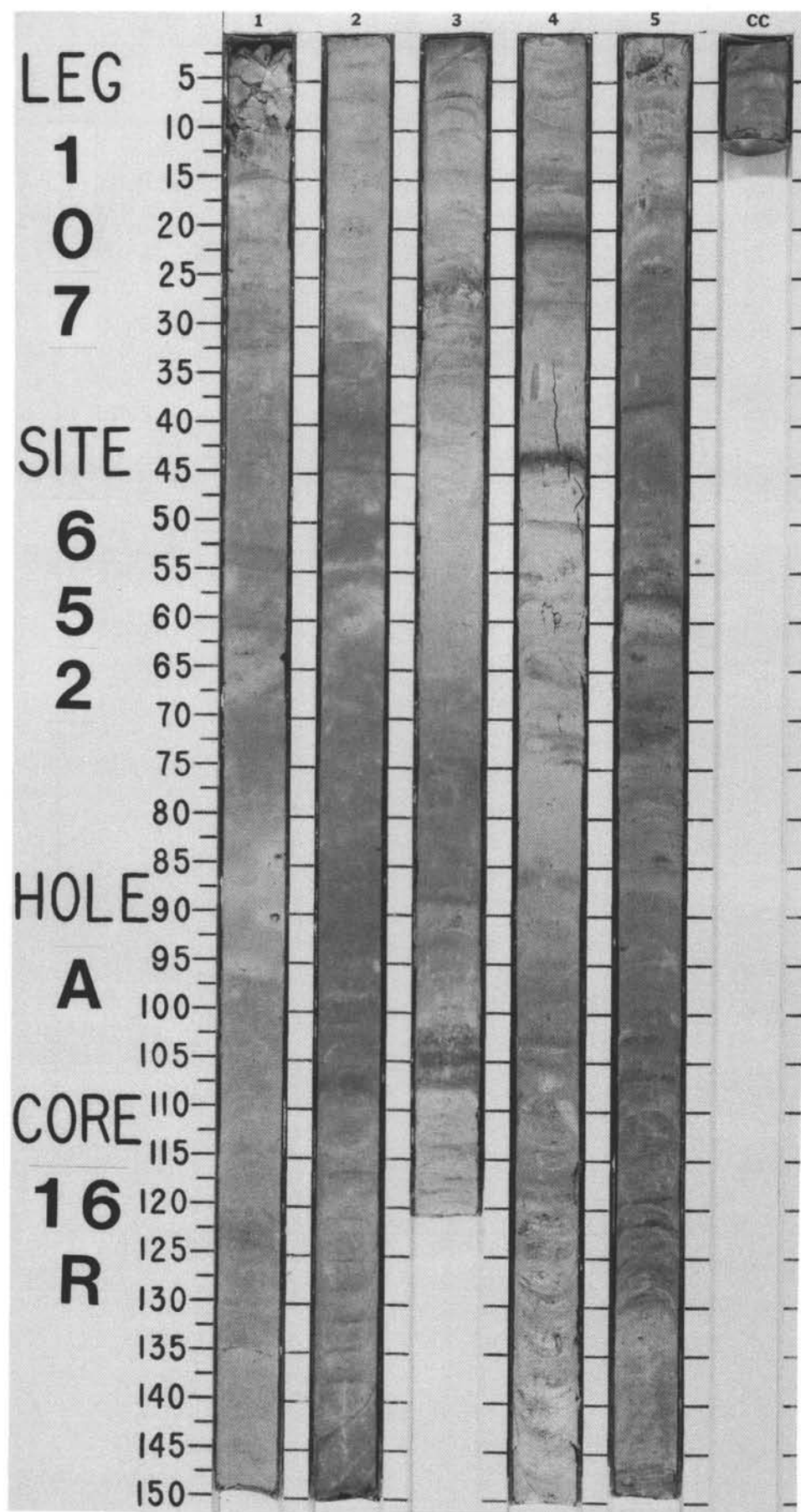
SITE 652 HOLE A CORE 15 R CORED INTERVAL 3577.9-3587.5 mbsl; 131.9-141.5 mbsf

TIME-ROCK UNIT	BIOSTRAT. ZONE/ FOSSIL CHARACTER				PALEOMAGNETICS	PHYS. PROPERTIES	CHEMISTRY	SECTION	METERS	GRAPHIC LITHOLOGY	DRILLING DISTURB.	SED. STRUCTURES	SAMPLES	LITHOLOGIC DESCRIPTION																													
	FORAMINIFERS	NANNOFOSSILS	RADIOLARIANS	DIATOMS																																							
EARLY PIOCENE	MPI 4				● V-1607	● 54	54 ●	1	0.5	VOID				MARLY NANNOFOSSIL OOZE and CALCAREOUS MUD																													
	MPI 3	NN14													38 ● ● 62	2						Marly nannofossil ooze grades downcore to calcareous mud, light olive-gray (5Y 6/2), pale olive (5Y 6/3), olive (5Y 5/3), and light gray (5Y 7/1, 10Y 7/1), to gray (10Y 6/1-6/2). Distinct intervals are overprinted with yellow-brown tones: olive-yellow (5Y 6/6), light brownish gray (2.5Y 6/2), and pale yellow (2.5Y 7/4). There are gradual and sharp gradations between colored intervals and many black speckled regions.																					
																							● 22	3					SMEAR SLIDE SUMMARY (%):														
																														Cochiti	4					TEXTURE:							
																																					Cochiti or Nun	5					COMPOSITION:
C/G	NN13			CC	6						Quartz 1 1 1 2 Mica 1 Tr 1 1 Clay 28 49 52 55 Volcanic glass Tr — 2 Tr Calcite 5 — — 5 Dolomite 3 5 — 3 Accessory minerals 2 1 3 1 Opales — — — 1 Foraminifers 5 8 3 — Nannofossils 50 35 35 30 Diatoms 1 Tr — Tr Radiolarians 1 1 — Tr Sponge spicules Tr Tr — 1 Silicoflagellates — Tr — — Fish remains — — 2 1 Plant debris — — 1 — Micrite 3 — — —																																



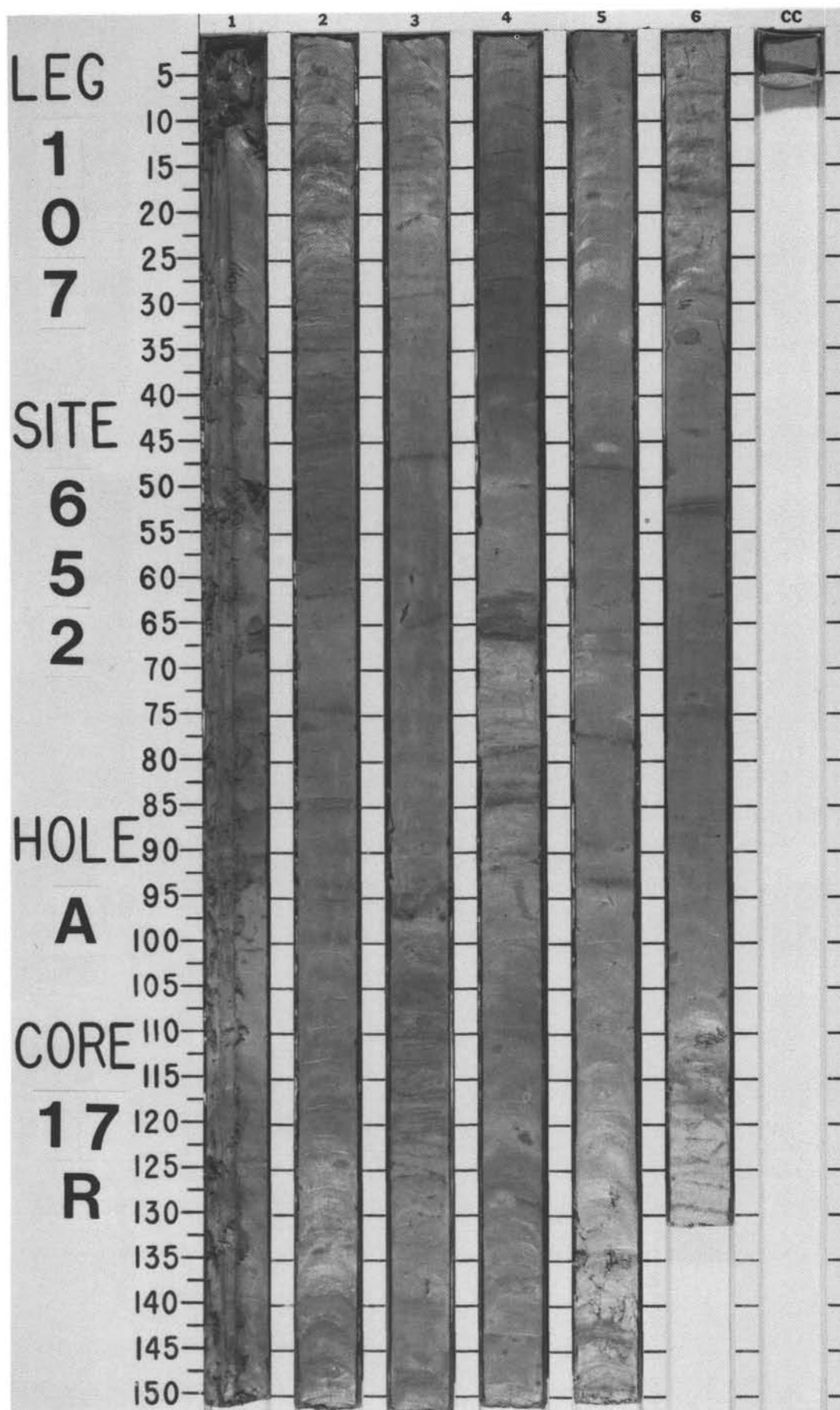
SITE 652 HOLE A CORE 16 R CORED INTERVAL 3587.5-3597.2 mbsl; 141.5-151.2 mbsf

TIME-ROCK UNIT	BIOSTRAT. ZONE/ FOSSIL CHARACTER				PALEOMAGNETICS	PHYS. PROPERTIES	CHEMISTRY	SECTION	METERS	GRAPHIC LITHOLOGY	DRILLING DISTURB.	SED. STRUCTURES	SAMPLES	LITHOLOGIC DESCRIPTION															
	FORAMINIFERS	NANNOFOSSILS	RADIOLARIANS	DIATOMS																									
EARLY PLIOCENE	MPI 3	NN13			Gibert	● $\gamma = 1.80$ $\phi = 57$ $V = 1652$	● 47	2	1					MARLY NANNOFOSSIL OOZE and NANNOFOSSIL OOZE															
															0.5				Marly nannofossil ooze with gradational contacts of pale yellow (2.5Y 7/4), light gray (2.5Y 6/2), and gray (2.5Y 6/0), and scattered patches of white (2.5Y 8/0) surrounding black cores (2.5Y 2/0), in Sections 1 through 3; secondary (diagenetic), black (2.5Y 2/0) laminations in Section 3, 115-120 cm; alternations of marly nannofossil ooze with sharp contacts of pale yellow (2.5Y 7/4), light gray (2.5Y 7/2), gray (5Y 6/1) and olive-gray (5Y 6/2), and centimeter-thick intervals of light yellowish brown (2.5Y 6/4) and olive-yellow (2.5Y 6/6), in Sections 4 and 5.										
																				1.0									
						2																							
											3																		
																4													
																					5								
CC																													

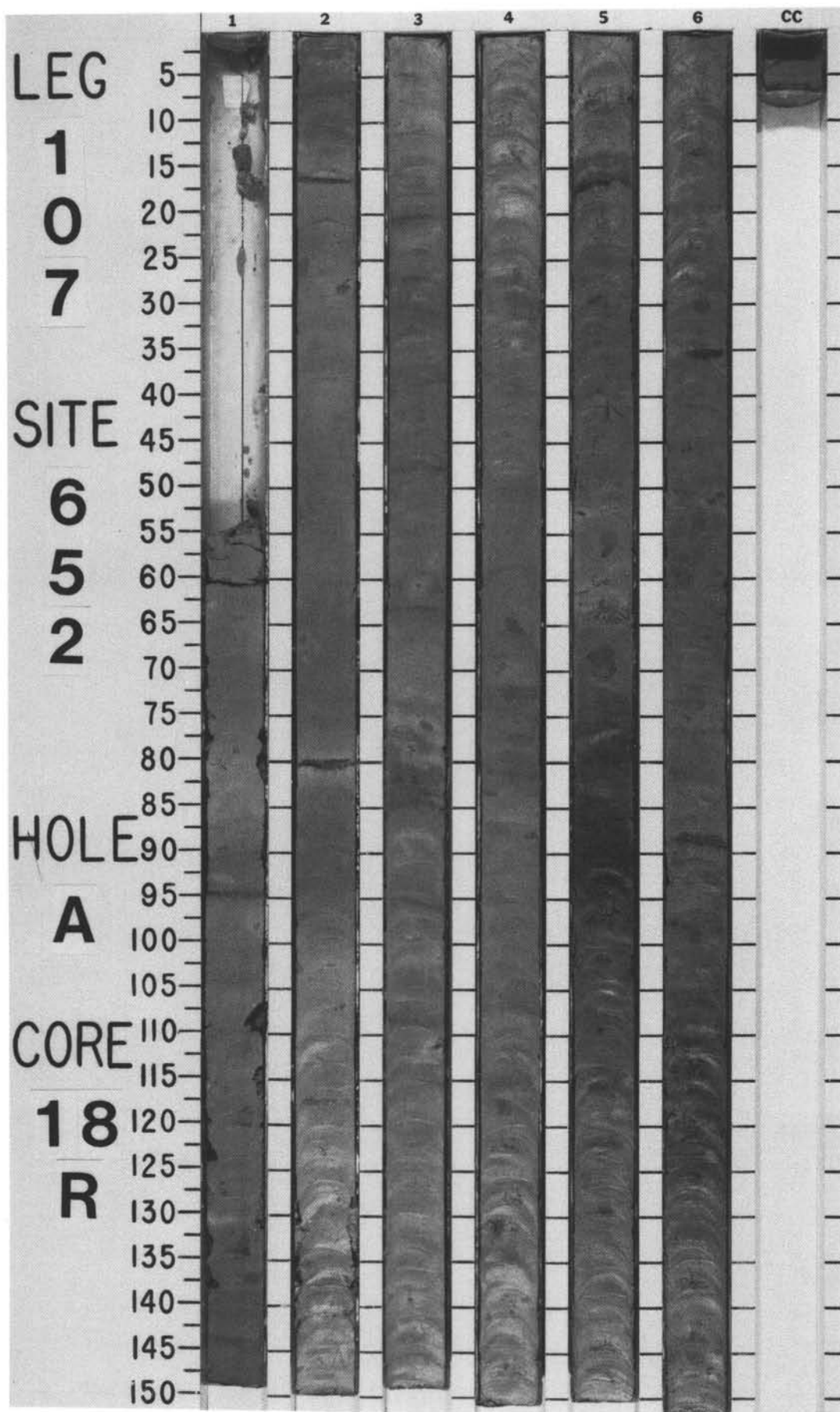


SITE 652 HOLE A CORE 17 R CORED INTERVAL 3597.2-3606.8 mbsl; 151.2-160.8 mbsf

TIME-ROCK UNIT	BIOSTRAT. ZONE/ FOSSIL CHARACTER				PALEOMAGNETICS	PHYS. PROPERTIES	CHEMISTRY	SECTION	METERS	GRAPHIC LITHOLOGY	DRILLING DISTURB.	SED. STRUCTURES	SAMPLES	LITHOLOGIC DESCRIPTION
	FORAMINIFERS	NANNOFOSSILS	RADIOLARIANS	DIATOMS										
EARLY PLIOCENE	C/G	MPI 2 NN12	NN13		Gibert	● $\gamma = 1.85$ $\phi = 57$ $\psi = 1736$	● 47%	1	0.5 1.0					MARLY NANNOFOSSIL OOZE Marly nannofossil ooze containing gradational (diffuse) intervals with gray tones: gray (10Y 5/1-6/1, 5Y 5/1), light olive-gray (5Y 6/2), pale olive (5Y 6/3), and light greenish gray (10Y 6/2). SMEAR SLIDE SUMMARY (%): 2, 69 5, 111 D D TEXTURE: Sand 5 10 Silt 10 10 Clay 85 80 COMPOSITION: Quartz Tr — Feldspar 3 3 Clay 24 23 Accessory minerals — 1 Zeolite Tr Tr Foraminifers 4 7 Nannofossils 66 60 Diatoms — 3 Radiolarians — Tr Micrite 5 3
								2						
								3						
								4						
								5						
								6						

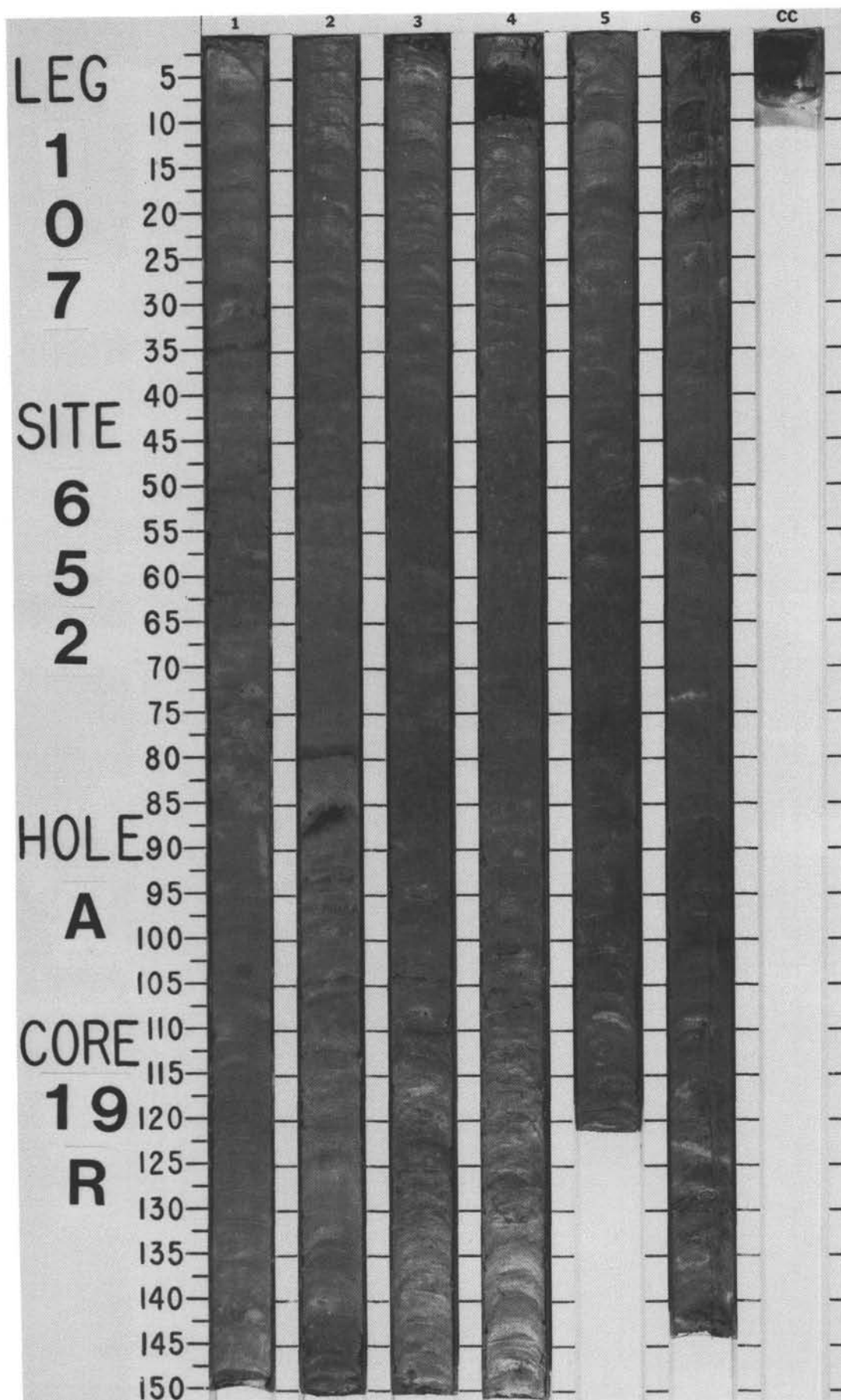


[illegible]



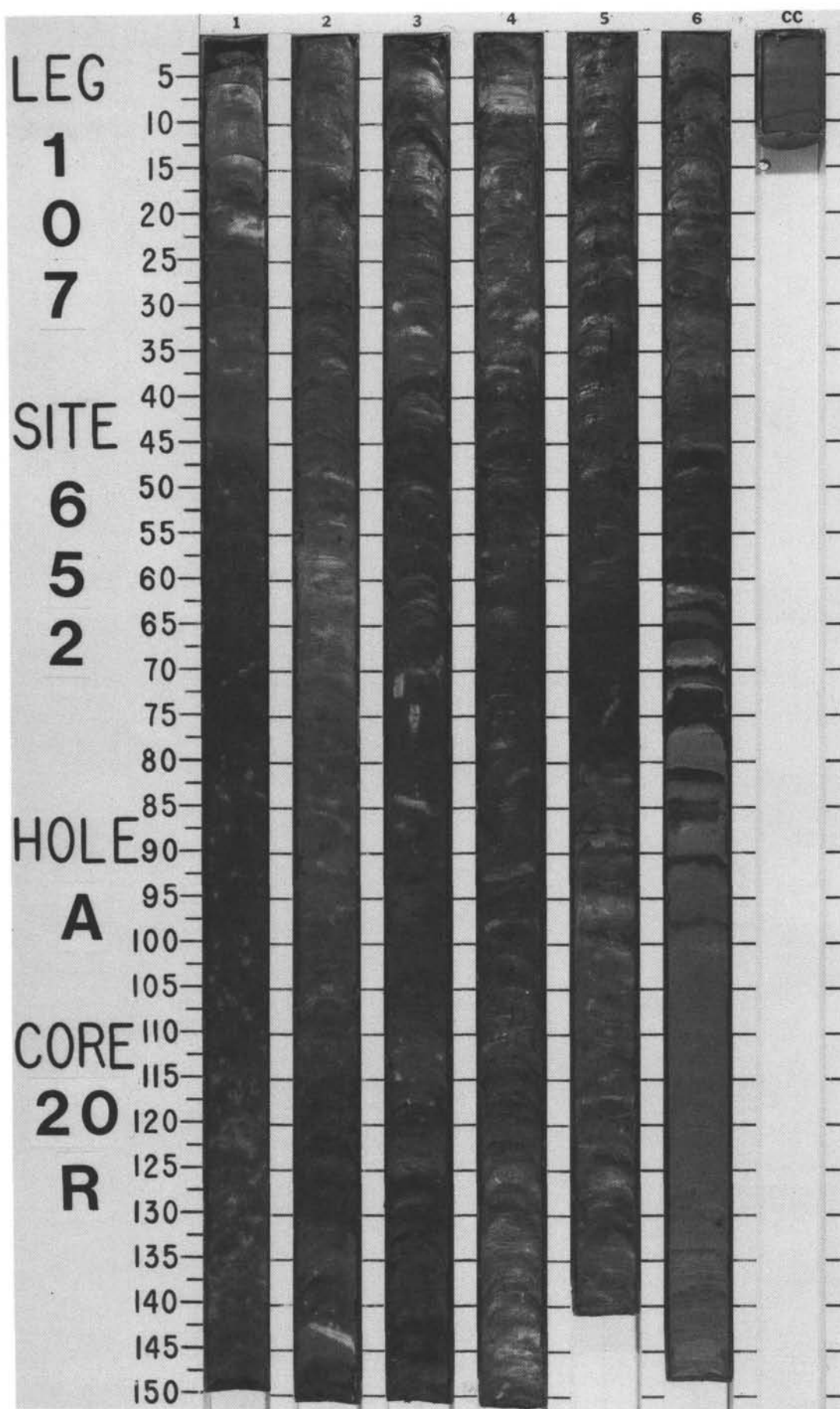
SITE 652 HOLE A CORE 19 R CORED INTERVAL 3616.5-3626.2 mbsf; 170.5-180.2 mbsf

TIME-ROCK UNIT														LITHOLOGIC DESCRIPTION													
BIOSTRAT. ZONE/ FOSSIL CHARACTER																											
FORAMINIFERS																											
NANNOFOSSILS																											
RADIOLARIANS																											
DIATOMS																											
PALEOMAGNETICS																											
PHYS. PROPERTIES																											
CHEMISTRY																											
SECTION																											
METERS																											
GRAPHIC LITHOLOGY																											
DRILLING DISTURB.																											
SED. STRUCTURES																											
SAMPLES																											
														MARLY NANNOFOSSIL OOZE													
														Homogeneous, marly nannofossil ooze with some diagenetic laminations, olive-gray (5Y 5/2) in Sections 1 and 2, light olive-gray (5Y 6/2) in Sections 3 and 4, and yellowish red (5YR 5/6) and brown-yellow (10YR 6/6) in Sections 5 and 6.													
														SMEAR SLIDE SUMMARY (%):													
														1, 48 2, 85 4, 8 5, 62 D M M D													
														TEXTURE:													
														Sand — — — — Silt 2 5 1 1 Clay 98 95 99 99													
														COMPOSITION:													
														Quartz Tr — — — Feldspar Tr — — — Mica — — Tr — Clay — 60 70 55 Volcanic glass 25 20 20 — Calcite/dolomite — — — Tr Accessory minerals Tr 10 10 — Clinoptilolite Tr — Tr Tr Foraminifers 8 — Tr Tr Nannofossils 52 10 — 35 Bioclasts 5 — Tr Tr Micrite 10 — — 10													



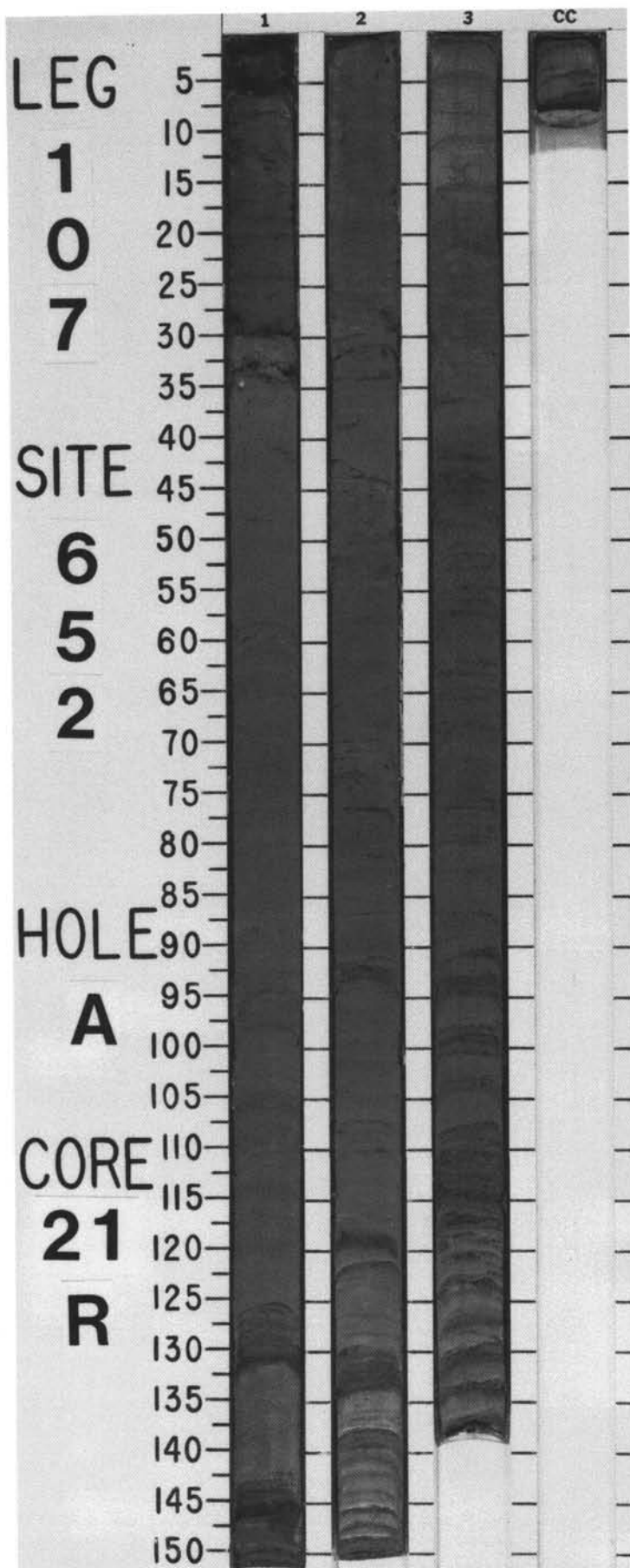
SITE 652 HOLE A CORE 20 R CORED INTERVAL 3626.2-3635.8 mbsl; 180.2-189.8 mbsf

TIME-ROCK UNIT	BIOSTRAT. ZONE/ FOSSIL CHARACTER				PALEOMAGNETICS	PHYS. PROPERTIES	CHEMISTRY	SECTION	METERS	GRAPHIC LITHOLOGY	DRILLING DISTURB.	SEC. STRUCTURES	SAMPLES	LITHOLOGIC DESCRIPTION																																																																																																																
	FORAMINIFERS	NANNOFOSSILS	RADIOLARIANS	DIATOMS																																																																																																																										
MESSINIAN	F/G NN11b	MPI 1	NN12		Thvera (C ₂)	γ=1.75 φ=64 V=1612 ●	46 ● ● 46	1	0.5 1.0			*		MARLY NANNOFOSSIL OOZE, CLAY, and DOLOMITIC-CALCAREOUS MUD																																																																																																																
EARLY PLIOCENE					Gilbert	γ=1.74 φ=63 ●	51 ●	2						Core is subdivided into three units: Unit 1 is the major part of the recovered sediment: Sections 1–5, and upper 51 cm of Section 6, are dominantly red (2.5YR 4/6) to strong brown (7.5YR 5/6) clay with a small number of nannofossils. Unit 2 is a 40-cm-thick interval (from 52 to 92 cm) of Section 6, with alternating varicolored levels of clay with some dolomitic intervals; gypsum is present. Color varies strongly from red (10R 5/6), deep brown (5Y 4/6), reddish gray (10R 6/1), light gray (7.5 YR), to grayish green (5G 5/2). Unit 3 is quartz and gypsum nannofossil clay, gray (5Y 6/1); nannofossils and foraminifers are reworked.																																																																																																																
								3						SMEAR SLIDE SUMMARY (%):																																																																																																																
								4						<table><tr><td></td><td>1, 100</td><td>5, 50</td><td>6, 74</td><td>6, 81</td><td>6, 130</td><td>6, 135</td></tr><tr><td></td><td>D</td><td>D</td><td>M</td><td>M</td><td>M</td><td>D</td></tr><tr><td>Texture:</td><td></td><td></td><td></td><td></td><td></td><td></td></tr><tr><td>Sand</td><td>—</td><td>—</td><td>—</td><td>—</td><td>—</td><td>—</td></tr><tr><td>Silt</td><td>2</td><td>1</td><td>—</td><td>50</td><td>5</td><td>30</td></tr><tr><td>Clay</td><td>98</td><td>99</td><td>100</td><td>50</td><td>95</td><td>70</td></tr></table>		1, 100	5, 50	6, 74	6, 81	6, 130	6, 135		D	D	M	M	M	D	Texture:							Sand	—	—	—	—	—	—	Silt	2	1	—	50	5	30	Clay	98	99	100	50	95	70																																																																						
	1, 100	5, 50	6, 74	6, 81	6, 130	6, 135																																																																																																																								
	D	D	M	M	M	D																																																																																																																								
Texture:																																																																																																																														
Sand	—	—	—	—	—	—																																																																																																																								
Silt	2	1	—	50	5	30																																																																																																																								
Clay	98	99	100	50	95	70																																																																																																																								
								5						COMPOSITION:																																																																																																																
								6						<table><tr><td></td><td>Quartz</td><td>—</td><td>—</td><td>—</td><td>—</td><td>10</td></tr><tr><td></td><td>Feldspar</td><td>—</td><td>—</td><td>—</td><td>—</td><td>2</td></tr><tr><td></td><td>Mica</td><td>Tr</td><td>—</td><td>—</td><td>Tr</td><td>—</td></tr><tr><td></td><td>Clay</td><td>55</td><td>73</td><td>100</td><td>20</td><td>35</td></tr><tr><td></td><td>Volcanic glass</td><td>—</td><td>—</td><td>—</td><td>—</td><td>1</td></tr><tr><td></td><td>Calcite/dolomite</td><td>Tr</td><td>—</td><td>—</td><td>75</td><td>25</td></tr><tr><td></td><td>Accessory minerals</td><td>5</td><td>7</td><td>—</td><td>—</td><td>1</td></tr><tr><td></td><td>Clinoptilolite</td><td>Tr</td><td>—</td><td>—</td><td>—</td><td>—</td></tr><tr><td></td><td>Unidentified</td><td>25</td><td>—</td><td>—</td><td>—</td><td>—</td></tr><tr><td></td><td>Analcime</td><td>—</td><td>Tr</td><td>—</td><td>—</td><td>—</td></tr><tr><td></td><td>Foraminifers</td><td>3</td><td>Tr</td><td>—</td><td>30</td><td>2</td></tr><tr><td></td><td>Nannofossils</td><td>10</td><td>20</td><td>—</td><td>—</td><td>35</td></tr><tr><td></td><td>Diatoms</td><td>—</td><td>—</td><td>—</td><td>—</td><td>1</td></tr><tr><td></td><td>Bioclasts</td><td>2</td><td>—</td><td>—</td><td>10</td><td>—</td></tr><tr><td></td><td>Gypsum</td><td>—</td><td>—</td><td>Tr</td><td>5</td><td>2</td></tr><tr><td></td><td>Glauconite</td><td>—</td><td>—</td><td>—</td><td>—</td><td>1</td></tr></table>		Quartz	—	—	—	—	10		Feldspar	—	—	—	—	2		Mica	Tr	—	—	Tr	—		Clay	55	73	100	20	35		Volcanic glass	—	—	—	—	1		Calcite/dolomite	Tr	—	—	75	25		Accessory minerals	5	7	—	—	1		Clinoptilolite	Tr	—	—	—	—		Unidentified	25	—	—	—	—		Analcime	—	Tr	—	—	—		Foraminifers	3	Tr	—	30	2		Nannofossils	10	20	—	—	35		Diatoms	—	—	—	—	1		Bioclasts	2	—	—	10	—		Gypsum	—	—	Tr	5	2		Glauconite	—	—	—	—	1
	Quartz	—	—	—	—	10																																																																																																																								
	Feldspar	—	—	—	—	2																																																																																																																								
	Mica	Tr	—	—	Tr	—																																																																																																																								
	Clay	55	73	100	20	35																																																																																																																								
	Volcanic glass	—	—	—	—	1																																																																																																																								
	Calcite/dolomite	Tr	—	—	75	25																																																																																																																								
	Accessory minerals	5	7	—	—	1																																																																																																																								
	Clinoptilolite	Tr	—	—	—	—																																																																																																																								
	Unidentified	25	—	—	—	—																																																																																																																								
	Analcime	—	Tr	—	—	—																																																																																																																								
	Foraminifers	3	Tr	—	30	2																																																																																																																								
	Nannofossils	10	20	—	—	35																																																																																																																								
	Diatoms	—	—	—	—	1																																																																																																																								
	Bioclasts	2	—	—	10	—																																																																																																																								
	Gypsum	—	—	Tr	5	2																																																																																																																								
	Glauconite	—	—	—	—	1																																																																																																																								



SITE 652 HOLE A CORE 21 R CORED INTERVAL 3635.8-3645.7 mbsl; 189.8-199.7 mbsf

TIME-ROCK UNIT	BIOSTRAT. ZONE/ FOSSIL CHARACTER				PALEOMAGNETICS	PHYS. PROPERTIES	CHEMISTRY	SECTION	METERS	GRAPHIC LITHOLOGY	DRILLING DISTURB.	SED. STRUCTURES	SAMPLES	LITHOLOGIC DESCRIPTION
	FORAMINIFERS	NANNOFOSSILS	RADIOLARIANS	DIATOMS										
						$\gamma = 2.03 \quad \phi = 44 \quad \nabla = 1754$ ● ● 22 ● 30		1	0.5 1.0			*		TURBIDITIC, GYPSUM-BEARING, SANDY, SILTY CLAY and CALCAREOUS MUDSTONE Succession of turbidites made of gypsum-bearing calcareous clay, light olive-gray (5Y 6/2); thin level (<10 cm) of calcareous mudstone or nannofossil-bearing mudstone, olive-gray (5Y 5/2); nannofossils are reworked. SMEAR SLIDE SUMMARY (%): 1, 30 1, 100 M D TEXTURE: Sand — — Silt 15 40 Clay 85 60 COMPOSITION: Quartz — 5 Mica 2 3 Clay 40 32 Calcite/dolomite 8 — Accessory minerals 5 — Gypsum detritus 20 — Foraminifers Tr — Nannofossils 20 60 Bioclasts 5 —
						$\gamma = 1.99 \quad \phi = 48 \quad \nabla = 1734$ ●		2		©			*	
								3						
								CC						

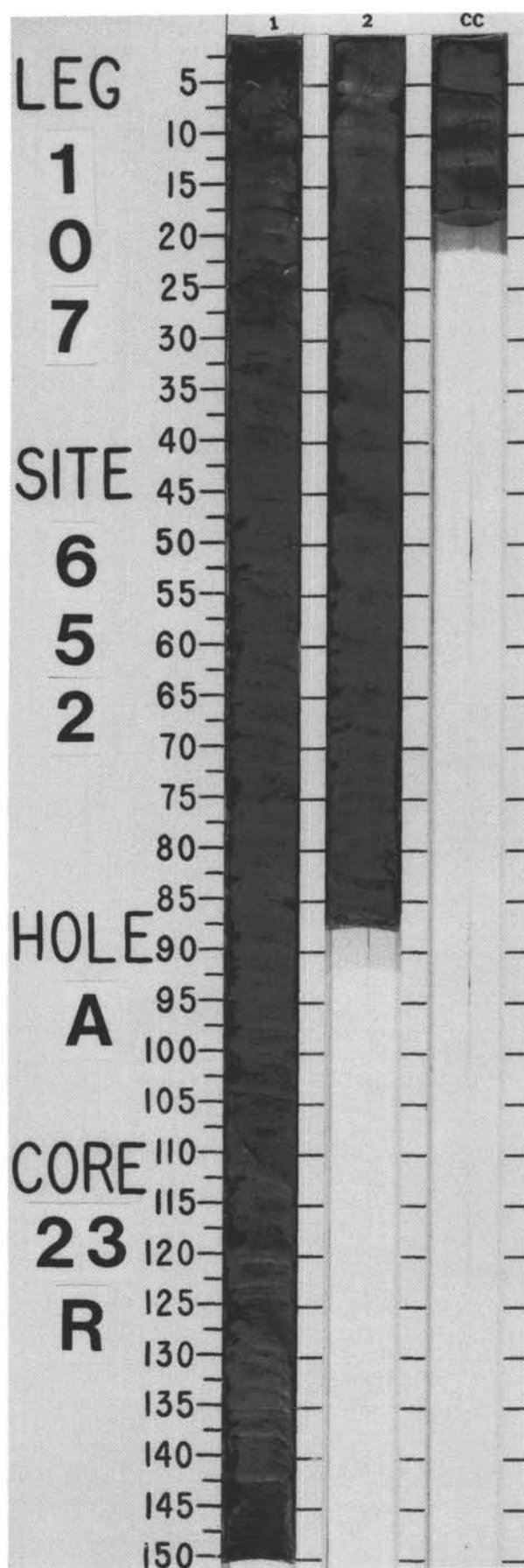
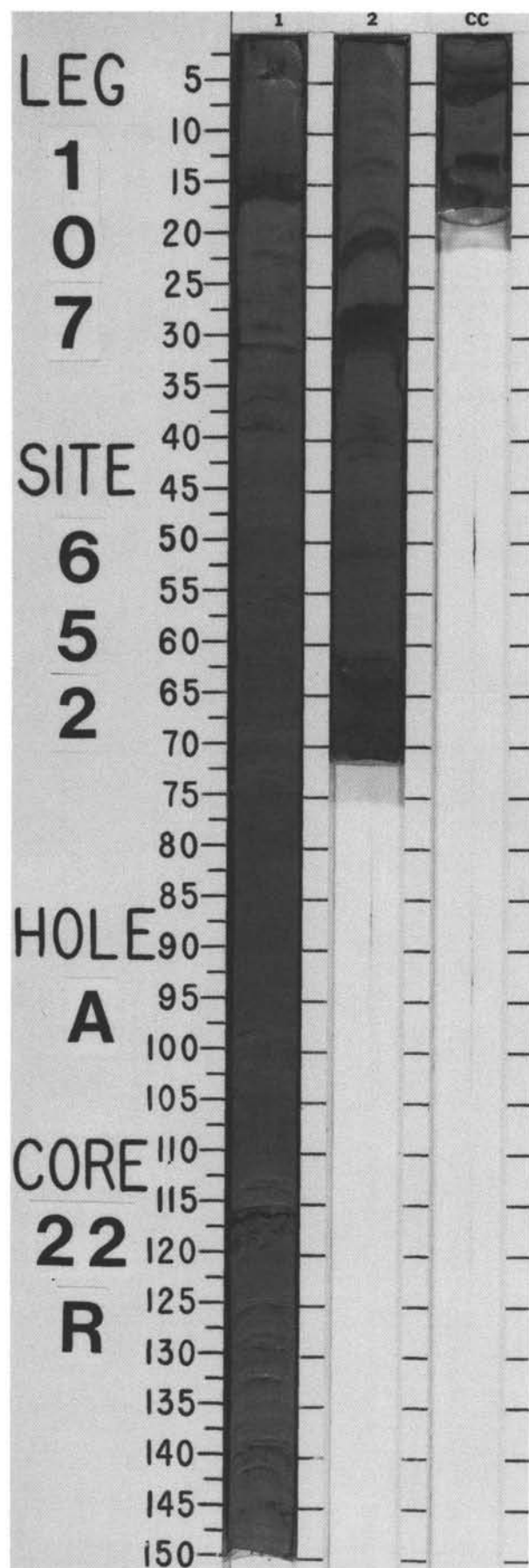


SITE 652 HOLE A CORE 22 R CORED INTERVAL 3645.7-3655.1 mbsl; 199.7-209.1 mbsf

TIME-ROCK UNIT	BIOSTRAT. ZONE/ FOSSIL CHARACTER				PALEOMAGNETICS	PHYS. PROPERTIES	CHEMISTRY	SECTION	METERS	GRAPHIC LITHOLOGY	DRILLING DISTURB.	SED. STRUCTURES	SAMPLES	LITHOLOGIC DESCRIPTION																																							
	FORAMINIFERS	NANNOFOSSILS	RADIOLARIANS	DIATOMS																																																	
						● $\gamma=2.02$ $\phi=45$ $V=17.2$	● 20		0.0 1 0.0 2				*	<p>CARBONATE-BEARING MUD with minor alternations of GYPSIFEROUS and CALCAREOUS SILTY SAND</p> <p>Thin layers (5 cm or less) of gypsum and carbonate, alternating with thick layers of gray (5Y 5/1), nannofossil-bearing clay; nannofossils are reworked.</p> <p>SMEAR SLIDE SUMMARY (%):</p> <table><tr><td></td><td>1, 100</td><td>2, 70</td></tr><tr><td>D</td><td></td><td>M</td></tr></table> <p>TEXTURE:</p> <table><tr><td>Sand</td><td>—</td><td>50</td></tr><tr><td>Silt</td><td>20</td><td>40</td></tr><tr><td>Clay</td><td>80</td><td>10</td></tr></table> <p>COMPOSITION:</p> <table><tr><td>Mica</td><td>—</td><td>Tr</td></tr><tr><td>Clay</td><td>10</td><td>10</td></tr><tr><td>Calcite/dolomite</td><td>5</td><td>—</td></tr><tr><td>Accessory minerals</td><td>—</td><td>4</td></tr><tr><td>Gypsum</td><td>—</td><td>43</td></tr><tr><td>Unidentified</td><td>75</td><td>—</td></tr><tr><td>Carbonate detritus</td><td>—</td><td>43</td></tr><tr><td>Nannofossils</td><td>10</td><td>—</td></tr></table>		1, 100	2, 70	D		M	Sand	—	50	Silt	20	40	Clay	80	10	Mica	—	Tr	Clay	10	10	Calcite/dolomite	5	—	Accessory minerals	—	4	Gypsum	—	43	Unidentified	75	—	Carbonate detritus	—	43	Nannofossils	10	—
	1, 100	2, 70																																																			
D		M																																																			
Sand	—	50																																																			
Silt	20	40																																																			
Clay	80	10																																																			
Mica	—	Tr																																																			
Clay	10	10																																																			
Calcite/dolomite	5	—																																																			
Accessory minerals	—	4																																																			
Gypsum	—	43																																																			
Unidentified	75	—																																																			
Carbonate detritus	—	43																																																			
Nannofossils	10	—																																																			

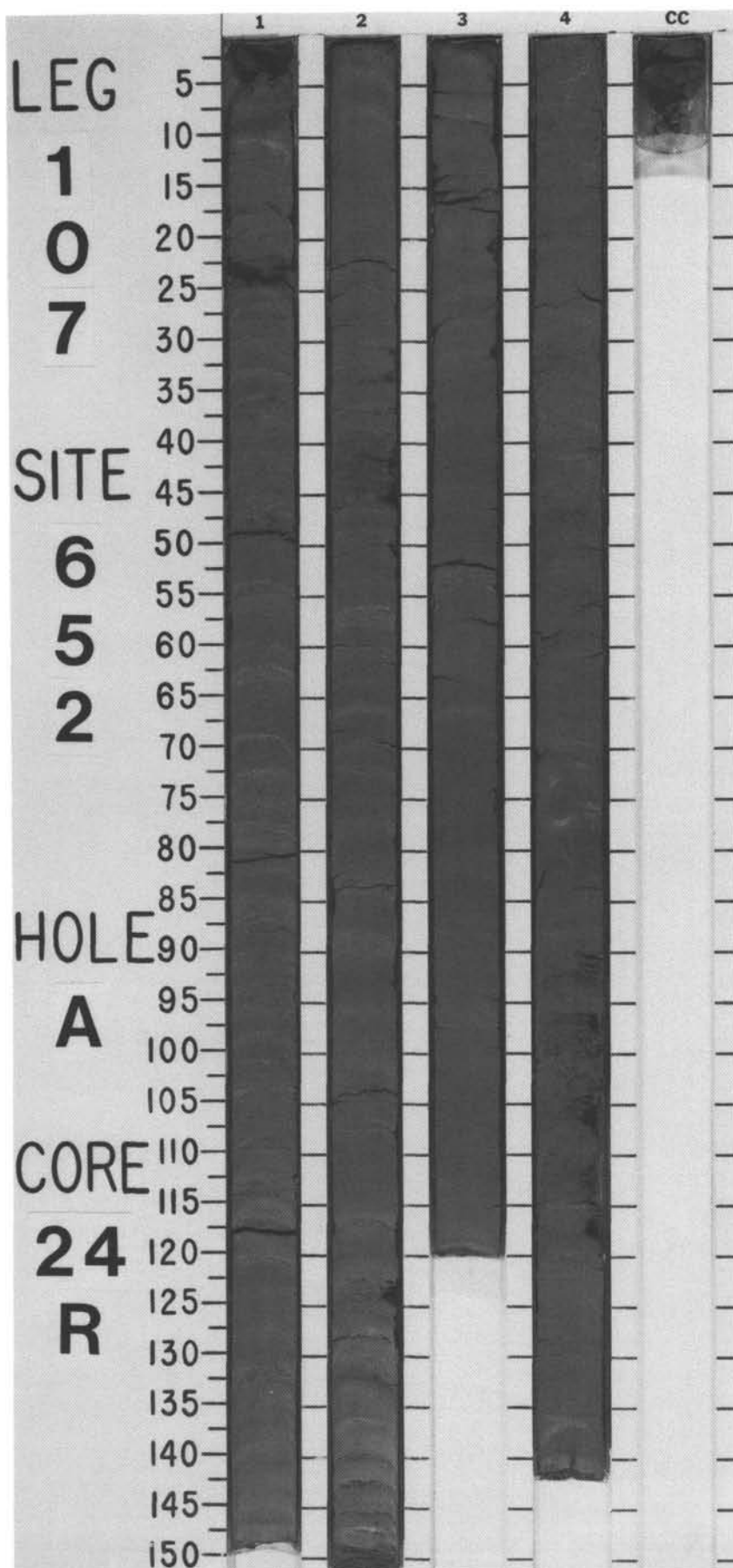
SITE 652 HOLE A CORE 23 R CORED INTERVAL 3655.1-3664.7 mbsl; 209.1-218.7 mbsf

TIME- ROCK UNIT	BIOSTRAT. ZONE/ FOSSIL CHARACTER				PALEOMAGNETICS	PHYS. PROPERTIES	CHEMISTRY	SECTION	METERS	GRAPHIC LITHOLOGY	DRILLING DISTURB.	SED. STRUCTURES	SAMPLES	LITHOLOGIC DESCRIPTION
	FORAMINIFERS	NANNOFOSSILS	RADIOLARIANS	DIATOMS										
						● $\gamma=2.04$ $\phi=48$ $V=1657$	● 29	1	0.5 1.0			Δ <		



SITE 652 HOLE A CORE 24 R CORED INTERVAL 3664.7-3674.4 mbsl; 218.7-228.4 mbsf

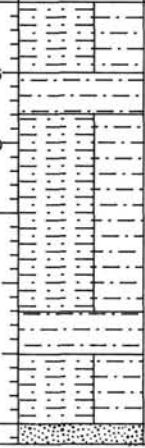
TIME-ROCK UNIT	BIOSTRAT. ZONE/ FOSSIL CHARACTER				PALEOMAGNETICS	PHYS. PROPERTIES	CHEMISTRY	SECTION	METERS	GRAPHIC LITHOLOGY	DRILLING DISTURB.	SED. STRUCTURES	SAMPLES	LITHOLOGIC DESCRIPTION
	FORAMINIFERS	NANNOFOSSILS	RADIOLARIANS	DIATOMS										
														</

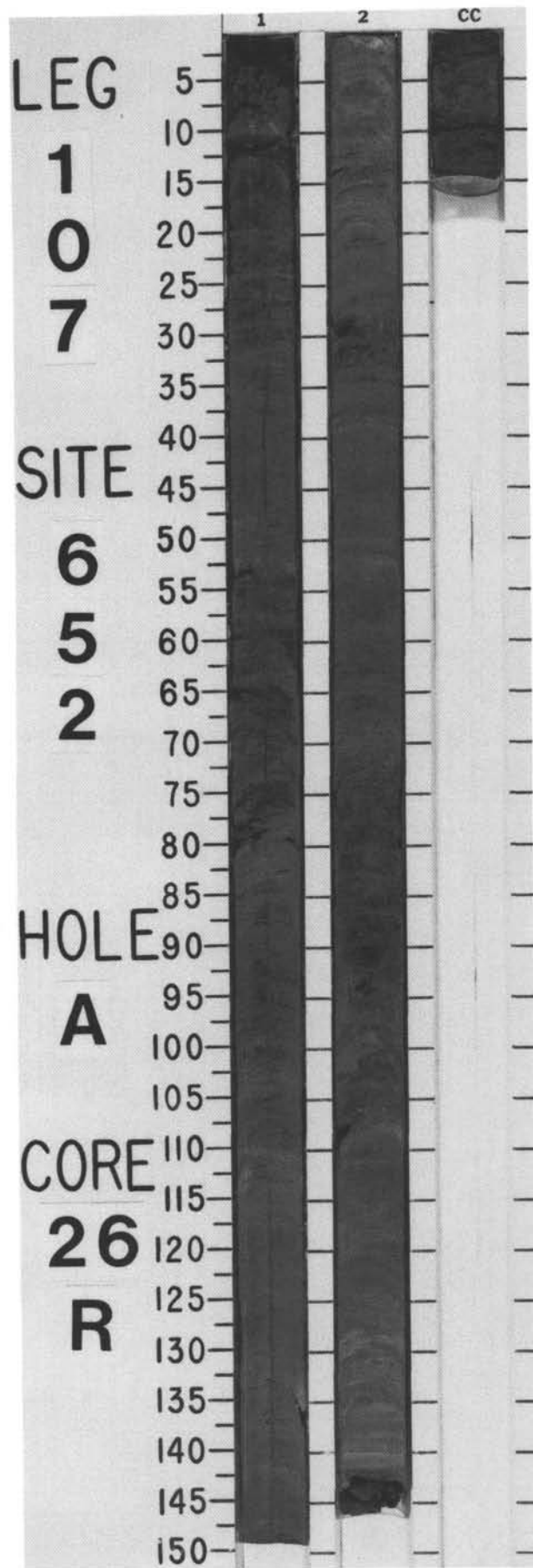
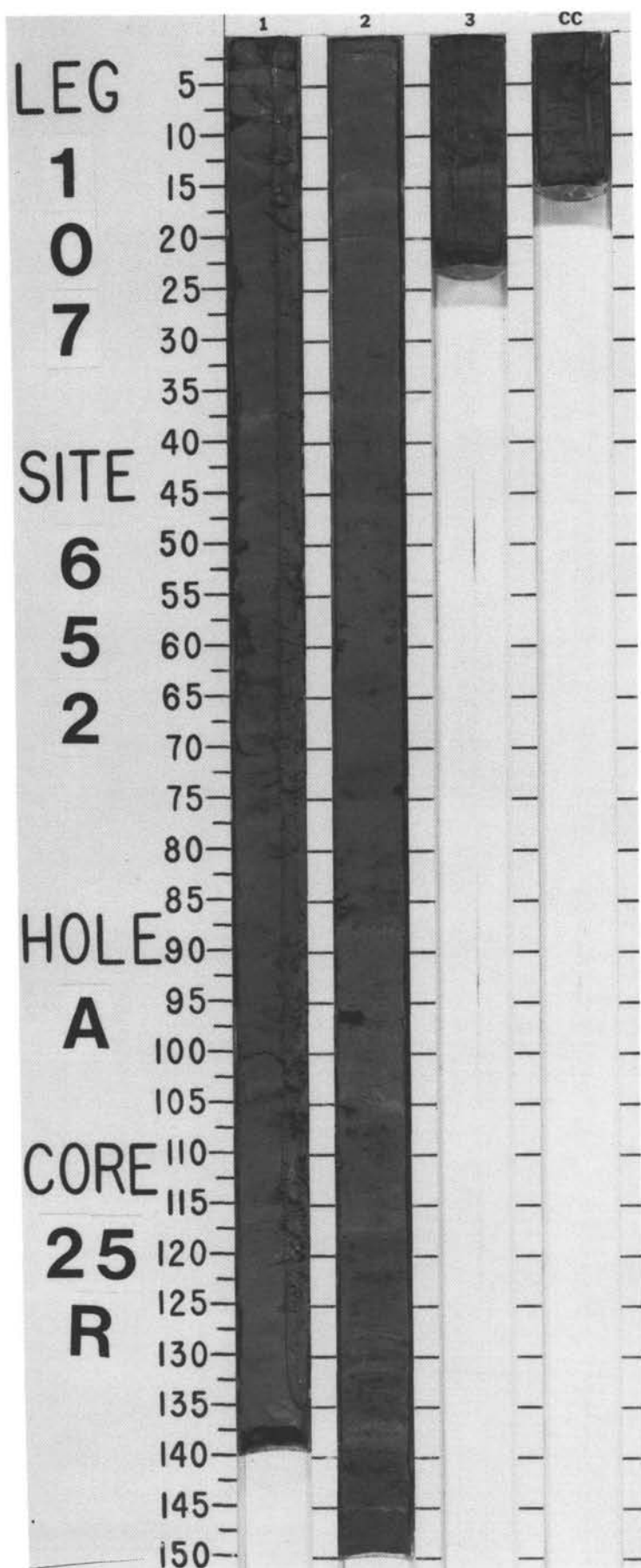


SITE 652 HOLE A CORE 25 R CORED INTERVAL 3674.4-3684.1 mbsl; 228.4-238.1 mbsf

TIME- ROCK UNIT	BIOSTRAT. ZONE/ FOSSIL CHARACTER				PALEOMAGNETICS	PHYS. PROPERTIES	CHEMISTRY	SECTION	METERS	GRAPHIC LITHOLOGY	DRILLING DISTURB.	SED. STRUCTURES	SAMPLES	LITHOLOGIC DESCRIPTION
	FORAMINIFERS	NANNOFOSSILS	RADIOLARIANS	DIATOMS										
						● $\gamma=2.08$ $\phi=42$ $V=1981$	● 23 ● 21 ● 35 ● 37	1	0.5 1.0			*** IV 		

SITE 652 HOLE A CORE 26 R CORED INTERVAL 3684.1-3693.7 mbsl; 238.1-247.7 mbsf

TIME-ROCK UNIT	BIOSTRAT. ZONE/ FOSSIL CHARACTER				PALEOMAGNETICS	PHYS. PROPERTIES	CHEMISTRY	SECTION	METERS	GRAPHIC LITHOLOGY	DRILLING DISTURB.	SED. STRUCTURES	SAMPLES	LITHOLOGIC DESCRIPTION																																																																				
	FORAMINIFERS	NANNOFOSSILS	RADIOLARIANS	DIATOMS																																																																														
						● $\gamma=2.15$ $\phi=42$ $V=1900$	● 23 ● 24 ● 25 ● 26 ● 27 ● 28 ● 29 ● 30 ● 31 ● 32 ● 33 ● 34 ● 35 ● 36 ● 37 ● 38 ● 39 ● 40 ● 41 ● 42 ● 43 ● 44 ● 45 ● 46 ● 47 ● 48 ● 49 ● 50 ● 51 ● 52 ● 53 ● 54 ● 55 ● 56 ● 57 ● 58 ● 59 ● 60 ● 61 ● 62 ● 63 ● 64 ● 65 ● 66 ● 67 ● 68 ● 69 ● 70 ● 71 ● 72 ● 73 ● 74 ● 75 ● 76 ● 77 ● 78 ● 79 ● 80 ● 81 ● 82 ● 83 ● 84 ● 85 ● 86 ● 87 ● 88 ● 89 ● 90 ● 91 ● 92 ● 93 ● 94 ● 95 ● 96 ● 97 ● 98 ● 99 ● 100	1 2 CC	0.5 1.0					<p>CALCAREOUS MUD; GYPSUM-BEARING, CALCAREOUS, SANDY MUD; and SAND</p> <p>Alternations of olive (5Y 5/3) and olive-gray (5Y 5/2) to grayish brown (2.5Y 4/2) calcareous mud; gypsum-bearing, calcareous (marly), sandy mud; and gypsum-bearing, calcareous, clayey, silty sand. Thick, gypsum-bearing, calcareous (marly), sandy, silt layers are found in Section 1, 52-80 cm and Section 2, 69-99 cm.</p> <p>Interpretation: a series of thin-bedded turbidites.</p> <p>SMEAR SLIDE SUMMARY (%):</p> <table><tr><td></td><td>2, 41</td><td>2, 88</td><td>CC, 4</td></tr><tr><td></td><td>D</td><td>D</td><td>D</td></tr></table> <p>TEXTURE:</p> <table><tr><td>Sand</td><td>—</td><td>30</td><td>40</td></tr><tr><td>Silt</td><td>15</td><td>35</td><td>30</td></tr><tr><td>Clay</td><td>85</td><td>35</td><td>30</td></tr></table> <p>COMPOSITION:</p> <table><tr><td>Quartz</td><td>5</td><td>20</td><td>15</td></tr><tr><td>Feldspar</td><td>4</td><td>15</td><td>8</td></tr><tr><td>Rock fragments</td><td>—</td><td>1</td><td>1</td></tr><tr><td>Clay</td><td>56</td><td>14</td><td>26</td></tr><tr><td>Volcanic glass</td><td>3</td><td>2</td><td>2</td></tr><tr><td>Calcite</td><td>—</td><td>35</td><td>30</td></tr><tr><td>Dolomite</td><td>2</td><td>3</td><td>2</td></tr><tr><td>Accessory minerals</td><td>1</td><td>—</td><td>—</td></tr><tr><td>Gypsum</td><td>Tr</td><td>10</td><td>15</td></tr><tr><td>Foraminifers</td><td>Tr</td><td>—</td><td>Tr</td></tr><tr><td>Nannofossils</td><td>4</td><td>Tr</td><td>1</td></tr><tr><td>Micrite</td><td>25</td><td>—</td><td>—</td></tr></table>		2, 41	2, 88	CC, 4		D	D	D	Sand	—	30	40	Silt	15	35	30	Clay	85	35	30	Quartz	5	20	15	Feldspar	4	15	8	Rock fragments	—	1	1	Clay	56	14	26	Volcanic glass	3	2	2	Calcite	—	35	30	Dolomite	2	3	2	Accessory minerals	1	—	—	Gypsum	Tr	10	15	Foraminifers	Tr	—	Tr	Nannofossils	4	Tr	1	Micrite	25	—	—
	2, 41	2, 88	CC, 4																																																																															
	D	D	D																																																																															
Sand	—	30	40																																																																															
Silt	15	35	30																																																																															
Clay	85	35	30																																																																															
Quartz	5	20	15																																																																															
Feldspar	4	15	8																																																																															
Rock fragments	—	1	1																																																																															
Clay	56	14	26																																																																															
Volcanic glass	3	2	2																																																																															
Calcite	—	35	30																																																																															
Dolomite	2	3	2																																																																															
Accessory minerals	1	—	—																																																																															
Gypsum	Tr	10	15																																																																															
Foraminifers	Tr	—	Tr																																																																															
Nannofossils	4	Tr	1																																																																															
Micrite	25	—	—																																																																															

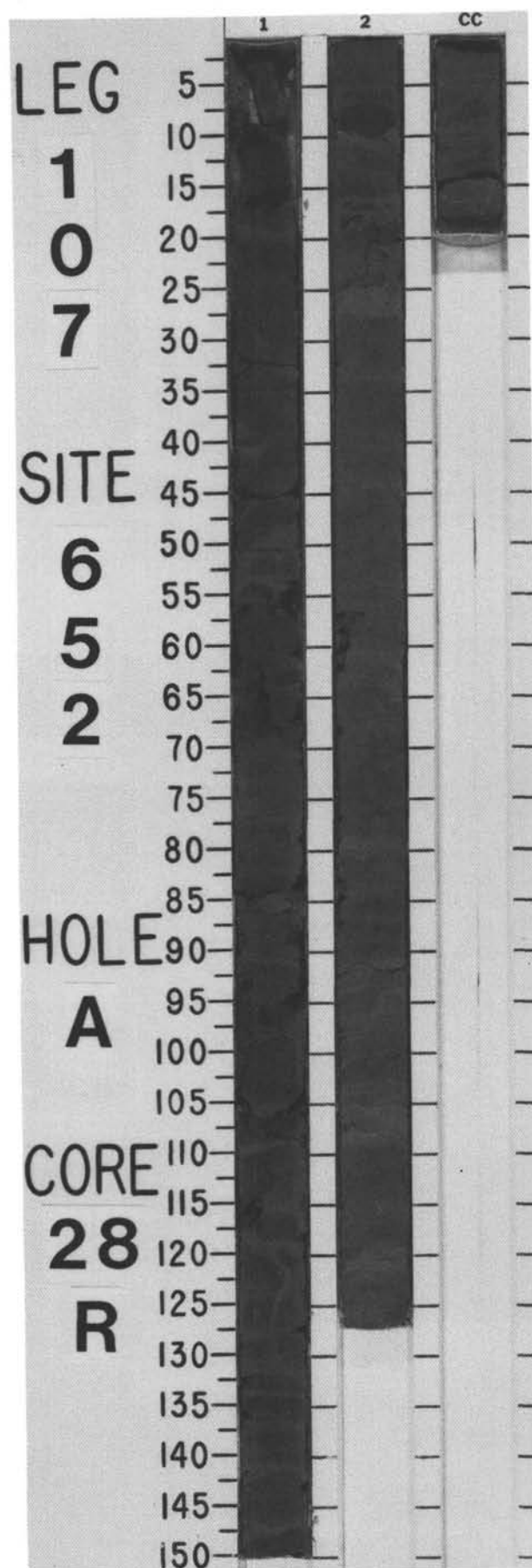
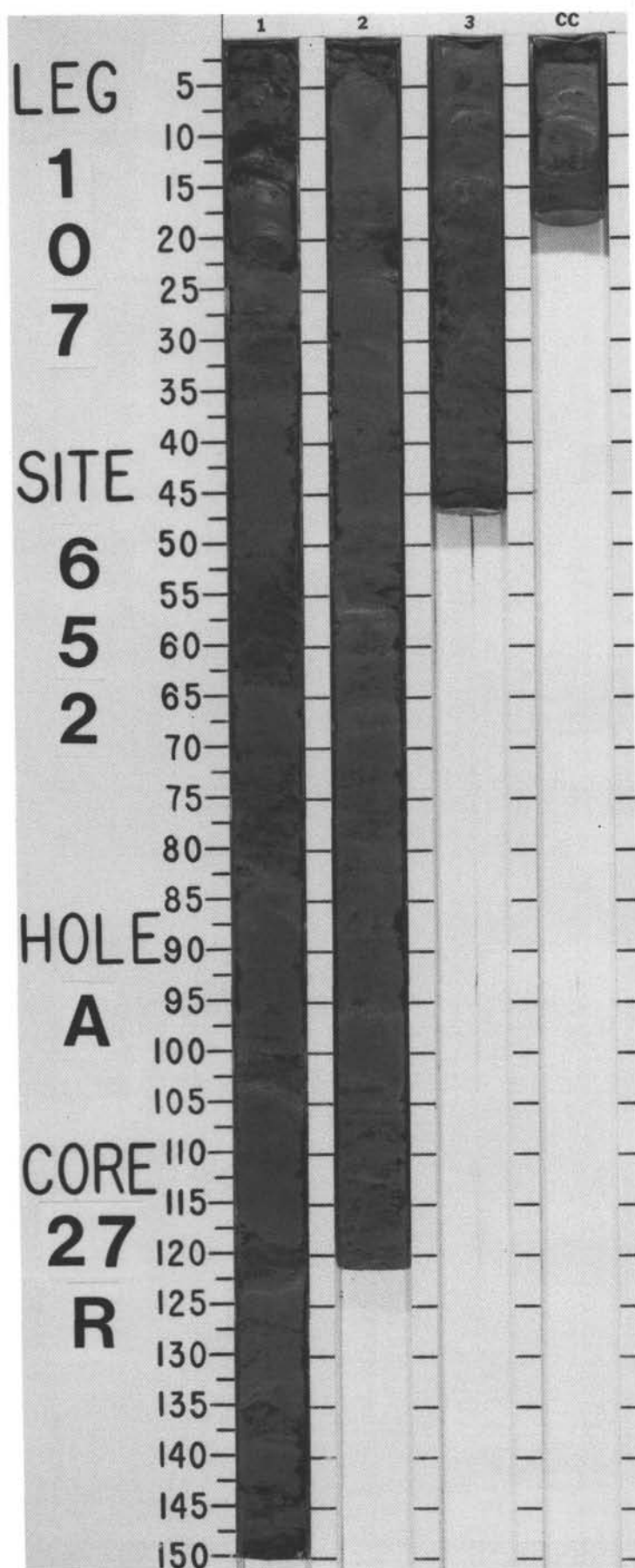


SITE 652 HOLE A CORE 27 B CORED INTERVAL 3693.7-3703.4 mbsl; 247.7-257.4 mbsf

[illegible]

SITE 652 HOLE A CORE 28 R CORED INTERVAL 3703.4-3713.1 mbsl; 257.4-267.1 mbsf

TIME - ROCK UNIT	BIOSTRAT. ZONE/ FOSSIL CHARACTER				PALEOMAGNETICS	PHYS. PROPERTIES	CHEMISTRY	SECTION	METERS	GRAPHIC LITHOLOGY	DRILLING DISTURB.	SED. STRUCTURES	SAMPLES	LITHOLOGIC DESCRIPTION
	FORAMINIFERS	NANNOFOSSILS	RADIOLARIANS	DIATOMS										
						●	●26	1	0.5 1.0			///	*	CALCAREOUS MUDSTONE, alternating with GYPSIFEROUS, SANDY MUDSTONE Gray (2.5Y 6/0), clastic layers, alternating with thicker, olive-gray (2.5Y 6/2), sandstone layers. Bases of clastic layers are sharp, laminated in millimeter-wide laminae, and cross-bedded; gypsum is an important percentage of the clastic content. Micro-meteorites in CC.
						●	●35	2					*	SMEAR SLIDE SUMMARY (%): 2, 100 1, 54 D M TEXTURE: Sand 5 25 Silt 20 35 Clay 75 40 COMPOSITION: Quartz Tr — Feldspar Tr — Mica Tr 1 Clay 71 64 Dolomite 5 5 Accessory minerals 2 2 Calcite detritus 15 — Zeolites 5 — Gypsum — 25 Nannofossils 2 5
								CC						

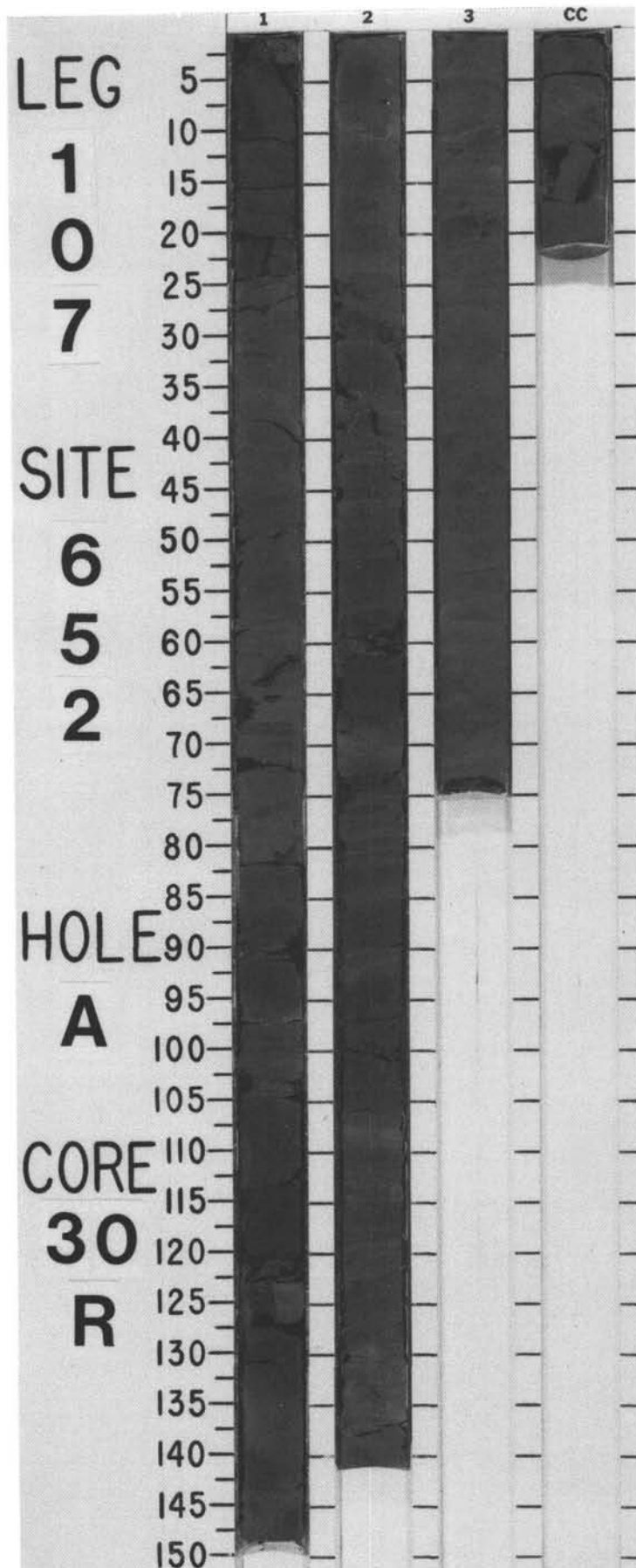
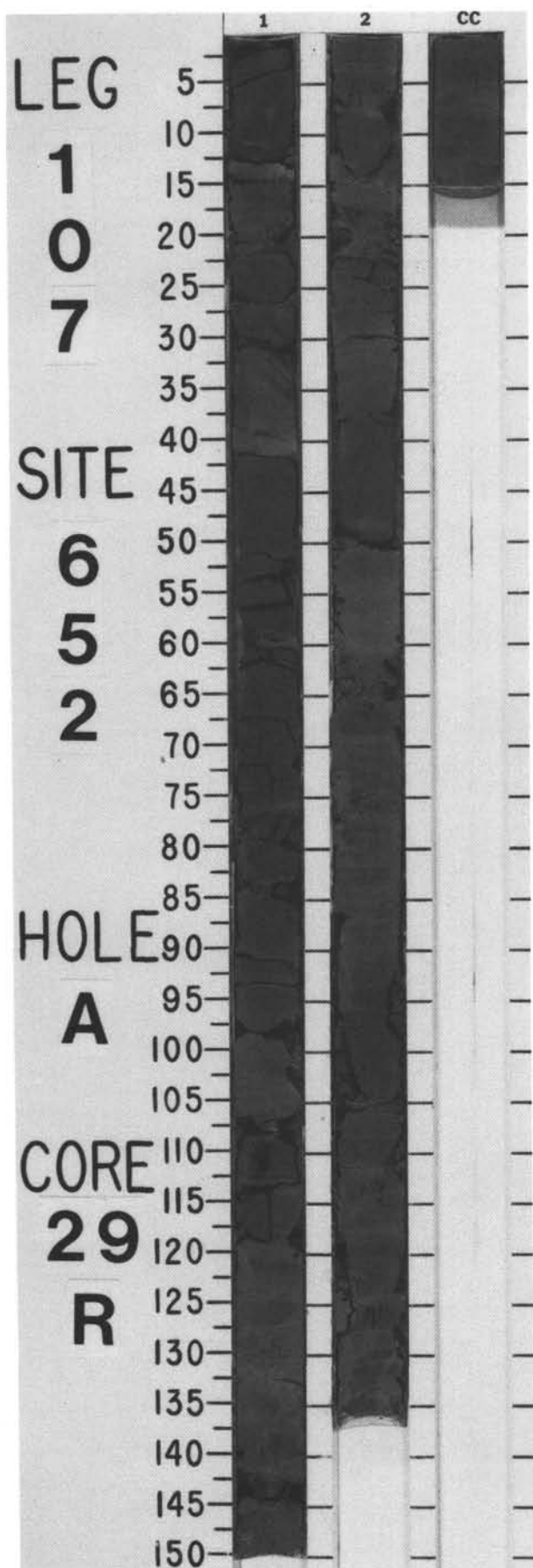


SITE 652 HOLE A CORE 29 R CORED INTERVAL 3713.1-3722.7 mbsl; 267.1-276.7 mbsf

TIME-ROCK UNIT	BIOSTRAT. ZONE/ FOSSIL CHARACTER				PALEOMAGNETICS	PHYS. PROPERTIES	CHEMISTRY	SECTION	METERS	GRAPHIC LITHOLOGY	DRILLING DISTURB.	SED. STRUCTURES	SAMPLES	LITHOLOGIC DESCRIPTION
	FORAMINIFERS	NANNOFOSSILS	RADIOLARIANS	DIATOMS										
						● $\gamma = 2.17$ $\phi = 39$ $\psi = 1852$	● 28	1	0.5 1.0			*		CALCAREOUS MUDSTONE, alternating with SANDY, GYPSIFEROUS MUDSTONE Light olive-gray (5Y 5/4), coarse-grained, sandy siltstone, alternating with gray (2.5Y 5/2), silty mudstone. Sandy silt contains a large amount of detrital carbonate and gypsum and is well graded and cross-bedded; silty mud is strongly disturbed by drilling. Traces of micro-meteorite are present. Interpretation: turbidite succession.
							● 28	2				*		SMEAR SLIDE SUMMARY (%): 1, 120 2, 48 D M TEXTURE: Sand — 15 Silt 15 65 Clay 85 20 COMPOSITION: Quartz — 3 Feldspar — Tr Mica Tr Tr Clay 52 20 Calcite/dolomite 7 Tr Accessory minerals 8 5 Analcime 2 — Clinoptilolite 1 — Gypsum Tr 20 Foraminifers Tr Tr Nannofossils 10 7 Carbonate detritus 20 45

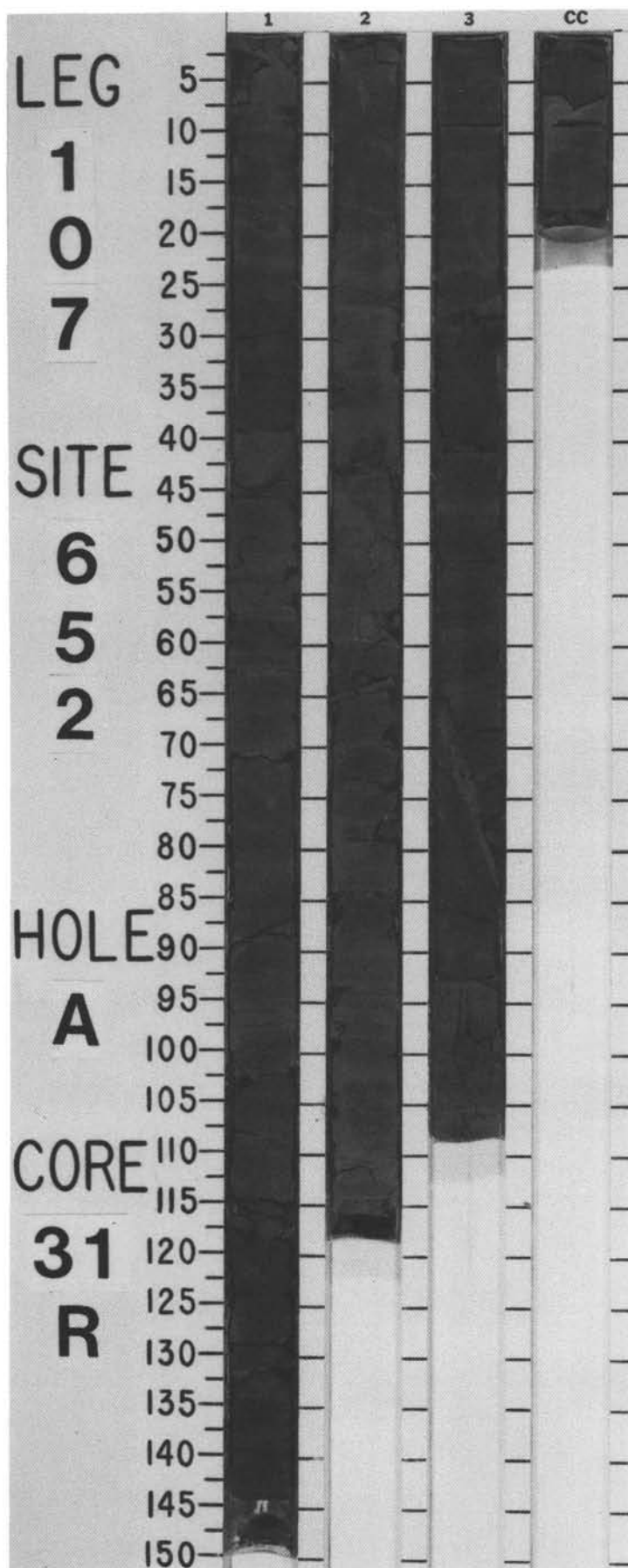
SITE 652 HOLE A CORE 30 R CORED INTERVAL 3722.7-3732.3 mbsl; 276.7-286.3 mbsf

TIME- ROCK UNIT	BIOSTRAT. ZONE/ FOSSIL CHARACTER				PALEOMAGNETICS	PHYS. PROPERTIES	CHEMISTRY	SECTION	METERS	GRAPHIC LITHOLOGY	DRILLING DISTURB.	SED. STRUCTURES	SAMPLES	LITHOLOGIC DESCRIPTION
	FORAMINIFERS	NANNOFOSSILS	RADIOLARIANS	DIATOMS										
						● $\gamma=2.25$ $\phi=34$ $\psi=1935$	● 33		0.5 1.0				*	CALCAREOUS, GYPSIFEROUS MUDSTONE, alternating with GYPSIFEROUS, SANDY MUDSTONE Grayish brown (10YR 5/2), gypsiferous, silty sand at the base, alternating with light olive-brown (2.5Y 5/2) silt and mud at the top. Silty sand layers include small black fragments of organic matter. Interpretation: turbidite succession. SMEAR SLIDE SUMMARY (%): 1, 100 D TEXTURE: Sand 5 Silt 50 Clay 45 COMPOSITION: Quartz Tr Feldspar 5 Clay 25 Calcite/dolomite 5 Accessory minerals 5 Gypsum detritus 25 Clinoptilolite Tr Carbonate detritus 25 Nannofossils 10
						● $\gamma=2.18$ $\phi=37$ $\psi=1784$	● 30	2						
								3				IVV		
								CC						



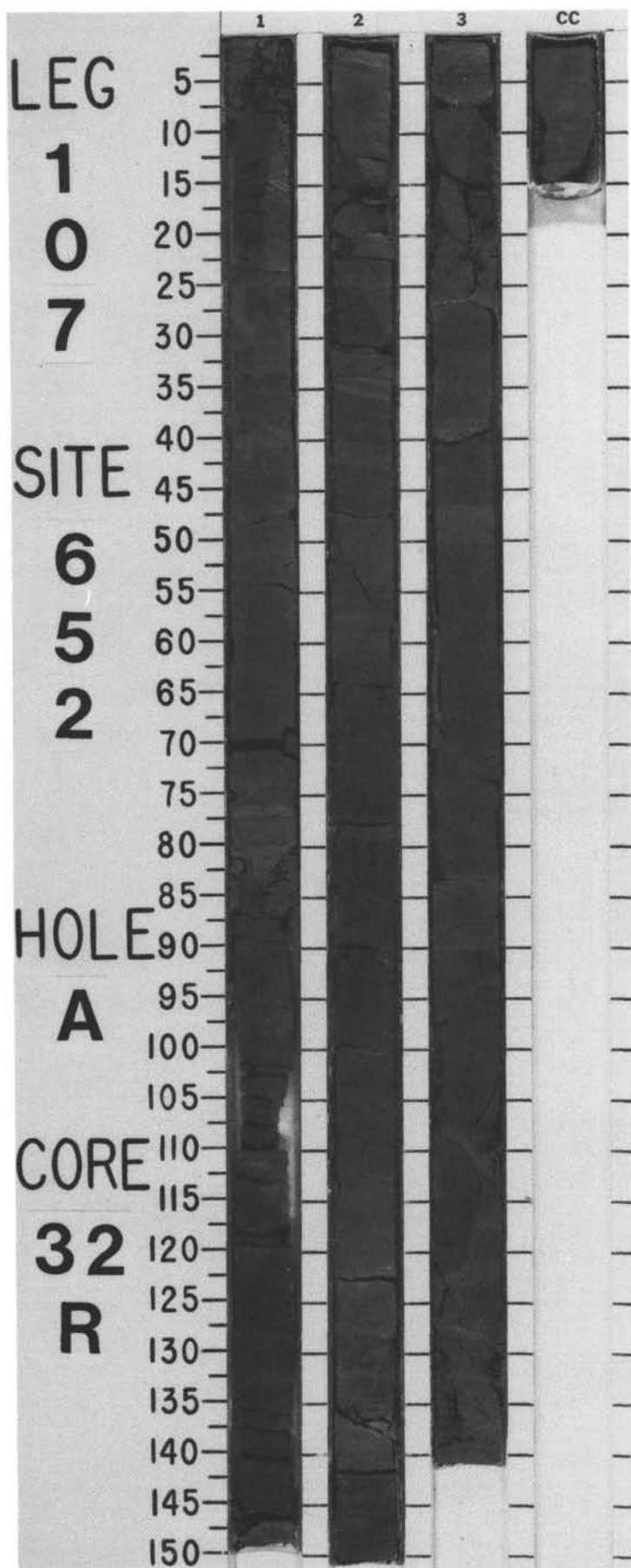
SITE 652 HOLE A CORE 31 R CORED INTERVAL 3732.3-3741.9 mbsl; 286.3-295.9 mbsf

TIME- ROCK UNIT	BIOSTRAT. ZONE/ FOSSIL CHARACTER				PALEOMAGNETICS	PHYS. PROPERTIES	CHEMISTRY	SECTION	METERS	GRAPHIC LITHOLOGY	DRILLING DISTURB.	SED. STRUCTURES	SAMPLES	LITHOLOGIC DESCRIPTION
	FORAMINIFERS	NANNOFOSSILS	RADIOLARIANS	DIATOMS										
						● $\gamma=2.25$ $\phi=36$ $V=1819$	● 35	1	0.5 1.0				*	CALCAREOUS, GYPSIFEROUS MUDSTONE, alternating with CALCAREOUS, GYPSIFEROUS, SANDY MUDSTONE Dark grayish brown (2.5Y 4/2), calcareous, gypsiferous sand at the base, alternating with brown (7.5Y 4/4), silty mud at the top. Succession of clastic sequences is strongly fractured by syndimentary tectonism.
						● $\gamma=2.28$ $\phi=33$ $V=1991$	● 36	2					*	SMEAR SLIDE SUMMARY (%): 1, 55 1, 110 D D TEXTURE: Sand 30 — Silt 30 30 Clay 40 70 COMPOSITION: Quartz 10 20 Mica 2 — Clay 15 30 Calcite/dolomite — 5 Accessory minerals 20 25 Gypsum detritus 20 10 Carbonate detritus 30 5 Nannofossils 3 5
								3						
								CC						



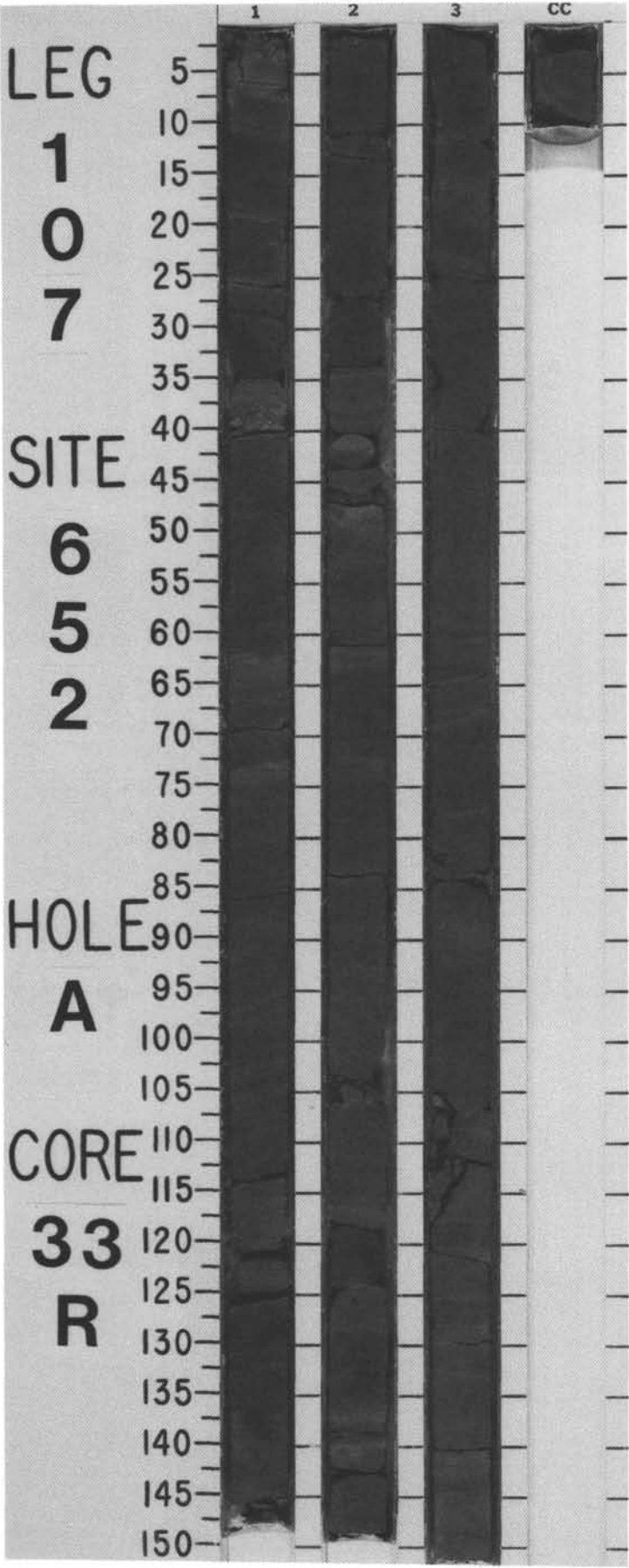
SITE 652 HOLE A CORE 32 R CORED INTERVAL 3741.9-3751.6 mbsl; 295.9-305.6 mbsf

TIME-ROCK UNIT	BIOSTRAT. ZONE/ FOSSIL CHARACTER				PALEOMAGNETICS	PHYS. PROPERTIES	CHEMISTRY	SECTION	METERS	GRAPHIC LITHOLOGY	DRILLING DISTURB.	SEL. STRUCTURES	SAMPLES	LITHOLOGIC DESCRIPTION
	FORAMINIFERS	NANNOFOSSILS	RADIOLARIANS	DIATOMS										
														GYPSIFEROUS, CALCAREOUS MUDSTONE, alternating with GYPSIFEROUS, CALCAREOUS, SANDY MUDSTONE
									0.5					Gypsiferous, calcareous mudstone, grayish brown (2.5Y 5/2), alternating with gypsiferous, calcareous, sandy mudstone, olive-gray (5Y 4/2) to gray (5Y 5/1). Sandy mudstone shows both fining- and coarsening-upward sequences, cross-stratification, and millimeter-thick fine laminations.
									1.0					Minor lithology: Section 3, 50-53 cm, diffuse, reddish brown (5YR 5/4) mudstone; Section 2, 50-62 cm, some microfaults.
														Apparent dip: approximately 5°.
														SMEAR SLIDE SUMMARY (%):
														1, 67 1, 83 1, 96 1, 98 1, 99 1, 113
														D D M M D D
														TEXTURE:
														Sand
														Silt
														Clay
														COMPOSITION:
														Quartz
														Feldspar
														Rock fragments
														Mica
														Clay
														Volcanic glass
														Calcite
														Dolomite
														Accessory minerals
														Gypsum
														Foraminifers
														Nannofossils
														Diatoms
														Radiolarians
														Sponge spicules
														2, 36 2, 40
														M M
														TEXTURE:
														Sand
														Silt
														Clay
														COMPOSITION:
														Quartz
														Clay
														Calcite
														Dolomite
														Accessory minerals
														Gypsum
														Nannofossils

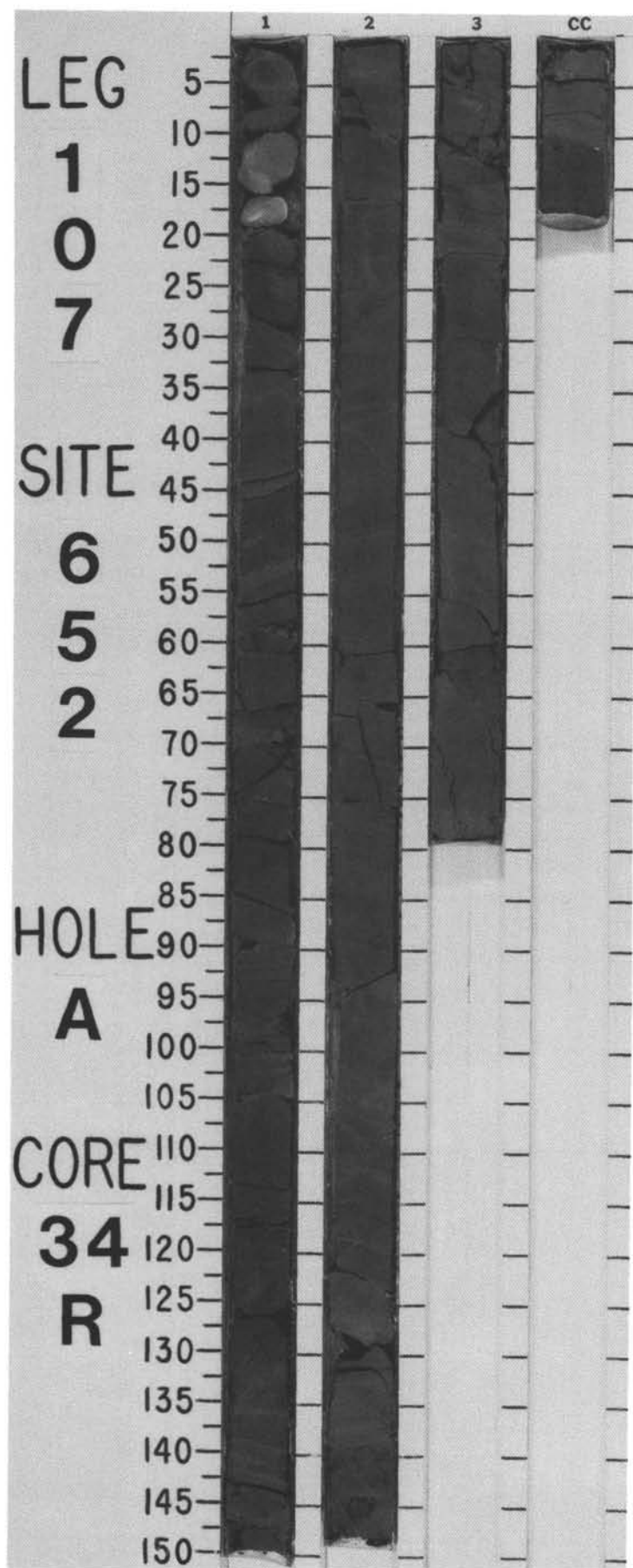


SITE 652 HOLE A CORE 33 R CORED INTERVAL 3751.6-3761.3 mbsl; 305.6-315.3 mbsf

TIME-ROCK UNIT	BIOSTRAT. ZONE/ FOSSIL CHARACTER				PALEOMAGNETICS	PHYS. PROPERTIES	CHEMISTRY	SECTION	METERS	GRAPHIC LITHOLOGY	DRILLING DISTURB.	SED. STRUCTURES	SAMPLES	LITHOLOGIC DESCRIPTION																																																									
	FORAMINIFERS	NANNOFOSSILS	RADIOLARIANS	DIATOMS																																																																			
						$\gamma = 2.28 \phi = 28 \vee = 2606$	●30	1	0.5 1.0				*	<p>GYPSIFEROUS, SALIFEROUS, SANDY SILTSTONES and MUDSTONE</p> <p>Section 1, dominant gypsiferous, calcareous sandy mudstone interbedded with 5-10-cm-thick intervals of gypsiferous, calcareous mudstone; minor sandstone layers occur. Section 3, predominantly halite- and gypsum-bearing sandy siltstone, grayish brown (2.5Y 5/2), light olive-brown (2.5Y 5/4), and gray (5Y 5/1); reddish brown (5YR 5/4) intervals also occur. Sandy mudstone and siltstone layers show fining- and coarsening-upward sequences, cross-lamination, and many fine parallel laminations.</p> <p>Minor lithology: Sections 1 and 2, slump and water escape structures in the mudstone; Section 1, 35-40 cm, fine- to coarse-grained sandstone with imbricated 1-2-cm mudstone pebbles. Halite dissolution molds (diameter from 0.5 to 3 mm) occur frequently in the coarser grained intervals. Section 3, authigenic crystals of gypsum.</p> <p>Dip: 5-9°, average 6-7°.</p> <p>SMEAR SLIDE SUMMARY (%):</p> <table><tr><td></td><td>1, 35</td><td>3, 47</td></tr><tr><td></td><td>M</td><td>D</td></tr></table> <p>TEXTURE:</p> <table><tr><td>Sand</td><td>75</td><td>40</td></tr><tr><td>Silt</td><td>20</td><td>50</td></tr><tr><td>Clay</td><td>5</td><td>10</td></tr></table> <p>COMPOSITION:</p> <table><tr><td>Quartz</td><td>20</td><td>20</td></tr><tr><td>Feldspar</td><td>5</td><td>12</td></tr><tr><td>Rock fragments</td><td>35</td><td>6</td></tr><tr><td>Mica</td><td>2</td><td>2</td></tr><tr><td>Clay</td><td>5</td><td>5</td></tr><tr><td>Volcanic glass</td><td>Tr</td><td>2</td></tr><tr><td>Calcite</td><td>15</td><td>15</td></tr><tr><td>Dolomite</td><td>1</td><td>6</td></tr><tr><td>Accessory minerals</td><td>2</td><td>1</td></tr><tr><td>Gypsum</td><td>15</td><td>30</td></tr><tr><td>Halite</td><td>—</td><td>1</td></tr><tr><td>Foraminifers</td><td>—</td><td>Tr</td></tr><tr><td>Nannofossils</td><td>—</td><td>Tr</td></tr><tr><td>Diatoms</td><td>—</td><td>1</td></tr></table>		1, 35	3, 47		M	D	Sand	75	40	Silt	20	50	Clay	5	10	Quartz	20	20	Feldspar	5	12	Rock fragments	35	6	Mica	2	2	Clay	5	5	Volcanic glass	Tr	2	Calcite	15	15	Dolomite	1	6	Accessory minerals	2	1	Gypsum	15	30	Halite	—	1	Foraminifers	—	Tr	Nannofossils	—	Tr	Diatoms	—	1
	1, 35	3, 47																																																																					
	M	D																																																																					
Sand	75	40																																																																					
Silt	20	50																																																																					
Clay	5	10																																																																					
Quartz	20	20																																																																					
Feldspar	5	12																																																																					
Rock fragments	35	6																																																																					
Mica	2	2																																																																					
Clay	5	5																																																																					
Volcanic glass	Tr	2																																																																					
Calcite	15	15																																																																					
Dolomite	1	6																																																																					
Accessory minerals	2	1																																																																					
Gypsum	15	30																																																																					
Halite	—	1																																																																					
Foraminifers	—	Tr																																																																					
Nannofossils	—	Tr																																																																					
Diatoms	—	1																																																																					
						$\gamma = 2.29 \phi = 30 \vee = 4220$	●25	2																																																															
								3					*																																																										
								CC																																																															



TIME- ROCK UNIT	BIOSTRAT. ZONE/ FOSSIL CHARACTER				PALEOMAGNETICS	PHYS. PROPERTIES	CHEMISTRY	SECTION	METERS	GRAPHIC LITHOLOGY	DRILLING DISTURB.	SED. STRUCTURES	SAMPLES	LITHOLOGIC DESCRIPTION
	FORAMINIFERS	NANNOFOSSILS	RADIOLARIANS	DIAZONES										

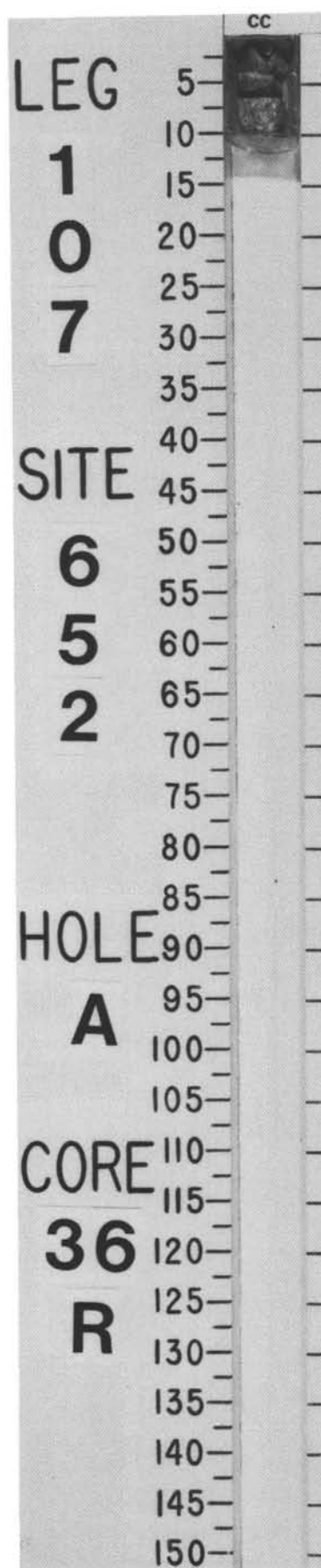
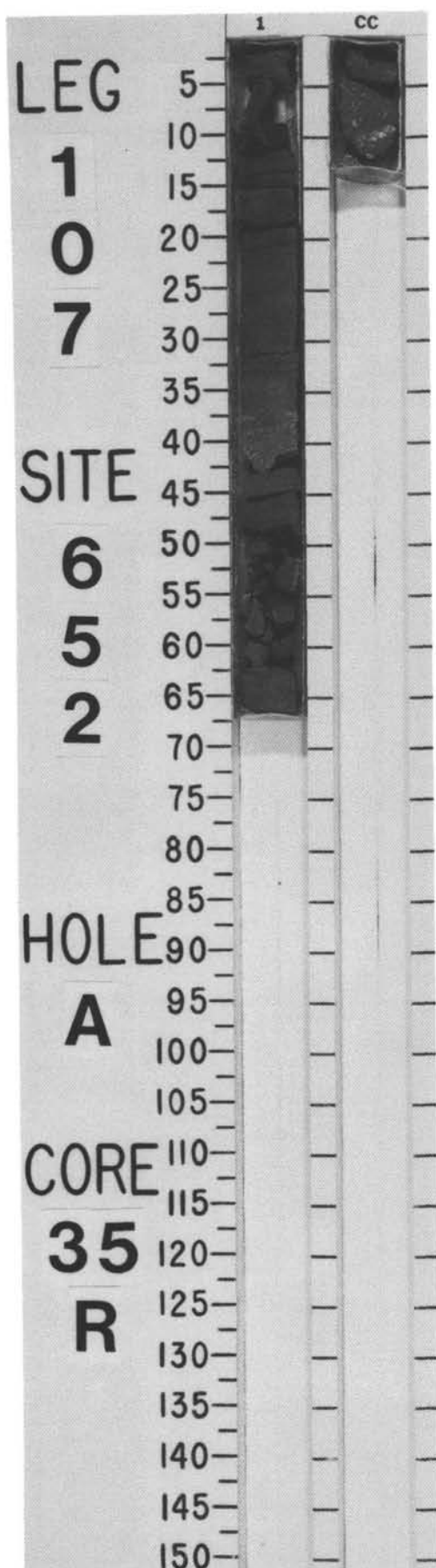


SITE 652 HOLE A CORE 35 R CORED INTERVAL 3771.0-3780.7 mbsl; 325.0-334.7 mbsf

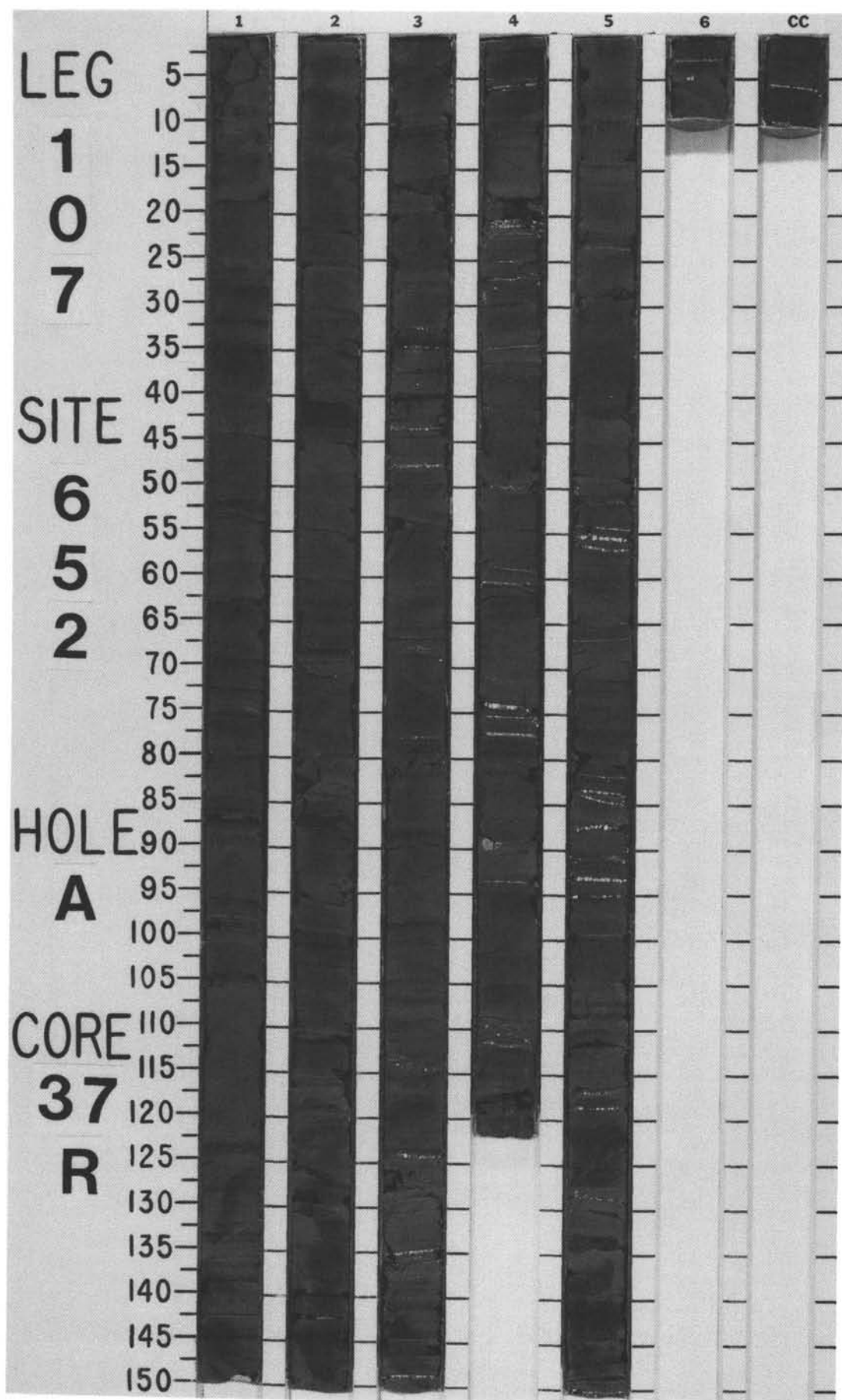
TIME-ROCK UNIT	BIOSTRAT. ZONE/ FOSSIL CHARACTER				PALEOMAGNETICS	PHYS. PROPERTIES	CHEMISTRY	SECTION	METERS	GRAPHIC LITHOLOGY	DRILLING DISTURB.	SED. STRUCTURES	SAMPLES	LITHOLOGIC DESCRIPTION
	FORAMINIFERS	NANNOFOSSILS	RADIOLARIANS	DIATOMS										
						$\gamma = 2.19 \phi = 35$			25 ●					<p>CALCAREOUS MUDSTONE, alternating with CALCAREOUS, SANDY MUDSTONE</p> <p>Calcareous mudstone, alternating with calcareous, sandy mudstone, olive (5Y 4/3) to olive-gray (5Y 5/2) or gray (10Y 4/1).</p> <p>Minor lithology: Section 1, 20-21 cm, reddish brown (5YR 4/3) interval; Section 1, 35-40 cm, mudstone with abundant white lenticular displacive crystals of calcium sulfate (gypsum); CC, calcareous mud, olive-gray (5Y 5/2), with nodules and clasts of white calcium sulfate (diameter as large as 5 mm).</p>

SITE 652 HOLE A CORE 36 R CORED INTERVAL 3780.7-3790.3 mbsl; 334.7-344.3 mbsf

TIME-ROCK UNIT	BIOSTRAT. ZONE/ FOSSIL CHARACTER				PALEOMAGNETICS	PHYS. PROPERTIES	CHEMISTRY	SECTION	METERS	GRAPHIC LITHOLOGY	DRILLING DISTURB.	SED. STRUCTURES	SAMPLES	LITHOLOGIC DESCRIPTION
	FORAMINIFERS	NANNOFOSSILS	RADIOLARIANS	DIATOMS										
								CC						<p>PEBBLES of SEDIMENTARY and LOW-GRADE METAMORPHIC ROCKS</p> <p>Pebbles 1 and 5: biocalcirudite with foraminifers.</p> <p>Pebbles 2 and 13: quartzarenite.</p> <p>Pebbles 3 and 6: biomicrite with foraminifers.</p> <p>Pebbles 4, 9, 12, and 14: biomicrite with radiolaria.</p> <p>Pebbles 7 and 10: polygenic sandstone.</p> <p>Pebble 11: low-grade calcareous phyllite.</p>

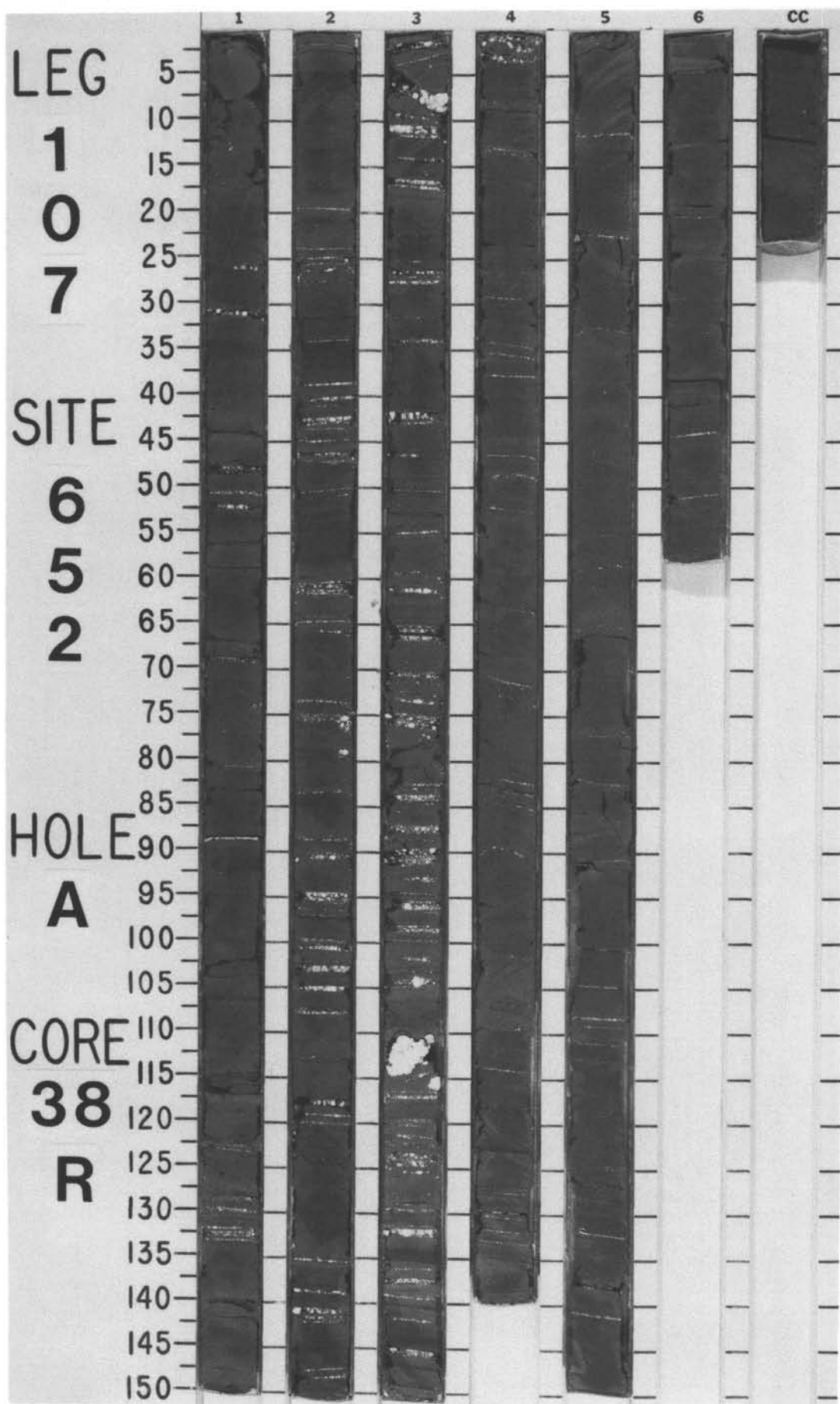


[illegible]



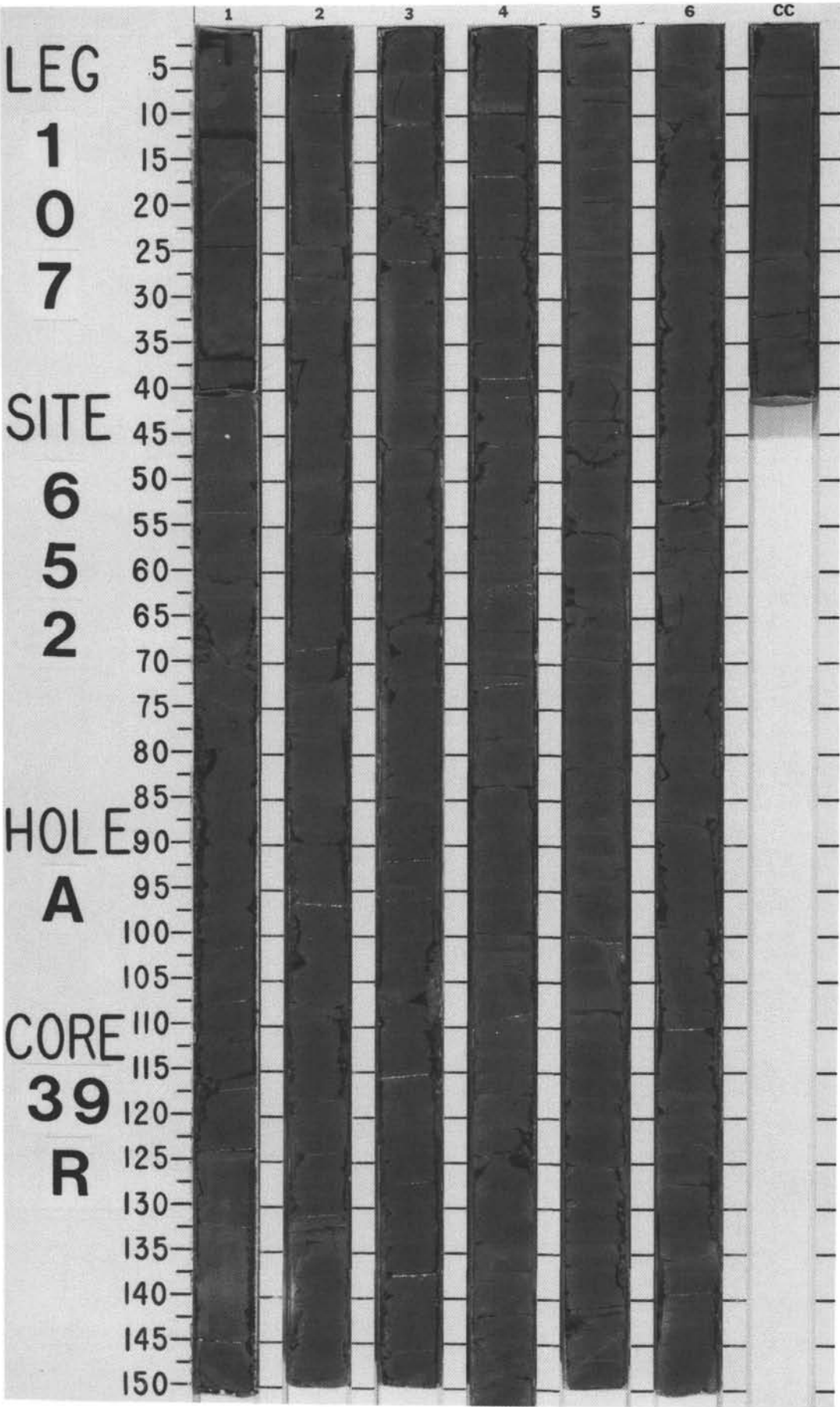
SITE 652 HOLE A CORE 38 R CORED INTERVAL 3800.0-3809.7 mbsl; 354.0-363.7 mbsf

TIME-ROCK UNIT	BIOSTRAT. ZONE/ FOSSIL CHARACTER				PALEOMAGNETICS	PHYS. PROPERTIES	CHEMISTRY	SECTION	METERS	GRAPHIC LITHOLOGY	DRILLING DISTURB.	SED. STRUCTURES	SAMPLES	LITHOLOGIC DESCRIPTION
	FORAMINIFERS	NANNOFOSSILS	RADIOLARIANS	DIATOMS										
						γ -2.28 ϕ -32 ∇ -1984 ●	19 ●	1	0.5 1.0					GYPSIFEROUS, CALCAREOUS MUDSTONE and SANDY SILTSTONE, alternating with NODULAR ANHYDRITE Gypsiferous, calcareous mudstone and sandy siltstones, alternating with nodular (chicken-wire texture) anhydrite layers. Thickness of sequences ranges from 1 to 25 cm. Sequence from top to base: Section 3, 5-7, and 110-115 cm, crystalline anhydrite with chicken-wire texture; Sections 1 and 3, olive (5Y 5/3) layered clay and mud; and Sections 4-6 and CC: black-gray (5Y 4/1) layered clay and mud and gypsum-bearing sand and silt, well-graded (fining-upward), often bedded and laminated. Basal contact is generally sharp, often scoured, black-gray (5Y 4/1), with salt and pepper texture; layers are frequently very thin (<1 cm). SMEAR SLIDE SUMMARY (%): 1, 102 3, 66 4, 100.5 M M D TEXTURE: Sand 20 — — Silt 70 12 40 Clay 10 88 60 COMPOSITION: Quartz Tr — — Mica 10 — 3 Clay 10 20 35 Calcite/dolomite 7 Tr 12 Accessory minerals 5 10 3 Limonite 3 — 2 Carbonate detritus 45 40 30 Gypsum detritus 20 30 5 Nannofossils — Tr 10
						γ -2.88 ϕ -5 ∇ -5212 ●	19 ●	2						
						γ -2.88 ϕ -5 ∇ -5212 ●	19 ●	3						
						γ -2.88 ϕ -5 ∇ -5212 ●	19 ●	4						
						γ -2.32 ϕ -30 ∇ -2040 ●	17 ●	5						
						γ -2.32 ϕ -30 ∇ -2040 ●	17 ●	6						
						γ -2.32 ϕ -30 ∇ -2040 ●	17 ●	CC						

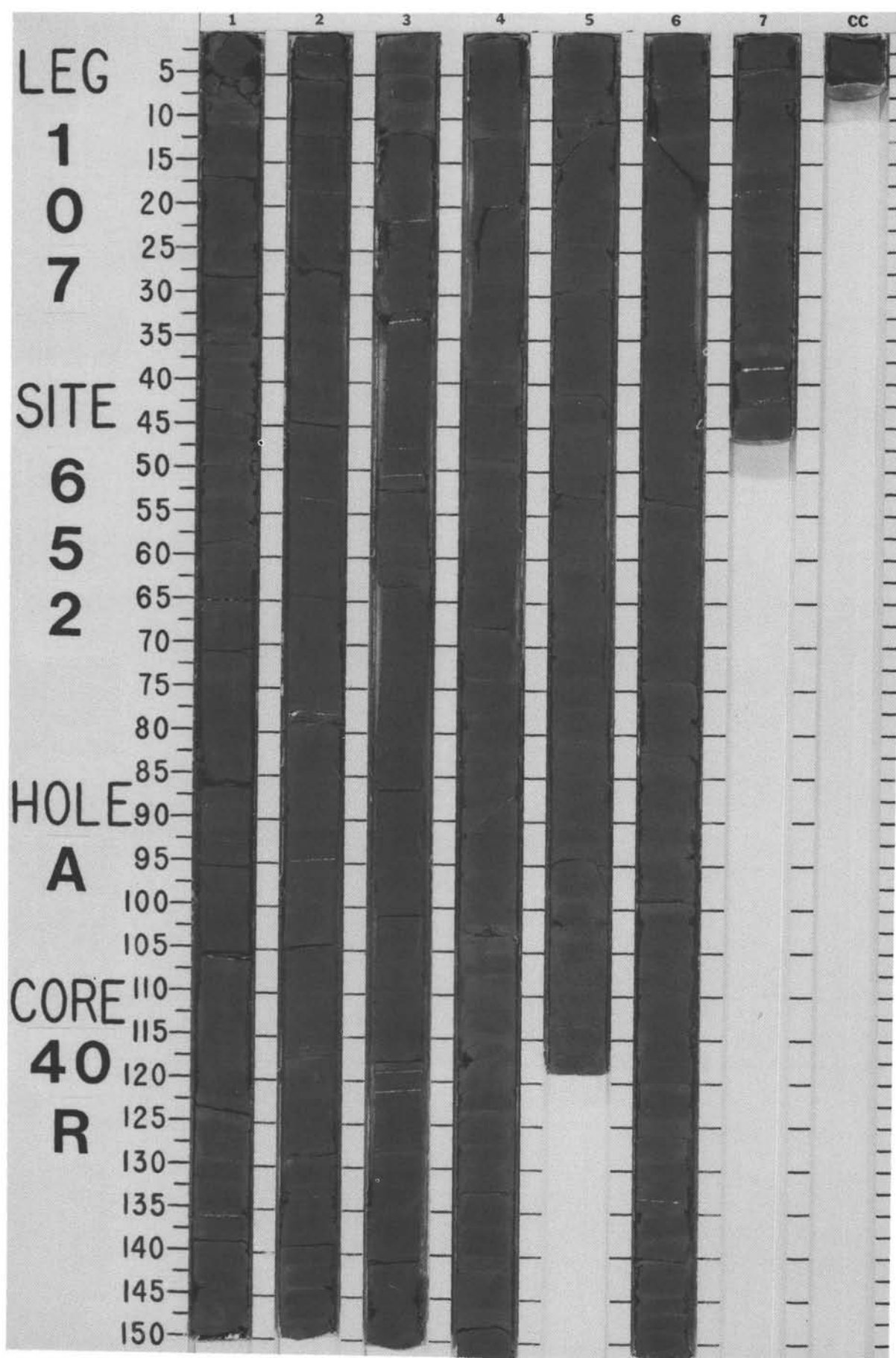


SITE 652 HOLE A CORE 39 R CORED INTERVAL 3809.7-3819.4 mbsl; 363.7-373.4 mbsf

TIME-ROCK UNIT	BIOSTRAT. ZONE/ FOSSIL CHARACTER				PALEOMAGNETICS	PHYS. PROPERTIES	CHEMISTRY	SECTION	METERS	GRAPHIC LITHOLOGY	DRILLING DISTURB.	SED. STRUCTURES	SAMPLES	LITHOLOGIC DESCRIPTION
	FORAMINIFERS	NANNOFOSSILS	RADIOLARIANS	DIATOMS										
						$\gamma = 2.22 \phi = 34 \sqrt{-1905}$	27 ●		0.5					<p>CALCAREOUS CLAYSTONE and MUDSTONE, alternating with NODULAR ANHYDRITE</p> <p>Calcareous claystone and mudstone, alternating with nodular anhydrite; succession of small sequences, ranging in thickness from 1 to 20 cm.</p> <p>Sequence from top to base: well-layered clay and mud, slightly calcareous, olive (5Y 5/2), with thin to very thin sandy, silty horizons, cross-bedded and graded (fining-upward); base is generally sharp and sometimes scoured; salt and pepper texture. Crystallized anhydrite (chicken-wire texture) occurs at the top of these sequences, but the layers are thinner (2-3 mm) and more scarce than in preceding (shallower) cores.</p> <p>SMEAR SLIDE SUMMARY (%):</p> <p style="text-align: right;">3, 80 D</p> <p>TEXTURE:</p> <p>Sand — Silt 10 Clay 90</p> <p>COMPOSITION:</p> <p>Clay 20 Volcanic glass Tr Calcite/dolomite 25 Accessory minerals 5 Carbonate detritus 27 Gypsum detritus 8 Zeolites? Tr Nannofossils 15</p>
							● 23		1.0					
								2						
							● 23	3						
								4						
								5						
								6						
						$\gamma = 2.22 \phi = 37 \sqrt{-1823}$								
								CC						

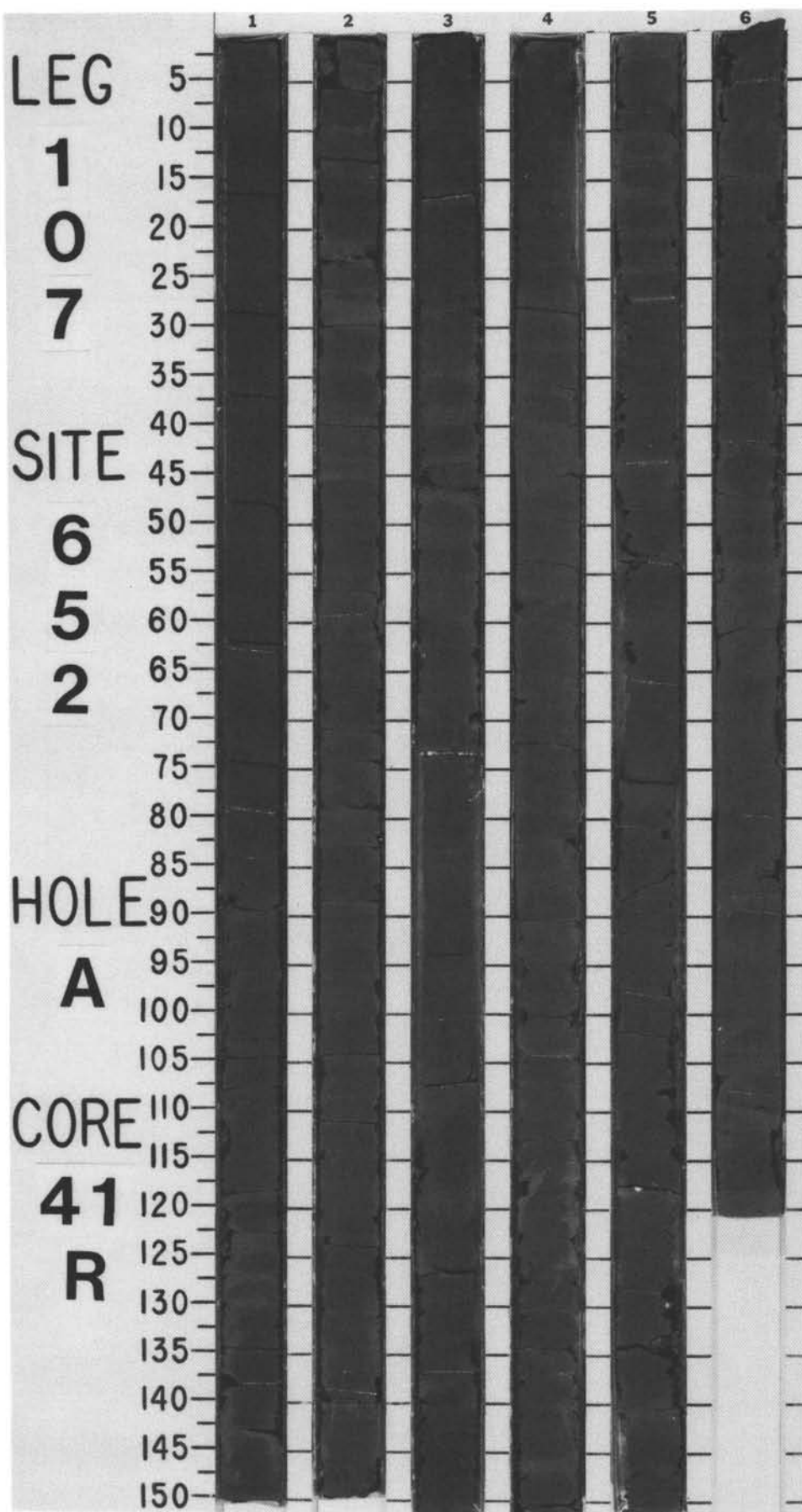


530



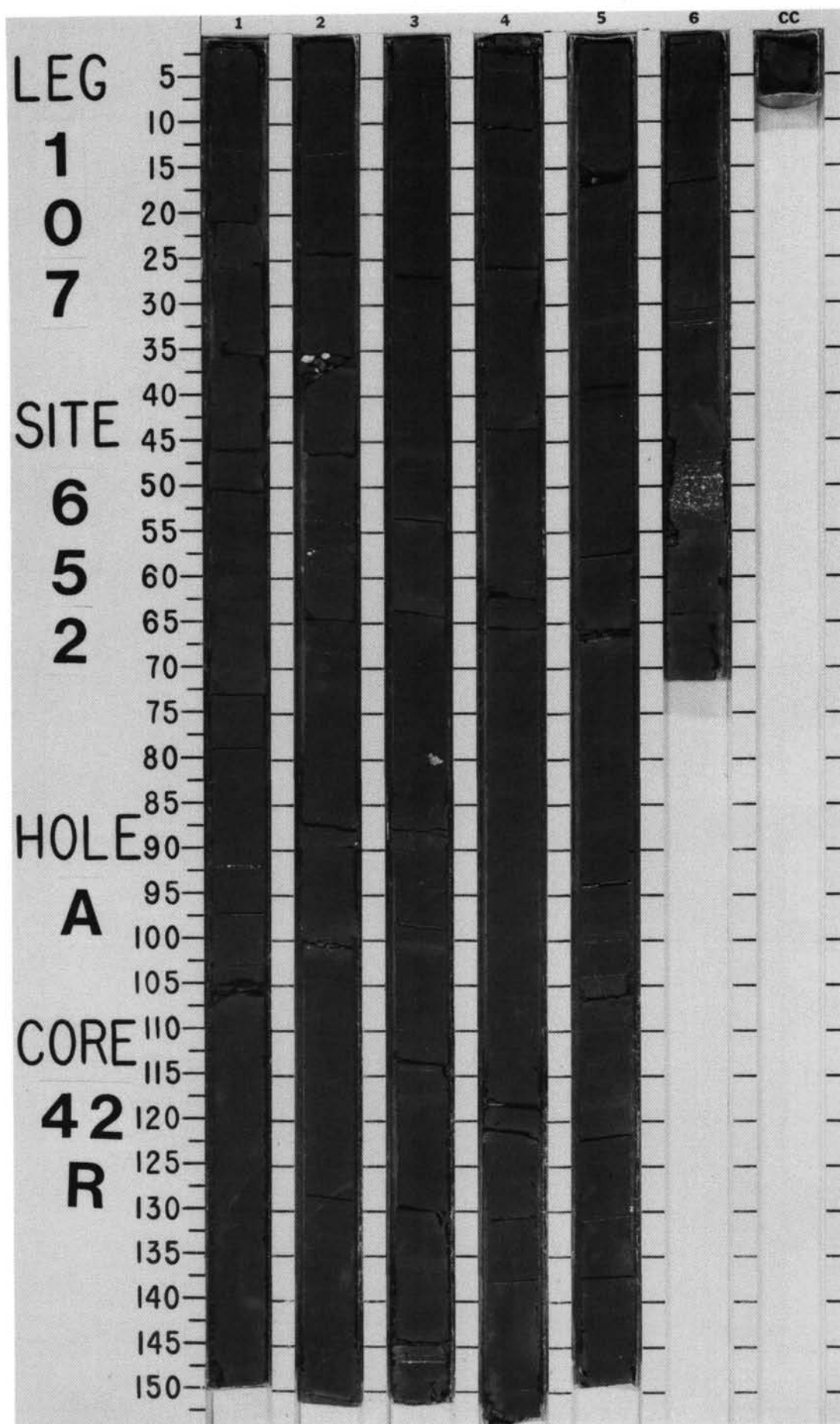
SITE 652 HOLE A CORE 41 R CORED INTERVAL 3829.0-3838.7 mbsl; 383.0-392.7 mbsf

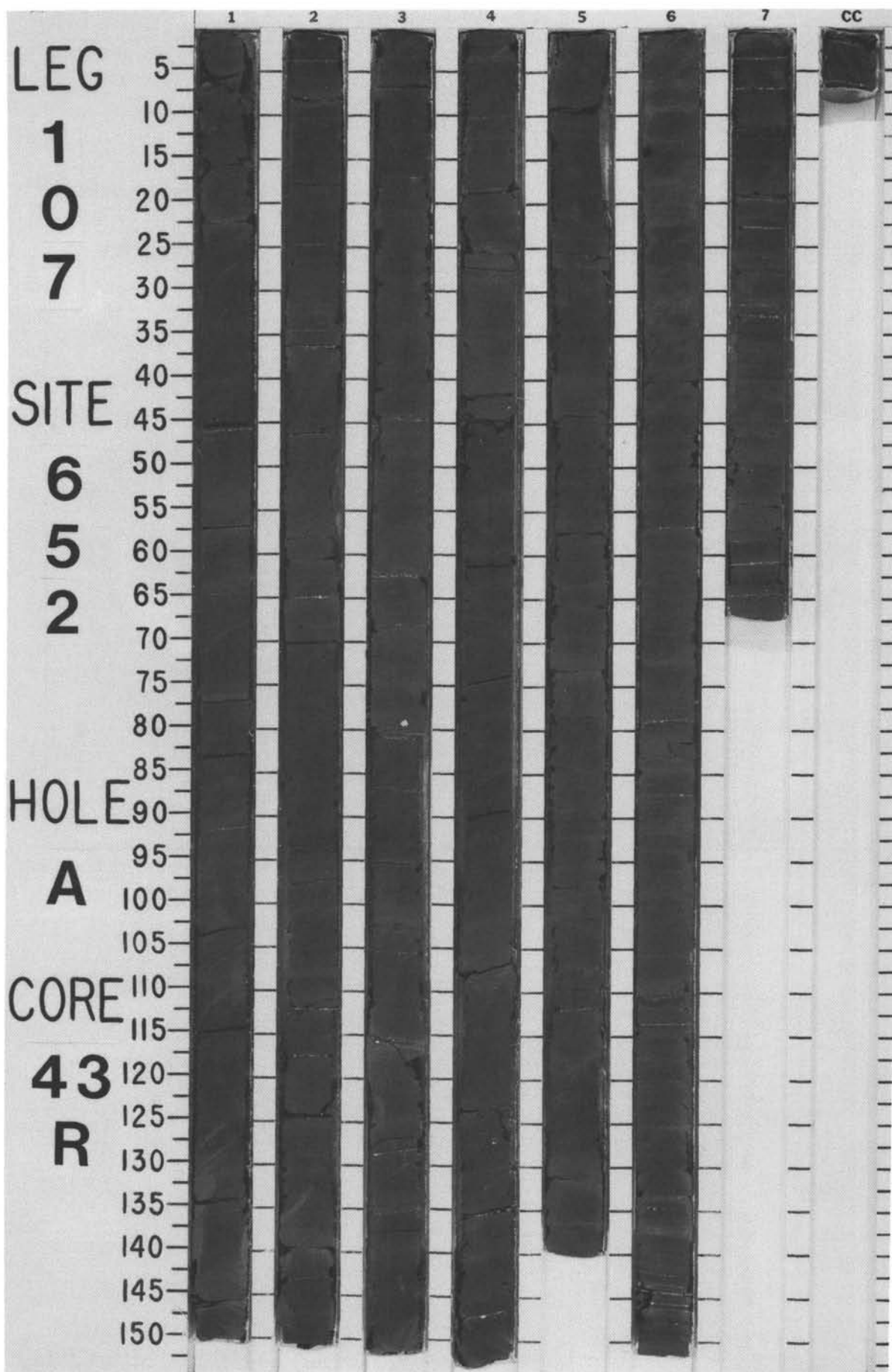
TIME-ROCK UNIT	BIOSTRAT. ZONE/ FOSSIL CHARACTER				PALEOMAGNETICS	PHYS. PROPERTIES	CHEMISTRY	SECTION	METERS	GRAPHIC LITHOLOGY	DRILLING DISTURB.	SED. STRUCTURES	SAMPLES	LITHOLOGIC DESCRIPTION
	FORAMINIFERS	NANNOFOSSILS	RADIOLARIANS	DIATOMS										
						● $\gamma=2.22$ $\phi=35$ $\sqrt{-1903}$	● 25	1	0.5 1.0					Alternations of GYPSIFEROUS, CALCAREOUS CLAYSTONE and MUDSTONE with ANHYDRITE
						● $\gamma=2.22$ $\phi=35$ $\sqrt{-1903}$	● 20	2						Monotonous succession of thin olive (5Y 4/3) sequences. The base of each sequence is represented by thin (3 mm) layers of graded, gypsiferous, sandy silt; the top shows layered silty mudstone. Between sequences a thin interval of white chicken-wire anhydrite sometimes occurs.
								3						SMEAR SLIDE SUMMARY (%):
														5, 78 D
								4						TEXTURE:
														Sand 10
														Silt 90
														Clay —
														COMPOSITION:
														Quartz Tr
														Clay 50
														Calcite/dolomite 5
														Accessory minerals 5
														Gypsum detritus 25
														Limonite 5
														Nannofossils 15
						● $\gamma=2.27$ $\phi=33$ $\sqrt{-1963}$	● 23	5					*	
								6						



SITE 652 HOLE A CORE 42 R CORED INTERVAL 3838.7-3848.4 mbsl; 392.7-402.4 mbsf

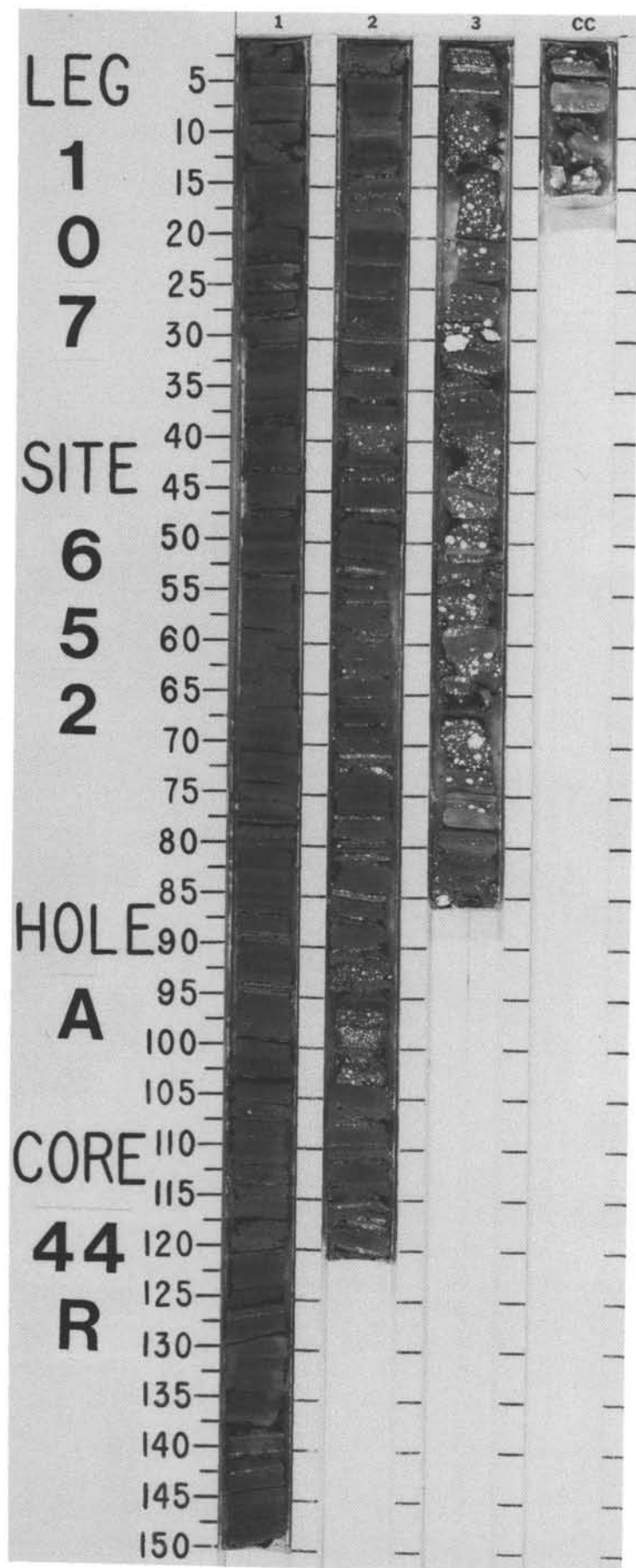
TIME-ROCK UNIT	BIOSTRAT. ZONE/ FOSSIL CHARACTER				PALEOMAGNETICS	PHYS. PROPERTIES	CHEMISTRY	SECTION	METERS	GRAPHIC LITHOLOGY	DRILLING DISTURB.	SED. STRUCTURES	SAMPLES	LITHOLOGIC DESCRIPTION																								
	FORAMINIFERS	NANNOFOSSILS	RADIOLARIANS	DIATOMS																																		
						● $\gamma=2.30$ $\phi=35$ $V=2095$	● 13	1	0.5 1.0					GYPSIFEROUS, CALCAREOUS MUDSTONE with NODULAR ANHYDRITE INTERCALATIONS																								
								2						Parallel-laminated gypsiferous, calcareous mudstone with discrete 1–2-mm thick laminae of white anhydrite. Sulfate layers are composed of tiny coalescing nodules. Matrix material is included in nodule layers and outlines surfaces; texture suggests that nodules are growing in the sediments. Large nodules (0.5–1-cm) are found in Section 2, 35–37 and 56–58 cm, and in Section 3, 80–82 cm; numerous small nodules (1–5-mm diameter) are found in Section 6, 40–55 cm, with a concentration toward the middle of the graded bed.																								
							● 30	3			ww	*		Minor lithology: finely-laminated sediments contain rare coarser (siltier) intervals, some showing normal grading; Section 4, some 1-mm-thick light reddish brown laminae; inorganic calcite component in core is recrystallized.																								
								4						Apparent dip: Section 1, 0–7°; Section 2, 7–8°; Section 3, 5–7°; Section 4, 6–7°; Section 5, 7–8°; Section 6, 6–8°.																								
							● 38	5						SMEAR SLIDE SUMMARY (%):																								
								6						<table><tr><td></td><td>3, 61</td><td>6, 47</td></tr><tr><td></td><td>D</td><td>M</td></tr></table>		3, 61	6, 47		D	M																		
	3, 61	6, 47																																				
	D	M																																				
							● 16	6					*	TEXTURE:																								
														<table><tr><td>Sand</td><td>—</td><td>10</td></tr><tr><td>Silt</td><td>20</td><td>20</td></tr><tr><td>Clay</td><td>80</td><td>70</td></tr></table>	Sand	—	10	Silt	20	20	Clay	80	70															
Sand	—	10																																				
Silt	20	20																																				
Clay	80	70																																				
														COMPOSITION:																								
														<table><tr><td>Quartz</td><td>2</td><td>10</td></tr><tr><td>Clay</td><td>60</td><td>50</td></tr><tr><td>Calcite</td><td>15</td><td>15</td></tr><tr><td>Dolomite</td><td>5</td><td>—</td></tr><tr><td>Accessory minerals</td><td>3</td><td>2</td></tr><tr><td>Gypsum</td><td>15</td><td>15</td></tr><tr><td>Opaques</td><td>—</td><td>3</td></tr><tr><td>Nannofossils</td><td>—</td><td>5</td></tr></table>	Quartz	2	10	Clay	60	50	Calcite	15	15	Dolomite	5	—	Accessory minerals	3	2	Gypsum	15	15	Opaques	—	3	Nannofossils	—	5
Quartz	2	10																																				
Clay	60	50																																				
Calcite	15	15																																				
Dolomite	5	—																																				
Accessory minerals	3	2																																				
Gypsum	15	15																																				
Opaques	—	3																																				
Nannofossils	—	5																																				





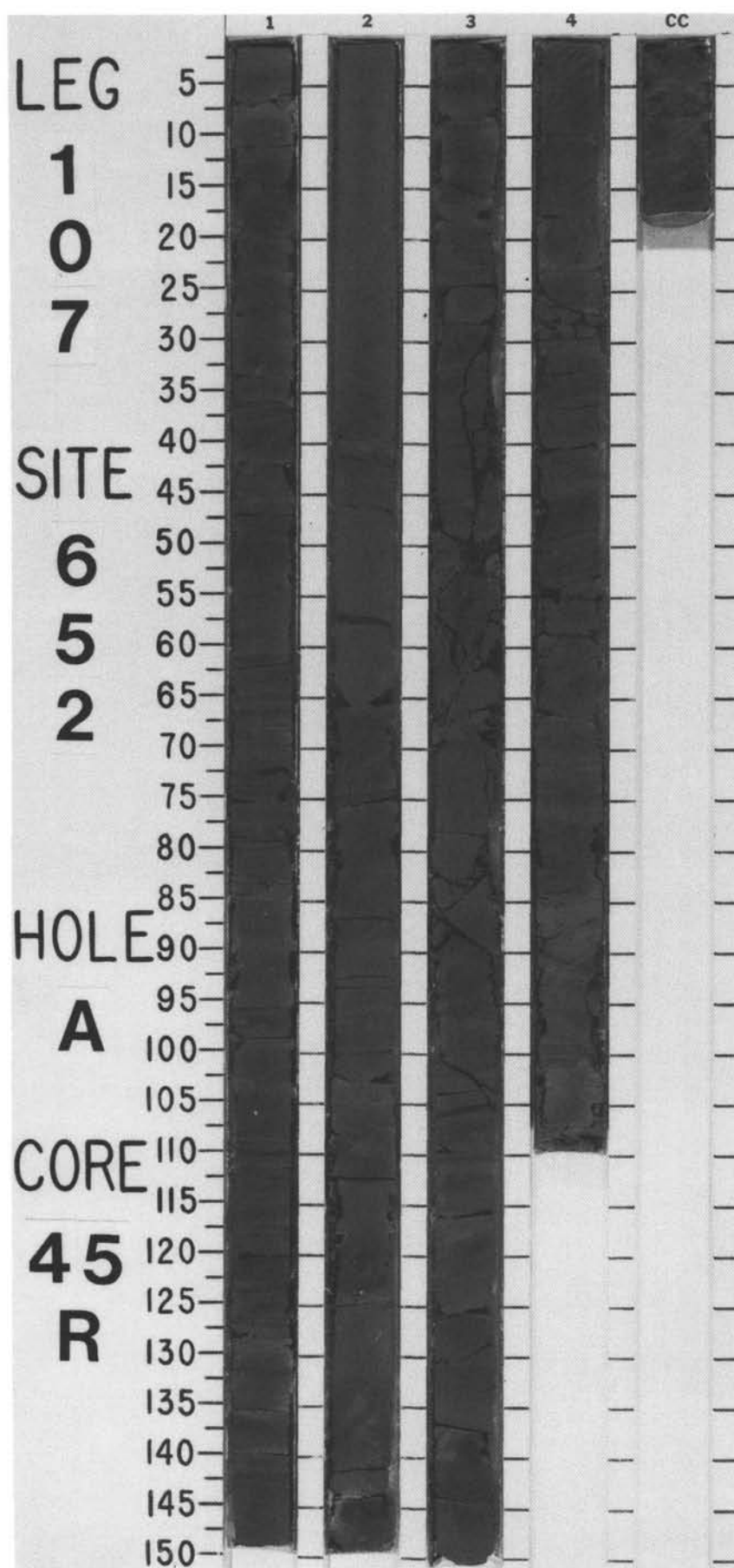
SITE 652 HOLE A CORE 44 R CORED INTERVAL 3858.1-3867.8 mbsl; 412.1-421.8 mbsf

TIME- ROCK UNIT	BIOSTRAT. ZONE/ FOSSIL CHARACTER				PALEOMAGNETICS	PHYS. PROPERTIES	CHEMISTRY	SECTION	METERS	GRAPHIC LITHOLOGY	DRILLING DISTURB.	SED. STRUCTURES	SAMPLES	LITHOLOGIC DESCRIPTION																																																																												
	FORAMINIFERS	NANNOFOSSILS	RADIOLARIANS	DIATOMS																																																																																						
						● 27			0.5				*	<p>GYPSEIFEROUS, CALCAREOUS CLAYSTONE, MUDSTONE, and NODULAR GYPSUM and ANHYDRITE</p> <p>Alternating parallel (varvelike) laminations (2 mm to 2 cm thick) of gypsiferous, calcareous claystone and mudstone in varying colors, olive-gray (5Y 5/2) to gray (5Y 5/1), dark gray (5Y 4/1), reddish brown (5YR 4/4, 5/3), dark grayish brown (10YR 4/2), and dark yellowish brown (10YR 4/4). Nodular gypsum and anhydrite layers (0.5–5 cm) and scattered nodules occur throughout.</p> <p>Minor lithology: below Section 2, 30 cm, the number and thickness of gypsum and anhydrite laminae as well as frequency of the nodules increases downsection; Section 3, 20–80 cm, finely-laminated microcrystalline gypsum and anhydrite, which has been deformed by later growth of gypsum and anhydrite nodules; laminae are displaced and appear to drape around nodules; Section 3, 49–51 cm, presence of anhydrite as well as authigenic feldspars was identified in a 2-cm-thick sandy mudstone layer; Section 2, 41 cm, micronodules of possible pyrite were identified in mudstone.</p> <p>Apparent dip: drilling deformation (biscuits) prevented measurement.</p> <p>SMEAR SLIDE SUMMARY (%):</p> <table><tr><td></td><td>1, 49</td><td>2, 41</td><td>3, 49</td></tr><tr><td></td><td>D</td><td>M</td><td>M</td></tr></table> <p>TEXTURE:</p> <table><tr><td>Sand</td><td>—</td><td>10</td><td>20</td></tr><tr><td>Silt</td><td>5</td><td>25</td><td>30</td></tr><tr><td>Clay</td><td>95</td><td>65</td><td>50</td></tr></table> <p>COMPOSITION:</p> <table><tr><td>Quartz</td><td>10</td><td>15</td><td>—</td></tr><tr><td>Feldspar (authigenic)</td><td>—</td><td>—</td><td>35</td></tr><tr><td>Mica</td><td>—</td><td>Tr</td><td>—</td></tr><tr><td>Clay</td><td>51</td><td>50</td><td>38</td></tr><tr><td>Calcite</td><td>10</td><td>5</td><td>—</td></tr><tr><td>Dolomite</td><td>1</td><td>1</td><td>—</td></tr><tr><td>Accessory minerals</td><td>—</td><td>3</td><td>—</td></tr><tr><td>Gypsum</td><td>25</td><td>20</td><td>2</td></tr><tr><td>Opakes (& micronodules)</td><td>—</td><td>3</td><td>—</td></tr><tr><td>Halite</td><td>—</td><td>1</td><td>—</td></tr><tr><td>Foraminifers</td><td>—</td><td>2</td><td>—</td></tr><tr><td>Nannofossils</td><td>3</td><td>—</td><td>—</td></tr><tr><td>Fish remains</td><td>—</td><td>—</td><td>Tr</td></tr><tr><td>Anhydrite</td><td>—</td><td>—</td><td>25</td></tr></table>		1, 49	2, 41	3, 49		D	M	M	Sand	—	10	20	Silt	5	25	30	Clay	95	65	50	Quartz	10	15	—	Feldspar (authigenic)	—	—	35	Mica	—	Tr	—	Clay	51	50	38	Calcite	10	5	—	Dolomite	1	1	—	Accessory minerals	—	3	—	Gypsum	25	20	2	Opakes (& micronodules)	—	3	—	Halite	—	1	—	Foraminifers	—	2	—	Nannofossils	3	—	—	Fish remains	—	—	Tr	Anhydrite	—	—	25
	1, 49	2, 41	3, 49																																																																																							
	D	M	M																																																																																							
Sand	—	10	20																																																																																							
Silt	5	25	30																																																																																							
Clay	95	65	50																																																																																							
Quartz	10	15	—																																																																																							
Feldspar (authigenic)	—	—	35																																																																																							
Mica	—	Tr	—																																																																																							
Clay	51	50	38																																																																																							
Calcite	10	5	—																																																																																							
Dolomite	1	1	—																																																																																							
Accessory minerals	—	3	—																																																																																							
Gypsum	25	20	2																																																																																							
Opakes (& micronodules)	—	3	—																																																																																							
Halite	—	1	—																																																																																							
Foraminifers	—	2	—																																																																																							
Nannofossils	3	—	—																																																																																							
Fish remains	—	—	Tr																																																																																							
Anhydrite	—	—	25																																																																																							
						● 22			1.0				*																																																																													
								2					*																																																																													
								3					*																																																																													
								CC					OG																																																																													



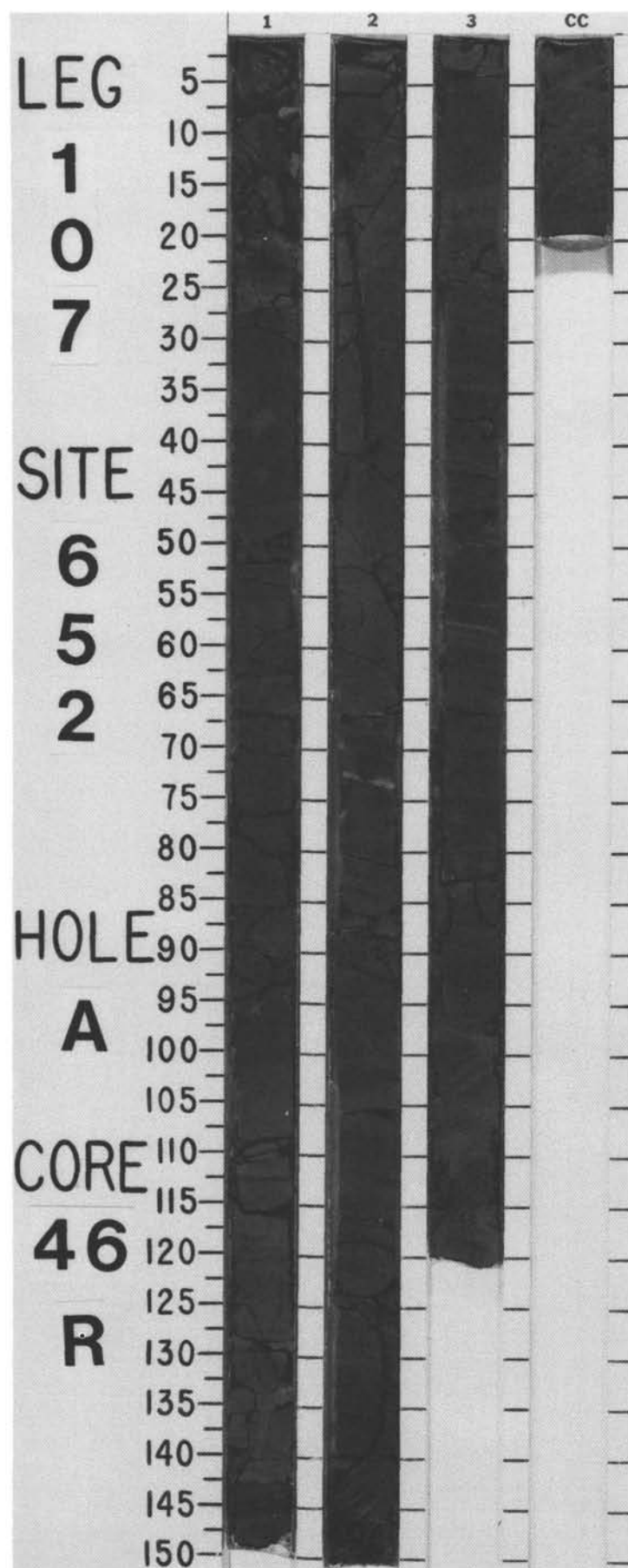
SITE 652 HOLE A CORE 45 R CORED INTERVAL 3867.8-3877.5 mbsl 421.8-431.5 mbsf

TIME-ROCK UNIT	BIOSTRAT. ZONE/ FOSSIL CHARACTER				PALEOMAGNETICS	PHYS. PROPERTIES	CHEMISTRY	SECTION	METERS	GRAPHIC LITHOLOGY	DRILLING DISTURB.	SED. STRUCTURES	SAMPLES	LITHOLOGIC DESCRIPTION																																																																				
	FORAMINIFERS	NANNOFOSSILS	RADIOLARIANS	DIATOMS																																																																														
						$\gamma = 2.32 \phi = 33$ $\gamma = 2.100$ $\gamma = 2.54 \phi = 22$ $\gamma = 3080$	$\phi = 43$ 22	1	0.5 1.0					<p>CALCAREOUS CLAYSTONE, alternating with SANDY, CALCAREOUS MUDSTONE</p> <p>Calcareous claystone (2-4 cm thick), alternating with sandy, calcareous mudstone (2 mm-1 cm thick), gray (5Y 5/1), olive-gray (5Y 4/2), pale olive (5Y 6/3), and dark gray (5Y 4/2). Sandy mudstone displays many primary sedimentary structures: cross-laminations, current ripples with mud drapes, normal and reverse grading, slumps, fine parallel laminations, and scours.</p> <p>Minor lithology: no evidence of evaporites, although gypsum is a common constituent in smear slides; inorganic calcite is partially recrystallized. Pyrite spherules and plant debris are associated with finely laminated intervals, rich in black particles, in Section 3, 8-10, 67-70, and 102-115 cm.</p> <p>Apparent dip: Section 1, 0-3°; Section 2, 0-3°; Section 3, 116-150 cm, 12°; Section 4, 40-53 cm, 15°.</p> <p>SMEAR SLIDE SUMMARY (%):</p> <table><tr><td></td><td>2, 85 D</td><td>3, 65 M</td><td>3, 105 M</td></tr></table> <p>TEXTURE:</p> <table><tr><td>Sand</td><td>—</td><td>25</td><td>2</td></tr><tr><td>Silt</td><td>5</td><td>25</td><td>15</td></tr><tr><td>Clay</td><td>95</td><td>50</td><td>83</td></tr></table> <p>COMPOSITION:</p> <table><tr><td>Quartz</td><td>10</td><td>15</td><td>10</td></tr><tr><td>Feldspar</td><td>—</td><td>—</td><td>1</td></tr><tr><td>Mica</td><td>—</td><td>—</td><td>1</td></tr><tr><td>Clay</td><td>40</td><td>30</td><td>—</td></tr><tr><td>Calcite</td><td>30</td><td>35</td><td>30</td></tr><tr><td>Dolomite</td><td>2</td><td>3</td><td>2</td></tr><tr><td>Accessory minerals</td><td>2</td><td>2</td><td>2</td></tr><tr><td>Gypsum</td><td>8</td><td>8</td><td>15</td></tr><tr><td>Anhydrite</td><td>—</td><td>2</td><td>—</td></tr><tr><td>Pyrite</td><td>—</td><td>1</td><td>—</td></tr><tr><td>Nannofossils</td><td>8</td><td>3</td><td>3</td></tr><tr><td>Plant debris</td><td>—</td><td>1</td><td>—</td></tr><tr><td>Opaques (pyrite spherules + organic matter (plant debris?), Unidentified</td><td>—</td><td>—</td><td>4</td></tr></table>		2, 85 D	3, 65 M	3, 105 M	Sand	—	25	2	Silt	5	25	15	Clay	95	50	83	Quartz	10	15	10	Feldspar	—	—	1	Mica	—	—	1	Clay	40	30	—	Calcite	30	35	30	Dolomite	2	3	2	Accessory minerals	2	2	2	Gypsum	8	8	15	Anhydrite	—	2	—	Pyrite	—	1	—	Nannofossils	8	3	3	Plant debris	—	1	—	Opaques (pyrite spherules + organic matter (plant debris?), Unidentified	—	—	4
	2, 85 D	3, 65 M	3, 105 M																																																																															
Sand	—	25	2																																																																															
Silt	5	25	15																																																																															
Clay	95	50	83																																																																															
Quartz	10	15	10																																																																															
Feldspar	—	—	1																																																																															
Mica	—	—	1																																																																															
Clay	40	30	—																																																																															
Calcite	30	35	30																																																																															
Dolomite	2	3	2																																																																															
Accessory minerals	2	2	2																																																																															
Gypsum	8	8	15																																																																															
Anhydrite	—	2	—																																																																															
Pyrite	—	1	—																																																																															
Nannofossils	8	3	3																																																																															
Plant debris	—	1	—																																																																															
Opaques (pyrite spherules + organic matter (plant debris?), Unidentified	—	—	4																																																																															
								2																																																																										
								3																																																																										
								4																																																																										
								CC																																																																										



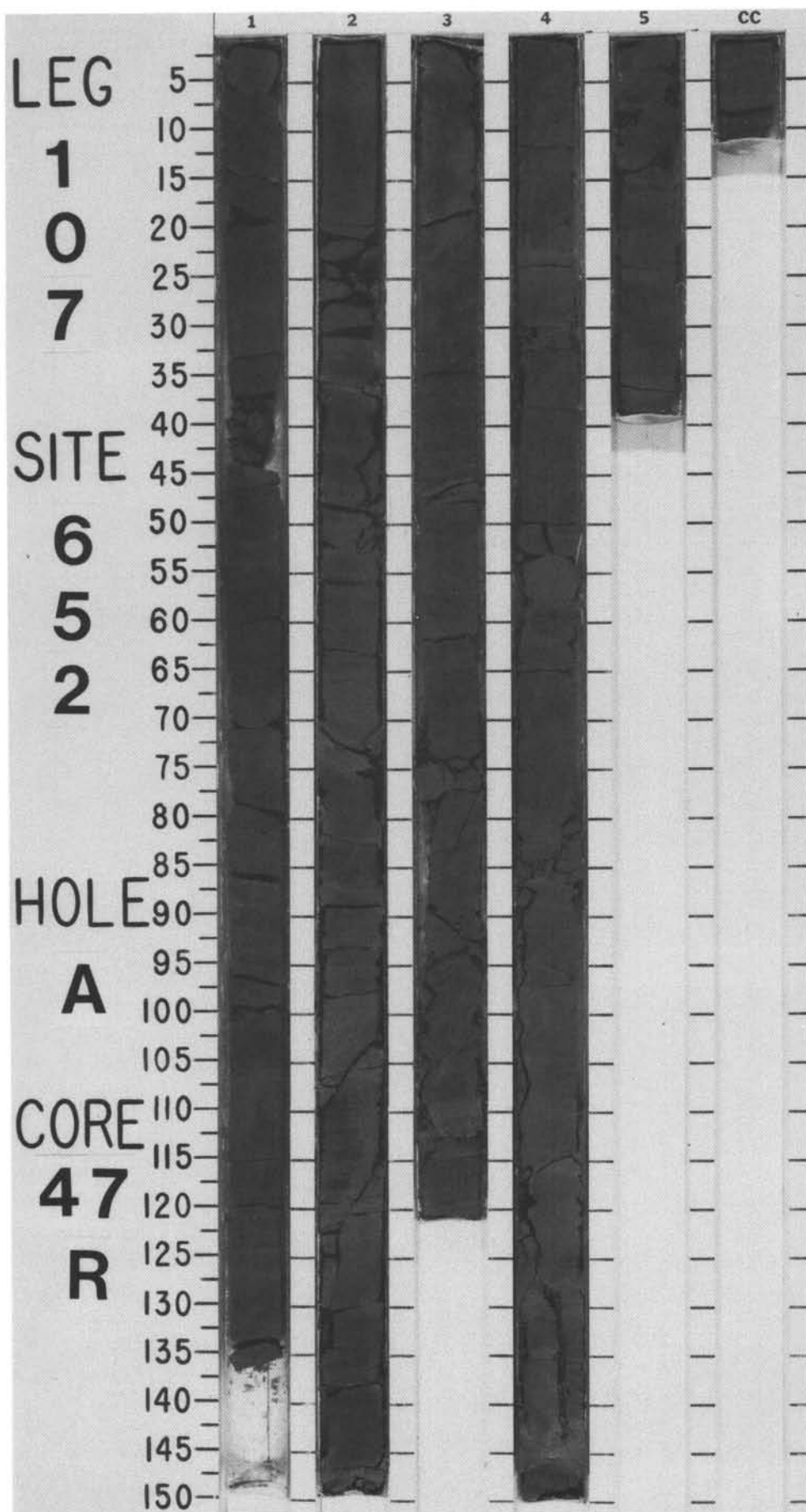
SITE 652 HOLE A CORE 46 R CORED INTERVAL 3877.5-3887.1 mbsl; 431.5-441.1 mbsf

TIME-ROCK UNIT	BIOSTRAT. ZONE/ FOSSIL CHARACTER				PALEOMAGNETICS	PHYS. PROPERTIES	CHEMISTRY	SECTION	METERS	GRAPHIC LITHOLOGY	DRILLING DISTURB.	SED. STRUCTURES	SAMPLES	LITHOLOGIC DESCRIPTION
	FORAMINIFERS	NANNOFOSSILS	RADIOLARIANS	DIAATOMS										



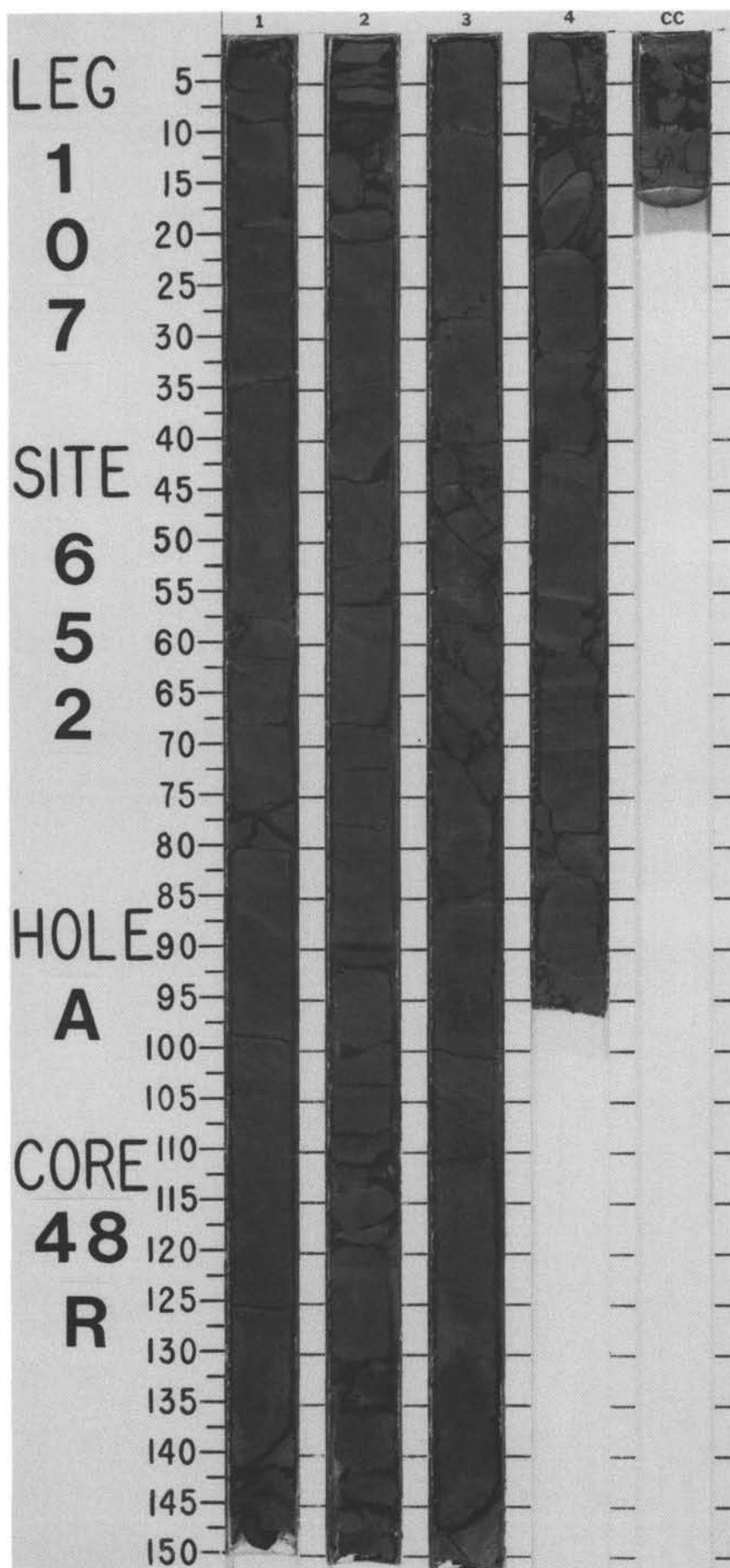
SITE 652 HOLE A CORE 47 R CORED INTERVAL 3887.1-3896.7 mbsl; 441.1-450.7 mbsf

TIME-ROCK UNIT	BIOSTRAT. ZONE/ FOSSIL CHARACTER			PALEOMAGNETICS	PHYS. PROPERTIES	CHEMISTRY	SECTION	METERS	GRAPHIC LITHOLOGY	DRILLING DISTURB.	SED. STRUCTURES	SAMPLES	LITHOLOGIC DESCRIPTION																																																								
	FORAMINIFERS	NANNOFOSSILS	RADIOLARIANS											DIATOMS																																																							
					$\gamma = 2.36 \phi = 29 \sqrt{-2197}$	24 ●	1	0.5 1.0			*		<p>GYPSEIFEROUS, CALCAREOUS, SILTY SANDSTONE; CLAYSTONE; and MUDSTONE</p> <p>Succession of detrital sequences of sandstone, claystone, and laminated mudstone. Sandstone and claystone are grayish brown (2/5Y 5/2), graded and laminated, often cross-bedded. Mudstone is reddish brown and laminated. Water escape structures are common. Coarsening-upward sequences occur randomly.</p> <p>Minor lithology: Section 1, 52 cm, deep (1 cm) scour structure; Section 3, 80 cm, small, tensional syn-sedimentary fault; Section 1, 95 cm, and Section 2, 120-130 cm, gypsum micronodules.</p> <p>Apparent dip: about 5°.</p> <p>SMEAR SLIDE SUMMARY (%):</p> <table><tr><td></td><td>1, 86</td><td>3, 100</td><td>4, 56</td></tr><tr><td>D</td><td>D</td><td>D</td><td>M</td></tr></table> <p>TEXTURE:</p> <table><tr><td>Sand</td><td>60</td><td>—</td><td>—</td></tr><tr><td>Silt</td><td>30</td><td>5</td><td>20</td></tr><tr><td>Clay</td><td>10</td><td>95</td><td>80</td></tr></table> <p>COMPOSITION:</p> <table><tr><td>Mica</td><td>5</td><td>—</td><td>10</td></tr><tr><td>Clay</td><td>8</td><td>60</td><td>40</td></tr><tr><td>Volcanic glass</td><td>2</td><td>—</td><td>—</td></tr><tr><td>Calcite/dolomite</td><td>—</td><td>Tr</td><td>—</td></tr><tr><td>Opaques</td><td>5</td><td>5</td><td>—</td></tr><tr><td>Gypsum detritus</td><td>45</td><td>5</td><td>30</td></tr><tr><td>Carbonate detritus</td><td>25</td><td>20</td><td>20</td></tr><tr><td>Nannofossils</td><td>10</td><td>10</td><td>—</td></tr><tr><td>Fish remains</td><td>Tr</td><td>—</td><td>—</td></tr></table>		1, 86	3, 100	4, 56	D	D	D	M	Sand	60	—	—	Silt	30	5	20	Clay	10	95	80	Mica	5	—	10	Clay	8	60	40	Volcanic glass	2	—	—	Calcite/dolomite	—	Tr	—	Opaques	5	5	—	Gypsum detritus	45	5	30	Carbonate detritus	25	20	20	Nannofossils	10	10	—	Fish remains	Tr	—	—
	1, 86	3, 100	4, 56																																																																		
D	D	D	M																																																																		
Sand	60	—	—																																																																		
Silt	30	5	20																																																																		
Clay	10	95	80																																																																		
Mica	5	—	10																																																																		
Clay	8	60	40																																																																		
Volcanic glass	2	—	—																																																																		
Calcite/dolomite	—	Tr	—																																																																		
Opaques	5	5	—																																																																		
Gypsum detritus	45	5	30																																																																		
Carbonate detritus	25	20	20																																																																		
Nannofossils	10	10	—																																																																		
Fish remains	Tr	—	—																																																																		
					$\gamma = 2.48 \phi = 24 \sqrt{-2578}$	● 15	2																																																														
						● 38	3																																																														
							4																																																														
							5																																																														



SITE 652 HOLE A CORE 48 R CORED INTERVAL 3896.7-3906.3 mbsl; 450.7-460.3 mbsf

TIME-ROCK UNIT	BIOSTRAT. ZONE/ FOSSIL CHARACTER				PALEOMAGNETICS	PHYS. PROPERTIES	CHEMISTRY	SECTION	METERS	GRAPHIC LITHOLOGY	DRILLING DISTURB.	SED. STRUCTURES	SAMPLES	LITHOLOGIC DESCRIPTION
	FORAMINIFERS	NANNOFOSSILS	RADIOLARIANS	DIATOMS										
						$\gamma = 2.36 \phi = 32 V = 2301$	36	1	0.5 1.0					<p>CALCAREOUS, GYPSIFEROUS MUDSTONE, alternating with SANDY MUDSTONE</p> <p>Calcareous, gypsiferous mudstone, alternating with sandy/silty mudstone. Calcareous mudstone is reddish brown (5YR 5/3); sandy/silty layers are graded (both fining- and coarsening-upward grading), cross-laminated (high angle), and olive-gray (5Y 5/2). Dewatering structures are common, observed in Section 1, 20-60 and 100-110 cm, and Section 3, 10-40, 60-90, and 100-120 cm; sediments are brecciated due to dewatering in Section 3, 100-120 cm.</p> <p>SMEAR SLIDE SUMMARY (%):</p> <p style="text-align: right;">2, 10 M</p> <p>TEXTURE:</p> <p>Sand 5 Silt 60 Clay 35</p> <p>COMPOSITION:</p> <p>Mica Tr Clay 40 Volcanic glass Tr Calcite/dolomite 8 Gypsum detritus 12 Carbonate detritus 40 Zeolites Tr Nannofossils Tr</p>
						$\gamma = 2.46 \phi = 25$	18	2				*		
							31	3						
								4						
								CC						

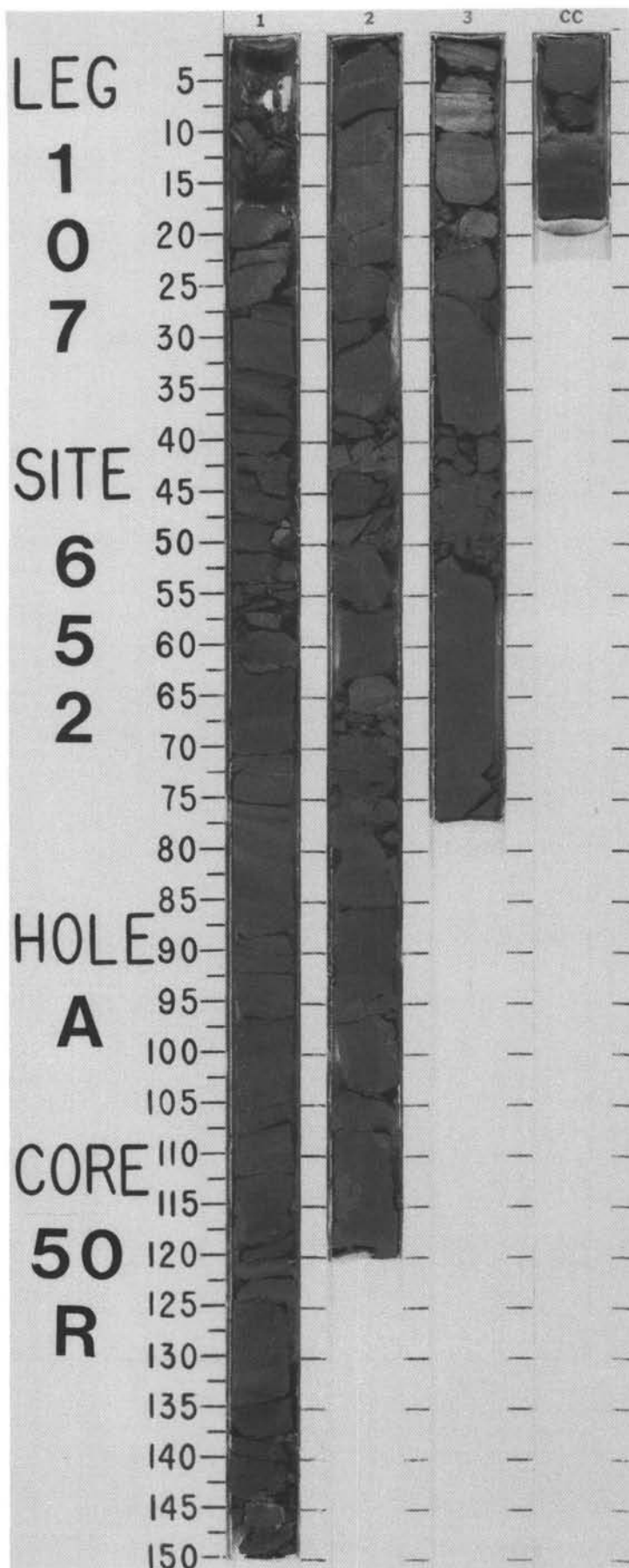
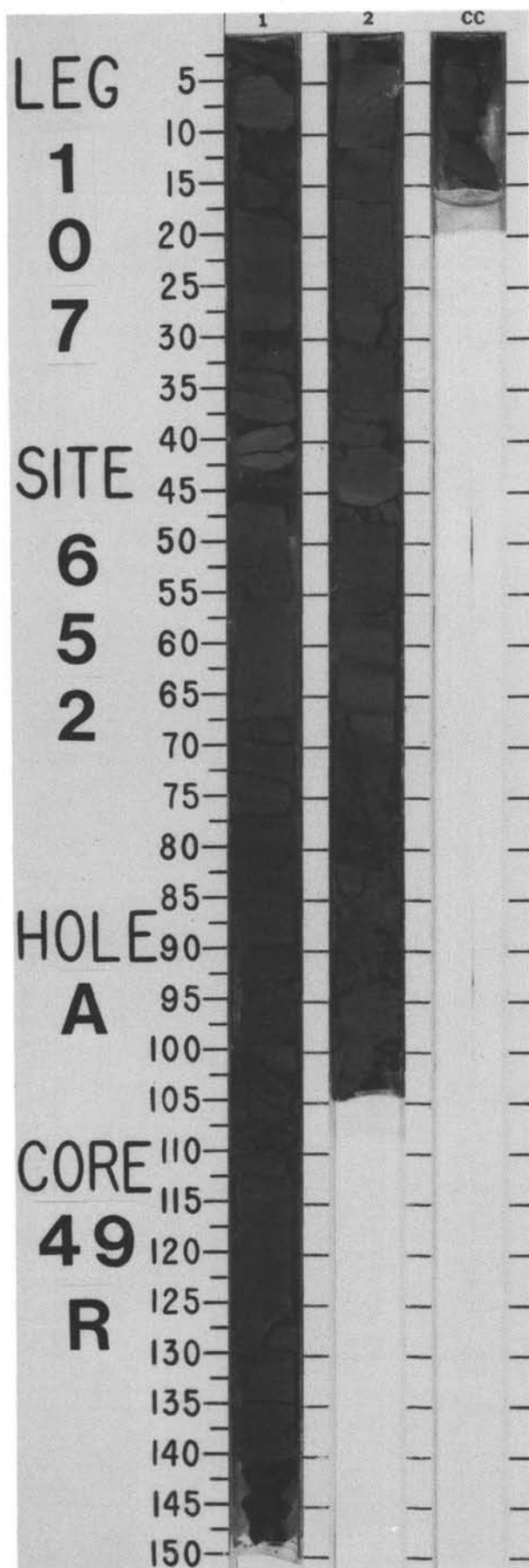


SITE 652 HOLE A CORE 49 R CORED INTERVAL 3906.3-3916.0 mbsl; 460.3-470.0 mbsf

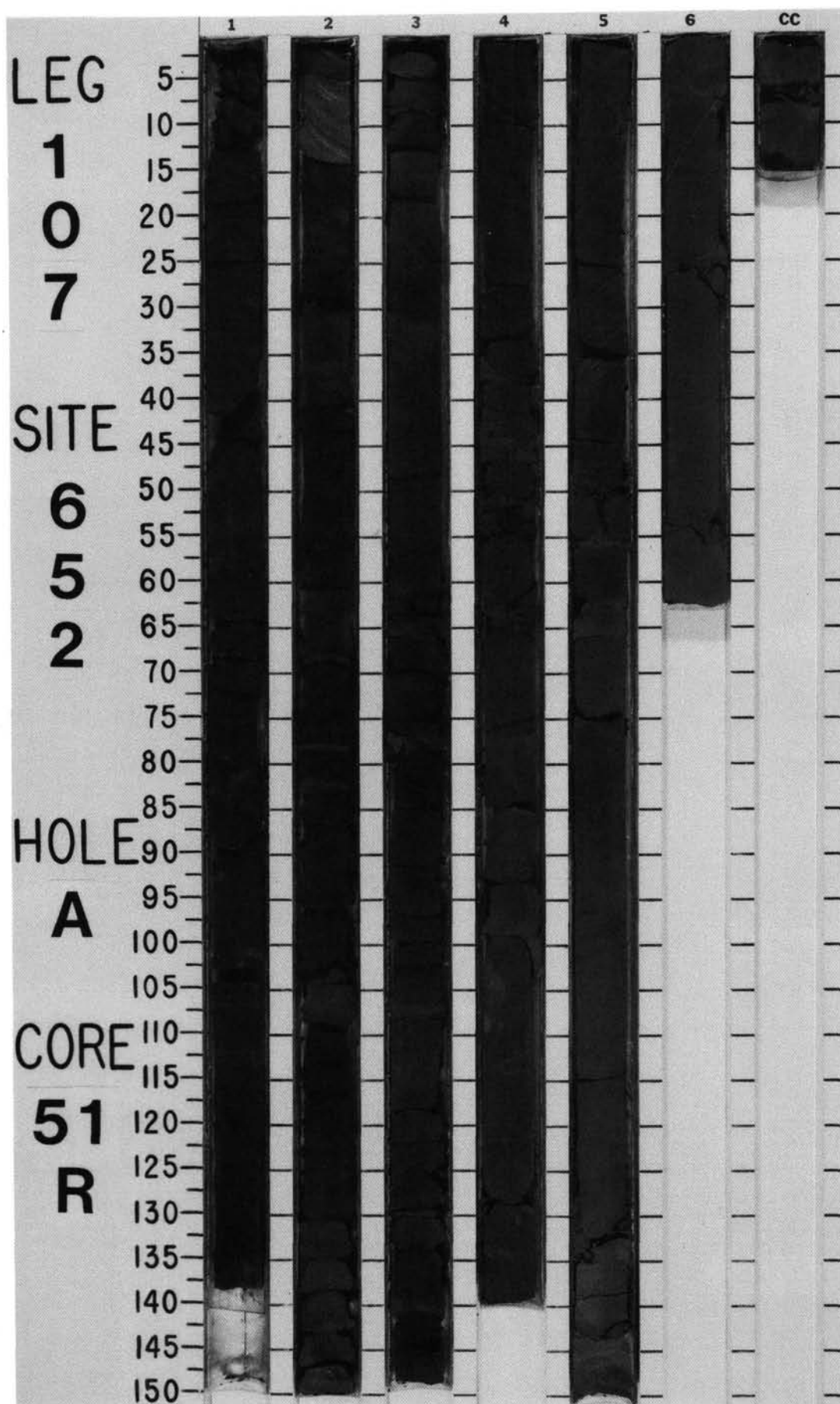
TIME-ROCK UNIT	BIOSTRAT. ZONE/ FOSSIL CHARACTER				PALEOMAGNETICS	PHYS. PROPERTIES	CHEMISTRY	SECTION	METERS	GRAPHIC LITHOLOGY	DRILLING DISTURB.	SED. STRUCTURES	SAMPLES	LITHOLOGIC DESCRIPTION																																										
	FORAMINIFERS	NANNOFOSSILS	RADIOLARIANS	DIATOMS																																																				
						$\gamma=2.40 \phi=28 \vee=2503$ ●	● 18		0.5 1.0				*	<p>CALCAREOUS, GYPSIFEROUS MUDSTONE, alternating with SANDY MUDSTONE</p> <p>Calcareous, gypsiferous mudstone, alternating with grayish brown (2.5Y 5/2), sandy silt layers; both are well-indurated. Mud layers are generally laminated with scattered organic matter; silt layers are graded (reverse or normal) and cross-bedded. Dewatering structures are numerous.</p> <p>Apparent dip: one tensional fault shows a dip of 35° and a throw of about 1 cm; pitch of slickensides is 65°.</p> <p>SMEAR SLIDE SUMMARY (%):</p> <table><tr><td></td><td>1, 55</td><td>2, 98</td></tr><tr><td>D</td><td>D</td><td>D</td></tr></table> <p>TEXTURE:</p> <table><tr><td>Sand</td><td>—</td><td>25</td></tr><tr><td>Silt</td><td>40</td><td>60</td></tr><tr><td>Clay</td><td>60</td><td>15</td></tr></table> <p>COMPOSITION:</p> <table><tr><td>Mica</td><td>—</td><td>2</td></tr><tr><td>Clay</td><td>30</td><td>20</td></tr><tr><td>Volcanic glass</td><td>—</td><td>Tr</td></tr><tr><td>Dolomite</td><td>10</td><td>15</td></tr><tr><td>Opacues</td><td>10</td><td>3</td></tr><tr><td>Gypsum detritus</td><td>25</td><td>5</td></tr><tr><td>Carbonate detritus</td><td>25</td><td>55</td></tr><tr><td>Zircon</td><td>Tr</td><td>—</td></tr><tr><td>Hornblende?</td><td>Tr</td><td>—</td></tr></table>		1, 55	2, 98	D	D	D	Sand	—	25	Silt	40	60	Clay	60	15	Mica	—	2	Clay	30	20	Volcanic glass	—	Tr	Dolomite	10	15	Opacues	10	3	Gypsum detritus	25	5	Carbonate detritus	25	55	Zircon	Tr	—	Hornblende?	Tr	—
	1, 55	2, 98																																																						
D	D	D																																																						
Sand	—	25																																																						
Silt	40	60																																																						
Clay	60	15																																																						
Mica	—	2																																																						
Clay	30	20																																																						
Volcanic glass	—	Tr																																																						
Dolomite	10	15																																																						
Opacues	10	3																																																						
Gypsum detritus	25	5																																																						
Carbonate detritus	25	55																																																						
Zircon	Tr	—																																																						
Hornblende?	Tr	—																																																						
						$\gamma=2.56 \phi=19 \vee=4275$ ●	● 54	CC					*																																											

SITE 652 HOLE A CORE 50 R CORED INTERVAL 3916.0-3925.6 mbsl.; 470.0-479.6 mbsf

TIME-ROCK UNIT	BIOSTRAT. ZONE/ FOSSIL CHARACTER				PALEOMAGNETICS	PHYS. PROPERTIES	CHEMISTRY	SECTION	METERS	GRAPHIC LITHOLOGY	DRILLING DISTURB.	SED. STRUCTURES	SAMPLES	LITHOLOGIC DESCRIPTION																																													
	FORAMINIFERS	NANNOFOSSILS	RADIOLARIANS	DIATOMS																																																							
						●	● 8		0.5 1.0					<p>CALCAREOUS, GYPSIFEROUS MUDSTONE, alternating with SANDY MUDSTONE</p> <p>Calcareous, gypsiferous mudstone, alternating with minor layers of sandy mudstone. Sandy silt, light reddish brown (2.5Y 6/4), is cross-laminated, graded (reverse and normal), and displays water escape structures and deep scour structures at the base; mudstone is homogeneous, generally light red-brown (2.5Y 6/4), with one gray layer in CC.</p> <p>Minor lithology: hematitic red or reddish layers in Section 2, 50–170 cm, in Section 3, 70 cm, and in CC, 16 cm, appear in zones disturbed by drilling. Layers in Section 2, 85 cm, and in CC, 13 cm, show small, yellowish, flat burrows in a horizon of plant debris.</p> <p>SMEAR SLIDE SUMMARY (%):</p> <table><tr><td></td><td>2, 50</td><td>CC, 4</td></tr><tr><td>D</td><td>D</td><td>M</td></tr></table> <p>TEXTURE:</p> <table><tr><td>Sand</td><td>5</td><td>—</td></tr><tr><td>Silt</td><td>75</td><td>35</td></tr><tr><td>Clay</td><td>20</td><td>65</td></tr></table> <p>COMPOSITION:</p> <table><tr><td>Quartz</td><td>Tr</td><td>2</td></tr><tr><td>Feldspar</td><td>Tr</td><td>Tr</td></tr><tr><td>Mica</td><td>Tr</td><td>—</td></tr><tr><td>Clay</td><td>57</td><td>65</td></tr><tr><td>Volcanic glass</td><td>3</td><td>Tr</td></tr><tr><td>Calcite/dolomite</td><td>5</td><td>3</td></tr><tr><td>Opacues</td><td>5</td><td>10</td></tr><tr><td>Gypsum detritus</td><td>10</td><td>5</td></tr><tr><td>Carbonate detritus</td><td>20</td><td>10</td></tr><tr><td>Nannofossils</td><td>—</td><td>5</td></tr></table>		2, 50	CC, 4	D	D	M	Sand	5	—	Silt	75	35	Clay	20	65	Quartz	Tr	2	Feldspar	Tr	Tr	Mica	Tr	—	Clay	57	65	Volcanic glass	3	Tr	Calcite/dolomite	5	3	Opacues	5	10	Gypsum detritus	10	5	Carbonate detritus	20	10	Nannofossils	—	5
	2, 50	CC, 4																																																									
D	D	M																																																									
Sand	5	—																																																									
Silt	75	35																																																									
Clay	20	65																																																									
Quartz	Tr	2																																																									
Feldspar	Tr	Tr																																																									
Mica	Tr	—																																																									
Clay	57	65																																																									
Volcanic glass	3	Tr																																																									
Calcite/dolomite	5	3																																																									
Opacues	5	10																																																									
Gypsum detritus	10	5																																																									
Carbonate detritus	20	10																																																									
Nannofossils	—	5																																																									
					● $\gamma=2.36 \phi=30$	● 25							*																																														
					● $\gamma=2.34 \phi=26 \vee=2871$	● 24						OG																																															
								CC					*																																														

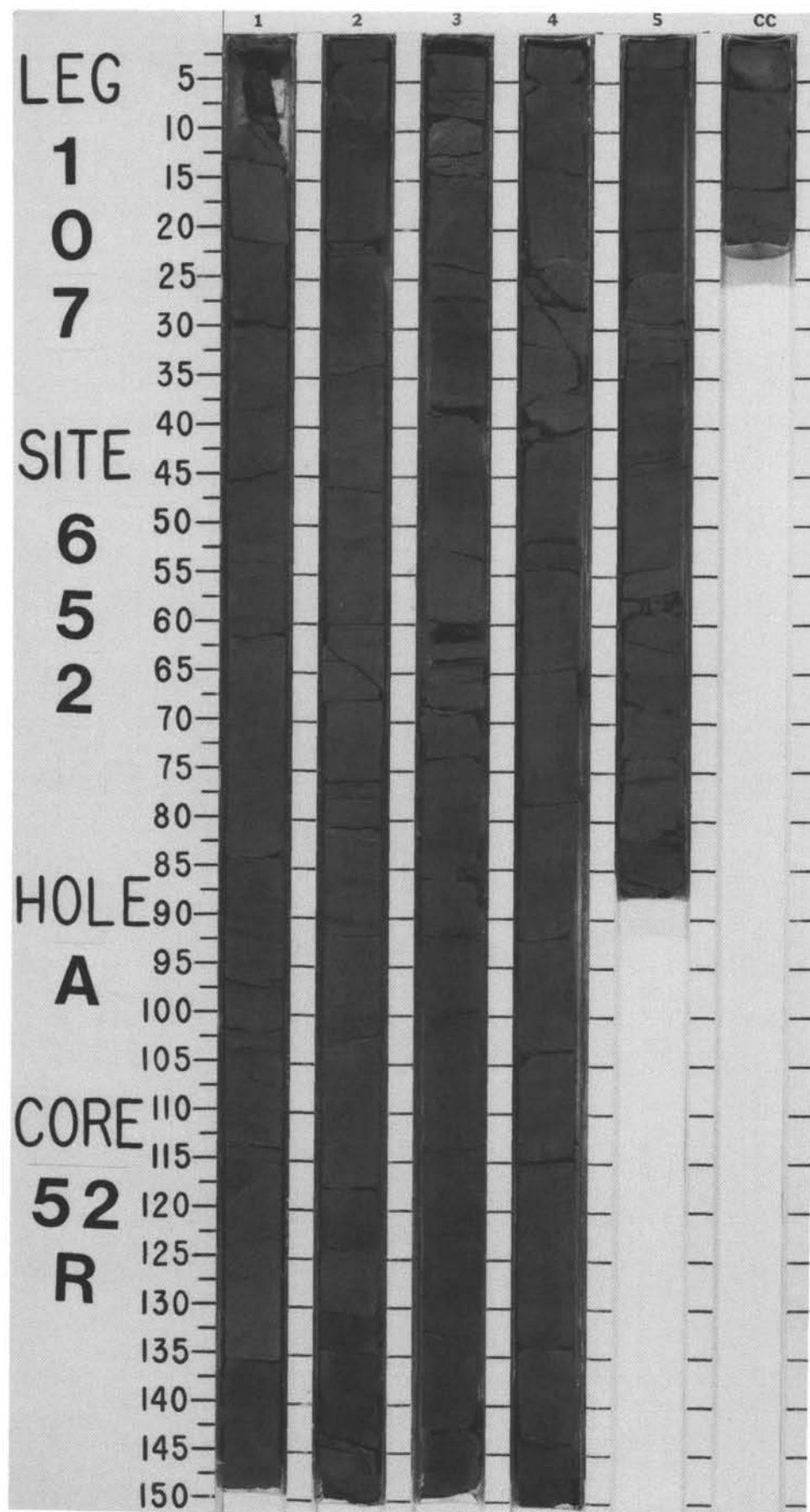


550

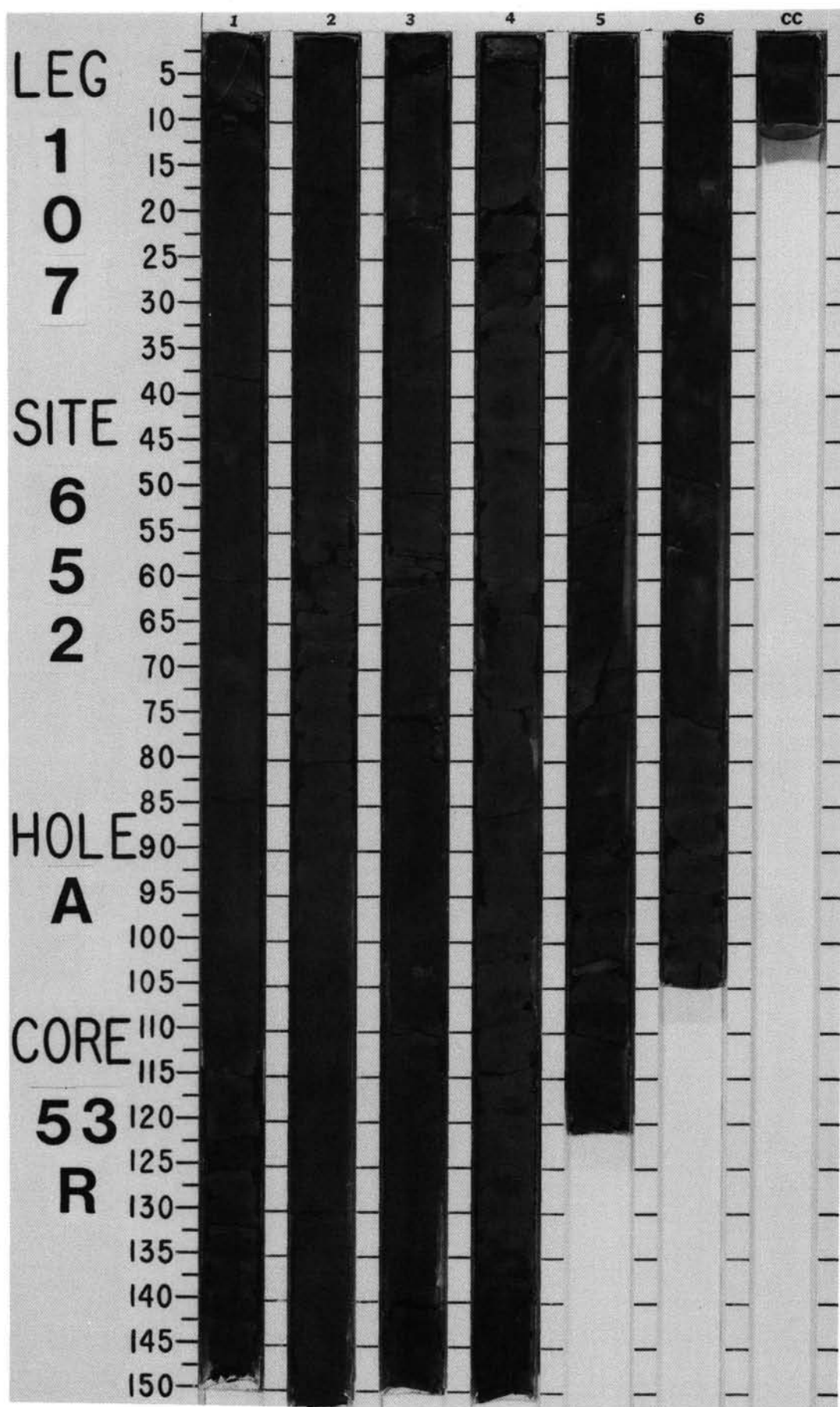


SITE 652 HOLE A CORE 52 R CORED INTERVAL 3935.2-3944.8 mbsl; 489.2-498.8 mbsf

TIME-ROCK UNIT	BIOSTRAT. ZONE/ FOSSIL CHARACTER				PALEOMAGNETICS	PHYS. PROPERTIES	CHEMISTRY	SECTION	METERS	GRAPHIC LITHOLOGY	DRILLING DISTURB.	SED. STRUCTURES	SAMPLES	LITHOLOGIC DESCRIPTION																																																																																								
	FORAMINIFERS	NANNOFOSSILS	RADIOLARIANS	DIATOMS																																																																																																		
						$\gamma = 2.42$ $\phi = 28$ $\psi = 2476$	31	1	0.5 1.0				*	<p>CALCAREOUS, SANDY MUDSTONE, alternating with CALCAREOUS MUDSTONE</p> <p>Calcareous, sandy mudstone, alternating with calcareous mudstone, dark grayish brown (10YR 3/2), dark gray (5Y 4/1), dark reddish gray (10YR 3/2), and gray (5Y 5/1).</p> <p>Primary sedimentary structures include numerous slumps in Sections 1, 2, and 3, parallel bedding of 1-mm- to 1-cm-thick layers, and normal grading. Section 4 also shows scoured basal contacts, lenticular and flaser bedding, cross-stratification, and small filled scours. Distinct dusty red (10R 3/4) to reddish brown (2.5YR 4/4), 1-2-mm-thick laminae of an iron-rich, possibly aluminum-rich, claystone occurs in Section 2, 40-45 cm, in Section 3, 28, 62, 63, and 145 cm, and in Section 5, 3, 68, and 73.5-75.7 cm. These red laminae are apparently associated with sandier units, which also frequently contain micro-lenses of black particles (pyrite?). Red claystone contains 8% limonite/goethite, often occurring just above sandier intervals.</p> <p>Apparent dip: Section 1, 10°; Section 2, 0-10°; Section 3, 3-7°; Section 4, 54-78 cm, 6°; Section 5, 33-55 cm, 10°.</p> <p>SMEAR SLIDE SUMMARY (%):</p> <table><tr><td></td><td>1, 41</td><td>4, 83</td><td>5, 3</td></tr><tr><td></td><td>D</td><td>D</td><td>M</td></tr></table> <p>TEXTURE:</p> <table><tr><td>Sand</td><td>30</td><td>10</td><td>15</td></tr><tr><td>Silt</td><td>45</td><td>10</td><td>25</td></tr><tr><td>Clay</td><td>25</td><td>80</td><td>60</td></tr></table> <p>COMPOSITION:</p> <table><tr><td>Quartz</td><td>10</td><td>6</td><td>3</td></tr><tr><td>Feldspar</td><td>10</td><td>4</td><td>7</td></tr><tr><td>Rock fragments</td><td>10</td><td>—</td><td>—</td></tr><tr><td>Mica</td><td>2</td><td>Tr</td><td>—</td></tr><tr><td>Clay</td><td>31</td><td>59</td><td>54</td></tr><tr><td>Volcanic glass</td><td>3</td><td>3</td><td>2</td></tr><tr><td>Calcite</td><td>23</td><td>15</td><td>10</td></tr><tr><td>Accessory minerals</td><td>Tr</td><td>—</td><td>—</td></tr><tr><td>Gypsum/anhydrite</td><td>1</td><td>5</td><td>Tr</td></tr><tr><td>Opacities (undetermined)</td><td>4</td><td>—</td><td>10</td></tr><tr><td>Limonite/goethite</td><td>—</td><td>—</td><td>8</td></tr><tr><td>Foraminifers</td><td>—</td><td>Tr</td><td>—</td></tr><tr><td>Nannofossils</td><td>Tr</td><td>Tr</td><td>1</td></tr><tr><td>Sponge spicules</td><td>—</td><td>1</td><td>—</td></tr><tr><td>Fish remains</td><td>—</td><td>—</td><td>2</td></tr><tr><td>Micrite</td><td>6</td><td>7</td><td>—</td></tr><tr><td>Unknown subhexagonal low birefringence</td><td>—</td><td>—</td><td>3</td></tr></table>		1, 41	4, 83	5, 3		D	D	M	Sand	30	10	15	Silt	45	10	25	Clay	25	80	60	Quartz	10	6	3	Feldspar	10	4	7	Rock fragments	10	—	—	Mica	2	Tr	—	Clay	31	59	54	Volcanic glass	3	3	2	Calcite	23	15	10	Accessory minerals	Tr	—	—	Gypsum/anhydrite	1	5	Tr	Opacities (undetermined)	4	—	10	Limonite/goethite	—	—	8	Foraminifers	—	Tr	—	Nannofossils	Tr	Tr	1	Sponge spicules	—	1	—	Fish remains	—	—	2	Micrite	6	7	—	Unknown subhexagonal low birefringence	—	—	3
	1, 41	4, 83	5, 3																																																																																																			
	D	D	M																																																																																																			
Sand	30	10	15																																																																																																			
Silt	45	10	25																																																																																																			
Clay	25	80	60																																																																																																			
Quartz	10	6	3																																																																																																			
Feldspar	10	4	7																																																																																																			
Rock fragments	10	—	—																																																																																																			
Mica	2	Tr	—																																																																																																			
Clay	31	59	54																																																																																																			
Volcanic glass	3	3	2																																																																																																			
Calcite	23	15	10																																																																																																			
Accessory minerals	Tr	—	—																																																																																																			
Gypsum/anhydrite	1	5	Tr																																																																																																			
Opacities (undetermined)	4	—	10																																																																																																			
Limonite/goethite	—	—	8																																																																																																			
Foraminifers	—	Tr	—																																																																																																			
Nannofossils	Tr	Tr	1																																																																																																			
Sponge spicules	—	1	—																																																																																																			
Fish remains	—	—	2																																																																																																			
Micrite	6	7	—																																																																																																			
Unknown subhexagonal low birefringence	—	—	3																																																																																																			
						$\gamma = 2.42$ $\phi = 23$ $\psi = 2846$	31	2																																																																																														
							37	3																																																																																														
							19	4																																																																																														
								5																																																																																														
								CC																																																																																														

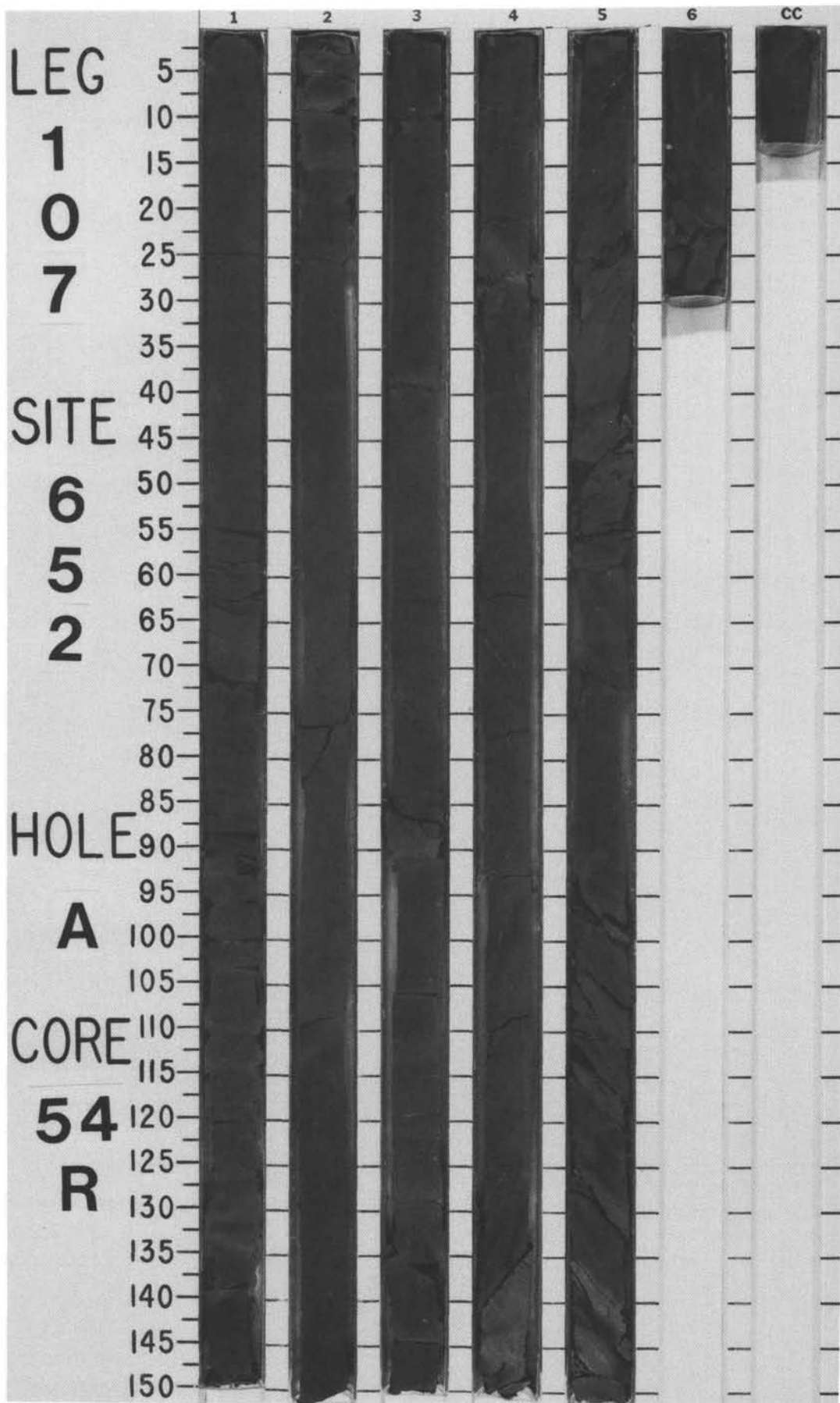


TIME - ROCK UNIT	BIOSTRAT. ZONE/ FOSSIL CHARACTER				PALEOMAGNETICS	PHYS. PROPERTIES	CHEMISTRY	SECTION	METERS	GRAPHIC LITHOLOGY	DRILLING DISTURB.	SED. STRUCTURES	SAMPLES	LITHOLOGIC DESCRIPTION																																																																																																																																				
	FORAMINIFERS	NANNOFOSSILS	RADIOLARIANS	DIATOMS																																																																																																																																														
														<p>CALCAREOUS MUDSTONE with interbedded SANDY, QUARTZOSE, CALCAREOUS MUDSTONE</p> <p>Dark gray (5Y 4/1) to gray (5Y 5/1) calcareous mudstone with less common (than previous cores) interbedded layers of sandy, quartzose, calcareous mudstone, often showing normal graded bedding. Slump structures dominate in the mudstone, and lenticular beds of sandier material occur.</p> <p>Minor lithology: small concretions of calcite (<2 mm in diameter) and plant filament and fish debris are found in the siltier intervals of Sections 1 and 6. A cemented calcite vein was noted in Section 3, 75 cm. Dusty red (2.5YR 3/2), thin laminae (<3 mm) of iron-rich (limonite about 5%) mudstone with recrystallized calcite and anhydrite occur in Section 1, 6 and 110 cm; Section 3, 3, 50, and 60 cm; Section 4, 3, 5, 26, and 33 cm; and Section 5, 88-90 and 110 cm.</p> <p>Apparent dip: Section 5, 22° maximum.</p> <p>SMEAR SLIDE SUMMARY (%):</p> <table border="1"> <thead> <tr> <th></th> <th>1, 70 D</th> <th>1, 100 M</th> <th>3, 49 M</th> <th>3, 75 M</th> <th>5, 88 M</th> </tr> </thead> <tbody> <tr> <td>TEXTURE:</td> <td></td> <td></td> <td></td> <td></td> <td></td> </tr> <tr> <td>Sand</td> <td>5</td> <td>10</td> <td>15</td> <td>—</td> <td>30</td> </tr> <tr> <td>Silt</td> <td>25</td> <td>20</td> <td>25</td> <td>—</td> <td>20</td> </tr> <tr> <td>Clay</td> <td>70</td> <td>70</td> <td>60</td> <td>—</td> <td>50</td> </tr> </tbody> </table> <p>COMPOSITION:</p> <table border="1"> <thead> <tr> <th></th> <th>15</th> <th>20</th> <th>20</th> <th>5</th> <th>5</th> </tr> </thead> <tbody> <tr> <td>Quartz</td> <td>15</td> <td>20</td> <td>20</td> <td>5</td> <td>5</td> </tr> <tr> <td>Feldspar</td> <td></td> <td></td> <td></td> <td></td> <td></td> </tr> <tr> <td>(some authigenic)</td> <td>2</td> <td>Tr</td> <td>1</td> <td>—</td> <td>3</td> </tr> <tr> <td>Mica</td> <td>1</td> <td>Tr</td> <td>Tr</td> <td>—</td> <td>—</td> </tr> <tr> <td>Clay</td> <td>40</td> <td>43</td> <td>31</td> <td>—</td> <td>29</td> </tr> <tr> <td>Volcanic glass</td> <td>?</td> <td>—</td> <td>—</td> <td>—</td> <td>—</td> </tr> <tr> <td>Calcite</td> <td>40</td> <td>30</td> <td>40</td> <td>93</td> <td>40</td> </tr> <tr> <td>Dolomite</td> <td>1</td> <td>—</td> <td>2</td> <td>—</td> <td>8</td> </tr> <tr> <td>Accessory minerals</td> <td>1</td> <td>1</td> <td>1</td> <td>—</td> <td>Tr</td> </tr> <tr> <td>Opauques</td> <td>—</td> <td>2</td> <td>3</td> <td>—</td> <td>5</td> </tr> <tr> <td>Gypsum</td> <td>—</td> <td>1</td> <td>1</td> <td>—</td> <td>—</td> </tr> <tr> <td>Anhydrite</td> <td>—</td> <td>—</td> <td>—</td> <td>2</td> <td>10</td> </tr> <tr> <td>Nannofossils</td> <td>—</td> <td>1</td> <td>—</td> <td>—</td> <td>Tr</td> </tr> <tr> <td>Fish remains</td> <td>—</td> <td>1</td> <td>1</td> <td>—</td> <td>—</td> </tr> <tr> <td>Plant debris</td> <td>—</td> <td>1</td> <td>—</td> <td>—</td> <td>—</td> </tr> <tr> <td>*Limonite(?)</td> <td></td> <td></td> <td></td> <td></td> <td></td> </tr> </tbody> </table>		1, 70 D	1, 100 M	3, 49 M	3, 75 M	5, 88 M	TEXTURE:						Sand	5	10	15	—	30	Silt	25	20	25	—	20	Clay	70	70	60	—	50		15	20	20	5	5	Quartz	15	20	20	5	5	Feldspar						(some authigenic)	2	Tr	1	—	3	Mica	1	Tr	Tr	—	—	Clay	40	43	31	—	29	Volcanic glass	?	—	—	—	—	Calcite	40	30	40	93	40	Dolomite	1	—	2	—	8	Accessory minerals	1	1	1	—	Tr	Opauques	—	2	3	—	5	Gypsum	—	1	1	—	—	Anhydrite	—	—	—	2	10	Nannofossils	—	1	—	—	Tr	Fish remains	—	1	1	—	—	Plant debris	—	1	—	—	—	*Limonite(?)					
	1, 70 D	1, 100 M	3, 49 M	3, 75 M	5, 88 M																																																																																																																																													
TEXTURE:																																																																																																																																																		
Sand	5	10	15	—	30																																																																																																																																													
Silt	25	20	25	—	20																																																																																																																																													
Clay	70	70	60	—	50																																																																																																																																													
	15	20	20	5	5																																																																																																																																													
Quartz	15	20	20	5	5																																																																																																																																													
Feldspar																																																																																																																																																		
(some authigenic)	2	Tr	1	—	3																																																																																																																																													
Mica	1	Tr	Tr	—	—																																																																																																																																													
Clay	40	43	31	—	29																																																																																																																																													
Volcanic glass	?	—	—	—	—																																																																																																																																													
Calcite	40	30	40	93	40																																																																																																																																													
Dolomite	1	—	2	—	8																																																																																																																																													
Accessory minerals	1	1	1	—	Tr																																																																																																																																													
Opauques	—	2	3	—	5																																																																																																																																													
Gypsum	—	1	1	—	—																																																																																																																																													
Anhydrite	—	—	—	2	10																																																																																																																																													
Nannofossils	—	1	—	—	Tr																																																																																																																																													
Fish remains	—	1	1	—	—																																																																																																																																													
Plant debris	—	1	—	—	—																																																																																																																																													
*Limonite(?)																																																																																																																																																		



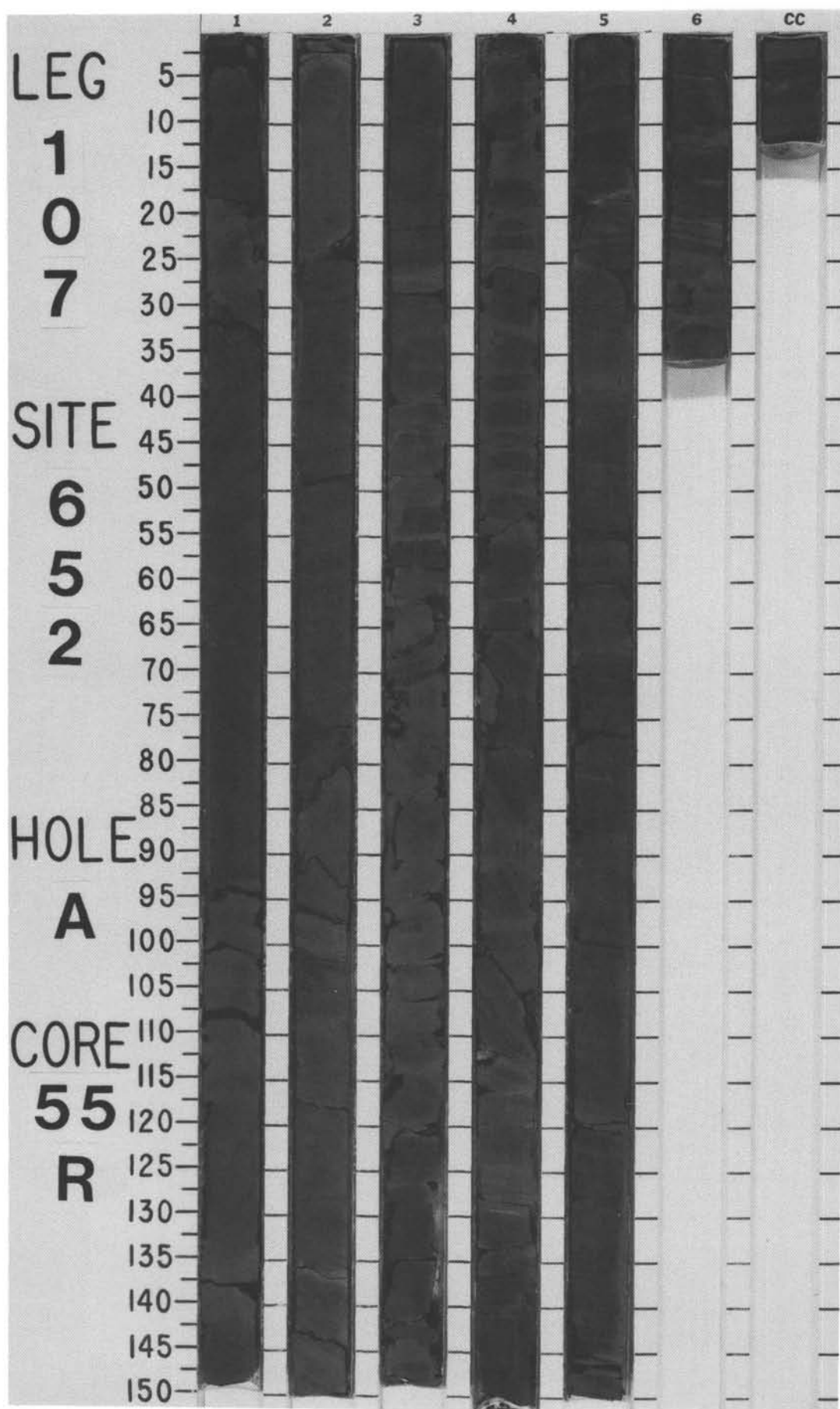
SITE 652 HOLE A CORE 54 R CORED INTERVAL 3954.5-3964.1 mbsl; 508.5-518.1 mbsf

TIME - ROCK UNIT	BIOSTRAT. ZONE/ FOSSIL CHARACTER				PALEOMAGNETICS	PHYS. PROPERTIES	CHEMISTRY	SECTION	METERS	GRAPHIC LITHOLOGY	DRILLING DISTURB.	SED. STRUCTURES	SAMPLES	LITHOLOGIC DESCRIPTION																																																				
	FORAMINIFERS	NANNOFOSSILS	RADIOLARIANS	DIATOMS																																																														
						$\gamma = 2.41 \quad \phi = 28 \quad \vee = 2228$	●25 ●26	1	0.5 1.0				*	<p>CALCAREOUS MUDSTONE</p> <p>Homogeneous calcareous mudstone, dark gray (5Y 4/1), gray (5Y 5/1), and reddish gray (5YR 5/2).</p> <p>Minor lithology: Section 1, 0-82 cm, noncalcareous (possibly dolomitic) mudstone. Section 3, 73 cm, to CC, large slump deposit of the gray mudstone with lighter dusky red (2.5YR 3/2), light gray (5Y 5/1), and white (2.5Y 8/2) laminae that accent and highlight the slump structures. Within the slump are irregular fillings of calcite cement and boudin-like, lenticular, sandy mudstone (in Section 5, 95-150 cm) that parallel the disturbed bedding plane. Section 5, 63 cm, a bright white, finely crystalline anhydrite/calcite layer occurring along the fault plane; this layer differs from irregular calcite filling.</p> <p>Apparent dip of the slump: 37°. Section 5, 59-74 cm, is a small reverse fault with an apparent displacement of 5 mm; dip angle of the fault plane is 70° and pitch of the slickensides is 75°, as seen with the fault plane deviation to the right.</p> <p>Interpretation: fault may post-date slump.</p> <p>SMEAR SLIDE SUMMARY (%):</p> <table><tr><td></td><td>1, 40</td><td>2, 100</td><td>5, 63</td></tr><tr><td>D</td><td>D</td><td>D</td><td>M</td></tr></table> <p>TEXTURE:</p> <table><tr><td>Sand</td><td>5</td><td>10</td><td>—</td></tr><tr><td>Silt</td><td>15</td><td>20</td><td>—</td></tr><tr><td>Clay</td><td>80</td><td>70</td><td>—</td></tr></table> <p>COMPOSITION:</p> <table><tr><td>Quartz</td><td>5</td><td>5</td><td>—</td></tr><tr><td>Clay</td><td>30</td><td>42</td><td>—</td></tr><tr><td>Volcanic glass</td><td>1</td><td>—</td><td>—</td></tr><tr><td>Calcite</td><td>60</td><td>50</td><td>40</td></tr><tr><td>Accessory minerals</td><td>1</td><td>2</td><td>—</td></tr><tr><td>Opauques (org. matter?)</td><td>3</td><td>—</td><td>—</td></tr><tr><td>Opauques</td><td>—</td><td>1</td><td>—</td></tr><tr><td>Anhydrite</td><td>—</td><td>—</td><td>60</td></tr></table>		1, 40	2, 100	5, 63	D	D	D	M	Sand	5	10	—	Silt	15	20	—	Clay	80	70	—	Quartz	5	5	—	Clay	30	42	—	Volcanic glass	1	—	—	Calcite	60	50	40	Accessory minerals	1	2	—	Opauques (org. matter?)	3	—	—	Opauques	—	1	—	Anhydrite	—	—	60
	1, 40	2, 100	5, 63																																																															
D	D	D	M																																																															
Sand	5	10	—																																																															
Silt	15	20	—																																																															
Clay	80	70	—																																																															
Quartz	5	5	—																																																															
Clay	30	42	—																																																															
Volcanic glass	1	—	—																																																															
Calcite	60	50	40																																																															
Accessory minerals	1	2	—																																																															
Opauques (org. matter?)	3	—	—																																																															
Opauques	—	1	—																																																															
Anhydrite	—	—	60																																																															
						$\gamma = 2.46 \quad \phi = 24 \quad \vee = 2320$	●26 ●18	2					*																																																					
								3																																																										
								4																																																										
								5					*																																																					
								6																																																										
								CC																																																										



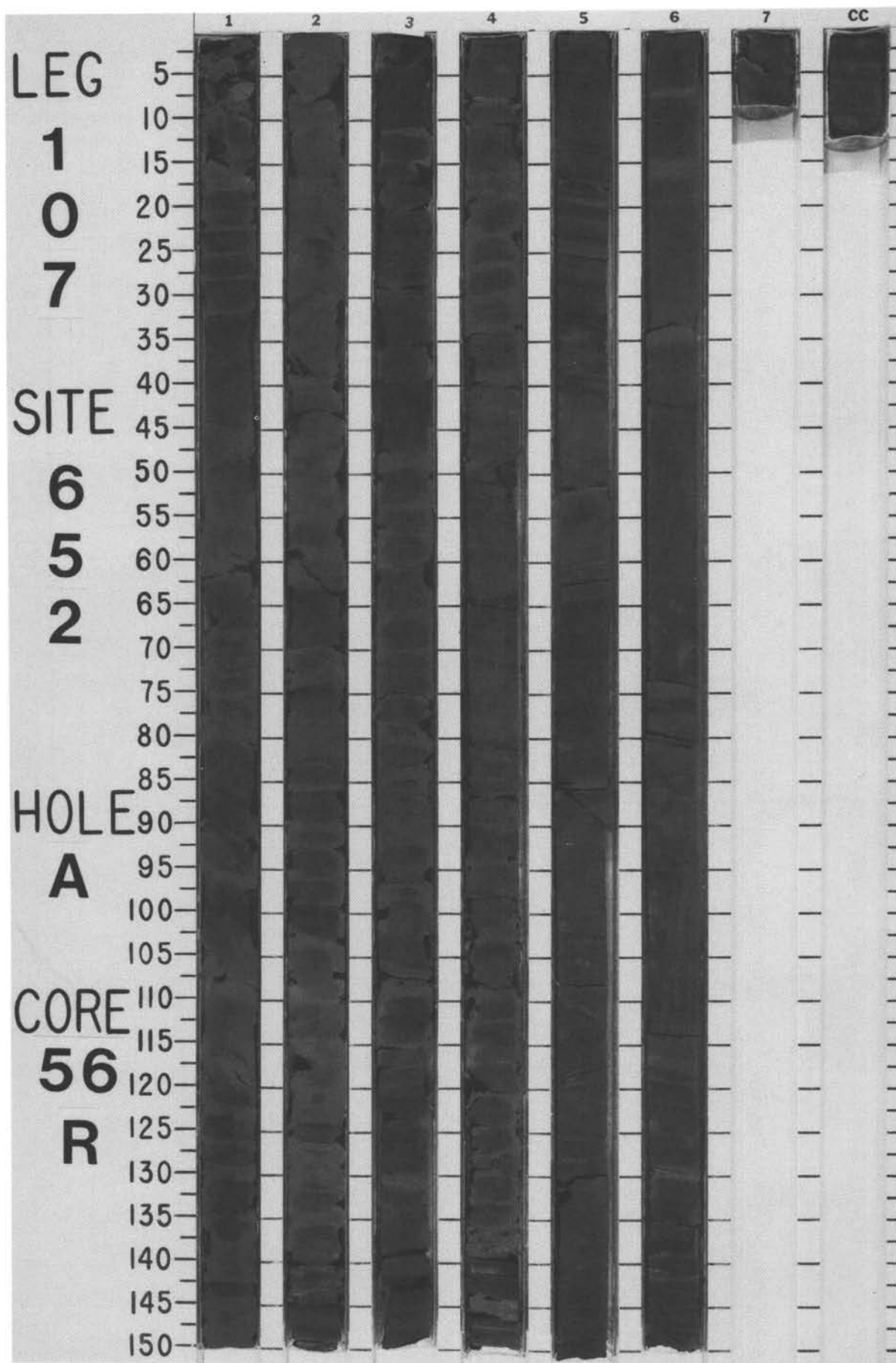
SITE 652 HOLE A CORE 55 R CORED INTERVAL 3964.1-3973.8 mbsl; 518.1-527.8 mbsf

TIME - ROCK UNIT	BIOSTRAT. ZONE/ FOSSIL CHARACTER				PALEOMAGNETICS	PHYS. PROPERTIES	CHEMISTRY	SECTION	METERS	GRAPHIC LITHOLOGY	DRILLING DISTURB.	SED. STRUCTURES	SAMPLES	LITHOLOGIC DESCRIPTION
	FORAMINIFERS	NANNOFOSSILS	RADIOLARIANS	DIAZONES										
														CALCAREOUS MUDSTONE and NONCALCAREOUS (DOLOMITIC?) MUDSTONE
									0.5			*		Intervals of calcareous mudstone, alternating with a noncalcareous (dolomitic?) mudstone. Noncalcareous portion contains a very fine-grained recrystallized carbonate that cannot be identified definitively as dolomite in smear slide, but does not fizz with 1 N HCl. Colors range from dark gray (5Y 4/1), gray (5Y 5/1), to reddish gray 5YR 5/20.
									1.0			*		Minor lithology: Section 2, 70-80 cm, vein fillings of white (2.5Y 8/2) anhydrite/calcite sediment; Sections 3-6, thin laminae of dusky red (2.5YR 3/2), iron-rich (limonite?) mudstone. Numerous slumps, with a particularly well-developed one in Section 4, 60-120 cm, showing fold hinges with initial foliation. Few sandier mudstone layers occur within interbeds or with lenticular bedding.
									2			*		SMEAR SLIDE SUMMARY (%):
														1, 60 2, 60 D D
														TEXTURE:
														Sand 10 5
														Silt 20 15
														Clay 70 80
														COMPOSITION:
														Quartz 15 15
														Mica 1 —
														Clay 33 44
														Calcite 45 35
														Dolomite — —
														Accessory minerals — 3
														Opaques (amorphous) 3 3
														Gypsum 3 —



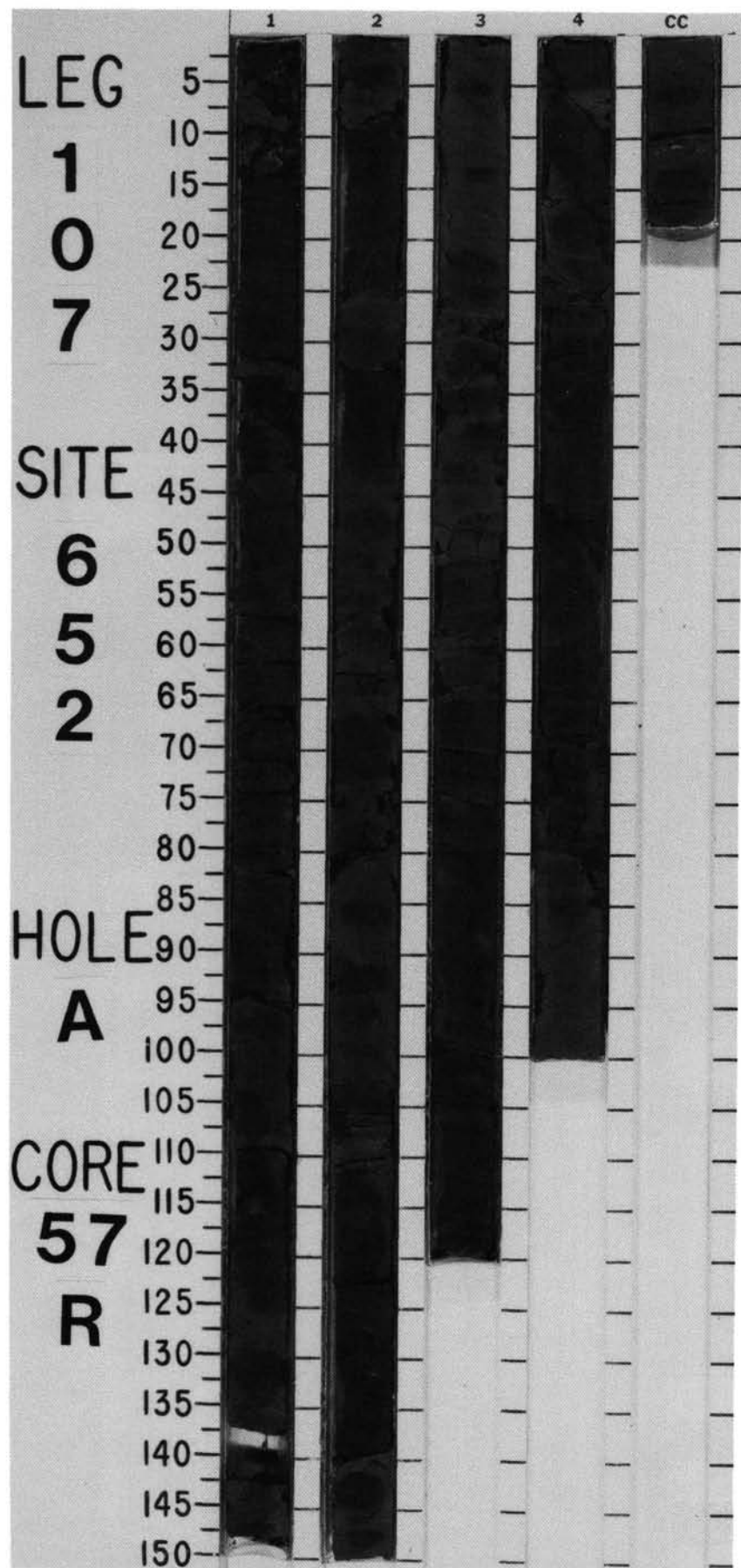
SITE 652 HOLE A CORE 56 R CORED INTERVAL 3973.8-3983.4 mbsl; 527.8-537.4 mbsf

TIME-ROCK UNIT	BIOSTRAT. ZONE/ FOSSIL CHARACTER				PALEOMAGNETICS	PHYS. PROPERTIES	CHEMISTRY	SECTION	METERS	GRAPHIC LITHOLOGY	DRILLING DISTURB.	SED. STRUCTURES	SAMPLES	LITHOLOGIC DESCRIPTION
	FORAMINIFERS	NANNOFOSSILS	RADIOLARIANS	DIATOMS										
						● $\gamma = 2.42$ $\phi = 24$ $V = 2368$	● 29	1	0.5 1.0		XX XX XX			<p>CALCAREOUS CLAYSTONE, alternating with MUDSTONE and SANDY SILTSTONE</p> <p>Calcareous claystone, alternating with mudstone and sandy siltstone. Mudstone is dark reddish brown (5YR 5/3), sometimes homogeneous, and often laminated (parallel and convolute laminations); thin, silty layers occur at the base of some sequences.</p> <p>Minor lithology: Sections 2, 3, and 5, a few red hematite-rich bauxitic horizons; Sections 1, 6, and CC, thin, less than millimeter-thick intervals of crystallized dolomite. A slump shows isoclinal folding with an associated axial plane, crenulation-type cleavage; Section 4, numerous tensional microfaults.</p> <p>Apparent dip: Section 5, fault dip of 45° was measured; angle between dip and fault plane is 40°; pitch of slickensides is 75°.</p> <p>Interpretation: sedimentary structures such as slumps and faults are related to syn-sedimentary instability.</p> <p>SMEAR SLIDE SUMMARY (%):</p> <p style="text-align: right;">5, 10 D</p> <p>TEXTURE:</p> <p>Sand — Silt 5 Clay 95</p> <p>COMPOSITION:</p> <p>Quartz Tr Mica 2 Clay 40 Volcanic glass Tr Calcite/dolomite 3 Cement 35 Accessory minerals 5 Anhydrite Tr Gypsum Tr Carbonate detritus 15</p>
						● $V = 2485$	● 24	2			XX XX XX			
								3			XX X			
								4						
								5						
								6						
								CC						



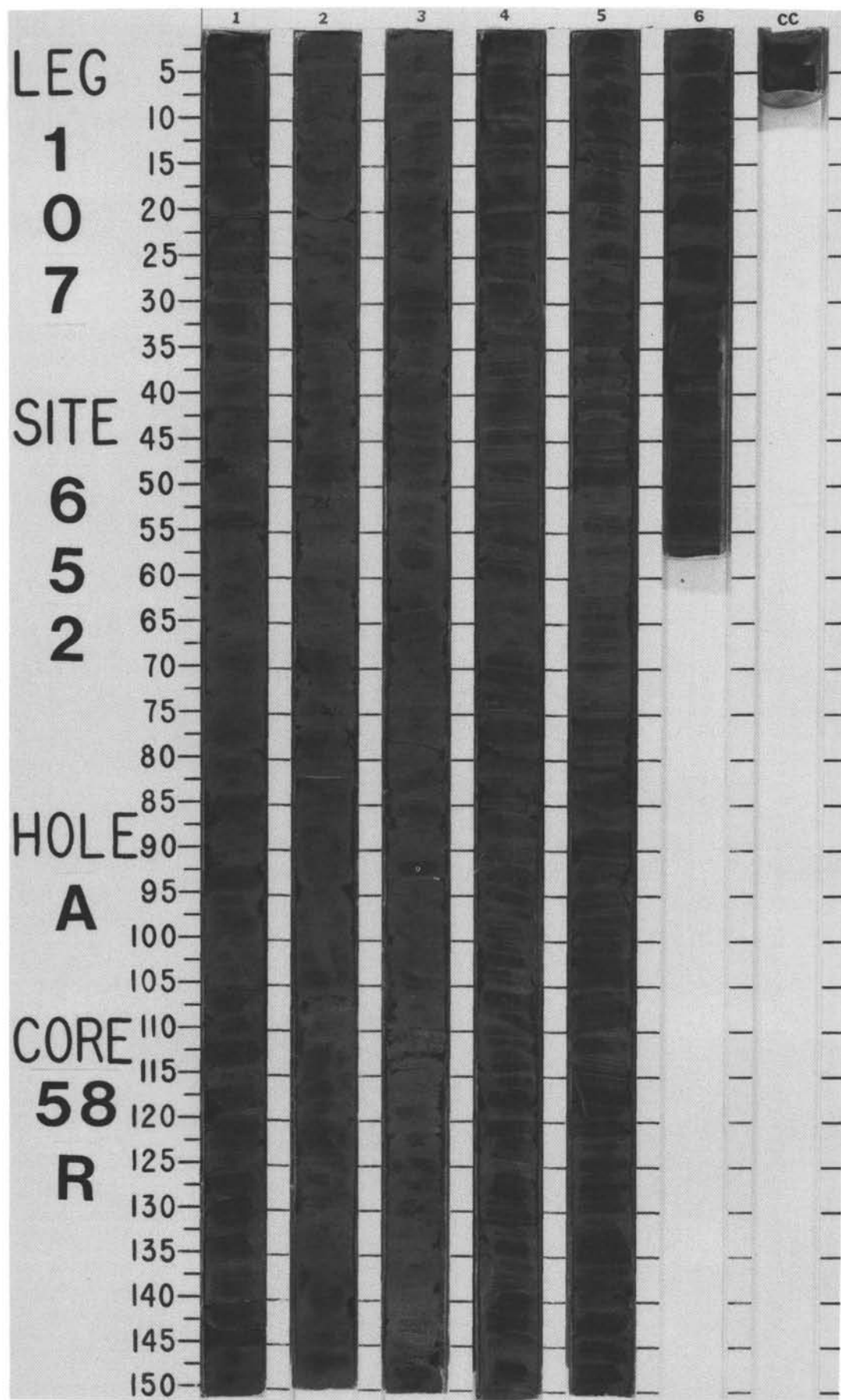
SITE 652 HOLE A CORE 57 R CORED INTERVAL 3983.4-3992.6 mbsl; 537.4-546.6 mbsf

TIME-ROCK UNIT	BIOSTRAT. ZONE/ FOSSIL CHARACTER				PALEOMAGNETICS	PHYS. PROPERTIES	CHEMISTRY	SECTION	METERS	GRAPHIC LITHOLOGY	DRILLING DISTURB.	SED. STRUCTURES	SAMPLES	LITHOLOGIC DESCRIPTION																															
	FORAMINIFERS	NANNOFOSSILS	RADIOLARIANS	DIATOMS																																									
						● γ -2.60 ϕ -19 \vee -2972		22 ● ●28 ● 44							<p>SILICEOUS MUDSTONE, alternating with SANDY SILTSTONE</p> <p>Alternation of weak red (2.5YR 4/2), fine-grained, siliceous mudstone and grayish brown (2.5Y 5/2), well-cemented, fine-grained sandy siltstones. Parallel and convolute laminations are common.</p> <p>Minor lithology: Section 1, 20 cm, and Section 2, 125-135 cm, boudinage of sand layers; Section 1, 120-130 cm, numerous tensional microfaults; Section 2, 28-34 cm, calcareous sandstone, well-cemented with thin, parallel, wavy laminations and small-scale dewatering structures; and Section 4, 55 cm, compressional fault.</p> <p>SMEAR SLIDE SUMMARY (%):</p> <table><tr><td>Sand</td><td>3, 30</td></tr><tr><td>Silt</td><td>D</td></tr><tr><td>Clay</td><td>90</td></tr></table> <p>TEXTURE:</p> <table><tr><td>Sand</td><td>—</td></tr><tr><td>Silt</td><td>10</td></tr><tr><td>Clay</td><td>90</td></tr></table> <p>COMPOSITION:</p> <table><tr><td>Quartz</td><td>2</td></tr><tr><td>Mica</td><td>Tr</td></tr><tr><td>Clay</td><td>83</td></tr><tr><td>Volcanic glass</td><td>Tr</td></tr><tr><td>Opauques</td><td>5</td></tr><tr><td>Anhydrite detritus</td><td>Tr</td></tr><tr><td>Gypsum detritus</td><td>Tr</td></tr><tr><td>Carbonate detritus</td><td>10</td></tr><tr><td>Nannofossils</td><td>Tr</td></tr></table>	Sand	3, 30	Silt	D	Clay	90	Sand	—	Silt	10	Clay	90	Quartz	2	Mica	Tr	Clay	83	Volcanic glass	Tr	Opauques	5	Anhydrite detritus	Tr	Gypsum detritus	Tr	Carbonate detritus	10	Nannofossils	Tr
Sand	3, 30																																												
Silt	D																																												
Clay	90																																												
Sand	—																																												
Silt	10																																												
Clay	90																																												
Quartz	2																																												
Mica	Tr																																												
Clay	83																																												
Volcanic glass	Tr																																												
Opauques	5																																												
Anhydrite detritus	Tr																																												
Gypsum detritus	Tr																																												
Carbonate detritus	10																																												
Nannofossils	Tr																																												
					● γ -2.39 ϕ -26 \vee -2508		29 ●		0.5																																				
									1																																				
									2																																				
									3																																				
									4																																				
									CC																																				



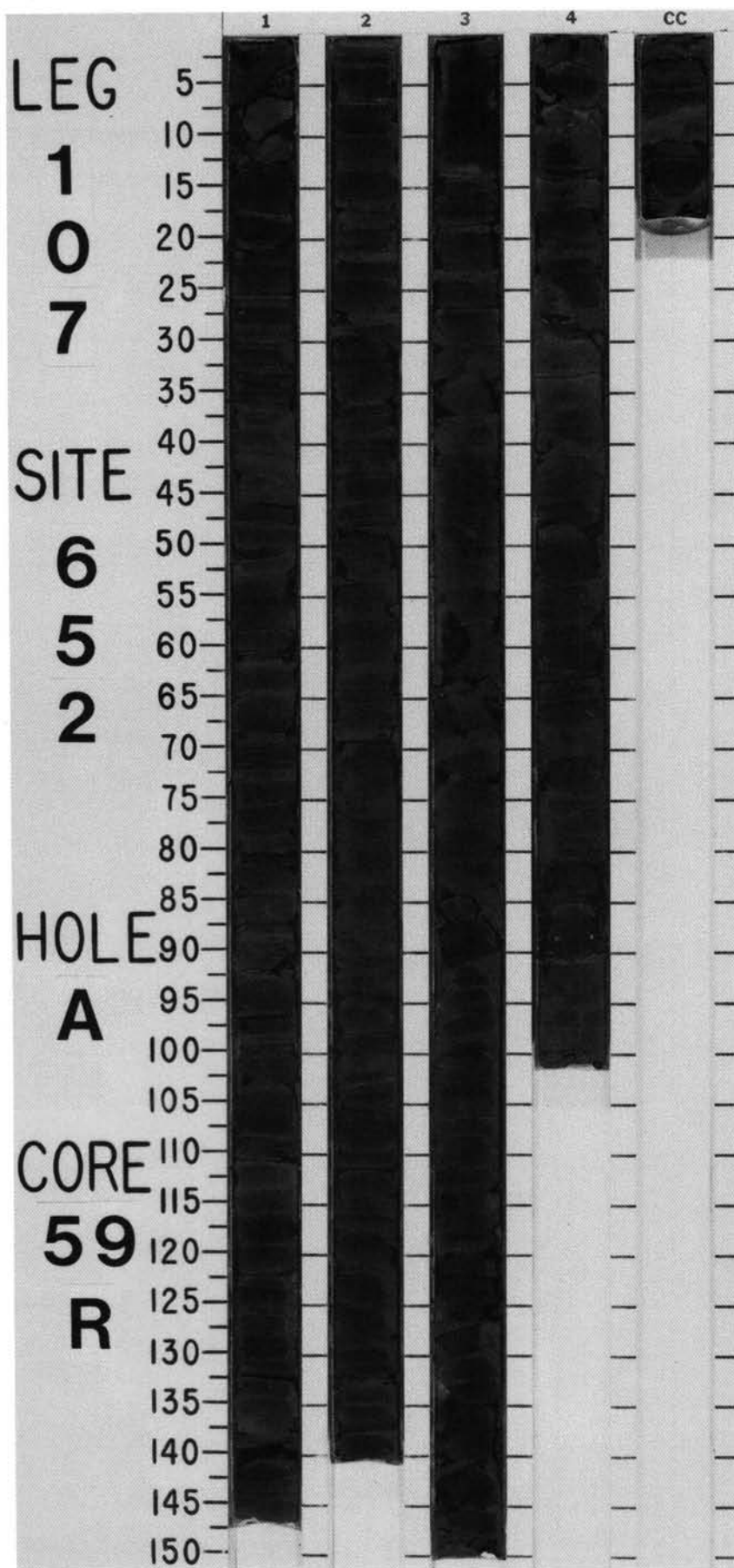
SITE 652 HOLE A CORE 58 R CORED INTERVAL 3992.6-4002.3 mbsl; 546.6-556.3 mbsf

TIME- ROCK UNIT	BIOSTRAT. ZONE/ FOSSIL CHARACTER				PALEOMAGNETICS	PHYS. PROPERTIES	CHEMISTRY	SECTION	METERS	GRAPHIC LITHOLOGY	DRILLING DISTURB.	SED. STRUCTURES	SAMPLES	LITHOLOGIC DESCRIPTION																																																														
	FORAMINIFERS	NANNOFOSSILS	RADIOLARIANS	DIATOMS																																																																								
						$\gamma=2.35 \phi=29 \quad V-2191 \bullet$	22 ● 33 ●	1	0.5				*	CALCAREOUS CLAYSTONE Calcareous claystone, olive (5Y 4/3), dark reddish brown (5Y 4/2), and olive-yellow (2.5Y 6/6). Variations in color may reflect rhythmically laminated alternations, interbedded with scarce, thin layers of siltstone. Minor lithology: Section 1, 102 cm, and Section 2, 125 cm, yellow or orange intervals of limonite-rich material and numerous dolomitic layers; Sections 3 and 4, striped, finely laminated mudstone of olive-brown, dark reddish brown, and olive-yellow. Apparent dip: maximum dip is 6–7°. SMEAR SLIDE SUMMARY (%) : <table><tr><td>1, 22</td><td>1, 106</td><td>3, 145</td></tr><tr><td>D</td><td>M</td><td>D</td></tr></table> TEXTURE : <table><tr><td>Sand</td><td>—</td><td>—</td><td>—</td></tr><tr><td>Silt</td><td>5</td><td>20</td><td>10</td></tr><tr><td>Clay</td><td>95</td><td>80</td><td>90</td></tr></table> COMPOSITION : <table><tr><td>Quartz</td><td>3</td><td>—</td><td>—</td></tr><tr><td>Clay</td><td>30</td><td>35</td><td>60</td></tr><tr><td>Calcite/dolomite</td><td>—</td><td>20</td><td>5</td></tr><tr><td>Cement (sl.)</td><td>40</td><td>—</td><td>—</td></tr><tr><td>Accessory minerals</td><td>—</td><td>—</td><td>10</td></tr><tr><td>Gypsum detritus</td><td>7</td><td>40</td><td>—</td></tr><tr><td>Anhydrite</td><td>Tr</td><td>—</td><td>—</td></tr><tr><td>Carbonate detritus</td><td>15</td><td>—</td><td>—</td></tr><tr><td>Nannofossils</td><td>5</td><td>—</td><td>—</td></tr><tr><td>Limonite</td><td>—</td><td>—</td><td>20</td></tr><tr><td>Albaurite</td><td>—</td><td>5</td><td>5</td></tr></table>	1, 22	1, 106	3, 145	D	M	D	Sand	—	—	—	Silt	5	20	10	Clay	95	80	90	Quartz	3	—	—	Clay	30	35	60	Calcite/dolomite	—	20	5	Cement (sl.)	40	—	—	Accessory minerals	—	—	10	Gypsum detritus	7	40	—	Anhydrite	Tr	—	—	Carbonate detritus	15	—	—	Nannofossils	5	—	—	Limonite	—	—	20	Albaurite	—	5	5
1, 22	1, 106	3, 145																																																																										
D	M	D																																																																										
Sand	—	—	—																																																																									
Silt	5	20	10																																																																									
Clay	95	80	90																																																																									
Quartz	3	—	—																																																																									
Clay	30	35	60																																																																									
Calcite/dolomite	—	20	5																																																																									
Cement (sl.)	40	—	—																																																																									
Accessory minerals	—	—	10																																																																									
Gypsum detritus	7	40	—																																																																									
Anhydrite	Tr	—	—																																																																									
Carbonate detritus	15	—	—																																																																									
Nannofossils	5	—	—																																																																									
Limonite	—	—	20																																																																									
Albaurite	—	5	5																																																																									
								2	1.0				*																																																															
								3																																																																				
								4																																																																				
								5																																																																				
								6																																																																				

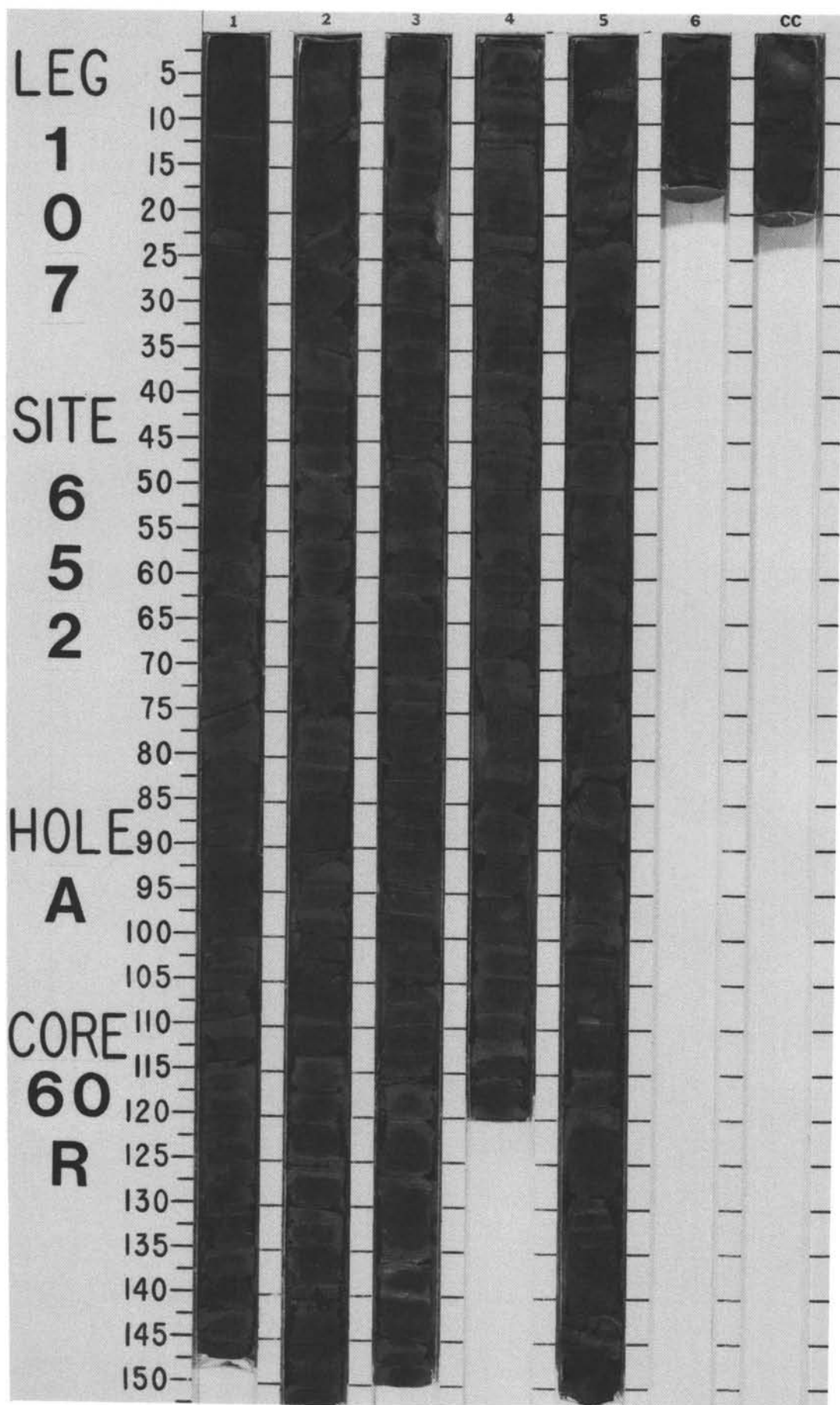


SITE 652 HOLE A CORE 59 R CORED INTERVAL 4002.3-4012.0 mbsl; 556.3-566.0 mbsf

TIME- ROCK UNIT	BIOSTRAT. ZONE/ FOSSIL CHARACTER				PALEOMAGNETICS	PHYS. PROPERTIES	CHEMISTRY	SECTION	METERS	GRAPHIC LITHOLOGY	DRILLING DISTURB.	SED. STRUCTURES	SAMPLES	LITHOLOGIC DESCRIPTION																																																												
	FORAMINIFERS	NANNOFOSSILS	RADIOLARIANS	DIATOMS																																																																						
						$\gamma=2.40 \phi=30 \vee-2026$	27	1	0.5 1.0				*	CLAYSTONE and DOLOMITIC CLAYSTONE Fine alternations (1-6 cm) of claystone with well-cemented dolomitic claystone, from very homogeneous weak red (10R 4/3) in the upper part of the core to light olive-brown (2.5Y 5/4). Thin, varicolored laminae appear randomly. Minor lithology: Section 1, 90, 130, and 140 cm, and Sections 3, 8, 10, and 12, red (10R 4/6), hematite-rich, bauxitic material; Section 1, 45 cm, Section 2, 36, 102, 131, and 148 cm, and Section 3, 7 and 10-13 cm, yellow (2.5Y 7/6), limonite-rich horizons; Section 4, 12-32 cm, two layers of crystalline dolomite. Apparent dip: 3-6°. SMEAR SLIDE SUMMARY (%): <table><tr><td></td><td>1, 62</td><td>2, 37</td><td>2, 133</td></tr><tr><td>D</td><td></td><td>M</td><td>M</td></tr></table> TEXTURE: <table><tr><td>Sand</td><td>—</td><td>—</td><td>—</td></tr><tr><td>Silt</td><td>5</td><td>5</td><td>5</td></tr><tr><td>Clay</td><td>95</td><td>95</td><td>95</td></tr></table> COMPOSITION: <table><tr><td>Quartz</td><td>Tr</td><td>Tr</td><td>—</td></tr><tr><td>Clay</td><td>35</td><td>50</td><td>55</td></tr><tr><td>Calcite/dolomite</td><td>15</td><td>2</td><td>3</td></tr><tr><td>Cement (si.)</td><td>25</td><td>—</td><td>—</td></tr><tr><td>Opaques</td><td>10</td><td>—</td><td>10</td></tr><tr><td>Gypsum</td><td>Tr</td><td>3</td><td>—</td></tr><tr><td>Carbonate detritus</td><td>10</td><td>—</td><td>—</td></tr><tr><td>Limonite</td><td>5</td><td>—</td><td>27</td></tr><tr><td>Anhydrite</td><td>—</td><td>Tr</td><td>—</td></tr><tr><td>Iron oxide</td><td>—</td><td>45</td><td>5</td></tr></table>		1, 62	2, 37	2, 133	D		M	M	Sand	—	—	—	Silt	5	5	5	Clay	95	95	95	Quartz	Tr	Tr	—	Clay	35	50	55	Calcite/dolomite	15	2	3	Cement (si.)	25	—	—	Opaques	10	—	10	Gypsum	Tr	3	—	Carbonate detritus	10	—	—	Limonite	5	—	27	Anhydrite	—	Tr	—	Iron oxide	—	45	5
	1, 62	2, 37	2, 133																																																																							
D		M	M																																																																							
Sand	—	—	—																																																																							
Silt	5	5	5																																																																							
Clay	95	95	95																																																																							
Quartz	Tr	Tr	—																																																																							
Clay	35	50	55																																																																							
Calcite/dolomite	15	2	3																																																																							
Cement (si.)	25	—	—																																																																							
Opaques	10	—	10																																																																							
Gypsum	Tr	3	—																																																																							
Carbonate detritus	10	—	—																																																																							
Limonite	5	—	27																																																																							
Anhydrite	—	Tr	—																																																																							
Iron oxide	—	45	5																																																																							
						$\gamma=2.43 \phi=24 \vee-2467$	7	2					*																																																													
							22	3					*																																																													
								4					*																																																													
								CC																																																																		

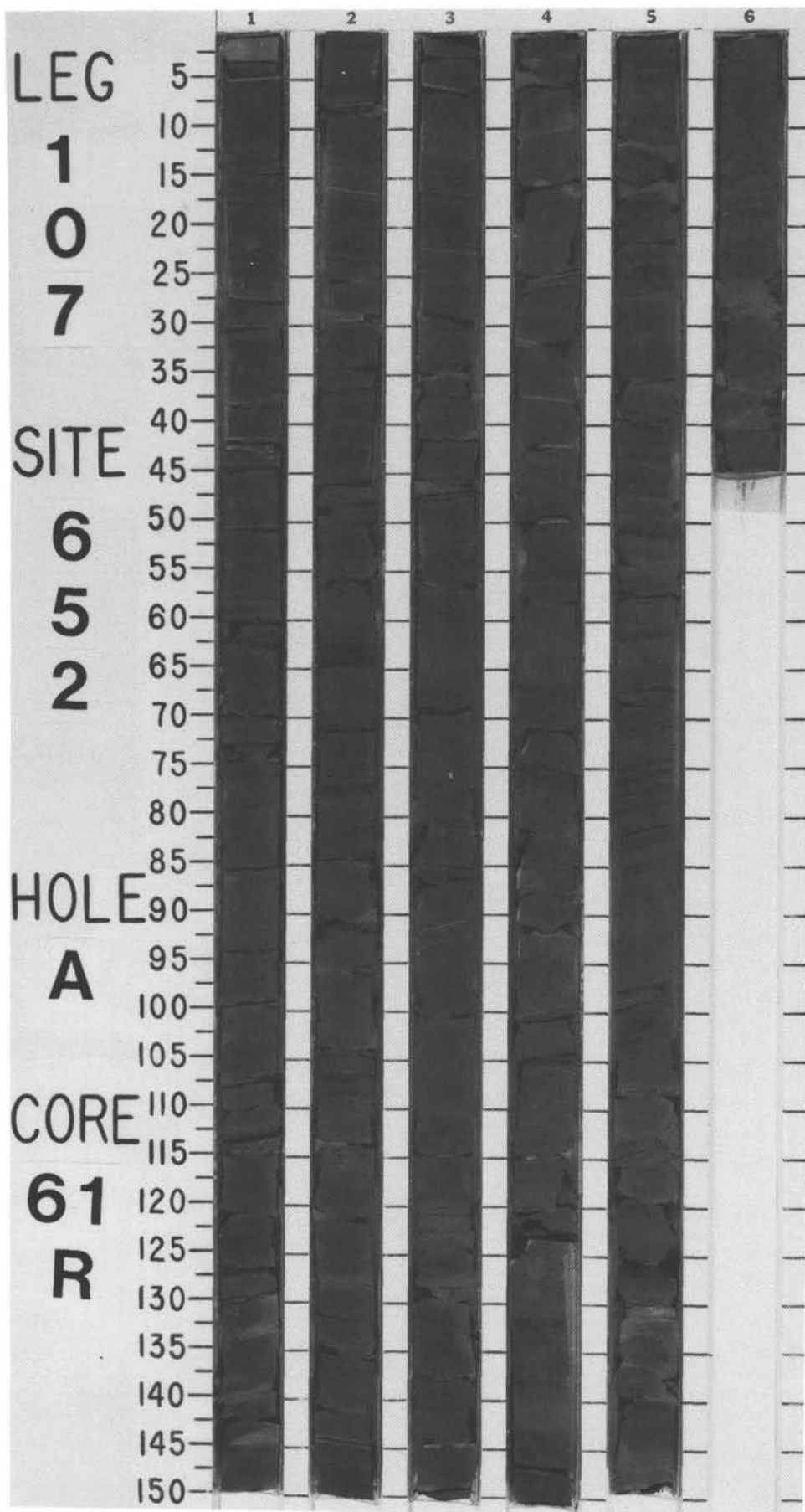


568

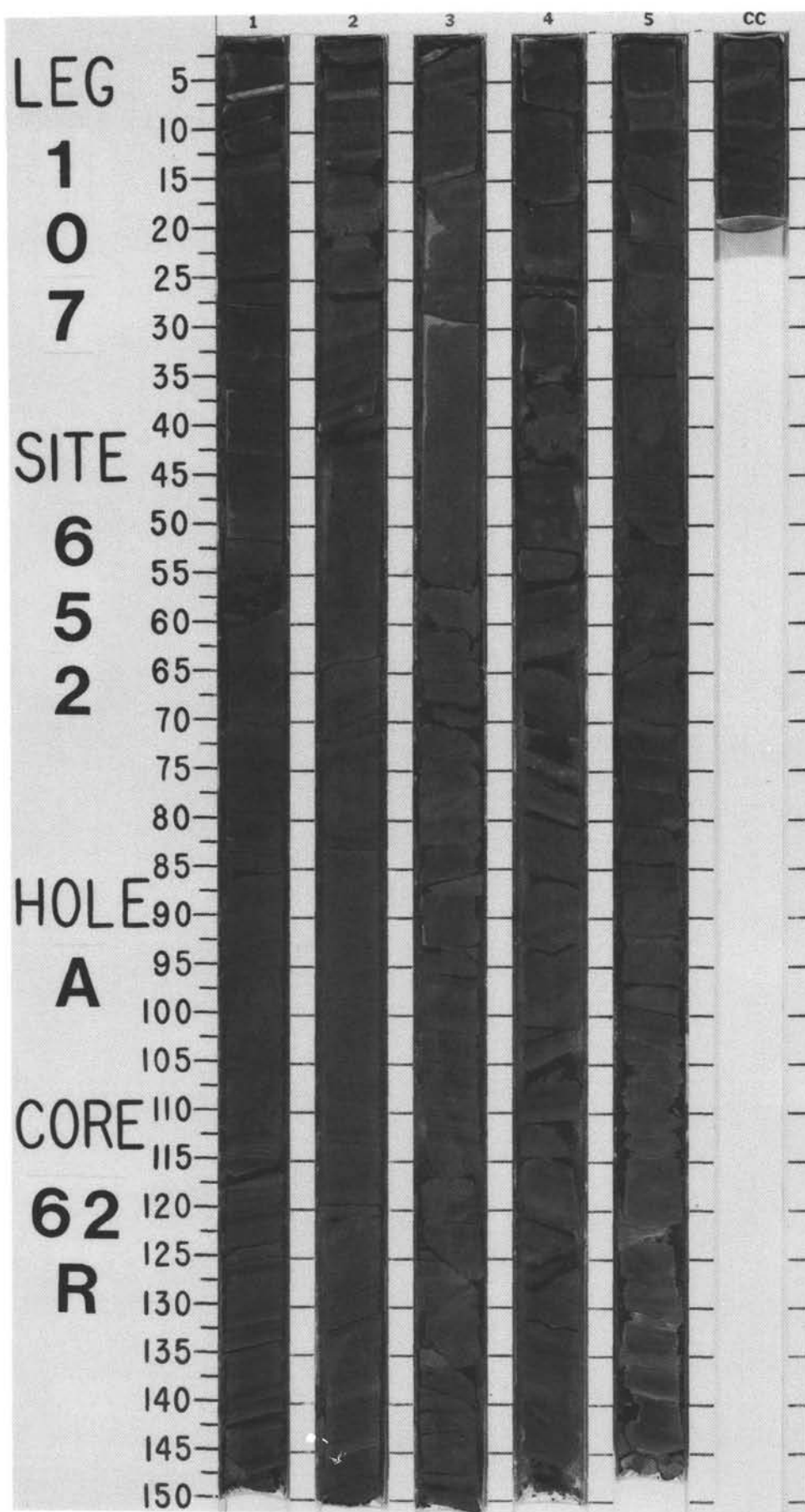


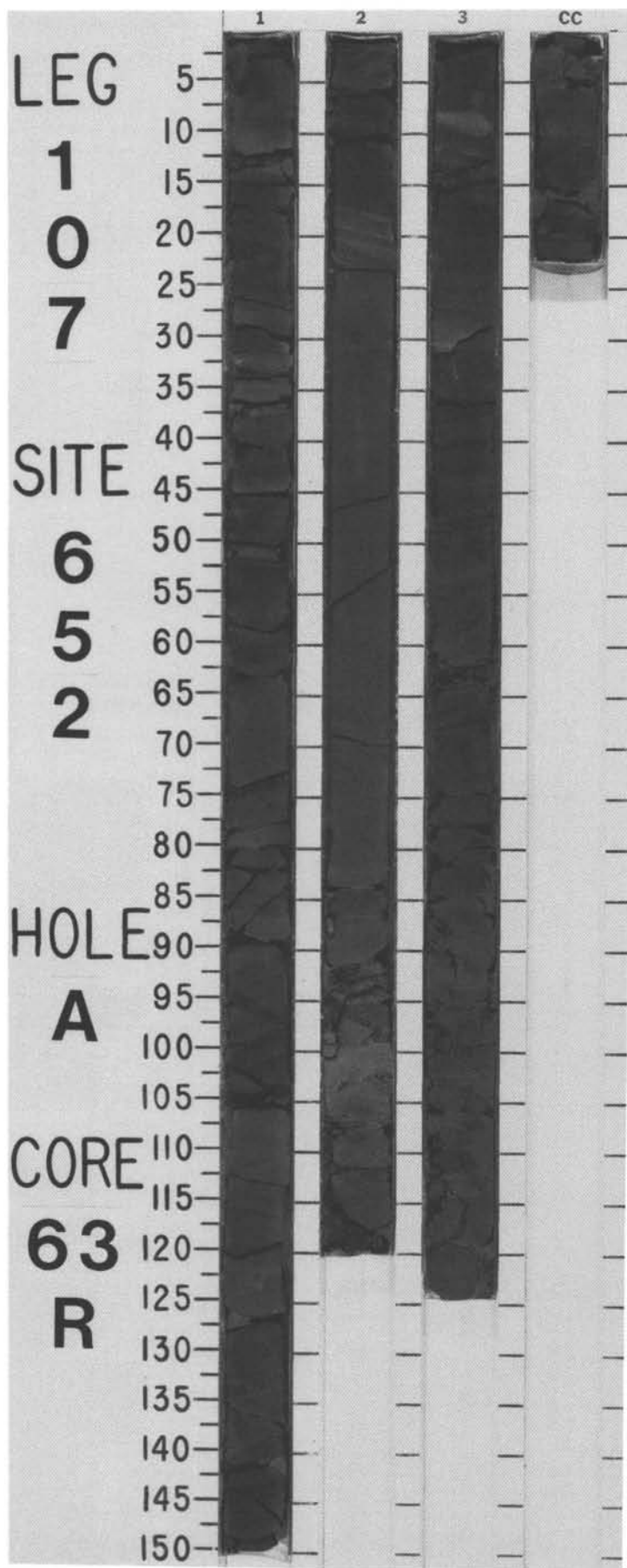
SITE 652 HOLE A CORE 61 R CORED INTERVAL 4021.6-4031.2 mbsl; 575.6-585.2 mbsf

TIME-ROCK UNIT	BIOSTRAT. ZONE/ FOSSIL CHARACTER				PALEOMAGNETICS	PHYS. PROPERTIES	CHEMISTRY	SECTION	METERS	GRAPHIC LITHOLOGY	DRILLING DISTURB.	SED. STRUCTURES	SAMPLES	LITHOLOGIC DESCRIPTION																																																				
	FORAMINIFERS	NANNOFOSSILS	RADIOLARIANS	DIATOMS																																																														
						● $\gamma=2.49$ $\phi=26$ $\gamma=2433$	21 ● 12	1	0.5 1.0					<p>CALCAREOUS and DOLOMITIC MUDSTONE</p> <p>Calcareous mudstone, very dark gray (10YR 3/1) to dark gray (10YR 4/1), in Sections 1, 2, 3, and Section 5, 0–36 cm, and dolomitic (noncalcareous) mudstone in Section 4, Section 5, 36–150 cm, and Section 6; intervals with very fine (1–5 mm), sharp, parallel black or grayish brown (10YR 5/2) laminae, often discontinuous. Gray (10YR 5/1), dolomitized, sandy mudstone layers containing authigenic feldspar, 1 m to 5 cm thick, occur at regular intervals (about every 15 cm); scours filled with laminated and cross-bedded material are notable sedimentary features.</p> <p>Minor lithology: Section 5, 71 cm, micronodule (about 3 mm in diameter) of pyrite growing in a finely laminated interval without disturbing it, with signs of gentle, current reworking of some laminae; Section 6, 0–25 cm, a slump containing elongated, rectangular pieces of the authigenic feldspar and dolomitized layers (crusts), indicative of early diagenesis.</p> <p>Apparent dip: 10–15°. Section 1, 25 and 43 cm, two faults dipping 65–70° with slickensides (about 90°) and a throw greater than 7 cm.</p> <p>SMEAR SLIDE SUMMARY (%):</p> <table><tr><td></td><td>2, 100</td><td>2, 107</td><td>5, 89</td></tr><tr><td>D</td><td></td><td>M</td><td>M</td></tr></table> <p>TEXTURE:</p> <table><tr><td>Sand</td><td>2</td><td>20</td><td>—</td></tr><tr><td>Silt</td><td>25</td><td>40</td><td>—</td></tr><tr><td>Clay</td><td>73</td><td>40</td><td>100</td></tr></table> <p>COMPOSITION:</p> <table><tr><td>Quartz</td><td>15</td><td>10</td><td>—</td></tr><tr><td>Feldspar (authigenic)</td><td>—</td><td>40</td><td>—</td></tr><tr><td>Mica</td><td>40</td><td>28</td><td>17</td></tr><tr><td>Calcite</td><td>40</td><td>5</td><td>—</td></tr><tr><td>Dolomite</td><td>4</td><td>15</td><td>80</td></tr><tr><td>Accessory minerals</td><td>1</td><td>2</td><td>—</td></tr><tr><td>Zeolites</td><td>Tr</td><td>—</td><td>—</td></tr><tr><td>Opauques</td><td>—</td><td>—</td><td>3</td></tr></table>		2, 100	2, 107	5, 89	D		M	M	Sand	2	20	—	Silt	25	40	—	Clay	73	40	100	Quartz	15	10	—	Feldspar (authigenic)	—	40	—	Mica	40	28	17	Calcite	40	5	—	Dolomite	4	15	80	Accessory minerals	1	2	—	Zeolites	Tr	—	—	Opauques	—	—	3
	2, 100	2, 107	5, 89																																																															
D		M	M																																																															
Sand	2	20	—																																																															
Silt	25	40	—																																																															
Clay	73	40	100																																																															
Quartz	15	10	—																																																															
Feldspar (authigenic)	—	40	—																																																															
Mica	40	28	17																																																															
Calcite	40	5	—																																																															
Dolomite	4	15	80																																																															
Accessory minerals	1	2	—																																																															
Zeolites	Tr	—	—																																																															
Opauques	—	—	3																																																															
						● $\gamma=2.45$ $\phi=32$ $\gamma=2309$	38 ● 27	2																																																										
								3																																																										
								4																																																										
								5																																																										
								CC																																																										



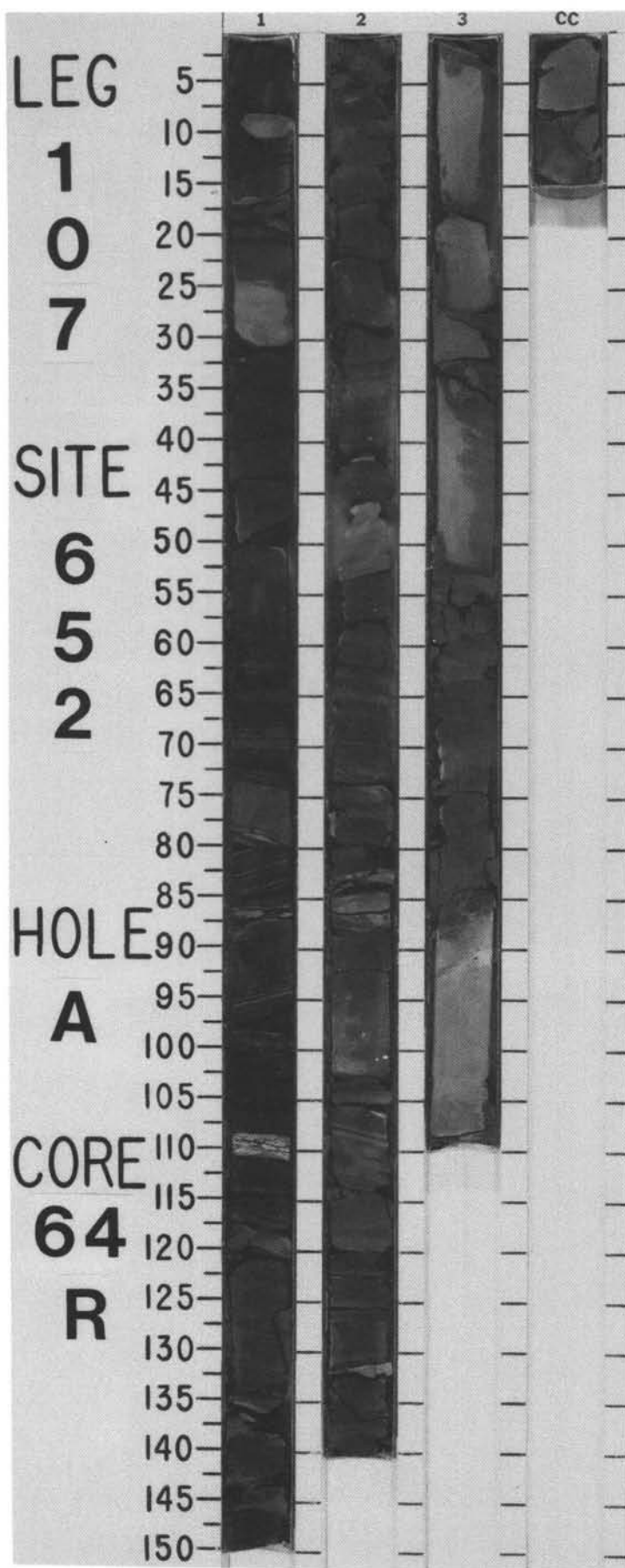
572





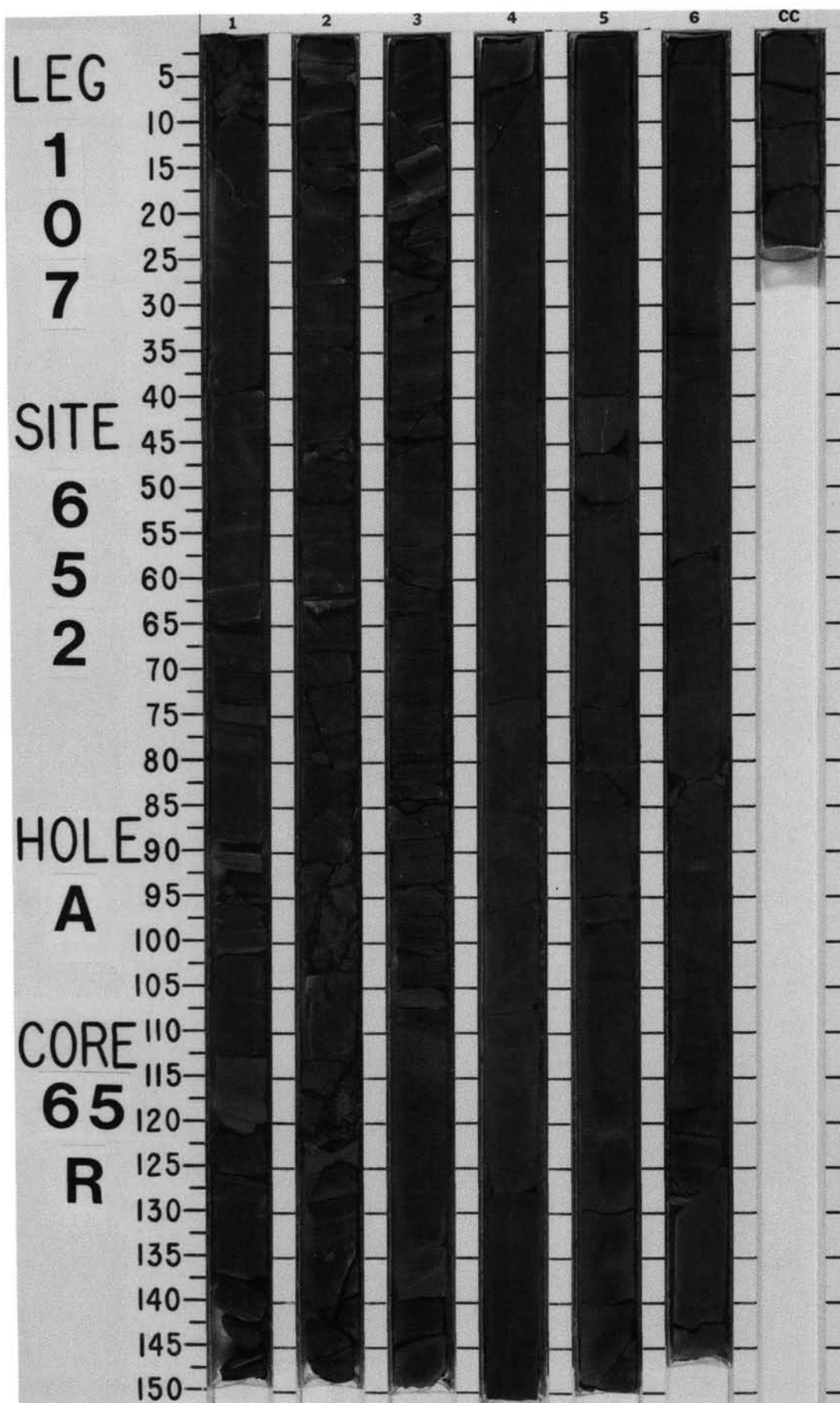
SITE 652 HOLE A CORE 64 R CORED INTERVAL 4050.5-4060.2 mbsl; 604.5 614.2 mbsf

TIME-ROCK UNIT	BIOSTRAT. ZONE/ FOSSIL CHARACTER				PALEOMAGNETICS	PHYS. PROPERTIES	CHEMISTRY	SECTION	METERS	GRAPHIC LITHOLOGY	DRILLING DISTURB.	SED. STRUCTURES	SAMPLES	LITHOLOGIC DESCRIPTION
	FORAMINIFERS	NANNOFOSSILS	RADIOLARIANS	DIAZONIS										



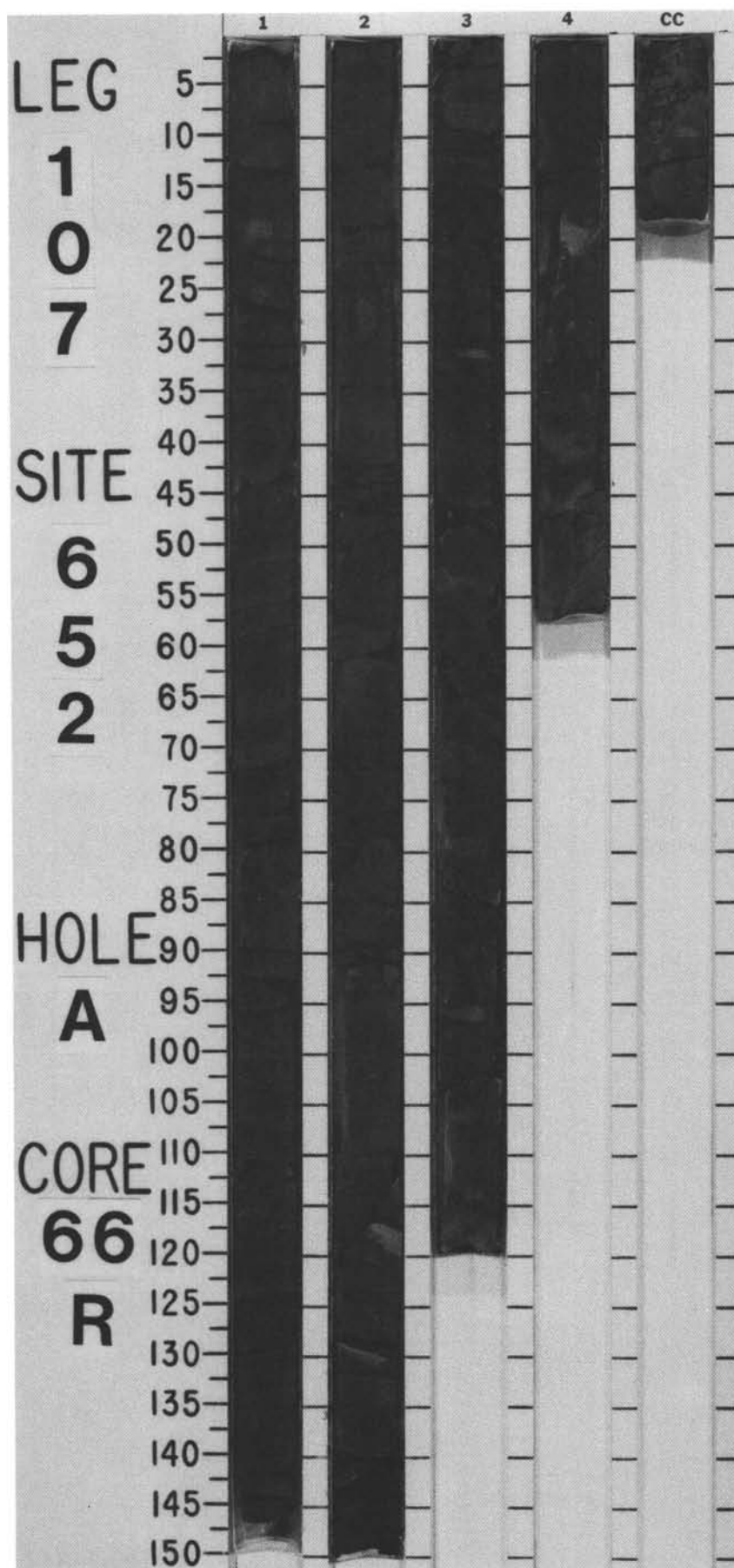
SITE 652 HOLE A CORE 65 R CORED INTERVAL 4060.2-4070.5 mbsl; 614.2-624.5 mbsf

TIME-ROCK UNIT	BIOSTRAT. ZONE/ FOSSIL CHARACTER				PALEOMAGNETICS	PHYS. PROPERTIES	CHEMISTRY	SECTION	METERS	GRAPHIC LITHOLOGY	DRILLING DISTURB.	SED. STRUCTURES	SAMPLES	LITHOLOGIC DESCRIPTION
	FORAMINIFERS	NANNOFOSSILS	RADIOLARIANS	DIATOMS										
						$\gamma=2.25 \phi=30$ V-2230 ●	11 ● 16 ● 17 ● 19 ●							
						$\gamma=2.77 \phi=31$ V-3960 ●	10 ●							
							●17							
								CC						

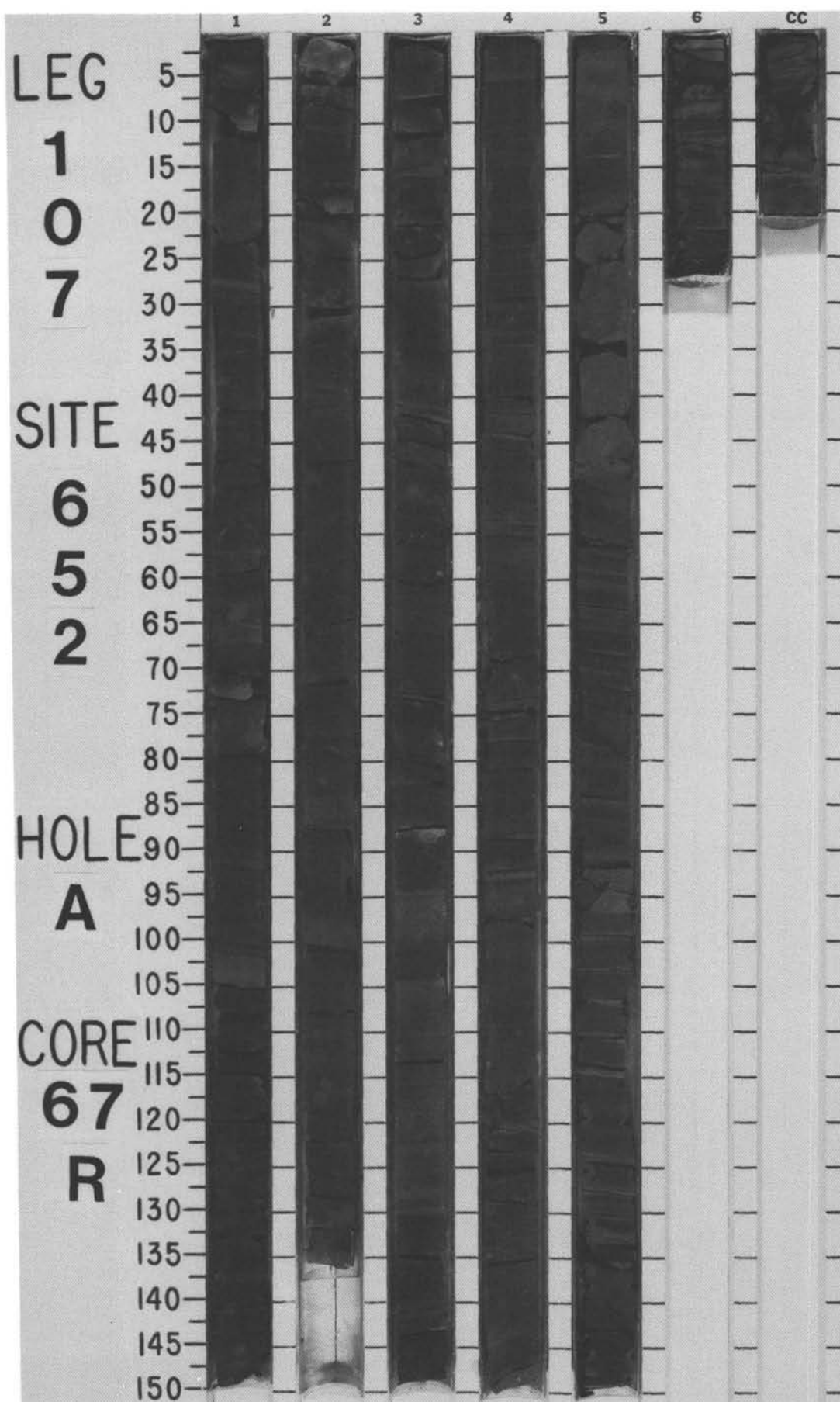


SITE 652 HOLE A CORE 66 R CORED INTERVAL 4070.5-4080.2 mbsl; 624.5-634.2 mbsf

TIME- ROCK UNIT	BIOSTRAT. ZONE/ FOSSIL CHARACTER				PALEOMAGNETICS	PHYS. PROPERTIES	CHEMISTRY	SECTION	METERS	GRAPHIC LITHOLOGY	DRILLING DISTURB.	SED. STRUCTURES	SAMPLES	LITHOLOGIC DESCRIPTION																																																												
	FORAMINIFERS	NANNOFOSSILS	RADIOLARIANS	DIATOMS																																																																						
						$\gamma=2.59 \phi=19 \vee-2764 \bullet$	38 ●	1	0.5 1.0					<p>CALCAREOUS MUDSTONE</p> <p>Monotonous succession of olive (5Y 5/2, 5/3) calcareous mudstone sequences. Sequences are generally 10 cm, beginning with well-indurated, graded (mainly normal), dolomitic, sandy siltstone with current marks; top of sequences is marked by parallel laminated calcareous mudstone. Convolute laminations occur in Section 1, 110-140 cm, and in Section 2, 80-140 cm.</p> <p>Dip reaches 52° in Section 2, 80-140 cm.</p> <p>SMEAR SLIDE SUMMARY (%):</p> <table><tr><td></td><td>1, 90</td><td>3, 95</td><td>4, 23</td></tr><tr><td>D</td><td>D</td><td>D</td><td>D</td></tr></table> <p>TEXTURE:</p> <table><tr><td>Sand</td><td>5</td><td>—</td><td>—</td></tr><tr><td>Silt</td><td>25</td><td>20</td><td>20</td></tr><tr><td>Clay</td><td>70</td><td>80</td><td>80</td></tr></table> <p>COMPOSITION:</p> <table><tr><td>Quartz</td><td>3</td><td>—</td><td>—</td></tr><tr><td>Mica</td><td>5</td><td>3</td><td>Tr</td></tr><tr><td>Clay</td><td>20</td><td>30</td><td>25</td></tr><tr><td>Dolomite</td><td>15</td><td>20</td><td>15</td></tr><tr><td>Cement (si.)</td><td>30</td><td>35</td><td>25</td></tr><tr><td>Opacues</td><td>—</td><td>Tr</td><td>5</td></tr><tr><td>Anhydrite detritus</td><td>5</td><td>—</td><td>—</td></tr><tr><td>Gypsum detritus</td><td>7</td><td>5</td><td>5</td></tr><tr><td>Carbonate detritus</td><td>15</td><td>—</td><td>20</td></tr><tr><td>Nannofossils</td><td>—</td><td>7</td><td>5</td></tr></table>		1, 90	3, 95	4, 23	D	D	D	D	Sand	5	—	—	Silt	25	20	20	Clay	70	80	80	Quartz	3	—	—	Mica	5	3	Tr	Clay	20	30	25	Dolomite	15	20	15	Cement (si.)	30	35	25	Opacues	—	Tr	5	Anhydrite detritus	5	—	—	Gypsum detritus	7	5	5	Carbonate detritus	15	—	20	Nannofossils	—	7	5
	1, 90	3, 95	4, 23																																																																							
D	D	D	D																																																																							
Sand	5	—	—																																																																							
Silt	25	20	20																																																																							
Clay	70	80	80																																																																							
Quartz	3	—	—																																																																							
Mica	5	3	Tr																																																																							
Clay	20	30	25																																																																							
Dolomite	15	20	15																																																																							
Cement (si.)	30	35	25																																																																							
Opacues	—	Tr	5																																																																							
Anhydrite detritus	5	—	—																																																																							
Gypsum detritus	7	5	5																																																																							
Carbonate detritus	15	—	20																																																																							
Nannofossils	—	7	5																																																																							
						$\gamma=2.52 \phi=22 \vee-3322 \bullet$	● 23	2																																																																		
							● 22	3																																																																		
								4																																																																		
								CC																																																																		

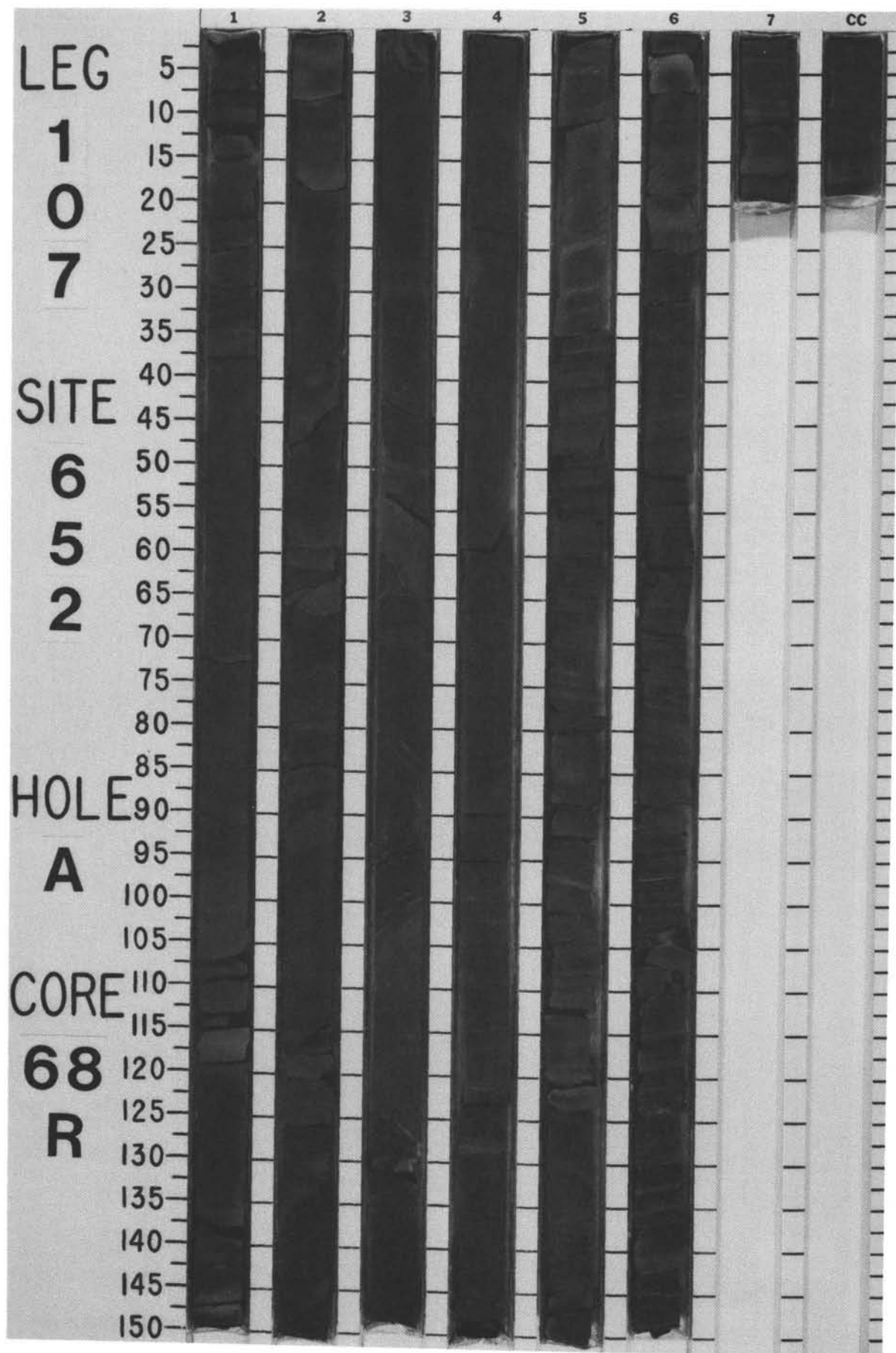


582



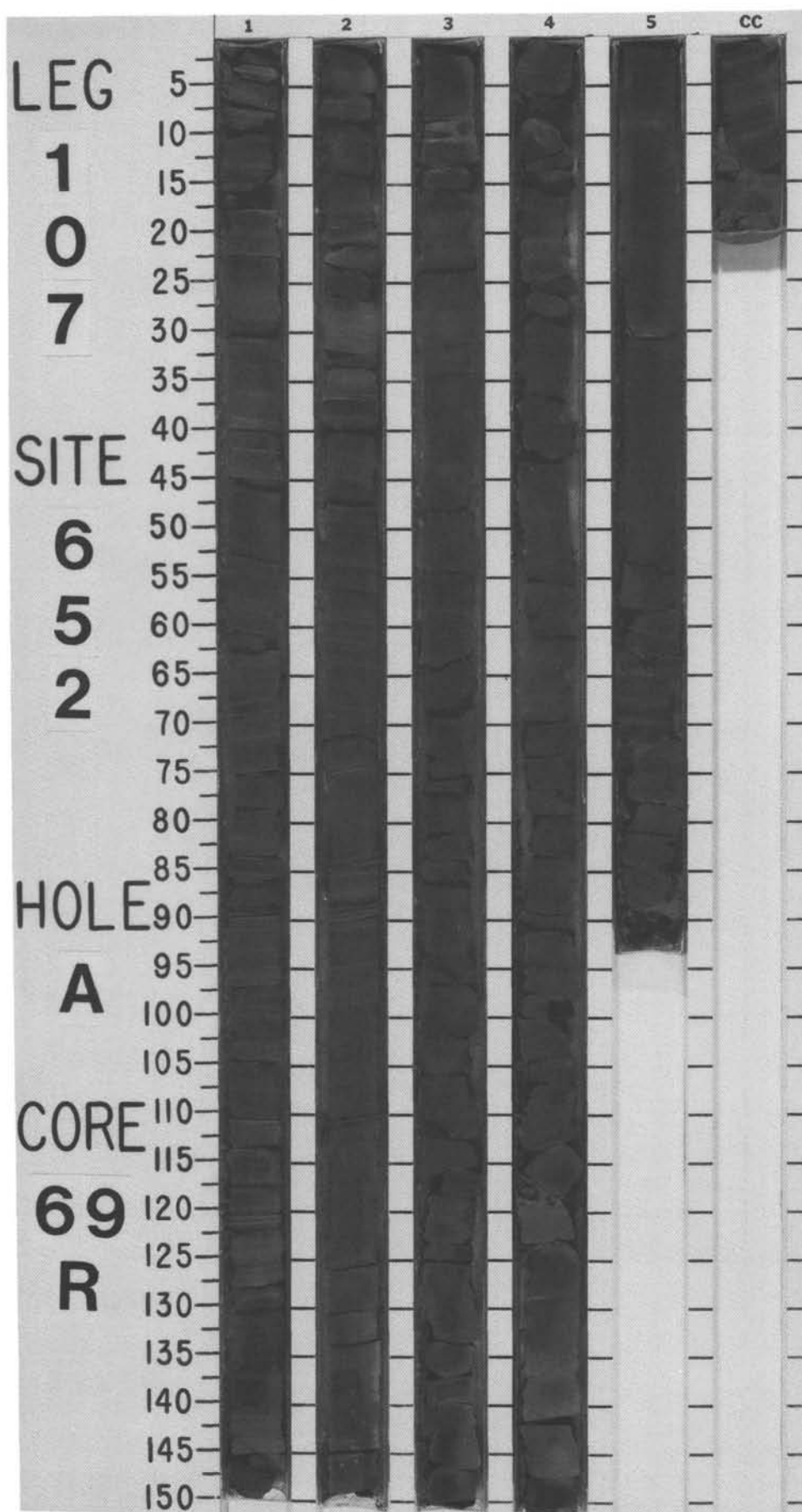
SITE 652 HOLE A CORE 68 R CORED INTERVAL 4089.8-4099.4 mbsl; 643.8-653.4 mbsf

TIME-ROCK UNIT	BIOSTRAT. ZONE/ FOSSIL CHARACTER				PALEOMAGNETICS	PHYS. PROPERTIES	CHEMISTRY	SECTION	METERS	GRAPHIC LITHOLOGY	DRILLING DISTURB.	SED. STRUCTURES	SAMPLES	LITHOLOGIC DESCRIPTION
	FORAMINIFERS	NANNOFOSSILS	RADIOLARIANS	DIAZONES										
						$\gamma = 2.55$ $\phi = 22$ $V = 2508$	46 15 20		0.5 1 1.0					
								2					*	CALCAREOUS or DOLOMITIC MUDSTONE
														Dark gray (5Y 4/1), gray (5Y 5/1), and light gray (5Y 6/1), calcareous mudstone, finely laminated with normally graded intervals; minor dolomitic mudstone occurs in Section 6, 10–25 and 80–150 cm, Section 7, and CC. Large slump feature in Section 1, 31 cm, to Section 5, 34 cm, includes disturbed layers of calcareous mudstone and minor sandy, calcareous mudstone. In Section 5, 48 cm, through CC, intercalations of sharp and diffuse laminae (about 1 mm thick); scattered blebs of sulfate minerals (anhydrite, celestite?, barite?) in both calcareous and dolomitic mudstone intervals.
														Apparent dip: Section 1, 12–15°.
														SMEAR SLIDE SUMMARY (%):
														1, 24 D 2, 65 M 6, 78 M
														TEXTURE:
														Sand 5 25 —
														Silt 25 25 —
														Clay 70 50 —
														COMPOSITION:
														Quartz 8 15 —
														Feldspar — 2 —
														Clay 35 32 —
														Calcite 40 40 —
														Dolomite 15 8 —
														Organic remains 2 1 —
														Pyrite Tr — —
														Zeolites — Tr —
														Gypsum? — 2 —
														Anhydrite — — 10
														Barite? — — 15
														Celestite? — — 75



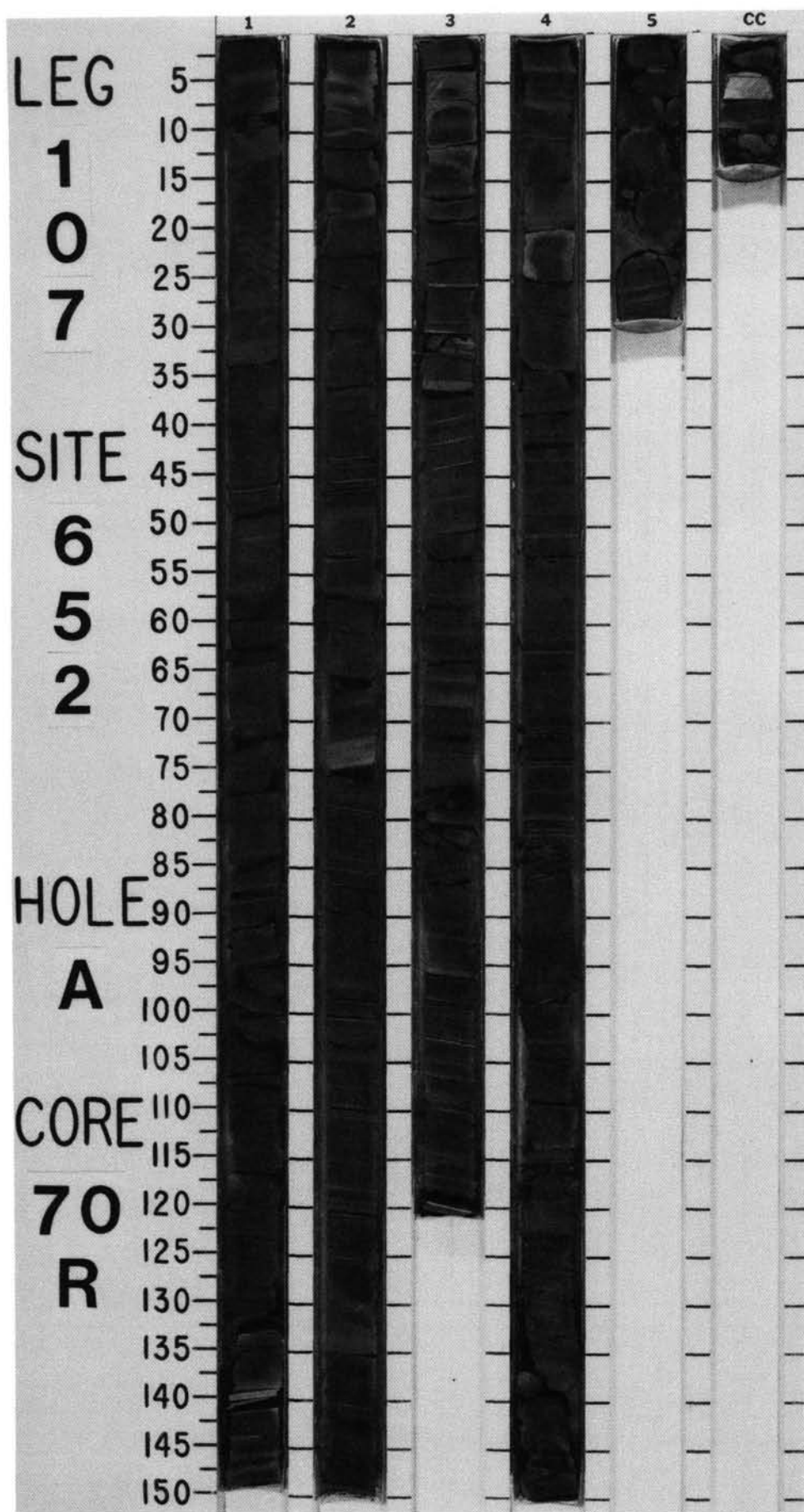
SITE 652 HOLE A CORE 69 R CORED INTERVAL 4099.4-4109.1 mbsl; 653.4-663.1 mbsf

TIME-ROCK UNIT	BIOSTRAT. ZONE/ FOSSIL CHARACTER				PALEOMAGNETICS	PHYS. PROPERTIES	CHEMISTRY	SECTION	METERS	GRAPHIC LITHOLOGY	DRILLING DISTURB.	SED. STRUCTURES	SAMPLES	LITHOLOGIC DESCRIPTION																																																												
	FORAMINIFERS	NANNOFOSSILS	RADIOLARIANS	DIATOMS																																																																						
						γ -2.56 ϕ -22 γ -2414 ●			1	0.5			*	<p>CALCAREOUS MUDSTONE</p> <p>Dark gray (5Y 4/1), gray (5Y 5/1), and light gray (5Y 6/1), calcareous mudstone with fine, parallel laminae, but commonly homogeneous (as seen in Section 4, 20–150 cm).</p> <p>Minor lithology: Section 1 and Section 2, 11–130 cm, numerous, fine, white laminae of sulfates of varying thickness from <1 mm to 5 mm and scattered, fine sulfate crystals (small blebs) occur within the dark mudstone; sulfates are predominantly anhydrite with lesser amounts of possible celestite; a notable sulfate layer occurs in Section 2, 125–126 cm. The boundaries between mudstone and sulfate layers are wavy and distorted, suggesting in situ growth of the sulfate. It also appears to begin growth as small discrete nodules that coalesce to form layers (as with typical nodular anhydrite).</p> <p>Apparent dip: Section 1, 5–8°.</p> <p>SMEAR SLIDE SUMMARY (%):</p> <table><tr><td></td><td>1, 66</td><td>2, 127</td><td>3, 48</td></tr><tr><td></td><td>M</td><td>M</td><td>D</td></tr></table> <p>TEXTURE:</p> <table><tr><td>Sand</td><td>—</td><td>90</td><td>10</td></tr><tr><td>Silt</td><td>20</td><td>10</td><td>25</td></tr><tr><td>Clay</td><td>80</td><td>—</td><td>65</td></tr></table> <p>COMPOSITION:</p> <table><tr><td>Quartz</td><td>8</td><td>—</td><td>12</td></tr><tr><td>Clay</td><td>36</td><td>—</td><td>22</td></tr><tr><td>Calcite</td><td>35</td><td>—</td><td>50</td></tr><tr><td>Dolomite</td><td>15</td><td>—</td><td>10</td></tr><tr><td>Pore space (org. remains)</td><td>—</td><td>2</td><td>—</td></tr><tr><td>Opaque (amorphous, org?)</td><td>2</td><td>—</td><td>—</td></tr><tr><td>Gypsum</td><td>2</td><td>—</td><td>2</td></tr><tr><td>Anhydrite</td><td>—</td><td>30</td><td>—</td></tr><tr><td>Celestite</td><td>—</td><td>68</td><td>2</td></tr><tr><td>Organic remains</td><td>—</td><td>—</td><td>2</td></tr></table>		1, 66	2, 127	3, 48		M	M	D	Sand	—	90	10	Silt	20	10	25	Clay	80	—	65	Quartz	8	—	12	Clay	36	—	22	Calcite	35	—	50	Dolomite	15	—	10	Pore space (org. remains)	—	2	—	Opaque (amorphous, org?)	2	—	—	Gypsum	2	—	2	Anhydrite	—	30	—	Celestite	—	68	2	Organic remains	—	—	2
	1, 66	2, 127	3, 48																																																																							
	M	M	D																																																																							
Sand	—	90	10																																																																							
Silt	20	10	25																																																																							
Clay	80	—	65																																																																							
Quartz	8	—	12																																																																							
Clay	36	—	22																																																																							
Calcite	35	—	50																																																																							
Dolomite	15	—	10																																																																							
Pore space (org. remains)	—	2	—																																																																							
Opaque (amorphous, org?)	2	—	—																																																																							
Gypsum	2	—	2																																																																							
Anhydrite	—	30	—																																																																							
Celestite	—	68	2																																																																							
Organic remains	—	—	2																																																																							
						● 15		2	1.0				*																																																													
								3					*																																																													
						● 25		4					*																																																													
								5					*																																																													
								CC					*																																																													



SITE 652 HOLE A CORE 70 R CORED INTERVAL 4109.1-4118.8 mbsl; 663.1-672.8 mbsf

TIME-ROCK UNIT	BIOSTRAT. ZONE/ FOSSIL CHARACTER				PALEOMAGNETICS	PHYS. PROPERTIES	CHEMISTRY	SECTION	METERS	GRAPHIC LITHOLOGY	DRILLING DISTURB.	SED. STRUCTURES	SAMPLES	LITHOLOGIC DESCRIPTION																																				
	FORAMINIFERS	NANNOFOSSILS	RADIOLARIANS	DIATOMS																																														
						$\gamma = 2.51$ $\phi = 21$ $\psi = 2970$	\bullet 21		0.5 1.0					<p>CALCAREOUS and DOLOMITIC MUDSTONE, ANHYDRITE</p> <p>Finely to very finely laminated mudstone interbedded with rare, sandy mudstone intervals, dark gray (5Y 4/1), gray (5Y 5/1), and light gray (5Y 6/1). Mudstone is calcareous in Section 1, Section 2, 0–65 cm, Section 4, 60–110 and 140–150 cm, and Section 5, 0–20 cm. Mudstone is dolomitic in Section 2, 65–150 cm, Section 3, Section 4, 0–60 and 110–140 cm, and Section 5, 20–29 cm. Sandy mudstone intervals are 2 mm to 2 cm thick, and contain current-reworking structures.</p> <p>Minor lithology: numerous intervals of dark bluish gray (5B 4/1) anhydrite, with possible celestite(?), varying in thickness from 1 mm to 5.5 cm. These intervals have wavy contacts at their upper and lower boundaries, probably due to the growth pattern of the sulfate nodules. Dispersed blebs are also common. Section 4, 112–118 cm, a 5.5-cm layer of sulfate shows a nodular, coalescing growth pattern on a macroscale (compared with the microlaminae).</p> <p>SMEAR SLIDE SUMMARY (%):</p> <table><tr><td></td><td>2, 74</td><td>4, 115</td></tr><tr><td></td><td>M</td><td>M</td></tr></table> <p>TEXTURE:</p> <table><tr><td>Sand</td><td>10</td><td>—</td></tr><tr><td>Silt</td><td>10</td><td>—</td></tr><tr><td>Clay</td><td>80</td><td>—</td></tr></table> <p>COMPOSITION:</p> <table><tr><td>Quartz</td><td>8</td><td>—</td></tr><tr><td>Feldspar</td><td>4</td><td>—</td></tr><tr><td>Clay</td><td>28</td><td>—</td></tr><tr><td>Volcanic glass</td><td>Tr</td><td>—</td></tr><tr><td>Dolomiticrite</td><td>60</td><td>—</td></tr><tr><td>Celestite</td><td>—</td><td>60</td></tr><tr><td>Anhydrite</td><td>—</td><td>40</td></tr></table>		2, 74	4, 115		M	M	Sand	10	—	Silt	10	—	Clay	80	—	Quartz	8	—	Feldspar	4	—	Clay	28	—	Volcanic glass	Tr	—	Dolomiticrite	60	—	Celestite	—	60	Anhydrite	—	40
	2, 74	4, 115																																																
	M	M																																																
Sand	10	—																																																
Silt	10	—																																																
Clay	80	—																																																
Quartz	8	—																																																
Feldspar	4	—																																																
Clay	28	—																																																
Volcanic glass	Tr	—																																																
Dolomiticrite	60	—																																																
Celestite	—	60																																																
Anhydrite	—	40																																																
						$\gamma = 2.58$ $\phi = 21$ $\psi = 2963$	\bullet 19 \bullet 37																																											
							</																																											

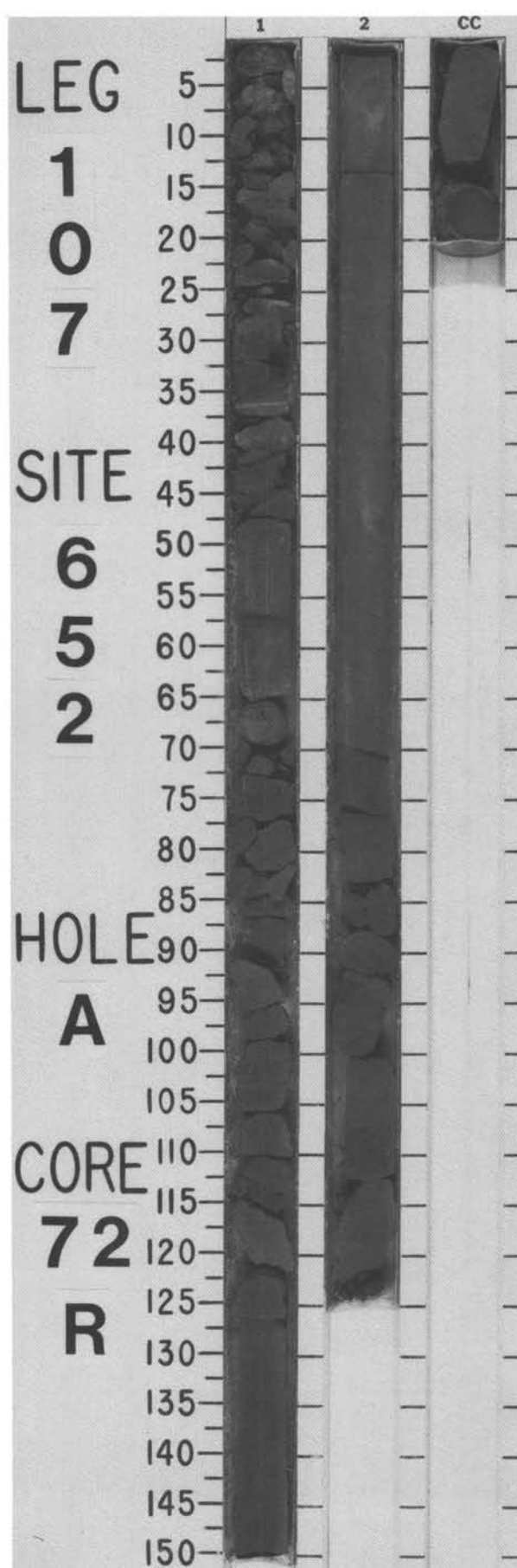
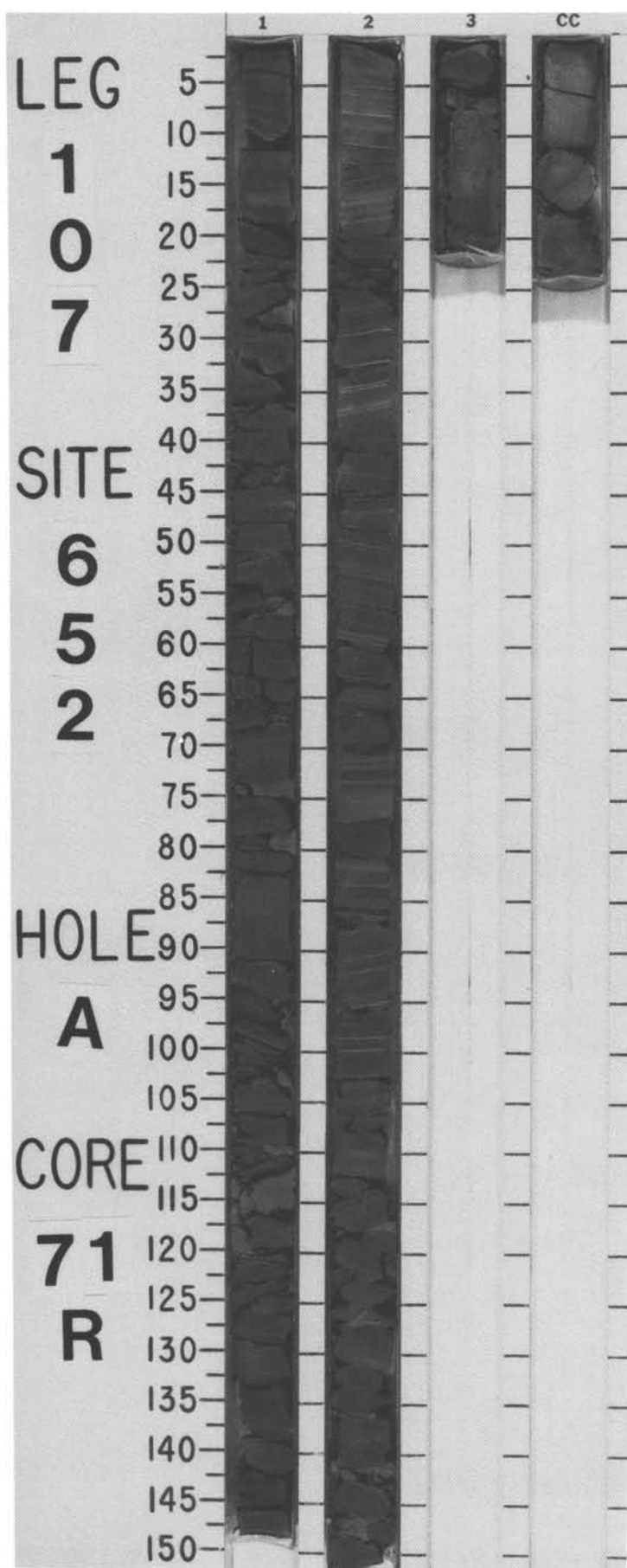


SITE 652 HOLE A CORE 71 R CORED INTERVAL 4118.8-4128.5 mbsl; 672.8-682.5 mbsf

TIME-ROCK UNIT	BIOSTRAT. ZONE/ FOSSIL CHARACTER				PALEOMAGNETICS	PHYS. PROPERTIES	CHEMISTRY	SECTION	METERS	GRAPHIC LITHOLOGY	DRILLING DISTURB.	SED. STRUCTURES	SAMPLES	LITHOLOGIC DESCRIPTION
	FORAMINIFERS	NANNOFOSSILS	RADIOLARIANS	DIATOMS										
						γ -2.58 ϕ =21 γ -2933 ϕ =20 γ -2491	●21 ●24	1 2 3 CC	0.5 1.0					<p>CALCAREOUS and DOLOMITIC MUDSTONE</p> <p>Finely to very finely laminated mudstone interbedded with rare sandy mudstone intervals; from dark gray (5Y 4/1) to gray (5Y 5/1) to light gray (5Y 6/1). The mudstone could be either calcareous or dolomitic. Core is similar to Core 70R, but with poorer recovery.</p>

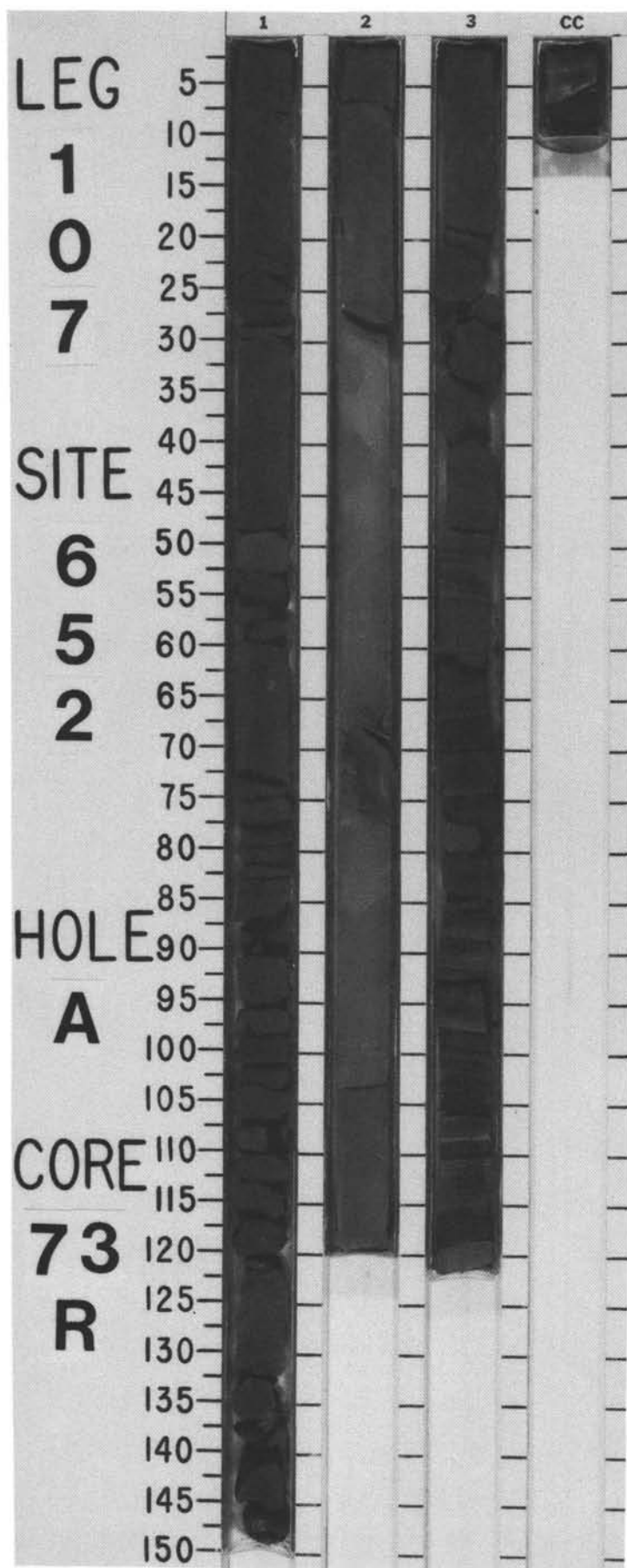
SITE 652 HOLE A CORE 72 R CORED INTERVAL 4128.5-4138.2 mbsl; 682.5-692.2 mbsf

TIME-ROCK UNIT	BIOSTRAT. ZONE/ FOSSIL CHARACTER				PALEOMAGNETICS	PHYS. PROPERTIES	CHEMISTRY	SECTION	METERS	GRAPHIC LITHOLOGY	DRILLING DISTURB.	SED. STRUCTURES	SAMPLES	LITHOLOGIC DESCRIPTION
	FORAMINIFERS	NANNOFOSSILS	RADIOLARIANS	DIATOMS										
						γ -2.58 ϕ =17 γ -3325 ϕ =15 γ -3338 ϕ =10	●12 ●32 ●35 ●10	1 2 CC	0.5 1.0					<p>SANDY MUDSTONE and CALCAREOUS, SILTY SANDSTONE</p> <p>Laminated, sandy mudstone, dark gray (2.5Y 4/0), progressively more sandy toward the base of the core, and predominately graded (normal), calcareous, silty sandstone in Section 2.</p> <p>SMEAR SLIDE SUMMARY (%):</p> <p style="text-align: right;">2, 50 D</p> <p>TEXTURE:</p> <p>Sand 50 Silt 30 Clay 20</p> <p>COMPOSITION:</p> <p>Quartz 7 Mica 3 Clay 20 Calcite/dolomite 7 Cement (si.) 35 Accessory minerals 3 Gypsum detritus 5 Carbonate detritus 20 Nannofossils Tr</p>



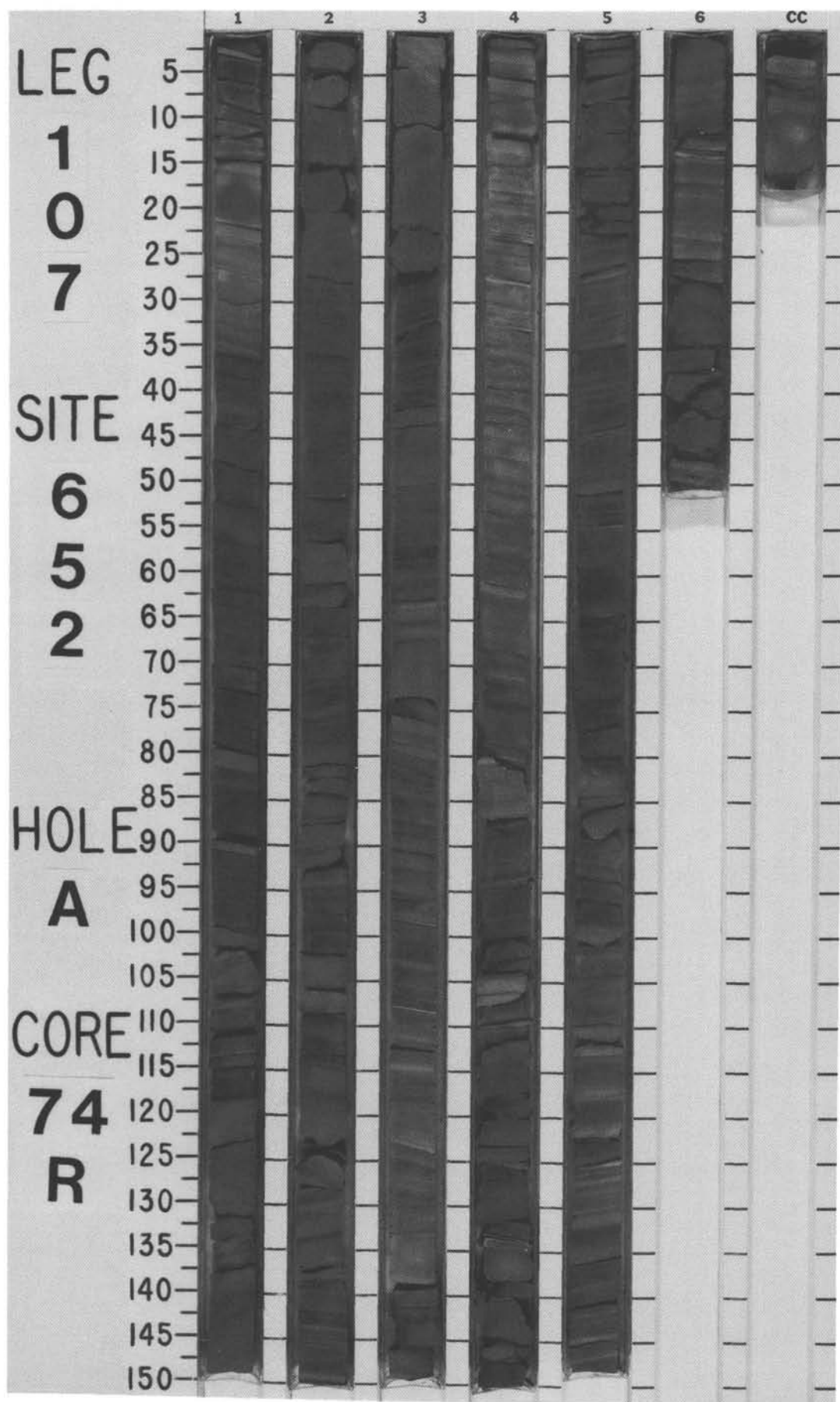
SITE 652 HOLE A CORE 73 R CORED INTERVAL 4138.2-4147.9 mbsl 692.2-701.9 mbsf

TIME-ROCK UNIT	BIOSTRAT. ZONE/ FOSSIL CHARACTER				PALEOMAGNETICS	PHYS. PROPERTIES	CHEMISTRY	SECTION	METERS	GRAPHIC LITHOLOGY	DRILLING DISTURB.	SED. STRUCTURES	SAMPLES	LITHOLOGIC DESCRIPTION
	FORAMINIFERS	NANNOFOSSILS	RADIOLARIANS	DIATOMS										
						$\gamma=2.77$ $\phi=20$ $\nabla=3263$ ●	● 28	1	0.5 1.0				*	CALCAREOUS, SANDY MUDSTONE; SANDY SILTSTONE; and MUDSTONE Dark gray, calcareous, sandy mudstone; sandy siltstone; and mudstone exhibiting salt and pepper texture. Small plant fragments and white mica grains are abundant. Sandy siltstone is generally massive or poorly laminated; a graded (normal) interval could exist. Slumps are numerous. Section 3, 60–120 cm, finer sediment (mudstone) is intercalated with the sandy siltstone.
						●	● 38	2					*	SMEAR SLIDE SUMMARY (%): 1, 68 2, 73 D D TEXTURE: Sand 25 5 Silt 55 60 Clay 20 35 COMPOSITION: Quartz 8 12 Mica 7 5 Clay 25 25 Dolomite 15 8 Cement (si.) 30 25 Gypsum detritus 5 5 Carbonate detritus 10 20
						$\gamma=2.51$ $\phi=18$ $\nabla=3208$ ●	● 24	3					OG	
								CC					X	



SITE 652 HOLE A CORE 74 R CORED INTERVAL 4147.9-4156.5 mbsl; 701.9-710.5 mbsf

TIME-ROCK UNIT	BIOSTRAT. ZONE/ FOSSIL CHARACTER				PALEOMAGNETICS	PHYS. PROPERTIES	CHEMISTRY	SECTION	METERS	GRAPHIC LITHOLOGY	DRILLING DISTURB.	SED. STRUCTURES	SAMPLES	LITHOLOGIC DESCRIPTION																																																																																				
	FORAMINIFERS	NANNOFOSSILS	RADIOLARIANS	DIATOMS																																																																																														
						● $\gamma = 2.75$ $\phi = 13$ V-3608	● 18 ● 36	1	0.5 1.0					CALCAREOUS, SANDY MUDSTONE; SILTY SANDSTONE; and CALCAREOUS MUDSTONE Gray (5Y 5/1 to 5Y 6/1), calcareous, sandy mudstone, alternating with silty sandstone. Sections 1 and 2. Convolute bedding and graded bedding (reverse and normal) are common. Sections 3, 4, 5, and 6 are dominantly gray (5Y 5/1-6/1), calcareous mudstone with minor layers of laminated sandstone. From the base of Section 4 to the end of the core are some intervals of anhydrite, about 1 mm thick. SMEAR SLIDE SUMMARY (%): <table><tr><td></td><td>2, 136 D</td><td>3, 96 M</td><td>4, 22 M</td><td>5, 54 M</td><td>CC, 10 D</td></tr></table> TEXTURE: <table><tr><td>Sand</td><td>25</td><td>—</td><td>—</td><td>—</td><td>—</td></tr><tr><td>Silt</td><td>55</td><td>—</td><td>10</td><td>—</td><td>—</td></tr><tr><td>Clay</td><td>20</td><td>100</td><td>90</td><td>100</td><td>100</td></tr></table> COMPOSITION: <table><tr><td>Quartz</td><td>15</td><td>Tr</td><td>—</td><td>—</td><td>5</td></tr><tr><td>Mica</td><td>5</td><td>—</td><td>—</td><td>—</td><td>—</td></tr><tr><td>Clay</td><td>20</td><td>40</td><td>30</td><td>—</td><td>55</td></tr><tr><td>Calcite/dolomite</td><td>15</td><td>—</td><td>5</td><td>—</td><td>Tr</td></tr><tr><td>Cement (si.)</td><td>20</td><td>25</td><td>—</td><td>—</td><td>25</td></tr><tr><td>Accessory minerals</td><td>—</td><td>5</td><td>3</td><td>—</td><td>—</td></tr><tr><td>Carbonate detritus</td><td>25</td><td>10</td><td>25</td><td>—</td><td>—</td></tr><tr><td>Anhydrite</td><td>—</td><td>—</td><td>30</td><td>100</td><td>—</td></tr><tr><td>Nannofossils</td><td>—</td><td>7</td><td>7</td><td>—</td><td>12</td></tr><tr><td>Micrite</td><td>—</td><td>13</td><td>—</td><td>—</td><td>3</td></tr></table>		2, 136 D	3, 96 M	4, 22 M	5, 54 M	CC, 10 D	Sand	25	—	—	—	—	Silt	55	—	10	—	—	Clay	20	100	90	100	100	Quartz	15	Tr	—	—	5	Mica	5	—	—	—	—	Clay	20	40	30	—	55	Calcite/dolomite	15	—	5	—	Tr	Cement (si.)	20	25	—	—	25	Accessory minerals	—	5	3	—	—	Carbonate detritus	25	10	25	—	—	Anhydrite	—	—	30	100	—	Nannofossils	—	7	7	—	12	Micrite	—	13	—	—	3
	2, 136 D	3, 96 M	4, 22 M	5, 54 M	CC, 10 D																																																																																													
Sand	25	—	—	—	—																																																																																													
Silt	55	—	10	—	—																																																																																													
Clay	20	100	90	100	100																																																																																													
Quartz	15	Tr	—	—	5																																																																																													
Mica	5	—	—	—	—																																																																																													
Clay	20	40	30	—	55																																																																																													
Calcite/dolomite	15	—	5	—	Tr																																																																																													
Cement (si.)	20	25	—	—	25																																																																																													
Accessory minerals	—	5	3	—	—																																																																																													
Carbonate detritus	25	10	25	—	—																																																																																													
Anhydrite	—	—	30	100	—																																																																																													
Nannofossils	—	7	7	—	12																																																																																													
Micrite	—	13	—	—	3																																																																																													
						● $\gamma = 2.69$ $\phi = 16$ V-3202	● 17 ● 8 ● 22	2																																																																																										
								3																																																																																										
								4																																																																																										
								5																																																																																										
								6																																																																																										
								CC																																																																																										



SITE 652 HOLE A CORE 75 R CORED INTERVAL 4156.5-4167.1 mbsl; 710.5-721.1 mbsf

TIME-ROCK UNIT	BIOSTRAT. ZONE/ FOSSIL CHARACTER				PALEOMAGNETICS	PHYS. PROPERTIES	CHEMISTRY	SECTION	METERS	GRAPHIC LITHOLOGY	DRILLING DISTURB.	SED. STRUCTURES	SAMPLES	LITHOLOGIC DESCRIPTION
	FORAMINIFERS	NANNOFOSSILS	RADIOLARIANS	DIATOMS										

